STRAIGHTENING OF BARS USING STATISTICAL CONSIDERATIONS

Thesis Submitted by

SANJIB ROY

Doctor of Philosophy (Engineering)

Department of Printing Engineering
Faculty Council of Engineering & Technology
Jadavpur University
Kolkata, India
2025

JADAVPUR UNIVERSITY

FACULTY COUNCIL OF ENGINEERING & TECHNOLOGY

KOLKATA-700032, INDIA

INDEX NO. 173/19/E

1. Title of the Thesis: **Straightening of Bars using Statistical Considerations**

2. Name, Designation & Institution of the Supervisor:

Dr. Arun Kiran Pal
Professor
Department of Printing Engineering
Jadavpur University
Salt Lake Campus
Plot-8, Sector-III, Block-LB
Bidhan Nagar Kolkata-700106
Phone: +91 79801 68930

3. List of Publications: **Papers published in international journals**

[1] Roy, S., Pal, A.K., "A Probabilistic Approach on the Estimation of Residual Curvature of Round Bars in Straightening Process with Cross-Roll Arrangements", International Journal of Science and Research (IJSR), ISSN:2319-7064, SJIF (2022): 7.942, Vol.11, Issue 6, June 2022, DOI:10.21275/SR22618185633

[2] Roy, S., Pal, A.K., "Theoretical Approach on Two Factorial Design on Residual Curvature of Bar Straightening in Cross-Roll Arrangements" , Journal of Production Engineering, JPE(2022), Vol.25, No.2, https://doi.org/10.24867/JPE-2022-02-030

[3] Roy, S., Pal, A.K., "Effect of Helix Angle in Cross-Roll arrangements of Bar Straightening Process with Kinematic Reverse Bending", Journal of Production Engineering, JPE(2022), Vol.25, No.2, https://doi.org/10.24867/JPE-2022-02-039

[4] Roy, S., Pal, A.K., "A Statistical Approach for Study of Roundness in Commercially Produced Round Metal Bars", European Journal of Theoretical and Applied Sciences, EJTAS ISSN 2786-7447, 1(5), 294-306. DOI:10.59324/ejtas.2023.1(5).20

[5] Roy, S., Pal, A.K., "A novel approach for study of straightness in commercially produced round metal bars based on deflection measurements", Applications in Engineering Science 16 (2023) 100161, https://doi.org/10.1016/j.apples.2023.100161

Papers published in International Conference

[1] Roy, S., Pal, A.K., Rawal, S., "A review on straightening of bars and application of probabilistic approach on Moment-Curvature relationship", IOP Conference Series: Materials Science and Engineering (ICEMEM-2019), 810 (2020) doi:10.1088/1757-899X/810/1/012080

[2] Roy, S., Pal, A.K., Das Talukder, N.K., "A Brief Review on Theoretical Aspects of Bar Straightening with Recent Developments in Its Modelling, Simulation, Control System, and Stabilization", Forming the Future, The Minerals, Metals & Materials Series, pp. 2135-2154, (2021), https://doi.org/10.1007/978-3-030-75381-8_180

Papers Communicated:

[1] Roy, S. Chaudhari, M., Pal, A.K., "Effect of straightening process on commercially produced round bars of ferrous and non – ferrous materials", Periodica Polytechnica Mechanical Engineering.

[2] Roy, S. Kar, A., Pal, A.K., "Predictive modeling of straightness in commercial round bars using machine learning", Periodica Polytechnica Mechanical Engineering.

Statement of Originality

I , Sanjib Roy, registered on the 10th June 2019 do hereby declare that the thesis entitled " Straightening of Bars using Statistical Consideration" contains literature survey and original research work done by the undersigned candidate as part of Doctoral studies.

All information in this thesis have been obtained and presented in accordance with existing academic rules and ethical conduct. I declare that, as required by these rules and conduct, I have fully cited and referred all materials and results that are not original to this work.

I also declare that I have checked this thesis as per the "Policy on Anti Plagiarism, Jadavpur University, 2019", and the level of similarity as checked by iThinkticate software is 3 %.

Sanjib Roy
Index No. 173/19/E
Date: 03/11/2025

Dr. Arun Kiran Pal
Professor.
Department of Printing Engineering
Jadavpur University, Salt Lake Campus
Plot-8, Block-LB, Sector-III,
Kolkata - 700106

Professor
Department of Printing Engineering
Jadavpur University, Salt-lake Campus
Kolkata - 700 098

CERTIFICATE FROM THE SUPERVISOR

Date: 03.11.2025

This is to certify that the thesis entitled "Straightening of bars using statistical considerations" submitted by Sanjib Roy who got his name registered on 10th June 2019 for the award of Ph.D. (Engineering) degree of Jadavpur University, is absolutely based upon his own work under supervision of Dr. Arun Kiran Pal and that neither his thesis nor any part of it has been submitted for any degree/diploma or any other academic award anywhere before.

Dr. Arun Kiran Pal
Professor
Department of Printing Engineering
Jadavpur University
Salt Lake Campus
Sector-III, Block-LB, Plot-8
Kolkata-700106, West Bengal, India

Professor
Department of Printing Engineering
Jadavpur University, Salt-lake Campus
Kolkata - 700 098

Dedicated to my father

Late Phanindra Mohan Roy

Who could not be here to see this day……..

Acknowledgement

कर्मण्येवाधिकारस्ते मा फलेषु कदाचन |
मा कर्मफलहेतुर्भूर्मा ते सङ्गोऽस्त्वकर्मणि ||
"Karmaṇy-evādhikāras te mā phaleṣhu kadāchana
Mā karma-phala-hetur bhūr mā te saṅgo 'stvakarmaṇi"
(Srimad Bhagavad Gita, Chapter 2, Verse 47)

"You have the right to perform your actions, but not to the fruits thereof. Let not your motive be the fruits of action, nor be attached to inaction."

I am grateful to The Almighty for his kind grace, blessings and direction during the studies and research work and at every moment of my life.

First of all, I take the privilege to pay sincere gratitude and homage to my supervisor Dr. Arun Kiran Pal, Professor, Department of Printing Engineering, Jadavpur University for his constant kind guidance, help and support in various forms. The undaunted encouragements and unforgettable inspirations have always motivated me towards completion of this thesis.

I am grateful to Prof. Dr. Amitabha Datta, Pro Vice-Chancellor, Jadavpur University, Kolkata for support and encouragement of this research work.

I am extremely thankful to Prof. P. P. Biswas, Dean, FET, Jadavpur University for encouraging and support of this research work.

I am also extremely indebted to Dr. Arpitam Chatterjee, Associate Professor & Head, Department of Printing Engineering, PhD Research Committee Chaiman and member of Doctoral Committee, Jadavpur University for his kind help of academic and administrative support during the journey of the thesis.

My thanks are due to all the members of Research Advisory Committee (RAC) and in particular to Dr. Apurba Kumar Santra, Professor, Department of Power, Jadavpur University and Expert from University outside department for providing important technical suggestions which enriched the research work and this thesis.

I take this opportunity to convey my deep gratitude to Dr. Kanai Chandra Paul, Professor, Department of Printing Engineering and member of Research Advisory Committee, PhD Research Committee and Doctoral Committee, Jadavpur University for various advices and encouragements all throughout this research work.

I take this opportunity to extend my sincere gratitude to Dr. Debasish Datta, Professor, Indian Institute of Engineering Science and Technology (IIEST), Shibpur, member of PhD Research Committee, Doctoral Committee and External member outside university.

I take this opportunity to extend my sincere gratitude to Dr. Bibhas Chandra Dhara, Department of Information Technology, member of PhD Research Committee, Doctoral Committee and External member outside department, Jadavpur University.

I take this opportunity to extend my sincere gratitude and thanks to Dr. Pradeep Kundu, Associate Professor and member of PhD Research Committee, Doctoral Committee and Departmental Subject Expert.

I express my sincere gratitude and thanks to Dr. Shilpi Naskar, Assistant Professor Department of Printing Engineering, Jadavpur University for constant encouragement and support during the entire research work.

I take this opportunity to extend my sincere gratitude and thanks to Prof. Soumen Basak, Associate Professor, Department of Printing Engineering, Jadavpur University for providing various administrative support and encouragements during the research work.

My sincere thanks to Shri Avijit Kar, Research Scholar, Printing Engineering, Jadavpur University for providing various technical assistance and constant encouragement during the research work.

My thanks are due to Shri Manoj Chaudhari, Assistant Professor, Alamuri Ratna Mala Institute of Engineering and Technology (ARMIET) for providing technical support during the research work and useful technical discussion.

My thanks are due to Shri Arjun Singh, Partner, M/s. Bhambra Engineering Works, Kolkata, manufacturer of two-roll Cross-Roll straightening machines for informative discussion on straightening machineries and M/s. Bright Bar Industries, Bhandardaha, Domjur, Howrah-711409 for facilitating straightening process which helped enormously in the research work.

I am grateful to all the nonteaching staff and laboratory assistants of the Printing Engineering Department, Library and workshop personnel of Jadavpur University for facilitating various services and help which was essential during the research work which was necessary at various times.

My sincere thanks are due to my friends Jadavpur High School, especially my friend Shri Animesh Roy and his family, my friends at BHU-IT (now IIT-BHU), my ex-colleagues of BHEL and NMIMS for various technical, moral supports and encouragements.

Lastly, my sincere thanks are due to my oncologist wife Dr. Chhaya Roy, MBBS, DMRT & MD, Retired Professor in Radiotherapy, my daughter Dr. Abhipriya Roy and all my family members who supported me in various forms without which this research work would not have been possible.

Sanjib Roy
Research Scholar
Department of Printing Engineering

Contents

LIST OF FIGURES

LIST OF TABLES

LIST OF NOTATIONS

σ	stress
C	an empirical constant
ε	strain
n	exponent of strain-hardening
E	Elastic Limit or Elastic Modulus
E_p	Plastic modulus, Linear work-hardening modulus
z	a value in z axis representing stress
c	a value in z axis representing stress
Y	Yield point
μ	A dimensionless parameter representing ratio of Young's modulus and plastic hardening modulus
σ_a	Stress at loading point a
σ_b	Stress at loading point b
σ_c	Stress at loading point c
ε_y	strain at yield point
ε_r	residual strain
c	constant
M	Moment
κ	Curvature
κ_r	Initial residual curvature
ε_{r1}	residual strain in the extreme fibre
h	depth of the studied section
y	a distance at z-axis
y_e	a value of y at elastic-plastic boundary
λ	a function dependent on the section parameters
κ_y	curvature at yield point or yield curvature
I_z	moment of inertia about z-axis
ΔM	extra moment required to produce a particular curvature
$\lambda_a, \lambda_b, \lambda_i, \lambda_{i+1}$	arbitrary intervals at length segments
P	Probability
X	a continuous random variable
$f(x)$	Probability density function
v_x	Throughput speed of bar
κ_f	Final curvature
θ	Angle between loading plane and osculating plane
$M_{\lambda a}$	Moment at length section 'a'

$M_{\lambda b}$	Moment at length section 'b'
$\kappa_{\lambda a}$	Curvature at length section 'a'
$\kappa_{\lambda b}$	Curvature at length section 'b'
$f_{\kappa}(\kappa_f)$	probability density function of final curvature
$d\kappa$	Differential curvature
R	Roller radius
r	Bar radius
$\dot{\theta}$	Angular speed of bar
ω	Angular velocity of rollers
v_t	Tangential velocity of any point on the surface of the bar
α	Cross-roll straighteners are set at an angle to the axis
N	r.p.m. of rollers
p	pitch length
$\Delta\kappa_r$	Residual curvature change
M^*	maximum loading moment
κ^*	corresponding curvature change due to M^*
M_y	Bending Moment at yield point
$\bar{M}$	Non-dimensional form of bending moment
l	Length of bar or beam length
$\bar{\kappa}$	Non-dimensional form of curvature as ratio of curvature and curvature at yield point
$\Delta\bar{\kappa}$	curvature change in non-dimensional form
$\bar{\kappa}_f$	Final curvature in non-dimensional form
$\bar{\kappa}_r$	Residual curvature in non-dimensional form
$\bar{m}$	the effective bending moment in non-dimensional form
$\bar{M}^*$	Non-dimensional form of maximum bending moment at any instant
$\bar{\kappa}_{rf}$	final residual curvature in non-dimensional form
ω	angular velocity of the rolls
$\bar{r}$	Ratio of bar radius and length of bar
$\bar{M}_x$	Non-dimensional form bending moment at section x
$\bar{m}_x$	effective bending moment at section x in non-dimensional form
t	time
π	angle in radian equivalent to 180 degrees
$\bar{x}$	Ratio of x and length of bar, x/l
$\bar{p}$	Ratio of pitch length and length of bar, p/l
$\bar{y}$	Ratio of y and bar radius r
κ_{rf}	Residual final curvature
κ_{ri}	Residual initial curvature

$\Delta\kappa_r$	change in residual curvature
$\kappa_{r\lambda i}$	residual curvatures at length segment λ_i
$\kappa_{r\lambda i+1}$	residual curvatures at length segment λ_{i+1}
$F_K(\kappa_r)$	cumulative distribution function (CDF) of residual curvature κ_r
κ_{rl}	initial residual curvature in the loading plane
μ_κ	Mean curvature
$g(\kappa_r)$	a function of residual curvature, κ_r
E	expected value of curvature
σ_{κ_r}	Standard deviation of residual curvature
Var	variance
LR	Linear Regression
SVR	Support Vector Regression
RFR	Random Forest Regression
XgBoost	Extreme Gradient Boost
DT	Decision Tree
MAE	mean absolute error
RMSE	root mean square error
R^2	R squared
RBF	Radial Basis Function
$\varphi(.)$	kernel function
w, b	normal direction of hyperplane
y	predicted value
$\hat{y}$	actual value
$\bar{y}$	mean of actual variable
n	number of observations or data points.
C	regularization parameter
l, L	Learning set l or L of input variable X and output variable y
$Err(\varphi l)$	Error function of kernel
$E_{X,Y}$	Estimator of X, Y

Note: Symbols not included in this list are defined where they appear.

CHAPTER – 1

INTRODUCTION

1.1 Background

Production of various types, sizes and lengths of metal round bars are quite a common requirement in several metal-based manufacturing industries. This is due to the fact that these round bars are used as raw materials either directly in fabrication of structures or as raw materials for production of designed product based on design specifications. Many products which are outcome of shop floor, require quality inspection for the purpose of ascertaining of quality uprightness to ensure imperfections are within control limits and product lot is within acceptable quality level. In the production of round bars, roundness or circularity and straightness of bars are considered important factors due to their likely applications as raw materials for direct use or as various machine components in both static and dynamic condition.

It is quite natural that commercial round bars or tubes are subjected to several material handling and transportation before the product reaches to the consumer end. Due to their variety of sizes, it is practically and economically not feasible to go for such proper packaging for shipping so as to no deformations will occur. The usual practice is mass loading and transportation where there is fair possibility of occurrence of deformations during loading, unloading and transportation. Hence, there are cases where such commercial round bars undergo bending loads at several sections along the length and consequently deformations are observed.

Therefore, an overall understanding of such round bars is actually necessary to take decisions as to whether for a round bar, it is actually necessary for straightening or not. Visual inspections are sometimes not adequate to take decisions for use. Therefore,

usage of deformation analysis as well as its statistical analysis will lead to definitive decision making on quality acceptance based on Acceptable Quality Level (AQL) depending on type of manufacturing process.

Round bars are used sparingly in large number of manufacturing industries for the purpose of producing various types of machine components. Among these machine components, spindles, shafts and links are in dominant numbers. Support rollers are also used largely in machines where conveying system plays significant roles. Most printing machineries includes large number of such support rollers, shaft, rods to facilitate conveying of printing substrates i.e. papers and plastic and also controlled flow of ink. Inkjet printing machines also include use of highly polished round bars to support sliding cartridge. Rolling components in almost all printing machines are primarily made up of round bars of various sizes. Several supporting bars are also round in shape which keeps the machine properly aligned and structurally rigid to take working load arising out of continuous printing, sometimes high-speed printing. Straightness and roundness of these round bars used in printing machines as various components are significantly important for the purpose of production quality uprightness which essentially demands a vibration free and smooth conveying operation.

Besides printing industries several other industries had different types of machines where round bars are used in the form of precise straightness required for the quality output. These straight bars are subjected to various kind of static and dynamic load sometimes continuously or sometimes intermittently. A small curvature in any of these straight round bars would naturally affect overall performance of machines as well as the output. While manufacturing of round bars it has been observed that there is lack of roundness and straightness in most of the cases which requires further straightening process for getting better quality output. However, straightening process does not require much time and expense which in turn leads to overall economically viable manufacturing process.

It is this background that caused interest to look into deeply and also necessitated to do further research work on the importance of straightness and roundness of commercially available bars. It is also essential to understand statistically to what extent they are readily acceptable for direct use of machining and also to look into the straightening of deformed bars through various standard straightening processes so that most of the raw materials can be used in production purpose which in turn will lead to minimum waste.

1.2 Straightening

Bars, bar sections and long parts are generally straightened by bending, twisting or stretching. Deviation in straightness in round bars can be expressed either as camber (deviation from a straight line) or as a total indicator reading (TIR) per unit of length.

In the production of round bars, roundness and straightness of bars are considered important factors due to their likely applications as raw materials for direct use or for various machine components. Long bars which are produced in rolling mills are sometimes seen that degree of straightness is compromised along the length of bar either at various sections or at entire length as a whole.

Therefore, it can be stated that straightness of such products like round bars is certainly an issue before their further actual deployment into either job or batch or mass production. However, actual requirement of further straightening may depend upon real time situation as whether the lot produced really needs further straightening or not. Often, it is considered that straightening as a process through rollers is vital step in the route of processing of long products like shafts, links, long screws and rails etc. [1].

Many standard straightening methods are available in industries. Among these methods, cross-roll straightening is widely used in industries due to its speed of operation. The pitch length of bar can be decided by the helix angle of cross-roll arrangement. The helix angle causes the bar to rotate and simultaneously proceed also through the rollers which acts as a self-conveying mechanism and straightening operation takes place.

Among different types of cross-rolls straightening processes, two-cross roll straightening process is quite a common technique where the round bars are bent cyclically with varying amplitudes. In two-roll cross-roll straightening process, the round bars are bent and simultaneously rotated as these bars are passed between a set of convex and concave rolls or some other arrangements. For bars having a large diameter, some stamping may also be applied by the rolls. Before the process of straightening, it is also essential to understand various causes of imperfections such as residual curvatures present at various sections and its theoretical background as what actually matters in the process and where it is necessary to focus on the qualitative aspects for a sound product.

The concept of applying a bending moment and consequently a curvature in a beam is not new but quite old. Though it is known that there will be a linear relationship between bending moment and curvature as given in Saint Venant's solution, but later it has been found that bending moment increases initially as curvature increases as in Bending Moment-Curvature diagram, bending moment reaches a maximum value at a point 'A' as shown in Figure 1.1 [2]. The value of bending moment will reduce as curvature increases further. However, it was also indicated that if bending moment increases beyond point 'A', the beam will collapse which means that this point 'A' can be considered as a point of instability.

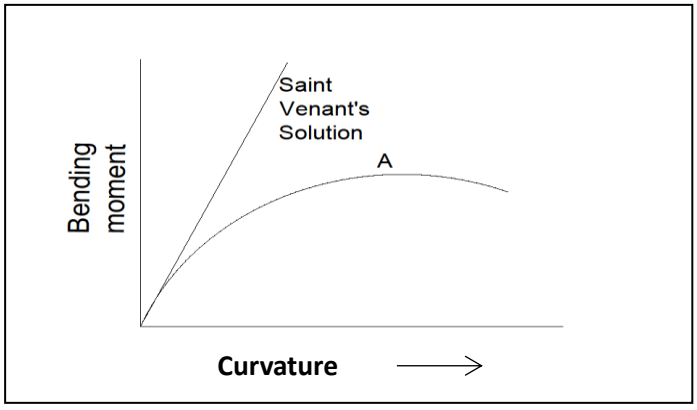

Figure 1.1 Bending Moment-Curvature Diagram

This analysis is sufficiently indicated on the relationship of bending moment and curvature when round tube or bars are subjected to both in elastic and plastic range. However, the present study has been focussed on solid metal round bars [3].

1.2.1 Straightness of round bars

It has been seen that profile of the round bars are often not straight and profile variations are visible when a surface plot is taken based on data which have been observed from dial gauge deflections at various sections of the round bars along the length of the bar [4]. It has been seen that variations in surface profile exists which means that curvatures exist at various sections of length segments, hence straightening may be required where curvatures are significant.

It is pertinent to mention that curvatures in commercially available round bars are actually residual curvatures which occurred during hot rolling process when bars were passed through rolling stands in steel rolling mills. The residual curvatures would further enhance due to material handling and transportation. These curvatures would occur due to deformation in elasto-plastic range. Deformations due to bending can be straightened through reverse kinematic bending process. Therefore, process of bar straightening can easily be considered as a standard process for reducing the curvatures in the bar.

It is quite imperative that researches continued with an aim of how better straightness can be achieved in round bars. Since, it is quite usual that commercially available round bars are sometimes not so straight and degree of straightness varies. Kemshall [5] indicated that degree of straightness depends on the selection of type of machine. Commercial straightness that is degree of straightness from 1 in 750, to 1 in 5000 can be achieved actually. Degree of straightness or simply straightness expressed as the distance or deviation from the longitudinal axis or centreline over a specified length, i.e., ratio of deviation to length as indicated in Arrow method. However, there is another

method of specifying degree of straightness that is Total Indicated Reading (TIR). TIR is defined as deviation measured on a dial gauge when the bar is rotated on "V" block supports or knife edge rolls at 1 m centres. The dial gauge is mounted in such a way that it is positioned on the centre of the span. It can be considered that TIR reading of 1 in 1000 is equivalent to straightness of 1 in 2000 of Arrow method. It is quite essential that straight bars as required at many places in industries are to be produced with necessary degree of straightness.

During straightening process, residual stress is developed in rounds bar and straightness of finished bar depends on the applied loads in straightening machine. Better straightness is desired on a round bar then the round bar has to be bent more severely with applied load so that curvature reduces and consequently straightness is improved [6]. In cross-roll arrangement, these feature of improvement of straightness were achieved through rolls. Consequently, it has been noticed that multiple rotary bending helps improving degree of straightness. However, it is also seen that for rotary plastic bending in a bar, direction of bending moment not necessarily coincide always with that of bending of the bar. As bars and tubing cannot obtain better straightness by parallel roller straighteners, hence rotary straighteners having oblique rollers are used. There is some angle between both directions of bending moments and bending of bar for rotary plastic bending of bar.

1.2.2 Plastic deformation

Round bars are subjected to elasto-plastic deformations when passed through straightening machine as the bars undergo alternate bending with loads of high magnitude. Surrounding the centre of the round bar two zones undergo plastic deformation which retains initial deformation [6]. Consequently, residual stress distribution of section of the bar and the zones left by compressive and tensile residual stresses surrounds the centre undergo no plastic deformation. At the plastic zone to the centre of the bar, residual stress builds up residual moments.

In straightening process, the bending moment arising out of residual stresses rotate accordingly during revolution of the bar as sections change between one pitch length to another. The pitch length is advancing of round bar during one revolution. The earlier research indicates that straightening of bar and tubing were more exactly which had comparatively smaller residual stresses while processing through rotary straightener by method that applies more severe bend and multiple rotary plastic bend during at period of the reducing bending moment.

Quite often by using Ludwik power law [3,69] (given in Eq.1.1), the effects of creep and plasticity are allowed for as an adjustment to initially elastic conditions.

$$\sigma = C\varepsilon^{n} \tag{1.1}$$

where σ is stress, C is stress constant, ε is strain and

n is strain-hardening exponent with range ($0 \leq n \leq 0.5$)

This can lead to conservative or pessimistic results of the structure. Hence, it is essential for a realistic prediction to have good 'constitutive relations' which may reflect true behaviour of material accurately. If the round bar in straightening can be considered that as it happens to 'remember' its previous loading history, then its subsequent behaviour can fairly be predicted using related equations. To some extent this is indicated by Bauschinger effect [3,7].

1.2.3 Bauschinger effect

The phenomenon of Bauschinger effect is defined as reduction of elastic limit or proportional limit (proportional limit is slightly below elastic limit) in compressive load after following previous tensile loading and vice versa. If deformation in one direction is considered, reloading in simple compression will show appreciably smaller elastic limit in magnitude compared to previous yield point. Bauschinger effect occurs whenever there is a reversal of stress. Lowering of the yield stress is primarily caused in reversed loading by the residual stresses as illustrated in Figure 1.2. In the specimen,

residual stress is actually left on a very small or microscopic scale due to materials individual crystal's different stress level [3,7].

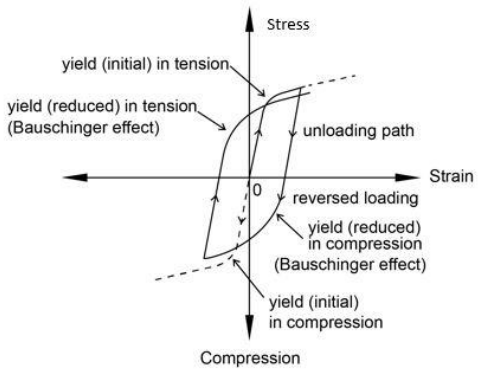

Figure 1.2 Illustration of Bauschinger Effect [7]

Interpretations made earlier are still effective and used today. It is considered as an internal 'back stress'. The back stress changes sign based on the epoch in the corresponding stress-strain cycle and takes the form of a hysteresis loop since plasticity is invoked. Although by mild annealing, bar materials are subjected to stress reduction, but it is seen that Bauschinger effect can actually be removed from materials.

In the theory of plasticity, Bauschinger effect is generally neglected and can be largely removed assuming that the material is having identical yield stresses both in compression and tension, irrespective of previous cold work [7]. In bar straightening it is quite significant that as bars are subjected to elasto-plastic bending while in the process of cold working.

The information on bar straightening have been arranged systematically chapter wise for easy understanding with due clarity. Residual stresses have been dealt briefly as residual stress is a major point of discussion in this work. Various types of straighteners are available in industries which have been discussed briefly. Keeping these theoretical observations in mind the objective of the present investigation has been decided and given below.

1.3 Objective of the present work

Since, there was practically hardly any research wok concerning statistical aspects in bar straightening process to the best of the knowledge of the author, the present research therefore had multiple objectives which are discussed below.

- To study probabilistic and statistical analysis in the process of bar straightening concerning final residual curvature and developing equation for probability of final residual curvatures along the bar length.
- To develop the criterion for helix angle of straightening process being a key parameter.
- To develop a theoretical framework by using factorial design by analysis of variance (ANOVA), one factor being the helix angle.
- To study circularity or roundness of straight round bars with feature of straightness using Statistical Process Control (SPC) analysis before and after straightening process.
- To measure the deformations of commercial metal round bars before and after straightening.
- To analyse the deformations of commercial metal round bars before and after straightening.
- To analyse deformations in the straight round bars using Finite Element Method (FEM) before and after straightening process for validation of deformation analysis obtained experimentally.
- To develop a novel methodology of prediction of straightness of metal bars on the basis of circumferential deformations along the length using machine learning models allowing forecasting of straightness after two cross-roll straightening for implementation in manufacturing process.

1.4 Scope of the present work

Previous investigations on straightness in general have stretched more on the qualitative aspects of deformation behaviour. In many cases investigators have also attempted to obtain the quantitative information of deformation behaviour. Unfortunately, many of early investigations are not easily accessible. Some of the earlier study indicate fairly good correlation with the results obtained from conventional measurements while others have failed. Research in this field has started in India for quite sometime possibly in 1980s. In spite of some inherent limitations of the theory of straightness (for instance, very long size of bar, absence of dynamic condition of bar, neglect of frictional effects on the surface of the bar etc.), it is possible to determine the deformation behaviour of round bars from simple experimental method by dial gauge and predictive modelling of straightness using machine learning. The overall results obtained using the present technique follow with the similar results obtained using finite element analysis and machine learning modelling.

The present investigation emphasizes the use of the dial gauge, finite element method and machine learning algorithm as experimental tools to study straightness of round bars. The usefulness of above tools is substantiated through the initial study conducted during the past few years at the Jadavpur University, India [4,7,8,9,10,11,12]. The experimental technique on commercially available round bars using dial gauge is quite simple and does not cost much excepting the equipment which, however, do not involve large funds and neither the gadgets or instruments are to procure indigenously. Other advantages of dial gauges include the absence of skilled personnel to conduct the experiment. The methods of experimentation are quite simple in comparison with experiments using other conventional optical devices.

In the present investigation, the developed predictive modelling technique and the finite element method [4] would be examined critically using different size of round bars of different materials. The experimental dataset obtained by using dial gauge method or round bars are applied to the above two numerical experiments. The

experimental technique of deformation measurement using dial gauge and the corresponding observations are presented in Chapter-5 & 6.

The study of the accessible literature pertaining to the use of dial gauge to study deformation behaviour by previous investigators has been made with a view to get a comprehensive status of research in this direction. This has been briefly described in Chapter-2.

Theoretical aspects being and integral part of the research work has been dealt at Chapter-3. In this chapter, straightness and straightening process by reverse bending has been discussed. The working principle and mechanics involved in bar straightening process has been discussed. This chapter also deals with various types of straightening machines. Criterion of setting of Helix Angle has also been discussed here. Derivation of helix angle shows its significance in the process. Application of straightening in various machines and machine components have been described briefly.

In Chapter-4, probabilistic approach has been considered in straightening process. Probability of residual curvature has been discussed based on initial and final residual curvatures. The expected value of residual curvature and variance thereof have been derived.

Based on the earlier works an appropriate experimental arrangement has been designed and constructed for measurement of deformations and also for single pass straightening of round bars. The size of the straightening machines is selected keeping in view the scope to accommodate different sizes (6-mm, 8-mm, 10-mm and 12-mm) diameters of round bars. The various design features and the methods followed during the experiments are presented in Chapter-5 & 6.

Along with the experimental work, it is also intended to address some of the above mentioned cases from analytical point of view. The experimental result of the deformation behaviour of round bars obtained by dial gauge are compared with the results obtained from finite element analysis. All these result are presented and discussed in Chapter-7.

For the sake of completeness of the study and ready availability, the predictive modelling of straightness by using different machine learning algorithms namely Linear Regression (LR), Support Vector Regression (SVR), Random Forest Regression (RFR), Extreme Gradient Boost Regression and Decision Tree Regression have been developed and discussed. As a part of developing predictive model these machine learning algorithms are applied to the experimentally acquired data. Computed metrices such as coefficient of determination (R^2), mean absolute error (MAE) and root mean square error (RMSE) etc. resulted in RFR better than all the other methods. These observations are presented in detail in Chapter-8.

At the end of each Chapter mainly Chapter-2, Chapter-4, Chapter-5, Chapter-6, Chapter-7 and Chapter-8 various investigations and observations are discussed. An overall discussions of the entire investigations caried out and scope of future investigations are also presented in Chapter-9. New contributions in this area have also been highlighted in this Chapter along with its limitations.

CHAPTER – 2

REVIEW OF PREVIOUS INVESTIGATIONS

2.1 Introduction

Considerable number of research papers had paid attention on straightening aspect of round bars. Arrangement of various types of straighteners or straightening machines in respect of degree of straightness and straightening theory developed by earlier researchers are in place. Discussions were on many aspects of elastic-plastic zone and applications of stress-strain relations up to non-linear regions where moment-curvature relationship played important role. Since, in bar straightening process loading have been in repeated nature, discussions included cyclic loads as well. Arrangement of rolls, residual stress distributions, multiple staggered rolls, the straightening speed, other geometrical parameters have played considered amount of role in the development of theories on bar straightening.

Researches in this area have been since year 1927 by Brazier [2] and by now large number of publications have taken place. The research works have therefore been reasonably classified with an aim to put the relevant information in proper perspective. Various work on numerical approaches including simulations have been done which enriched the subject in various forms.

Earliest reference in bar straightening is found in the work of Haruo Tokunaga in the year 1961 in the publication titled “On the Roller Straightener” [6]. However, most significant development of the theory has taken place in 1980s. In particular, work of N. K. Das Talukder, W. Johnson and T. X. Yu [13,14,15,16] made significant contributions in the development of theoretical part. Later on, many researchers worked in bar straightening which have been discussed subsequently. However, there are gaps

in the research work of various authors as well, which formed some basis of the present work. Bar Straightening using statistical consideration of various important parameters has not practically been looked into. Statistical consideration has its own importance from industrial point of view as production and pricing of a product largely depends on statistical approaches and management decisions which need to be rational and should be based of the foundation of statistics. Although there are large number of research papers in the area of bar straightening but, it has been felt prudent to consider most relevant research papers which have been further classified and reviewed accordingly. After reviewing these research papers, it has been found that following areas have been looked into primarily by various researchers and researches have been done. The research papers can actually be classified in certain groups based on area of researches. Accordingly, the classification has been done as below:

(i) Group-1: Researches related to "Theoretical aspects of straightening process"

(ii) Group-2: Researches related to "Measurements/Residual Stress Measurements"

(iii) Group-3: Researches related to "Modelling / Numerical Modelling and Simulation"

(iv) Group-4: Researches related to "Control Systems on Straightening Process"

(v) Group-5: Researches related to "Stabilisation of the process"

(vi) Group-6: Researches related to "Statistical Consideration"

In this chapter an attempt has been made to bring the important works in the field together as found in open literature till date. For ready reference and convenience, it is intended to make a critical study of the relevant works published in this direction. Substantial work has been done in some of the above-mentioned areas which have been briefly presented in the sub-sections. However, there are still some areas where researchers are yet to look into.

2.2 Review of Previous Investigations

As mentioned in previous paragraph that several researchers have worked on bar straightening in various areas, above classification has been made where previous researches tried to explain each classified area systematically to the extent possible. The classification has been done based on certain common areas where researchers have given thrust in order to get an insight of the subject matter. The development in bar straightening has taken place over long span of time. While in initial years thrust was much more in the understanding of theoretical aspects of straightening process of bars but later on other areas were picked up viz. measurement, numerical modelling, control systems etc. Theoretical development is the root of the researches which have been successfully done by some of the researchers. The mathematical relationship on reverse kinematic loading was looked into by early researchers. T.X. Yu and W. Johnson worked on initial and final curvatures and brought out clarity [13]. In particular, the mechanics part was developed in early years by Das Talukder et al. [14, 15, 16].

Numerical modelling has been quite a useful method in many scientific researches through the use of certain standard software which enables simulation of actual situation. This way a computer-generated model helps in predicting a real-life situation which often gives fairly reasonable result to derive useful conclusion. In the bar straightening process also, several researchers have used computer software for numerical modelling and simulation. Generally, for the purpose of numerical modelling and simulation of the process, software like ANSYS, ABAQUS, LS-DYNA, DEFORM-3D etc. have been used by the researchers.

In advance design and engineering, application of finite element method (FEM) helps in assessment of deformation and stress calculation. In the process of bar straightening, FEM has been used for the purpose of structural analysis based on given loads using above-mentioned software. FEM is no doubt a quite useful and powerful tool to assess deformations and stresses in the bars as well as on the rollers that is in contact. The generated mesh on the bar and rollers can indicate desired values of deformation and

stresses at any nodal point of the mesh. Researchers have taken the advantage of simulation technique in order to understand stress patterns in various types of cross-roll arrangements in the bar straightening process. It has been seen that in recent researches on bar straightening, there is substantial use of finite element model and simulation technique for the purpose of thorough understanding of various parameters involved in the bar straightening process. Large number of nodes in the mesh helps in correct assessment of stresses and strains over the bars and rollers. The values of stresses and strains in the straightening process form the basis of roller design.

2.2.1 Straightness and Roundness

Straightness and roundness being a major engineering concern for circular section bars, it has drawn attention of many researchers on theoretical and experimental basis. A general concern for straightness and roundness by researchers can be seen from various publications. Some of these researches have been mentioned here to highlight the importance given by various researchers in this area of bar straightening. Straightness may be considered as a general requirement in many industries unless specified. Therefore, straight round bars are not only highly sought items but also have tremendous industrial application practically in all range of industries whether small, medium or large scale.

The earliest reference on bar straightening is found in a publication by Haruo Tokunaga in the year 1961 in his paper titled "On the Roller Straightener" [6]. In his findings, Tokunaga indicated about residual stress distribution in bars straightened through rotary straightener which shows an alternate vortex of tensile and compressive zones around the center of the bar. This alternate vortex of tensile and compressive zones is not affected by the repeated rotary bending. Tokunaga also stated that in order to obtain improved or better straightness, it is somewhat essential that the bar requires to be bent more severely at the points in bar under the rolls and that receive more multiple rotary bending. An important point has been surfaced here that for straightening of the round bars and tubing, oblique rollers are to be used in the rotary straighteners, because better

straightness cannot be obtained by parallel roller straighteners as used for straightening of shapes and profiles. Tokunaga assumed following conditions while dealing deformation of the bars by rotary plastic bending in rotary straightener [6].

- The outside shapes of sections of bars and tubing are round and for pipe and tubing are having uniform thickness.
- The cross-section of the bar remains on a plane during the process of bending, and always at right angles to the axis of the bar.
- Other than the stress in the longitudinal direction, all stress components are zero.
- The material of the round bar is to be considered as perfectly elastic-plastic, i.e. its stress-strain relations in uniaxial tension and compression are same. Elastic modulus and yield point in tension and compression is same.

These assumptions are probably quite essential, else too much of complexities will emerge even at initial stage. Tokunaga also dealt with distribution of compressive and tensile residual stresses surrounding the center of the bar which undergoes no plastic deformation. Consequently, residual stress of the plastic zone builds up the residual moment to the centre of the bar. Measurements of the residual stresses of the straightened bar were done on an experimental set up. Residual stresses are left in the bar after straightening by the rotary straightener which is in the state of equilibrium to hold the straightness of the bar. Tokunaga also indicated relationship on radius of residual bend after straightening and moment of the core of the bar.

By the year 1974, there have been tremendous advancement in the design of straightening machines for light bar and section product which was highlighted by G. E. Kemshall in a publication titled “Bar Straightening and Bundling Equipment” [5]. Kemshall indicated various types of machines were in use. Most popular machine was Reeler or Reeling machines or cross-roll straightening machine. Cross-roll machines are available in various combinations of driven and idle roll arrangements. Other machines include section straightening and stretch straightening machines. Kemshall classified cross-roll straightening machines for round bars. These machines are of four basic types viz. two-roll, multi-staggered, six-roll types and cluster-roll machines.

Details of each type of machine have been discussed in separate chapter. Kemshall indicated about surface finish stating that all cross-roll straighteners will remove mill scale to a greater or lesser extent, and also improve surface finish [5]. Two roll straighteners are used frequently for improving surface finish. Two fundamental requirements have been indicated in straightening theory, i.e.

(i) material must be plastically deformed;

(ii) imposed stresses must be reversed progressively.

Circular section is one of the most fundamental forms in engineering components. There are numerous applications in engineering where circular forms arise. Consequently, it became apparent to look into the surface of material with circular section, hence measurement of surface got its own importance. Surface smoothness is having deep concern due to its mechanical aspects as most machine components demand surface smoothness in industrial arena. Surface smoothness is an important factor when dealing with performance of a component in tribology as explained by Whitehouse in 1997 [17]. It is obvious that variation of roundness needs to extremely low for improving smoothness of round bar unless specifically designed a component for a special purpose. In general, most machine components require uniform roundness and surface smoothness too to meet general industrial requirement.

A study of roundness was made by Marcos-Barcena et al. in 2005 [18]. Marcos-Barcena studied on Aluminium-copper alloyed cylindrical bars with specification of UNS A92024. The authors studied that these Aluminium alloys were broadly employed for the production of the different elements in aerospace industries which conform the requirement of airships. The research was focused on roundness and difference of roundness through measurements have been considered as response variable. These light alloys are widely employed for producing elements of pieces that integrates the products in industrial sectors. Roundness of precision elements are real concern here. Based on the work of Marcos-Barcena et al. further research was done using neural network by Kalos et al. in 2007 on roundness control of turned cylindrical bars [19].

In 2009, according to Lu et al., to improve upon the straightness of metal bar, straightening techniques is one of important means [20]. The authors used stroke-

deflection model, a mathematical method for their bending experimental and numerical simulation which may be considered a novel way of predicting the straightening stroke. Lu et al. stated that metal bars viz. metal pipes, rods, rails etc. are often essential parts for various mechanical manufacturing industries. It is highlighted that the straightness of metal bars is usually not sufficiently precise that would meet the industrial requirements. Hence, such metal bars need to be straightened before deploying for various kinds of high precision products. It is pertinent to mention that the straightening technology is reckoned as one of the most important processes in many manufacturing industries and therefore has been adopted in their production system. Lu et al. stated that for different processing objects, there are different methods which could be chosen to straighten the bar part. So, based on requirement, different method could be chosen to straighten the bar part.

There are different straightening methods which will be discussed separately at appropriate chapter/section. These frequently used methods include press straightening, parallel roller straightening, inclined roller straightening, turning hub straightening, tensile straightening and stretch bend straightening. In comparison to roller straightening, method of recurvation press straightening which accompanies large straightening force, best possible flexibility along with high controllability and precision could extensively be applied to straightening process of metallic bars such as large size pipes, rods, guides, irregular sectional long shaft parts, non-symmetrical section profiles and some special steel parts. As the automatic straightening machines came into being the concept of straightening techniques gradually started getting focus of the current precise straightening controlling research. However, it is not so easy to make improvement on the precision of the theoretical model.

Straightness of bar is a major concern in most industries where round bars are required as raw materials. The present work has largely focused on straightness of bar and also the process of straightening. Straightness evaluation has therefore been an area of research for obvious reason. In 2015, Kume et al. have attempted evaluation of straightness using inclinometers [21]. According to Kume et al. usually, straightness evaluation is performed using a scanning a detector along an object. It is also stated

that errors in the scanning locus directly affect this evaluation. Authors proposed several kinds of error separating techniques and also developed for eliminating errors. A simple and classical technique is straightness evaluation detecting tangential angles or differential straightness. On the whole, use of inclinometer is actually advantageous for large size objects because there is no requirement of transferring mechanism that scans the detector with sufficient accuracy.

In 2018, Tangjitsitcharoen & Chanthana worked on the prediction of roundness. The research was based on dynamic cutting forces [22]. The paper published in 2015 is an advanced work of same authors [23]. The authors have investigated the relations of dynamic cutting forces, roundness, and cutting conditions. In this paper authors have realized that an intelligent machine is essential to control reduction of roundness errors during turning process. The process would then increase productivity and simultaneously efficiency also. To accept the mechanical parts, one of the important criteria is to roundness error especially in turning of a long slender bar. Critical importance has been given to the measurement of roundness as indicated by Roy & Pal [5].

2.2.2 Group-1: Review on Theoretical Aspects of Straightening Process of Metal Bars

As mentioned earlier that all the previous work has been reviewed and found that the researches could be classified in some groups. There have been several researches in the area of theoretical aspects of bar straightening. The researches on theoretical aspects practically started in the year 1911 which is evident from the publication of Tokunaga [6] and later by Yu & Johnson [13] and Das Talukder et al. [14] both in the year 1981. There have been other researchers subsequently. General analysis of bar straightening process and developed mechanics of bar straightening. It can be stated that theoretical researches in initial years have actually made foundation which helped many researchers to work on bar straightening at a later date. Basic governing

equations were developed in these early researches which helped tremendously to look into deeply on various aspects of bar straightening.

The mathematical relationship has been established for actual effective moment applicable during reverse kinematic loading. Consequently, components of throughput speed were established with helix angle. The pitch length of cross-roll arrangement is equated in terms of helix angle and bar diameter. In the same year Yu and Johnson researched further based on above work and brought out clarity on initial curvature and final curvature through their publication [13]. In this publication Yu and Johnson assumed that

(i) the bars are to be considered elastic/linear work-hardening

(ii) the bar is having a circular cross-section

(iii) when bar is subjected to pure bending, the neutral axis is mid-way through the bar.

The assumptions are no doubt at basics of theory of elasticity and plasticity. Mathematical relationships of final and initial curvatures were established with graphical representation. Obviously, their work is of immense importance in the study of bar straightening process. The change in curvature of straightened bar was elaborately discussed. The bending moment distribution in cross roll arrangements play most significant role. The concept was also explained graphically. Graphical illustrations on bar straightening process can be considered as key features of this publication.

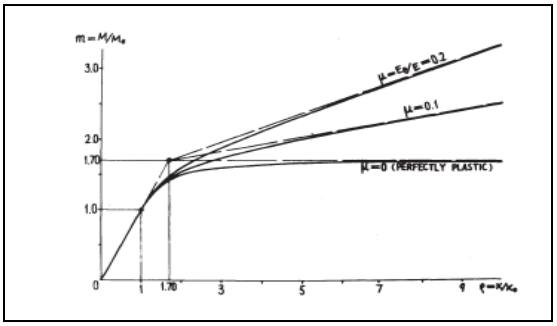

Figure 2.1 Moment – Curvature Relationship for Circular Bars [13]

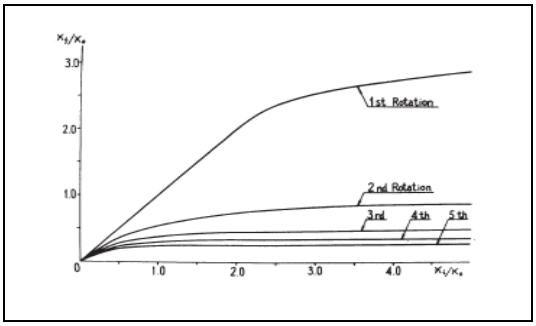

Figure 2.2 The Reductions of Curvature after Several Rotations, for Bars with $\mu = E_p/E = 0.1$, [13]

E = Young's modulus, E_p = Linear work-hardening modulus

In the year 1999, the work on profile determination of roller came into being through the publication by Li et al. [24] as indicated clearly that irrespective of accuracy of industrial process in the production of steel tubes or bars, straightening process is almost essential. This is required in order to correct the out-of-straightness and out-of-roundness of the produced bars or tubes. It has been found that in straightening process, roller profile is an important factor. Li et al. presented a new method for determination of roller profile of a tube straightening machine. Envelope theory has been applied for a family of spatial curves. In this study Li et al. used six-roll straightening machine and rolls are skewed. In six-roll straightening machine, there are supporting rollers which are driving roller while the driven rollers are actually loading rollers. In this six-roll straightening arrangement, the skewed angles can be adjusted to suit different requirement of tube or bar sizes.

To manufacture a quite precise roller surface with an acceptable quality, profile of roller needs to be defined analytically for getting reasonably accurate roller data which can be employed in the processes of machining and inspection. A roller is essentially an object of three-dimensional curved surface. When the bars are subjected to straightening process, i.e. within the curved surfaced rollers, the rolls are actually subjected to a series or repeated bending and unbending operation.

Li et al. [24] presented a method and applied envelop theory for a three-parameter family of spatial curves to determine the profile of roller of a tube-straightening machine. Based on envelope theory, the roller contour is regarded simultaneously as an envelope of the three-parameter family of spatial circular curves in implicit form in a simultaneous process of rotation, translation and rotation. The spatial curves can be expressed as a function in a three-dimensional x,y,z space where rotating angle φ along the first axis, translating angle ρ along the second axis and rotating angle θ along the third axis are three independent parameters of motion. Li et al. used solid modeling of a roller with tube-straightening element to develop envelopes. Various profile design is possible by changing data in solid modeling. Analytical mathematical expression for the determination of the roller profile of tube-straightening element based on envelope

theory, coordinate transformation matrices, and differential geometry is essence of the research work. The method indeed provides a versatile technique which is convenient also for the design of three-dimensional roller contours.

In 2001, Marcus Paech came up with another publication titled "Roller Straightening process and peripherals" [25]. The focus was on wire straightening like previous publication. Straightening process as a classical function is to create material that is quite straight or having a defined curvature. However, these days straightening process is also expected to do several other jobs as well. These jobs include identification of material's characteristics and changing them in a predefined manner. These characteristics are modulus of elasticity, yield point, sectional geometry, initial curvature and helix angle. Paech thrust was in designing the straightening process and on peripherals. It can be stated that every straightening unit and system comes with a specification indicating range which is fixed by diameter of straightening rollers and spacing as mentioned earlier.

It is quite common that use of latest technology is beneficial for increasingly high-quality level products demanded by customer. In the year 2008, Marcus Paech [26] has shown in his publication titled "Advanced semi-automatic straightening technology" that intelligent and flexible machinery technology, excellent process planning and optimization are essential for production process design. Paech's concern was primarily on wire production. Straightening process in wires is primarily intended to remove or modify curvature in the process material. Curvature may be induced by mechanical and thermal effects which may be considered as undesirable or desirable too. In the straightening process as a secondary effect, mechanical properties and residual stress potential are affected. Paech mentioned an important feature i.e. a straightener having rolls in two alternating rows, can either eliminate or effectively modify one dimensional curvature. Paech indicated that positioning of the straightening rolls with adjustability facility plays a significant role. This is due to that it causes alternate elastic/plastic deformation.

Like most machines, straightening machines are also made with certain specification based on certain design criteria to suit usually a range of input data. Therefore, at

market most manufacturers of straightening machines produce straighteners with specific straightening range which is usually determined by the roller spacings i.e. distance between straightening rolls or more technically beam length in case of cross-roll straighteners. Paech also indicated that straightening range has limiting values in terms of round bar dimensions. Range of cross-sectional dimension of process material is probably the first criterion that comes when going for a selection of straightening machines. As larger diameter process materials cannot be used in small diameter range machines due to machine capability restriction, similarly a straightening machine which suits for straightening of higher diameter process material is not useful for smaller diameter materials. This is evident from practical experiences of bar straightening industries.

In the process of straightening of bar, position of bending rolls plays an important part. Therefore, beside profile of rollers, deriving position of bending rolls is a significant factor. Yoshonori Sasaki et al. presented a schematic diagram in their publication in the year 2014 [27]. Sasaki has used the concept in glass frame which is made of titanium wire. There has been use of eight rolls of different sizes at varied position to give proper curvature of frames. Hence, position of rolls is quite significant in the straightening process. However, in the present scope of study we are interested not for adding curvature but for reducing or elimination of curvature to the extent possible.

In the year 2014, Kato et al. [28] stated in their publication that in order to improve quality of round bar products and productivity, researchers have looked into various aspects of cross-roll arrangements. Various equipment has been used in order to achieve improvement in quality and productivity. With the application of high-speed rotary straightener, it became a necessity for straighteners to correct the shape of round bar product, widening diameter range of straightening machine from 17 mm to 80mm which may be considered more than conventional one. Roll gap, rotational speed of top and bottom rolls and skew angles happen to be playing significant roles. Hence proper setting of these parameters is essential for quality and productivity [28].

Next year, in 2015 Ma et al. worked on neutral layer offset of bar [29]. Ma et al. indicated that to ensure the quality of bar produced, straightening is key process which

is the final finishing step. Their study reveals that with all likelihood original bending of bar may exist in any direction. Therefore, straightening process is particularly suitable for cross-roll straighteners. There are two main forms in cross-roll straighteners i.e. two-roll and multi-roll. Ma et al. stated that there have been several problems in existing multi-roll straightening machines. The significant problems are disability of full-length and full-continuous straightening. After straightening, a need arises for removal of head and end portion. Beside this, generally multi-roll straighteners cost high due to the complex structure and large volume. High precision of bar straightening cannot be realized in multi-roll straightener. Ma et al. specified that two-roll straighteners can achieve straightening with residual deflection in the range 0.1 – 0.5 mm/m. This however meets requirements of current accuracy in high precision bar. Two-roll straightening is certainly a complex elastic-plastic deformation process. Offset of neutral layer changes distribution of stresses in bar cross-section that affects bending moment ratio and calculated curvature of reverse bend which finally affects roll shape design accuracy. Ma et al. concluded that when bar is in the process of straightening, neutral layer offset is related with structural parameter of reverse bending radius and mechanical properties and of materials. With the decrease of reverse bending radius, neutral layer offset increases. It also increases with the increase of plastic deformation. However, offset being small usually it can be neglected for small degree of inflection and small diameter [29].

In another publication in the year 2019, Ma et al. [30] indicated that in bar straightening process it is very difficult to meet good surface quality and high straightness precision at the same time. Due to this problem, Ma et al. have put forward a roll shape design method of continuous variable curvature and studied the straightening process setting method. Shape of the straightening roll is connected tangentially by several arc segments of uniform curvature changes. From middle to both ends the curvature decreases uniformly [30].

Poltarak and Ferro proposed a continuous straightening formulation in the year 2019 in order to smooth the transition between the curved and straight sectors in a continuous

caster of metals. In the straightening sector, this is done by minimizing variation of curvature considering boundary conditions [31].

2.2.3 Group-2: Review on Measurement / Residual Stress Measurement

Measurement of any parameter gives a quantitative value which usually helps in portraying a realistic picture of any system. Measurement of required parameter is therefore is most sought aspect in our daily life. Be it a temperature of a heating system or a furnace in industry or a place at day time or night, it is a general concept to understand the gravity of the ambient situation. Measurement of weights or volumes or quantity in our daily life plays most significant roles as economy is connected with measurement value of a parameter. It is possible to discuss on the utility of measurement at length, however most people understand the significance of measurement as a natural system. In scientific community measurement is obviously a key feature. Many decisions in our daily life are based on measurement only.

Attempt of measurement of parameter in bar straightening was done as early as in 1966 by Olson and Bert [32]. One such parameter is residual stresses in bars. Since bar straightening undergo kinematic loading through reverse bending, there is an impact on residual stresses and residual curvatures on the bar. Olson & Bert analysed cylindrically orthotropic materials theoretically in bars and tubes after successive borings. Surface-strain data were measured based on equations for calculating residual stresses that led to determination of elastic constants [32].

Residual stresses are obviously present in the bars before straightening. It has been seen that many researchers have used Finite Element Model for evaluation of stresses. Earliest reference on this has been found in a publication by Schleinzer and Fischer in the year 2000 [1]. Although rails are bars with a specific section but like any bar straightening process, residual stresses are also present in rails. Rails as produced by hot rolling when brought to room temperature, rails are often seen not sufficiently straight enough and needs straightening process as terminal step in the production. Roller straightening is used as most common method. The cold rail is drawn through

and bent up and down by a series of rollers. After this process, the rails should not exceed a certain range of residual stresses, since tensile residual stresses near the surface can support the initiation and propagation of cracks. Schleinzer & Fischer considered merit of the model and accounts for the correct bending moments and forces. Simulated results have shown residual stress pattern.

In the year 2004, Talamani and Perlman [33] researched on to develop models to predict accurately residual stresses due to the roller straightening of railroad rails. Finite Element estimation of residual stresses in roller straightened rail was done. However, present work is limited to round bars only. The reference of rails has been brought in due to similarity of the process.

2.2.4 Group-3: Review on Modeling / Numerical Modelling and Simulation

A numerical model is said to be a mathematical model with a combination of a large number of mathematical equations to find an approximate solution to the underlying physical problem through computation of digital computers. These days, role of computer modelling in the research of industrial objects and physical objects and has increased significantly. So is the quality of programs for numerical modelling processes. A successful use in this is application of finite element modelling in the study of metal forming processes. This also allowed to study phenomena and improve technology [34].

It is pertinent to note that minimisation of residual pipe curvature is important. However, straightening machines are usually constrained by certain difficulties. These difficulties are setting up the process of straightening of round bars or pipes at the entry and exit from the edge rolls. There is a possibility of occurring of buckling defects at entrance and exit. Finite element is carried out in order to predict the stress-strain state and force modes of tube dressing which revealed the character of influence of design and technological parameters of the dressing process with symmetrical profiling of pairs of edge rolls. Computer modelling results show overlapping conditions of crossed

rolls which were established and allowed the reduction of residual curvature of the pipe as much as three times.

A well-known fact is that an industrial process for producing steel rods or tubes may be done with high accuracy but there will be some out-of-roundness and out-of-straightness which is practically unavoidable in rolled products. So, it becomes quite necessary to go through a straightening process after rolling is done. In the year 1989, Dvorkin & Medina developed and presented finite element model to analyze the straightening and rounding of steel tubes of low carbon in a 6-roll type straightening machine [35].

In the year 1992, Mischke and Jonca [36] worked on simulation of the roller straightening process. Mischke and Jonca stated that the roller straightening itself is a pretty complicated process. The process has three different periods of state:

- the entry period of the material to be straightened
- the period of stabilised process conditions and
- the period of exit of the material after straightening.

It is imperative that position of roller plays significant role in the process of straightening. Theoretically by controlling position of only roller, straightness of a product can be achieved. Therefore, there will be at least $n!$ combinations of position of n independent rollers positioning devices that would assure product straightness.

An optimum of the position of rollers and various parameters of straightening machine i.e. distance of rollers, roller diameters, etc. exits but there are many factors that affect the final outcome of straightening process.

In the year 1996, Macura & Petruska used a finite element system in ANSYS software by 3D simplified numerical model through the for the purpose of numerical analysis of plastic deformation of the bar [37]. Wu et al. (2000) also used a mathematical model on precision of straightened bar considering continuous alternating and reverse bending process of straightening involving iterative function in the treatment [38]. Their investigation analysed the mechanics of the straightening process in detail. Their analysis led to the development of theoretical model that enables predicting the precision of bars which are produced in given rolls based on a series reverse bending

process. This theoretical model was subsequently successfully applied to the industrial designs of rolls in two cross-roll straighteners.

In the year 2000, Wu et al. systematically studied on precision modelling of round bars that are produced in two cross-roll straightening process. Mathematical model was developed considering continuous straightening process with alternate bending and reverse bending process. Wu et al. indicated that in the process of bar straightening it is assumed that there is an initial curvature at any section of the bar subjected to reverse bending and spring-back of the bars in straightening assume that any section that has an initial curvature, finally bent to another curvature [37]. It is natural that during the straightening process, plastic bending will occur. Wu et al. have dealt with curvature change in bar straitening process. In particular in order to ease the study of bar straightening, the condition of equivalent curvature has been examined and mentioned that bar straightening is actually a process of a multiple plastic reverse bending. Through this plastic reverse bending, it makes different initial curvatures of a bar to converge to the same curvature.

Widmark et al. also worked in the year 2000 on roller levelling in order to straighten steel plates or strips. Plates or strips after final rolling undergo heat treatment process followed by cooling operations [39]. Widmark et al. indicated that although it is believed that metals are mere rigid or dead bodies, but actually it is not. A material can very well be considered as having endowed with its own life. It may result in to lead to complex processes which may be quite inherent. Considering the model for the Bauschinger effect during stress reversal, it can be stated that a metal may be considered as possessing a limited memory arising out of its earlier or past history of hardening. It can be further stated that mathematically the constitutive laws of stress-strain behavior for engineering assessment depend on the following:

(a) Deformation characteristics of the material

(b) Structural complexity and

(c) Loading spectrum.

Ideally, the above-mentioned constitutive models should take following into account:

- Stress-strain's non-linear response

- Material's repeated cyclic behavior viz. cyclic hardening and softening or steady-state response
- Kinematic hardening or softening due to change in plastic slope
- Isotropic hardening or softening due to change in yield stress
- Mean stress relaxation under strain control, or strain ratchet under stress control
- Bauschinger effect
- Other past deformation memory

Although, Widmark et al. work is related to straightening of plates, but the above points actually hold good for round bars also.

Since, straightening calls for reverse loading with a load somewhat acting in between of a simply supported beam like arrangement, both the end portions are obviously not subjected to similar load, hence reverse bending at both the ends is not effective. This is true for all kind of bars irrespective of types of cross sections. In the year 2005, Srimani et al. (2005) analysed end straightness of rail. Using ANSYS, process of straightening was simulated by application of finite element package. For the purpose of simulation of loadings on rail straightening, it is considered that the rollers move with respect to stationary rail. The rails are bent up and down alternatively during the process of straightening. Therefore, it can be said that in the form of a bi-linear stress-strain curve cyclic plastic behaviour has been assumed [40].

Next year in 2008, Mutrux et al. have studied about the cross-roll straightening process in a simulated situation using LS-Dyna [41]. Mutrux et al. highlighted similarity between cross-rolling straightening and three points bending. For the purpose of testing the ability of simulation process of straightening, a bent bar has been used as an input and compared the curvatures of input and output bars. Based on above, it has been stated that prediction of reduction of curvature can be done.

In straightening of bent rod, the plastic zone is also propagated along the helix as shown in Figure 2.3. Study indicated that by changing the helix angle α between rolls and bar (shown in Figure 2.4), bending can be controlled. It has been observed that more bending occurs with smaller helix angle α. Optimum helix angle will be

when degree of straightness is at its highest level. It is necessary that a economically viable transition speed is ensured. Mutrux et al. indicated that similitude between the stress state bending and in cross-roll straightening. Consequently, it has been inferred that the curvature of a bent bar can be significantly reduced by passing through the rolls [41].

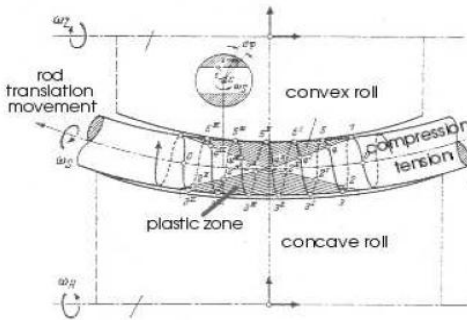

Figure 2.3 The Plastic Zone is Propagated along a Helix in the Bent Rod [41].

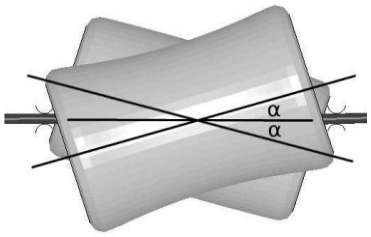

Figure 2.4 The Helix Angle α between the Rolls and the Bar

Mutrux et al. also defined that the straightness of the product through its curvature in the middle of a rod segment of 100 mm length. For references, a plane is fitted across the nodes taken on the middle axis of the rod. On this plane a parabola is fitted through various points in a two-dimensional coordinate system.

Local curvature of the round bar would correspond to the second derivative of the parabola. It is a delicate issue that for the fit adequate number of points to be taken since for few points numerical errors are more and obviously gain higher importance. However, it is quite normal that output round bar will have a three-dimensional curvature in general. If the nodes are farther from the fitted plane, it will possibly induce errors. Therefore, it is recommended that number of nodes to be considered depends on curvature which may be decided heuristically.

Numerical analysis is quite a preferred method using Finite Element Analysis Model by many researchers. In the year, Tian et al. [42] used finite element analysis software DEFORM-3D on pressure straightening process. The specific use was in seamless high pressure boiler tubes which are used in the manufacture of various boiler super-heater, re-heater etc. Tian et al. analysed different straightening forces through the model and

arrived for best straightening force. The straightening force has practical value and important scientific significance [42].

In 2010, Song et al. [43] also worked on straightening but of rail. FEM was used for the rail model which was meshed into large number of elements and nodes. Orthogonal experiment was done 50 times, residual stresses and straightness were tabulated. Song et al. has found that out of 15 rollers, 8^{th} roller has the most effect on residual stress in the bottom of rail which led to optimization of straightening plan [43].

Yi Yali and Jin Herong worked on triple-roller rotation blocking mechanism using mechanical model of bars for straightening in the year 2012 [44]. Their research discussed that most of minor diameter i.e. round bars with less than 12 mm diameter that were supplied from rolling industries as coiled stock. This coiled stock readily as such not straightway due to curvatures which however can be used easily after straightening process. It is generally known that traditional hub-straightening machine has somewhat quite low productivity which usually can't meet the production requitement. The device parallel-roll straightening gives better straightening speed. However, the bar is found to be rotating during straightening process. The straightening accuracy is low. Therefore, Yali and Herong [44] provided a roll-layout of equivalent curvature and a straightening mechanism with standstill-locking system. It also guarantees the straightening accuracy and increases straightening speed. The authors Yali and Herong [44] indicated that reinforced bar is pre-straightened in the straightening processes and its residual error reduces after the bar passes through the three-roll large deformation. In stand still mechanism the deformation occurred in the bar reaches equivalent curvature. The process also somewhat guarantees that the reinforced bar in the system does not rotate. The reinforced bar in the process gets straightened due to reverse bending through cyclic deformation in two orthogonal leveling flats as shown in Figure 2.5.

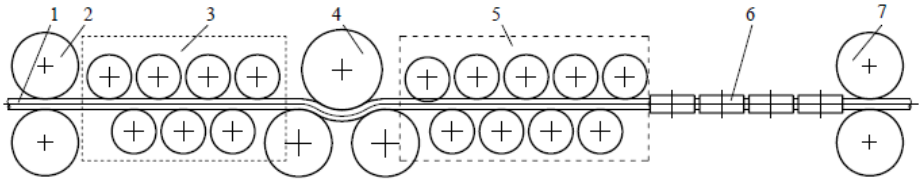

1-straightening bar; 2-pinch roll; 3-pre-straightening rolls; 4-three-roll large-deformation and standstill-locking rolls; 5-finish-straightening rolls; 6-vertical straightening rolls; 7-pull roll

Figure 2.5 Schematic Diagram of Straightening Rolls System [44]

Yali and Herong dealt substantially on rolls design of straightening system and have described that the bar is twisted since the wire rods are usually of minor diameter bar which adopts axial-feed wire coiling technology. To set-out before straightening, shelf of vertical coiled stock is used. As the torque is released in the bar and due to autorotation of the bar it causes the uncertainty of straightening plane which is basically osculating plane. Three-roll large-deformation technology has been used in the straightening processes. The bar can be kept rotating around its own axis. It ensures that two-dimensional straightening is fulfilled as the two orthogonal leveling planes don't change. Yali and Herong [44] also stated that the process guarantees straightening accuracy of the bar while curvature residual of the same bar reaches equivalent curvature.

In the same year 2012, Huang et al. [45] worked on numerical analysis using FEA model for small diameter seamless tube using straightening process of heavy caliber seamless steel tube with ten cross-roll. Their research indicated that seamless tube of heavy caliber was widely used in the field of general piping, oil and gas pipeline, in tubular structure, in pressure vessels, military usage etc. In the production process of heavy caliber seamless tube, the size and roundness tolerance are usually inevitable after rolling and heat treatment [45]. For the purpose of getting high-quality products, shape of geometry and tube size control plays a key role in the straightening process., Several studies were made aiming small-diameter seamless tube.

Huang et al. observed high technical difficulties in the study of about ten cross roll straightening process of heavy caliber seamless steel tube. The difficulties faced were

when considering the influence of the radial stiffness between the tube and straightening rollers. The difficulty was also with the non-linear elastic-plastic deformation on the cross-sectional rounding. There were problems in longitudinal straightening, and the contact state between the tube and straightening rollers which is also complex in nature. Huang et al. have used FEA model and indicated that for getting a quantitative analysis after straightening and selected sixty nodes with intervals of 6 degrees on the cross-section outline. Polar radius of the selected nodes was calculated and subtracted one by one to the ideal or the perfect radius.

Thereafter, these values of difference were plotted into a curve that would show the cross-sectional roundness tolerance. Huang et al. further stated that by using ten cross rollers straightening machine, roundness tolerance of the heavy caliber seamless tube could nearly be eliminated. Using process parameters, the geometry shape and the tube size may be controlled. From the simulation results, it reveals that equivalent stress and strains are distributed spirally. This coincides with motion form of the tube during the straightening process.

It has been found that straightening force emerged maximum at 2nd and 4th pair rollers. The amount of impact load was proportional to roundness tolerance. This may be considered in the straightening process for establishing designing of straightening machine.

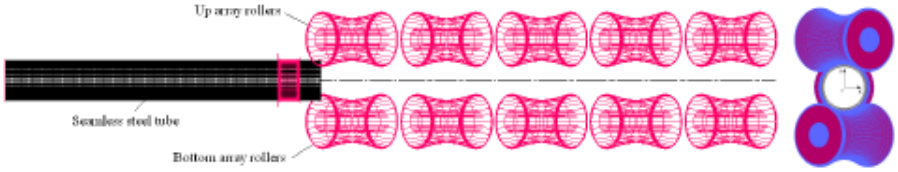

Figure 2.6 A Finite Element Model of Ten-Roller Straightening Process [45]

A quantitative analysis has shown that tolerance of roundness ranged initially from -3.5 mm to 3.5 mm got reduced to -0.5 mm to 0.5 mm range after straightening which ascertains that elimination of defect on roundness tolerance can be done greatly. It can be seen that several researchers have worked on numerical simulation of cross roll

straightening process. In 2012, Raab & Hynek [46] also worked on cyclic bending test of a tube in a six-roll straightener and used FEM model for the numerical simulation.

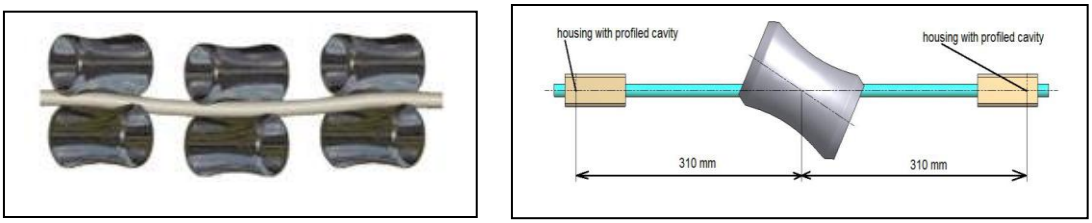

(a) (b)

Figure 2.7(a) Bending of a Tube Using Six-Roll Straightener with Concave Roller[46]

Figure 2.7(b) Substitutive Test on Bending with One Concave Roller [46]

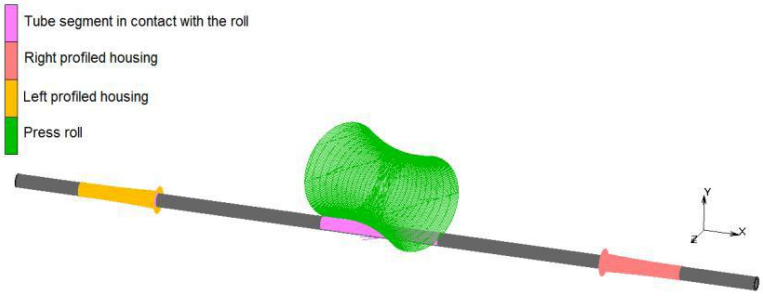

Figure 2.8 FEM Model for The Numerical Simulation of the Cyclic Bending Test [46]

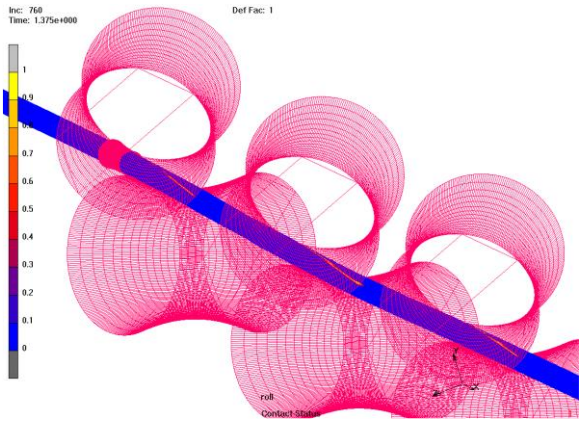

Figure 2.9 FEM Simulation with Properly Set-Up Between Tube and Cross Rolls During the Straightening Process [46]

Raab & Hynek found that it is extremely time consuming as well as unstable for numerical simulation of 3D straightening processes in a six-roll straightener, and therefore not widely used. While working out with products like small diameter metal ropes and cables it has been found by Khromov and Kawalla [47] in the year 2012 that one of the most vital quality factors is straightness.

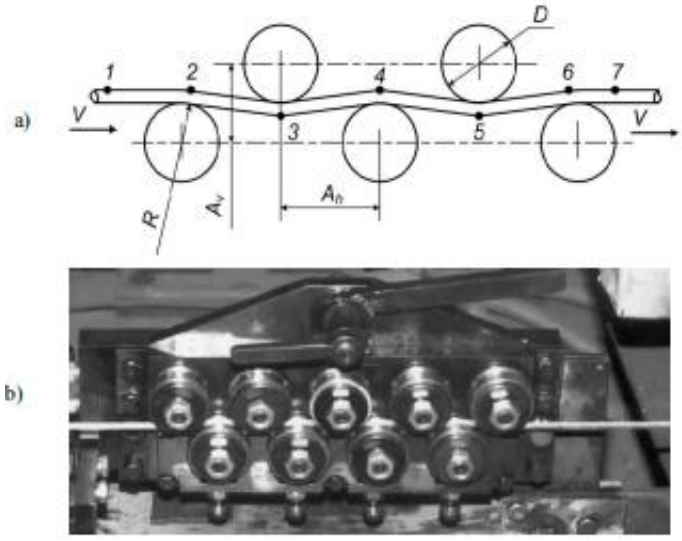

Figure 2.10(a) Diagrammatic Scheme of Straightening Process [47]

Figure 2.10(b) Pictorial View of Straightening Device for a Long-Length Product [47].

The fact is that in terms of mechanical implementation, straightening seems to be a simple process. However, it is actually quite difficult to find a thorough analysis of the process simulation related to steel wire rope production. Bar straightening is essentially a multiple alternating elastic-plastic bending of a workpiece of round bar on the rolls of a straightener. A kinematic scheme with sketch on the same is shown in Figure 2.10(a). A pictorial view of straightening device for a long-length product is shown in Figure 2.10(b) [47].

Khromov and Kawalla developed flow chart of general algorithm for computer simulation of a wire straightening process which includes several one-type cycles that

are executed consecutively [47]. The number of one-type cycles are equal to the number of alternating bending stages. They concluded that the technique developed by them provides a method for choosing number of bending cycles required at the stage of technological procedure designing which is on the basis of real material properties and simultaneously for visual evaluation of stress distribution in wire cross section at various different stages of deformation.

In the year 2012, Liu et al. presented mechanics model which is on the basis of curvature integration method [48]. Although most focus is on straightening of round bars and tubes, but this paper has dealt with levelling of plates. Plates are generally used for various engineering purposes as raw materials for fabrication industries. Liu et al. indicated that with the stringent demand of plate quality where perfection in flatness is desired with distribution of small internal stress, plates should have high level of improvement. As straightness is desired in round bars and tubes, in the similar manner flatness is desired for plates. It is quite a common phenomenon to have some number of defects as curl, gutter, middle waves and wedge waves which arise due to transformation on account of differential cooling, when not placed properly during transportation and distribution of non-uniform residual in-plane normal stress along the direction of thickness. The paper dealt with a new mechanics model of levelling process. Liu et al. conducted the plate levelling process by using a nine-roller leveler with an assumption of neglecting elastic behavior of rollers. The paper indicates substantially that residual stresses get reduced after levelling with change in distribution pattern. Figure below depicts this.

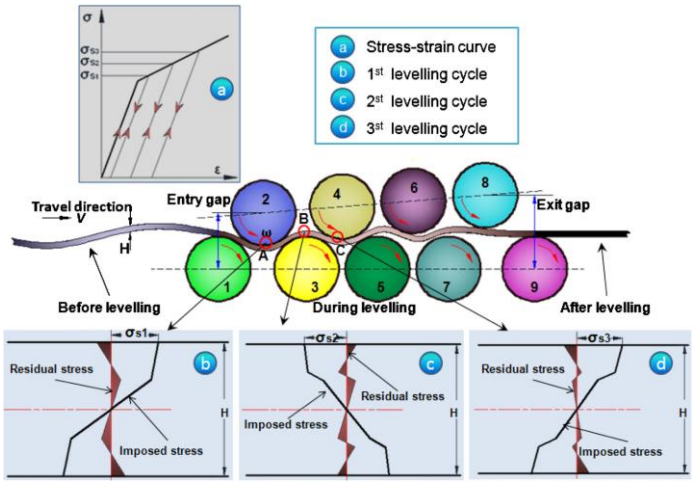

Figure 2.11 Stress Distribution During Levelling [48]

Petruska and Navrat (2013) dealt in the year 2013 with numerical analysis of cross roll straightening process of circular bars in a straightening machine of seven-roll. The curved bar progressing through laterally staggered rolls rotates initially along its axis. The loading is caused by a fluctuating bending moment beyond its elastic limit [49].

For efficient process simulation, a special computer program was developed on the basis of Euler scheme of material flow along the straightened bar, non-linear iterative solution of the elasto-plastic material behaviour and beam-type finite element. A reversed procedure was suggested by Petruska and Navrat starting from roll staggering. To evaluate curvatures, fast algorithm was used. Evaluation of curvatures done along the bending moments, roll loadings, leveled product, residual stress distribution and final curvature. In each material point, roll loadings included full stress/strain history. The program was made in MATLAB and was based on Finite Element Method. A simple beam element was used with Euler description of material flow thus through the levelling machine.

In the year 2014, Navrat & Petruska further worked in rails on numerical analysis of roller straightening process and repeated elasto-plastic bending problem was solved using MATLAB based on FEM algorithm [50]. In the same year Kaiser et al. [51] researched on simulation of process of roller straightening with respect to residual stresses and curvature trend. The thrust was primarily on the adjustment of roller. It is

quite essential that the rollers have to be adjusted to realise the desired curvature trend [51]. Analytically, the deflection line cannot be calculated because of elastic-plastic bending. Geometrical situation cannot be simply estimated around the contacting points but to be taken into account. Due to these facts, it however necessitates that using beam model, roller adjustment be determined. During analysis, in nine-roller configuration the beam passes and gets straightened. At the same time the program subroutine evaluates the peaks of the curvature trend in the plastic zones which is absolute maximum of the curvature. The rollers adjustment is done consecutively. The adjustment is done till defined trend is achieved. Several times the process is repeated since interaction of rollers and beam is complex in nature and at different positions its consequences for the curvature. Kaiser et al. used nine roller straightening model.

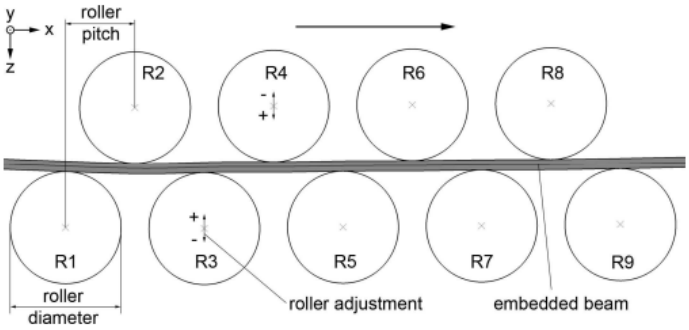

Figure 2.12 A Schematic Diagram for Plane Strain Model Straightening Process of Nine-Rollers for Detecting the Curvature with an Embedded Beam in the Middle of the Section [51]

In the year 2016, Petruska et al. indicated again that straightening of circular bars with cross roll straighteners is based on repeated elasto-plastic bending and simultaneously moving ahead with rotation about its longitudinal axis while the bar is through the straightening machine [52]. It is hereby stated that vertical intermeshing of rollers with angular deviation causes bending in a system of straightening rollers of a typical straightening machine.

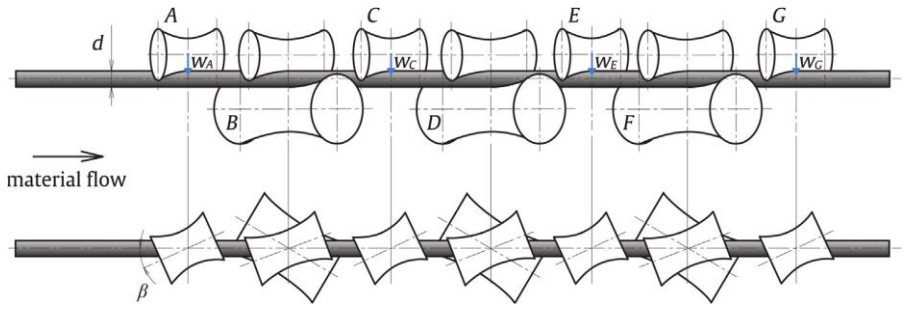

Figure 2.13 Schematic Diagram of a Typical Multi-Roller Straightening Machine [52]

Petruska et al. have indicated that optimal setting of parameters related to vertical intermeshing and angular deviation will likely to give best performance of the machine. Best performance will be for different material with input curvature or bar diameters. However, it is indeed to be reckoned as somewhat complicated engineering problem. It is apparent from Moment-Curvature relationship that the classical approach in bar straightening starts from known beam curvatures. Known beam curvature is applied as kinematic reversed forced loading to a rotating about axis along the length of the round bar or tube that has constant initial curvature. The materials are to be considered as ideally plastic. Petruska et al. indicated that when cyclic changes of curvature take place it results in the redistribution of stress, strain and bending moment over the bar cross section which have also been indicated by Tokunaga [6]. The central idea of the analysis is to establish a mathematical relationship between curvature and bending moment, but necessary intermeshing of rollers to reach the desired moment and curvature is actually difficult and can be considered as not so easy for evaluation. The problem has been dealt with curvature integration as described by Liu et al. [48] as already mentioned.

In the year 2016, Zhu et al. studied on modelling and simulation of straightening machine where the research work was focused on the process of straightening and its core technology about modelling and simulation thus making the process of straightening fully and realistically rendered on a digital computer through algorithm and program [53]. In the process users are thoroughly allowed to understand the

straightening machines and its working process. Straightening process flow was presented with brief description of straightening equipment [53].

In 2017, Yu et al. [54] used numerical simulation and analysed theoretically two-roller straightening mechanism. Two-roller straightening using cross-rolls for metal bars in the finishing process has an irreplaceable position. Yu et al. adopted mathematical induction and graphical method to analyze the deformation process of bar section. It was highlighted that ratio of plastic modulus to elastic modulus mainly determines the speed of curvature unification [54]. If the ratio of plastic modulus to elastic modulus is greater, then curvature uniformity speed is slower thus requiring higher bending time. There are many advantages in Two-roller straightening process. Straightening takes place in all-direction. Moreover, it is done with good surface quality and high precision. The straightening equipment or straightener is also very simple machine and may be considered as an irreplaceable one in the process of finishing of metal bars. Yu et al. stated that the theory is still not so mature in connection with roller shape design aspect and determination of process parameters. The operators rely mainly on their experience which ultimately lead to poor accuracy of straightening and low efficiency of straightening. The primary reason being that the technical foundation on theoretical basis and accumulated experiences are not sufficient. Therefore, it is quite necessary to understand deeply the mechanism involved in the process of two-roller straightening.

2.2.5 Group-4: Review on Control System on Straightening Process

Concern for control system is visible as early as 1984 from a publication by Hardt and Hale [55] where they mentioned that application of closed-loop control techniques to the bump forming process could improve significantly the efficiency of method of straightening, but the process will be a slow in comparison to continuous roll bending [55]. Hardt & Hale stated that the relationship between moment and curvature for the workpiece material as well as a relationship between relationship between the centre roll position and the maximum bending moment and loaded curvature must be known if open-loop or conventional predictive control is used on this process. From the

experimental data the authors have shown that steel material appears to get straightened for smaller deflections in comparison to aluminium.

Smooth operation of any system is possible only when control system is effective in any process. Springback control in metal forming and real-time identification was looked into by Chandra [56]. The concept of multi-step straightness control system (MSSC) was indicated by Kim and Chung in 2002 which is obviously considered as a very important feature in straightening process [57]. Kim and Chung developed a three-point bending and a multi-step straightening process (MSSP) for the MSSC.

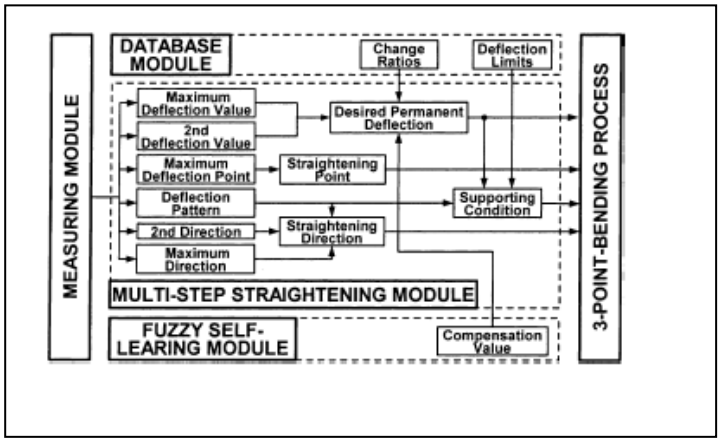

Figure 2.14 Schematic Diagram of Multi Step Straightening Process[57]

A schematic diagram of the MSSP can be used as a guideline. The pertinent point here is that fuzzy logic has been used. A schematic diagram has been shown in Figure 2.14 on the fuzzy self-learning control algorithm. A conclusion has been drawn that MSSC system straightens the shaft within the specified straightness tolerance. In order to compensate for straightness errors of deflected shafts, deflections values of some measuring points are measured and then loading the points. The work on MSSC may be considered of immense utility to researchers since it gives substantial indication as how to compensate for straightness errors of deflected shafts.

It is apparent that work on control system on straightening process will be considered important after MSSC. An application took place on longitudinally submerged arc welding of pipes. Zhao and Song [58] researched on control strategy of multi-point

bending one-off straightening process for longitudinally submerged arc welding (LSAW) pipes.

Needless to say, that straightness is certainly a significant indicator in measuring the quality of such pipes. Often a demand arises in the LSAW manufacturing process for straightening of the end of LSAW pipes. This is due to the fact that they fail to meet the overall straightness requirements. This is because of influence of such factors like forming equipment, welding thermal stress and overall straightness of the mould. Zhao and Song worked on the initial curvature distribution of a specific pipe LJ23-1 which is bell shape curve [58].

2.2.6 Group-5: Review on Stabilisation

Geometrical stability is a generally sought feature in any mechanical or production engineering. For obvious reason, shape is considered as an utmost important feature for any product. Therefore, assurance of geometrical stability is one of the most important problems in the production engineering. As already mentioned, geometrical stability is extremely desired feature not only in production engineering but also in automatic assembling.

A systematic study in the process of straightening of a bar was made by Wu et al. in the year 2000 using a two cross-roll straightener and concluded through their study on precision modelling that to improve the precision level of the bars produced it is essential to select a proper curvature of the gap of the rolls and a sufficient length of the contact region between rolls and bars. For the purpose of improvement of stability during the straightening operation, it is better to select as small radial tolerance [38].

Nastran & Kuzman [59] indicated that fluctuation of mechanical properties of input materials contributes a lot to the geometry of final product during cold forming. Final products' geometrical accuracy depends mainly on the quality aspect of final assembly lines and also semifinished products' accuracy level. Nastran and Kuzman discussed about stabilization of mechanical properties of wire through use of roller straightening

machine and stated, a note to be taken that it is quite possible to influence properties of material of the wire while passing through the rollers of straightening machine. From the experimental results, it is visible that reversed cyclic deformation has primary influence on reduction of tensile stress, yield stress, and also springback of the straightened product [59]. Nastran & Kuzman have shown that wire curvature varies with the position of rollers. The variation progressively gets reduced along the length. However, in this process there is only one precondition for such a stabilization system. The precondition is that for the wire bent products in the straightening machine there should be sufficient number of rollers.

In the year 2006, Aron discussed on certain elastic annular cylindrical sectors and its plane-strain straightening deformation which have been in conjunction with the closely related deformation of uniaxial extension of elastic rectangular strips [60]. A case was chosen of mixed boundary conditions i.e. of traction and place. The discussion was on sufficient and necessary conditions for the infinitesimal stability of these deformations. Aron has provided several illustrative examples and analysis. The results based on the relationship of an isotropic elastic solid were employed for obtaining general strain-energy function for which certain deformations in this class are possible in the absence of any body forces. An analogy with the case of a uniaxial extension, some deformations are very small i.e. infinitely small and stable provided stress is non-negative. Also, when stress is regarded as a function of the material radial coordinate. Firstly, Aron has shown that the stability conditions are sufficient for the infinitesimal stability of all deformations in this class. Secondly, these deformations satisfy dead-load mixed boundary conditions of place and tractions. Further, using the results for obtaining necessary conditions for stability has been done along with extensive mathematical formulation.

2.2.7 Group-6: Review on Statistical Consideration

In the year 2013, Mishra et al. [61] made an attempt to consider statistical approach on the roundness of cylindrical bar by the application of Taguchi method. In the present

machine era, our life somewhat depends on machines, more specifically machines with rotating parts. However, only few of the researchers studied the effect of machining parameters on the roundness of the turned part [61]. Mishra et al. worked on Experimental Design and worked on mean value of roundness. Mishra et al. also used S/N ratio in L9 Orthogonal array. This work indicated that statistics can be used for optimization of machining parameters. Although lot of research has been done in various areas pertaining to bar straightening but unfortunately research papers in statistical consideration are barely available in the process of bar straightening. Roundness as a general measure using X-Bar and R Charts is very usual in any manufacturing industry since products are to be produced within acceptable quality level (AQL). Producing long straight bar is certainly difficult particularly when large quantities of round bars need to be handled through machineries for loading, transportation, unloading and stacking. It has been seen that strictly statistical approach in respect of straightening of round bars has not been considered earlier by any researchers. In general bar straightening happens to be a process prior to actual manufacturing process in many occasions.

2.3 Status of Works in India

From the various research work, it can be understood easily that although the subject of bar straightening was somewhat originated in the United Kingdom which is reflected in a publication by Kemshall [5] in the year 1974 that Bronx Engineering Company, Lye, Stourbridge (Worcs), United Kingdom and Joshua Bigwood & Sonsat Wolverhampton, UK have been pioneers in this field and worked on the advancement of straightening machine design, but some work have been done in India also. The theoretical development has taken place in India and Das Talukder et al. [14,15,16] were major contributors in this. Beside developing mechanics of bar straightening various types of rolls were suggested too. Significance of the equations developed so far helped other researchers to look into deeply on various aspects including roll design and positions of rolls and its consequences on straightening of round bars.

Importance of position of rolls has been reflected by Ashvin S. Patel & J.M. Prajapati in their publication in the year 2011 [62]. Although, their focus was on wire straightening, but the concepts apply very much in the process of general bar straightening. Wire may be considered as bar of low diameter and usually available in coiled form for easy storage and transportation as mentioned earlier. Wires and wire like rods are available both in ferrous and non-ferrous materials. Non-ferrous wires are mostly used as cable for usage in electrical and electronic applications. Patel & Prajapati considered that in the process of straightening, there is apparent removal or elimination of stresses induced into the material which is to be straightened during its manufacturing due to force and torque related influences. This applies to tube straightening, cable straightening, wire straightening and rotary arbor straightening of wire. In this process of straightening of wire there is a series of rolls. These rolls are at offset which causes bending of the wire beyond the elastic limit a number of times. As the wire runs through, the bending in the wire takes place in two or more planes. The rolls are as such adjustable in the machine set up. The adjustments of rolls are done by the operators, hence the straightness so obtained depends upon operator's skill. The method is restricted to shaped wires in general for sections such as flats, squares and hexagons except for minor straightening of round wire for removing coil bow before further forming. In case of rotary straightened arbor, it rotates around the stock and imparts bending stresses in an overlapping helical pattern. This causes achieving a high degree of straightness into inbound stock. The principle is that straight wire is produced due to beam affect that moves around and along the wire and at the same time. Various factors like speeds, feeds and the condition of straightening dies control straightness. The rotary arbor is friction device with the die material which is compatible with the wire. To support the load of bending, the contour presents enough area. To give the correct beam effect and bending stress to produce a straight product, the center distance between the straightened dies must be within specific limits for a particular wire diameter. Patel & Prajapati described various methods for straightening process.

In the year 2016, Biju et al. worked on commercial steel bars. The project work was on design and analysis of straightening mechanism [63]. The work particularly focused on

developing a technique for straightening in an economic manner. Round bars keep rotating with a helix angle in the process of bar straightening which actually causes the bar to proceed inside the cross-rollers. Biju et al. highlighted that the bar rotates during the straightening processes and straightening speed raises greatly in the parallel-roll straightening device. In this case, straightening accuracy is too low. Biju et al. used the concept of equivalent curvature and standstill-locking mechanism. Considering low straightening accuracy, a roll-layout of equivalent curvature standstill-locking cum bidirectional straightening system has been provided which can straighten these round bars with better accuracy.

Straightness of commercially produced bars were analyzed by Roy & Pal [4] in an experimental set up for four different materials of approximately same diameter. Surface plots generated from the data of these four bars indicate that over the length segments, straightness is compromised and curvatures exist at various sections. For many applications, the roundness measurement is certainly of critical importance. Needless to say, that circular cross-section may be considered as one fundamental form amongst engineering components. Circular forms arise in many applications particularly in bearing surface. Circular forms arise in rotating shafts and ball bearings too. At this point it can be stated that in case of a shaft and rotational bearing whose components are not sufficiently and accurately round will likely to produce noise possibly due to vibration and possibility occurs for premature failure. Therefore, an accurate roundness is to be considered as vital to ensure proper functioning of such rotating parts. Roy and Pal [12] highlighted that the measurement of roundness is an extremely important assessment. Roundness of commercially available bars without any machining were assessed and checked for the roundness variations at various desired sections within the bar length.

While the round bar is progressing ahead between the straightening rolls, the round bar also rotates about its own axis. During the straightening process, at different instants, the plane of loading of initial curvature also makes different angles. For simplicity, considering a round bar with uniform initial curvature, the change of the curve i.e. a plot of curvature-resisting moment can be drawn. In the straightening machine, the rolls

are staggered in such a manner that whilst progressing through the rolls, the maximum loading-moment developed and corresponding change in curvature can be reckoned parametrically. It can be stated here that the change in residual curvature is likely to be equal and opposite to the above-mentioned initial curvature. A probabilistic approach has also been considered on theoretical basis by Roy et al. in 2019 [7] as probability of final curvatures at any given length segments. A more detailed theoretical work on probabilistic approach has been considered later in 2022 by Roy & Pal on the estimation of residual curvature of round bars in straightening process [9].

2.4. Research Gap

It is obvious that like most research areas, researches in bar straightening also have certain gaps. The classification as done in the beginning of the chapter shows clearly that most research work has been done with certain specific goals. Initial researches were more on development of the theoretical background for straightening process which was followed by measurement of residual stresses. Moment-curvature relationship was an important criterion in the development of theoretical background. Later, research thrust was given in modelling or numerical modelling and simulation using software like ANSYS, LS-DYNA, MATLAB etc. Researches were carried out on optimization and stabilization also. While going through individual publications, certain significant features have been noticed along with research gaps and presented in tabular form in Table 2.1 for publications from year 2000 onward.

Table 2.1. Literature Survey on Bar Straightening since year 2000 onward

SN	Literature Review on Bar Straightening	Research area and problem addressed	Method and Tools used	Significant Features	Research gap
1	Wu et al. (2000) [38]	Precision modelling of round bars	Theoretical formulation and experimental approach	Geometry of axis of bar in straightening	-Statistical aspect and Modelling not addressed

2	Widmark et al. (2000) [39]	Straightness of sheet	Mechanical approach	Simulation of straightening operation	Roundness and statistical aspects not featured
3	Schleinzer and Fischer (2000) [1]	Residual stresses in new rails	FEM and simulation	Model accounts for correct bending moments and forces.	Round bars not addressed.
4	Marcus Paech (2001) [25]	Wire Straightening process	Positioning of peripherals and Fuzzy logic	-Analysis of straightened material -Fuzzy system for necessary number of rolls	Statistical aspects not covered
5	Kim and Chung (2002) [57]	Shaft straightening	Multi step straightening process	-Multi step straightening control (MSSC) -Fuzzy Logic	-do-
6	Nastran & Kuzman (2002) [59]	Wire straightening	Numerical simulation, MATLAB	-Stabilisation of mechanical properties -curvature variation with roller positions	-do-
7	Talamani et al. (2004) [33]	Residual stresses in rails	3D & FEM	Prediction of residual stresses in rails	-do-
8	Srimani et al. (2005) [40]	End Straightness of rail	Finite Element Method and ANSYS	Simulated model of straightening process	-do-
9	Marcos-Barcena et al. (2005) [18]	Roundness of precision elements Aluminum-Copper alloyed cylindrical bars.	Experimental set up for measurement of roundness	- Surface plot generated with roundness as response variable. -Result shows improved roundness at lower cutting speed.	Statistical measure on overall straightness not addressed.
10	Aron (2006) [60]	Stability conditions of deformations	Theoretical analysis	Equations for sufficient and necessary conditions.	Statistical aspects not covered
11	Kalos et al. (2007) [19]	Control of roundness. Feed and roundness were studied.	Artificial Neural Network andMATLAB	- Algorithm developed. - 3D plot for prediction of roundness	Straightness not addressed

12	Marcus Paech (2008) [26]	Automation in straightening	Model for Synchronous positioning of rolls	Use of advanced semi-automatic machine. Position	Statistical aspect not addressed
13	Mutrux et al. (2008) [41]	Simulation of straightening process	LS-DYNA	Bending can be controlled by changing helix angle.	-do-
14	Lu Hong et al. (2009) [20]	Improvement on straightness of beam	FEM & Simulation. MATLAB & ANSYS.	Stroke Deflection model	Roundness not addressed.
15	Tian et al. (2010) [42]	Numerical analysis and simulation for straightening force	FEM, DEFORM-3D software	Best straightening force and curvature is determined	Statistical aspect not addressed
16	Song et al. (2010) [43]	Straightening of rail	FEM and optimisation. Orthogonal experiment done.	Statistical aspects used only on rails	Round bars not addressed
17	Yali & Herong (2012) [44]	Straightening of bars	FEM and Standstill Locking mechanism	Roll-layout of equivalent curvature and straightening mechanism.	Statistical aspect not addressed
18	Huang et al. (2012) [45]	Simulation analysis of straightening	FEM on platform MSC.MARC	-Maximum straightening force -Simulation of equivalent stress and strain.	-do-
19	Raab & Hynek (2012) [46]	Numerical simulation of straightening process and cyclic bending	FEM model	Extremely time consuming and unstable for numerical simulation of 3D processes.	-do-
20	Khromov & Kawalla (2012) [47]	Simulation of wire straightening	Graphical Stress Analysis using MathCad software.	General algorithm for computer simulation of wire straightening process	Statistical aspect not addressed
21	Liu et al. (2012) [48]	Straightening of plate	FEM simulation in MSC. Marc	Curvature integration method	Round bars not considered
22	Mishra et al. (2013) [61]	Optimisation of roundness	Taguchi method	Experimental Design for S/N in Orthogonal array	Straightness not addressed.
23	Petruska & Navrat (2013) [49]	Straightening of circular bars	FEM, Simulation & MATLAB	Fast algorithm for curvature evaluation	Statistical aspects not considered

24	Petruska & Navrat (2014) [50]	Roller straightening of Rails	FEM & MATLAB	Numerical analysis of roller straightening process	-do-
25	Sasaki et al. (2014) [27]	Deriving positions of rolls for bending of Titanium wire	Bending machinery	Roll positions	-do-
26	Kato et al. (2014) [28]	Straightening	Cross-roll straighteners	Roll skew angle and roll gap	-do-
27	Kaiser et al. (2014) [51]	Roller straightening process, Residual stresses and curvature trend	Simulation	Roller adjustment	-do-
28	Zhao & Song (2014) [58]	Theoretical analysis in Straightening system	Application on Longitudinally Submerged Arc Welding (LSAW) pipes.	-Multi-point bending - Initial curvature distribution of a specific pipe LJ23-1 which is bell shape curve.	-do-
29	Kume et al. (2015) [21]	Straightness evaluation	Inclinometers with a pair of offset bars	Comparative plots generated showing Inclinometer, Laser and Telescope.	Roundness not addressed. Statistical approach not considered
30	Ma et al. (2015) [29]	Neutral layer offset	Theoretical approach and FEM& Simulation	Simulation of neutral axis	Statistical consideration not addressed
31	Petruska et al. (2016) [52]	Straightening of circular bars and simulation	MATLAB	Vertical intermeshing of rollers with angular deviation	-do-
32	Biju et al. (2016) [63]	Straightening of bar	Standstill locking mechanism	Equivalent curvature	-do-
33	Zhu et al. (2016) [53]	Straightening machine	Modelling and Simulation	Algorithm and program for straightening process	-do-
34	Yu et al. (2017) [64]	Straightening process mechanism	Theoretical analysis &FEM	Numerical simulation	-do-
35	Tangjitsitcharoen & Chanthana (2018) [22]	In-process prediction of roundness in CNC machine	Surface Plot on roundness	Prediction on roundness	Straightness not addressed

36	Ma et al. (2019) [30]	Surface quality and high straightness precision	Design method of continuous curvature and FEM	Application of variable curvature, surface stress profile	Statistical aspect not addressed
37	Poltarak & Ferro (2019) [31]	Straightening process	Theoretical analysis	Continuous straightening with minimum curvature variation	-do-

Several researches have been done using FEM through software to assess deformations and stresses in the bar and rollers as well. Modelling and simulation have been a preferred area of many researchers which is evident from number of publications. While dealing with control systems researches emerged the necessity of multi-step straightening process. The use of Fuzzy logic has also been seen while working for multi-step straightening control. However, a glaring gap has been noticed in the area of statistical consideration. Mishra et al. initiated research work in 2013 on optimization of roundness only using Taguchi method but straightness was not addressed. Hence, for all practical purpose it can be stated that so far statistical consideration in bar straightening has not been looked into. Therefore, it is essentially a significant research gap in this area.

2.5 Aim of the Present Work

The present research work was therefore focused to fill up this particular gap so as to enrich the bar straightening research area in the application of statistics into it which will possibly reap scientific and industrial benefits in terms of production of bars. The research in statistical consideration and experimental & numerical approach for deformation analysis of both normal and straightened metal bars will possibly open up a new front where researchers may now look into it to further augment various process parameters. Therefore, in the present investigation following objectives have been aimed to fulfil the research gap to the extent possible with their scopes.

1. **To develop the orientation of probability and statistics in the process of straightening. For this equations of probability of final residual bar curvatures after straightening considering residual curvature as a continuous variable are formulated.**
2. **To determine a criterion of maximum permissible Helix Angle in two cross-roll straightening machine to keep a balance between the process speed and helix angle.**
3. **To develop theoretical framework by using two factor factorial design using analysis of variance (ANOVA), one factor being the helix angle. This may help to take a practical decision for choosing appropriate roller diameter and helix angle combination.**
4. **To study the circularity or roundness of commercially available bars along with features of straightness using various statistical tools. This may help to take decision on the quality aspect of commercially available round bars.**
5. **To study the deformation analysis of round metal bars of different size and materials before and after straightening process with single pass. This will help to take practical decision of requirement of straightening process and if required then more than single pass may be necessary for commercially acceptable product.**
6. **To conduct SPC analysis of commercially available round bars for both before and after straightening to see requirement of straightening process.**
7. **To conduct finite element analysis of round bars both before and after straightening process to validate the results obtained from SPC analyses.**
8. **To identify an appropriate machine learning regression model which would help in precise prediction of straightness of commercially available round bars after single pass of two cross-roll straightening process.**

2.6. Research Methodology

Based on the objectives and scope of work, certain methodologies have been considered for analysis of bar straightening process. Theoretical work has been done to see the significance of helix angle in the bar straightening process. A statistical approach was made with Two Factorial Design on residual curvatures where one factor was helix angle and the other factor was roller diameter.

Since round bars are produced in rolling mills, there are deformations at various sections of the bars which needed to be studied for an overall understanding of commercially available round bars. An experimental set up was made therefore to understand the deformations in these round bars. It has been kept in mind that the process and measurement system should be simple enough to make observation and data recording easy. The experimental set up primarily consisted of an arrangement of using V-Blocks on a small structural arrangement and dial gauge was placed on the sample bars with a mounting arrangement. Use of electronic and optical gadget has been avoided due to non-availability and higher cost.

Observations of the deformations at various sections of the bars along the length were measured and data recorded systematically for various angular positions circumferentially at the interval of about 15^{o} in small length segments of the sample round bars. Initial observations were carried out on four different sizes and four different types of materials before straightening and the sample bars were then passed through two cross-roll bar straightening process. Similar observations were made for straightened bars through dial gauge measurements. These experimental data sets were analysed using various statistical methods which have been validated using finite element techniques. Also, predictive modelling of deformation of straightened bars have been conducted by using different machine learning regression algorithms to obtain accurate forecasting of straightness of metal bars. Figure 2.15 illustrates the framework of proposed methodology followed in the present research work.

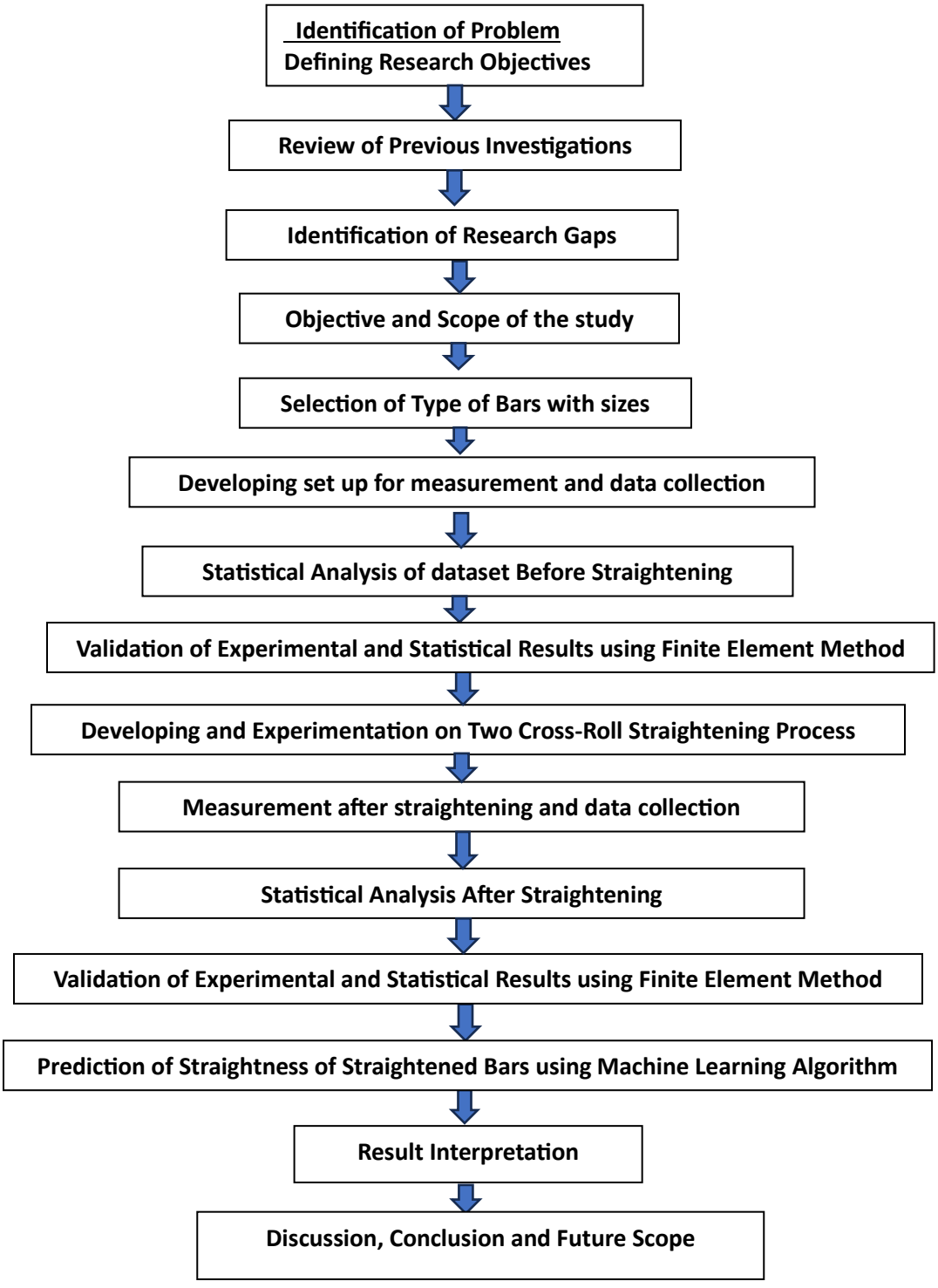

Figure 2.15 Framework of Proposed Methodology

2.7 Summary

To summarize the previous work in this area or literature review, it can be stated that several researchers have worked in this area and contributed in various forms. Although, at initial stages, thrust was primarily on the development of theoretical aspects but over the time other areas were looked into. Measurement of residual stresses were considered important. Substantial work has been done in numerical modelling and simulation. Several authors contributed in numerical modelling and simulation. The usage of finite element method has found an important place which enabled a clear insight of the deformation and stress levels along with residual curvatures. Control system is an important feature in any engineering field. Multi-step control system has opened up an engineering application for precise results. Consequently, optimization and stabilization were looked into by researchers. At present bar straightening may be considered as an industrial application-based engineering field where final product will have precision and possibly could be used directly as input material for the production of various final products viz. spindles, bolts, studs, shafts, linkages, tie rods, support rollers in paper and printing industries, long screws, pins etc. Since straight round bars are a general requirement in many industries, all the researchers mainly focused into developing the process either on theoretical aspects or improvement in required machine tools to enable precision-based engineering output.

Research work on straightening of round metal bars has been started in the early part of twentieth century. A number of countries, including America, Japan, United Kingdom, China etc. took part in the research of bar straightening. In India theoretical and experimental work has been done and more researches are in progress. The main reason that has encouraged this research work in India particularly at Jadavpur University is due to availability of bar straightening industries and manufacturers of this type of machines in and around the city of Kolkata. Therefore, it has been considered as a possible emerging area which may have direct industrial and commercial benefits. Many small scale industries in and around Kolkata and other

cities are supplying round bars after straightening operation. Small size industries are often engaged as ancillary to medium or large-scale industries with this process and supply straight bars in bulk quantity to medium and large size industries. For small diameter round bar straightening operation, small scale industries can cater the need conveniently with a smaller set up. However, for larger diameter round bars, there is a requirement of heavy-duty straightening machines. For industries both roundness and straightness of round bars is a general concern and requirement for obvious reasons i.e. straight bars are required as input material for manufacturing of various straight bar related items. Statistical consideration as well as circumferential deformation study before and after straightening of bars is therefore very significant from industrial production point of view.

CHAPTER – 3

THEORETICAL ASPECTS OF STRAIGHTENING

3.1 Introduction

Theoretical aspects are an important and essential part of the entire work since these forms a basis of working on the subject of bar straightening. Theoretical aspect deals with certain basics of theory of elasticity and plasticity. Beside discussion on basics there is some detailing on the mechanics of bar straightening. Statistical consideration is also dealt to the required extent which is necessary for this research work. This is quite necessary for a clear understanding of bar straightening process. Certain assumptions have been taken into account based on previous researches in this area. Stress-strain relationship and moment-curvature relationship is primary consideration to go ahead on the theoretical aspects of bar straightening. Since, the process involves repeated plastic deformation and cyclic loading and unloading, Bauschinger effect is considered for an insight in the process. A detailed discussion on Bauschinger effect will appear in subsequent chapter at a relevant place.

A probabilistic approach has been taken into consideration for evaluation of residual mean curvature of bar. Primarily, normal distribution has been considered for estimation of residual curvatures to compare different groups of data and make estimates about data population using different types of metal bars of different materials. With the evaluation of mean residual curvature, variance can also be evaluated using relevant equations and standard deviation. Statistical aspect of bar straightening using analysis of variance (ANOVA) has been dealt to some extent for choosing the significant factors related with straightening process.

Experimental design is an integral part of statistical consideration. Factorial design is therefore used in the present work. Based on the gap of earlier research work on bar straightening, it has been seen that two factorial design can be successfully

implemented in the area of bar straightening. Use of factorial design in statistical analysis helps in decision making by virtue of test hypothesis for quality criterion of residual curvatures in acceptable range.

In cross-roll arrangement, diameter of rollers and helix angle of the rollers play a significant role. However, various diameters of rollers and helix angles can be chosen for straightening purpose. Through experimental design it can be logically decided through ANOVA based on F-Test results. Hence, a theoretical approach has been attempted on two factorial designs on residual curvature to enable an insight for justification of various factors of bar straightening process.

It is pertinent to see how one of the factors i.e. Helix Angle contributes in straightening process in cross-roll arrangement. The effective bending moment at the bar section will vary continuously due to rotation of bar. Effective bending moment on the bar will be increased progressively and will attain a maximum position then again will decrease to minimum and again will increase in next cycle. The throughput speed of the bar can be controlled by choosing a helix angle of the rollers.

A brief study of the straightening process is presented here. The detailed analysis presented here are mainly based on the experimental and numerical methodology applied on cross-roll straightening process with the measurement of deformation of different types of round metal bars available in the commercial market.

This chapter deals with straightening aspect of bars where theoretical background has been discussed with an overview of the process. The basics of straightness and tolerance limits as referred by Geometric Dimensioning and Tolerancing (GD&T) has been discussed. The working principle and mechanics of straightening process have been dealt sufficiently. Bauschinger effect and residual stresses are part of analysis of bar straightening process which have been reflected in the chapter. Moment-curvature relationship being most significant aspect of bar straightening process has been discussed thoroughly. Probabilistic approach as well as statistical approach on residual curvature due to kinematic bending has been included briefly. The significant part of this chapter is discussion on various types of straighteners and mathematical approach in mechanics of straightening. Effect of Helix Angle in the process of bar straightening

has been shown with the help of mathematical model. The criterion for setting helix angle has been evaluated which is actually a key finding of the work on bar straightening in this dissertation. The chapter also includes a brief discussion on applications of straightening in various machines.

3.2 Straightening of Bars

3.2.1 Overview of the Straightening processes

Bar straightening deals with a process of reverse kinematic bending. A simply supported beam or bar have supports at both ends while the load at centre causes bending of the bar. After the bending, the bent bar has a different shape. To make the bar straight again it requires a reverse process i.e. loading of the bar at same centre on the bent portion in reverse direction while the supports at both ends remain same. Figure 3.1 (a-d) explains the process in brief. In case of Air-bend Reeling machine, two horns of concave roller act as a simply supported system when a bar is inside and the convex roller exerts a concentrated load at mid span of the bar which causes reverse bending i.e. straightening of the bar occurs through cross-roll arrangement [65].

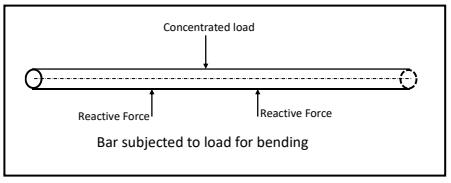

(a) Bar before Bending with Concentrated Load at Centre

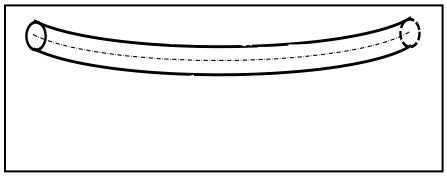

(b) Bar after Bending Occurred

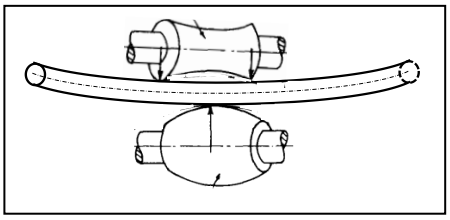

(c) Initiation of Reverse Kinematic Bending

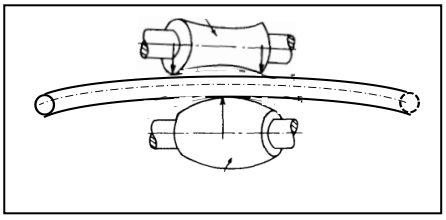

(d) Reverse Bending Occurred beyond Yield Point for Straightening

Figure 3.1 Schematic Diagram of Various Stages of Bending and Reverse Kinematic Bending of a Round Bar.

Although bar straightening through air-bend reeling machine can be done, however, there are other types of roller arrangements available for bar straightening. In air-bend reeling system a point load acts at centre by the convex roller while in six-roll straightening system a line contact takes place. For the purpose of bar straightening, various types of rolls can be used. Each type of rolls has specific advantages over other type. Selection of rolls are largely based on actual technical requirement. The process in its basics involve plastic deformation since a permanent deformation is required but in reverse direction. It will be quite relevant to deal with certain basics of plastic deformation as reverse bending ultimately requires plastic deformation. A brief discussion on Bauschinger effect is pertinent here as straightening often involves repeated kinematic reverse bending.

In light of material science, a metal may be regarded as macroscopically homogeneous and isotropic when the small crystal grains forming the aggregate are distributed with random orientations. As a result of plastic deformation, the crystallographic directions gradually rotate towards a common axis, producing a preferred orientation. An initially isotropic material thereby becomes anisotropic, and its mechanical properties vary with direction [3].

The present case of bar straightening actually involves that a bent bar where plastic deformation has already occurred as a permanent feature now needs to be straightened. Technically this is possible by reverse bending and practically also same process is done. Straightening process requires reverse bending where material will be loaded kinematically through rollers in the straightening machine. For the purpose of straightening, bars are subjected to elasto-plastic deformations. During the process bar undergoes alternate bending under high magnitude of loads [15]. Tokunaga (1961) indicated that two zones surround the centre of the bar where it retains initial deformations and no plastic deformation takes place [6]. Residual stress distribution of bar section and zones left by the tensile and compressive residual stresses respectively surround bar centre which don't undergo any plastic deformation. Residual stresses of the plastic zone build up residual moment to the centre of the bar.

In the process of straightening as the bar advances along the length during revolution, the bending moment arising out of residual stresses rotates accordingly as sections change between pitch lengths. The bar is straightened using rotary straightener and it may be considered as spring coil form having very small coil diameter and pitch length. It can be postulated that bar is straightened more exactly with smaller residual stress, when rotary straightener is used by a method which applies more reverse bending beyond yield point so that final curvature at that segment is reduced. There is an involvement of multiple rotary plastic bending at the period of the reducing bending moment.

3.2.2 Straightness

The most important single factor in achieving quality and reliability in the service of any product is dimension control, and demand for the qualitative aspect of a product is increasing day by day with emphasis on the geometric integrity. Straightness, flatness, squareness, parallelism, roundness and cylindricity are important terms used to specify the quality of a product under consideration [66].

Perfect straightness is one of the important geometrical parameters of many of the surfaces on an object/part of machine in order to serve its intended function. It is very easy to define a straight line as the shortest distance between two lines. But it is very difficult to define straightness exactly. A ray of light, though it is affected by environmental conditions (temperature, pressure and humidity in the air), for general purposes is straight. For a small area, spirit level is considered for the measurement of straightness and flatness. In a broader sense, straightness can be defined as one of the qualitative representations of a surface in terms of variations of its geometry from a predefined straight line or true mean line. A line or surface is said to be straight if the deviation of the distance of the points from two planes perpendicular to each other and parallel to the general direction of the line remains within a specific tolerance limit [66]. The value of tolerance limit varies from case to case depending on actual requirement. As already indicated that industrially produced bars from rolling mills are seldom straight, it is therefore a general requirement to have a measure of straightness

of these bars. Straightness, from industrial perspective, is considered as a control that requires axes or surface to follow a straight line within a given tolerance. This can be applied in two- or three-dimensional systems [67].

Straightness is generally applied on a 'per unit length' basis as zone of tolerance. Straightness in a simple form can be explained as below. Considering the diagram Figure 3.2 below where all points along the measured line if falls within two bounding lines, then the component is passed from quality point of view. If any of the points falls outside the two lines then from quality check it is failed, no matter how the lines are adjusted keeping the separation fixed.

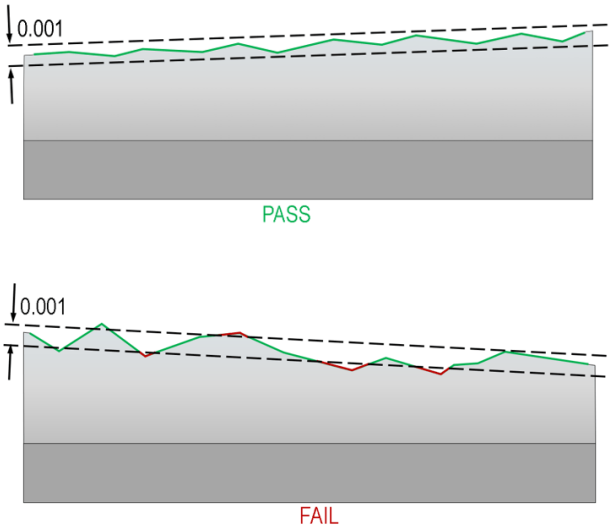

Figure 3.2 Diagram Showing Products where Straightness can be Accepted or Rejected based on Tolerance and Irregularities [67].

It may be noted here that "highest" and "lowest" points (the greatest deviations from a straight line will ultimately control the reported straightness value, and one or two single outlier points in a measurement can determine if a part passes or fails). It is essential that statistically all the highest and lowest points between the tolerance limits remain within the boundaries. As an example, in above mentioned Figure 3.2, tolerance limit is shown as 0.001, a ⏥ 0.001 measure of per unit length which means that in this case it is 1-mm tolerance over a 1000-mm length. This value is certainly not an absolute value for all products. Geometric Dimensioning and Tolerancing (GD&T)

uses the symbol for straightness tolerance [67]. The tolerance numerical value is preceded by straightness symbol. The present perspective is focussed on straightening of industrially produced bars. Degree of straightness in industrially produced commercial bars is a major concern in bar straightening industries.

Kemshall (1974) stated that commercially produced bars can achieve level of straightness ranging from 1 in 750 to 1 in 5000. Degree of straightness is specified as deviation from centerline over a given length or simply the length divided by the deviation which is referred as arrow method. Straightness is specified in another method i.e. Total Indicated Reading (TIR) system which is defined as the deviation reading obtained on a dial gauge when the bar is rotated on "V" block supports or knife edge rolls at 1-meter centers, the dial gauge being positioned on the center of the span. As an equivalent system, a TIR reading of 1 in 1000 is equivalent to Arrow straightness of 1 in 2000 [5].

Degree of straightness in bars depends on type of machines used for straightening purpose. Residual stresses are also developed in the straightening process. Straightness of final products or finished goods depends on applied loads while the bar is subjected in straightening machines. If better straightness is required to be achieved then it is essential that bar in question should be reversely bent beyond yield point at application point of load such that existing curvature is reduced and as a consequence straightness is improved. These improvement features are achieved in cross-roll arrangements. Moreover, it can be stated that multiple-rotary bending actually helps in improving degree of straightness. Simultaneously, it is seen that straighteners having oblique rollers are preferred for use in straightening processes of round bars. An elaborate discussion on this has been done in subsequent sections.

3.2.3 Working Principle

Working principle primarily includes mechanics of bar straightening. Bar straightening involves application of stresses by the rolls during axial travel of the bars. Loads are applied externally in bar straightening process since bar remains essentially in between the rollers. The response of deformation in bar or tubular structure may be analysed to

assess structural integrity [68]. Using Ludwik power law equations, Stress (σ) – strain (ε) relationship can be expressed as below [3,8,69].

$$\sigma = C\varepsilon^n \tag{3.1}$$

where C is an empirical constant,

n is an exponent of strain-hardening ($0 \leq n \leq 0.5$)

This relationship of stress-strain can lead to conservative or pessimistic results of the structure [68]. If it is intended for realistic predictions, then it is quite essential to have good constitutive relations. It may accurately reflect true behavior of material. An interesting feature of material in question is that if it happens to 'remember' its previous loading history, then its subsequent behavior can fairly be predicted with the help of related equations. Bauschinger effect indicates this to some extent [7,70] which has been described in section 3.2.3.2

3.2.3.1 Mechanics of Bar Straightening

Bar straightening involves applications of stresses by the rolls during the axial travel of the bars. Like many scientific and technological researches, certain assumptions have been taken into account in the area of bar straightening also while developing the theory and mathematical treatment. These assumptions are given below.

ASSUMPTIONS

i. Work hardening in elastic region is present in the straightened bar.
ii. Cross-sectional area of round bar is circular in pure bending condition and neutral axis passes through the centre.
iii. Bars outside shapes are round.
iv. Cross section of the bar remains on a plane and at right angles to the axis.
v. Strain variation in bar section at any point is proportional to the distance from perpendicular point on neutral axis.
vi. Material is perfectly elastic-plastic, yield point and its stress-strain relations is same in uniaxial tension and compression.
vii. Other than longitudinal direction all stress components is zero [6].

The basics of stress-strain relationship have been stated for enabling understanding how the analysis has actually proceeded. We are familiar with the stress-strain relationship of any isotropic material having elastic modulus, E up to elastic limit and plastic modulus, E_p beyond E. A simplified diagram on the same is presented below as shown in Figure 3.3(a) [13].

Straightening of bar essentially involves moment-curvature relationship as reverse bending due to applied moment results in reduction of curvature. This phenomenon is well explained by Bauschinger effect.

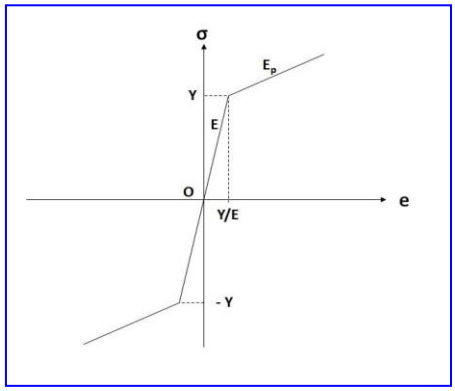

Figure 3.3(a) The Stress-Strain Relationship of a material [13]

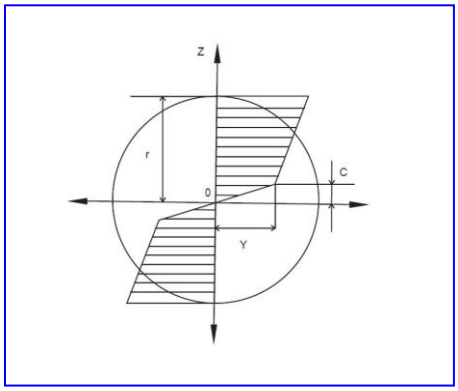

Figure 3.3(b) The Stress distribution through the section of a circular bar when subjected to pure elastic-plastic bending [6].

The distribution of stresses in the bar cross section when subjected to elastic-plastic pure bending which can be observed in Figure 3.3(b). The parameter z is the coordinate perpendicular to the axis of the bar and c is the distance between fibres which are just at yield and the neutral axis.

The stress-strain relationship is customarily expressed as below:

$$\sigma = E\varepsilon \qquad \text{for } z < c \qquad (3.2)$$

$$= Y + E_p [\varepsilon - Y/\,] = (1-\mu)\, Y + E_p\varepsilon \qquad \text{for } z > c \qquad (3.3)$$

where, σ = stress, ε = strain, Y = Yield point and $\mu = E_p/E$. E is the Young's modulus and E_p is the linear work hardening or plastic hardening modulus.

3.2.3.2 Bauschinger Effect

The phenomenon of Bauschinger effect is defined as reducing the proportional limit or elastic limit in compressive load after following previous tensile loading and vice versa. The elastic limit happens to be slightly above the proportional limit. Considering that if the deformation caused is in one direction only, reloading of the specimen in simple compression will exhibit appreciably smaller elastic limit in magnitude that of previous yield point. This will occur whenever there is stress reversal. Yield stress lowering in reversed loading is primarily caused by the residual stresses. This residual stress is actually left in the specimen on a microscopic scale due to the different stress states in the individual crystals of the specimen material made of [3].

Previous research findings have found that repeated plastic deformation introduces three major effects in pipes and bars: strain hardening, Bauschinger effect and strain aging. However, point of interest is much restricted to mainly on Bauschinger effect.

Bauschinger effect is a metallurgical phenomenon wherein the stress/strain characteristics of the studied material change due to the influence of microscopic stress distribution in the material [3]. The effect is notably observed in real metals, whenever there is a reversal of stress. In the process of rerolling, consequently there is a change in yield point in reverse loading. The above-mentioned loadings are widely regarded as the cause for occurrence of Bauschinger effect.

Bauschinger effect is generally neglected or can be largely removed in the theory of plasticity with the assumption that the material is having identical yield stresses both in tension and compression, irrespective of involvement of any previous history of cold working of that material [71]. In bar straightening it is quite significant as bars are subjected to elasto-plastic bending and the process cold working.

There are three different known residual stresses, viz. Type-1, Type-2 and Type-3 residual stresses. Commercially manufactured components possess all three residual stresses in varying degrees that are generated during the process of manufacturing. Type-2 and Type-3 residual stresses are primary causal agents of Bauschinger effect [72, 38]. The physical presence of these stresses could be imperceptible or in the form

of minute cracks. Cast and welded components can fail catastrophically even without loading at room temperature due to residual stresses. They are a proven agent in reducing the working lifespan of metal components [73]. As further discussion is mainly on reverse loading of bars, our consideration will be made on such analysis where discussion is centered around reverse loading and its impact on final curvature, consequently to degree of straightness and statistical consideration on the same.

3.2.3.3 Analysis of Bar Straightening

In the analysis of bar straightening, it has been assumed that metal bars behave both anisotropically as well as non-homogeneously, along with the degree of straightness of the finished component [15]. When analysing the process of general straightening under the action of reverse kinematic loading, prime considerations are of curvature change and resisting moments. Assumption is made that stress-strain curve on the basis of the findings of Davis et al. [71] are indicative curves showcasing the results for ductile nature of materials. The stress-strain relationship, between the reverse loading stress, σ and the change in longitudinal strain, ε [Figure 3.4(a)] is collectively demonstrated in Figure 3.4(b). Based on the results as reported, it shows that reverse loading does not have a clearly defined yield point and instead curves show sharp changes in the yield region [15, 71].

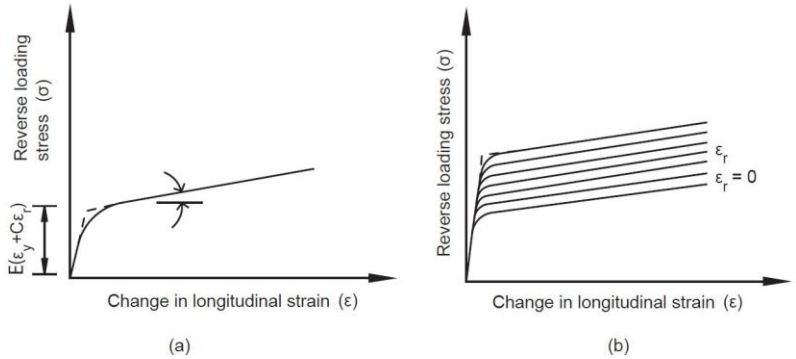

Figure 3.4 Stress-Strain Change Curves for Various Different Initial Residual Strains [15]

In addition to assumptions made earlier, it is also necessary that following assumptions are made:

(a) Yield point stress is the same in tension and in compression for an initially unstrained bar.

(b) During reverse loading, stress-strain relation is bilineal. This relationship is very close to the results reported by Das Talukder et al. [15]. The bilineal relationship as assumed can be expressed as

$$\sigma = E\varepsilon \quad ; \qquad \varepsilon < (\varepsilon_y + c\varepsilon_r) \qquad (3.4)$$

$$\sigma = E\,(\varepsilon_y + c\varepsilon_r) + E_p\,[\varepsilon - (\varepsilon_y + c\varepsilon_r)]\ ; \qquad \varepsilon \geq (\varepsilon_y + c\varepsilon_r) \qquad (3.5)$$

Where, $\sigma =$ stress

$\varepsilon =$ strain, $=$ strain at yield point, $\varepsilon_r =$ residual strain,

and $c =$ constant and c «1

$E =$ *E*lastic modulus, $E_p =$ Plastic modulus.

3.2.3.4 Moment-Curvature (M- κ) Relationship for Circular Bars

Considering a bar with the following characteristics:

i. Sectional symmetry about two axes in the y and z directions such that they are mutual perpendicular.

ii. Initial residual curvature κ_r in one plane of symmetry which will be different at different distances since strains in fibre at different distances will be different from z-axis.

Figure 3.4(b) shows the variation in strain change-stress curves as a result of an induced strain change [15]. Considering any arbitrary point on the surface of the round bar which is subjected under stress-strain due to bending moment, the outermost layer of the bar will have maximum stress and strain. The value of stress and strain at inner layers will be less than the maximum. Now, points joining together on the same surface along the axis can be considered as a fibre which is under bending load. Similar points on any inner layer can be considered as other fibres till the neutral axis. During bending

all the fibres above the neutral axis will be under tensile load and fibres below the neutral axis will be under compressive load. {During rotation of the bar while the bar is in straightening process, a cyclic stress-strain will take place}. Also, at yield point the residual strain will be zero since there will not be any permanent deformation of the bar. Following explanation using the equations of stress-strain gives more clarity in the matter.

According to the fibre in consideration, the curve of the initial residual strain is noted to calculate the stress. If residual strain in the extreme fibre is ε_{r1} and the residual strain in the fibre at a distance y from the z-axis is ε_r then assuming h to be the depth of the studied section, ε_r to be the residual strain at a distance of y units from the z-axis and the residual strain in the furthest fibre to be ε_{r1} then

$$\frac{\varepsilon_{r1}}{h/2} = \frac{\varepsilon_r}{y} = \kappa_r \tag{3.6}$$

The variation of stresses across different depths in bending is shown in Figure 3.5. Due to straightening if κ is the change in curvature along the length of the bar, it can be written as follows.

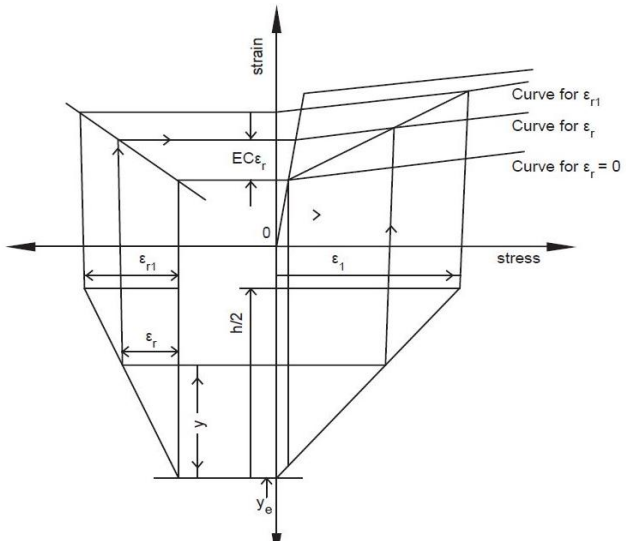

Figure 3.5 Variation of Stress across the Depth in Bending [15]

$$\kappa = \frac{2\varepsilon_1}{h} \tag{3.7}$$

$$= \frac{2y\varepsilon_1}{h} \tag{3.8} [7]$$

where the change in strain in the fiber at distances y and $h/2$ are given by ε and ε_1 respectively.

If the value of y at elastic-plastic boundary is given by y_e then from equation (3.8)

$$\sigma = \kappa E y \qquad -y_e \le y \le y_e \tag{3.9}$$

$$= (E - E_p)\,\varepsilon_y + \xi y \qquad -y_e \le |y| \le h/2 \tag{3.10}$$

where $\xi = (E - E_p)\, c\kappa_r + E_p\, \kappa$

Thus, the moment required to produce this change, M, can be found as follows [15].

$$M = [\lambda E\kappa + (1 - \lambda)\,\xi]\, I_Z \qquad \kappa \ge (\kappa_y + c\kappa_r) \tag{3.11} [7]$$

$$0 \le \lambda \le 1$$

$$= \kappa E\ ; \qquad \kappa \le (\kappa_y + c\kappa_r) \tag{3.12} [7]$$

where λ is a function dependent on the section parameters and change in curvature and I_Z is the moment of inertia about z-axis.

We know, $y_e = \varepsilon_y / h$ (3.13)

If the moment required to produce the same curvature change κ in a bar length, having zero initial curvature is represented by $M_o(\kappa)$, then from equations (4) and (5),

$$M_o = [E + (1 - \lambda)\, E_p]\, \kappa I_z \tag{3.14}$$

from equations (3.11) and (3.14)

$$\Delta M = M - M_o = (1 - \lambda)(E - Ep\ ]\, c\kappa_r\, I_z \tag{3.15}$$

where ΔM is the extra moment required to produce a particular curvature, due to initial curvature in the bar. It has been seen that the curvature falls down from roller to roller [74] when a round bar is subjected to reverse bending according to the absolute values [63].

3.2.3.5 Statistical Approach to the Bar Straightening

It has been observed through experimentation that deflection reduces after initially bent bar passes through straightening process by reverse bending. It has been observed that [63] changes in deviation from central axis are much dominant in the first pass and subsequent changes in deviation are lesser in comparison to initial change. It actually confirms that with every pass deflection data gets reduced which means straightness improves at every pass. However, improvement is more significant in the first pass itself than other passes, but at every pass straightness is improved even if it is marginal. It can be ascertained from the above that with reduction of deflections, curvatures are actually reduced and degree of straightness is therefore improved significantly with initial pass of reverse bending and also to some extent at subsequent passes. This is also in line with the very purpose of manufacturing of bar straightening machines. As each specimen enters the roller arrangement for reverse bending, bending moments thus faced by specimen causes improvement in reduction of curvature. However, due to insufficient experimental data, the frequency distribution followed by the reduction of deflection cannot be accurately ascertained.

Straight round bars are primary requirement in many industries. Therefore, use of straight round bars is necessary in industries due to requirement of raw material as input for production of value-added products. Round bars are often available in bent condition at several sections along the length; hence straightening is a necessity before deploying for commercial use. Therefore, choosing a proper lot of straightened bars with acceptable level of residual curvature is a quality requirement. Use of statistical analysis by Factorial Design will help in decision making through appropriate Test Hypothesis for quality criterion of acceptable range of residual curvatures. The author has made an attempt to look into the applicability of Factorial Design in bar straightening process by publishing a research article [10].

Commercially produced ferrous and non-ferrous metal round bars are available at various sizes. These bars have tremendous engineering use in multiple areas like automobile, aerospace, power, manufacturing, paper, printing, packaging and

construction industries. Due to its wide range of utility of round bars, it is naturally pertinent to understand and ascertain quality aspect of these bars. Quite often it has been observed that round bars as available are not completely geometrically round at various sections along the length, also straightness is also somewhat compromised. Therefore, it is necessary to check the uniformity of diameters at various sections. In this paper statistical process control has been used to ascertain whether such round bars as commercially available can be utilized for industrial application or not. Control limits in terms of diameter measurement along the length of bars help to evaluate the characteristics of data variation which is needed to take decision about confirmation of utility of commercially produced bars.

3.2.3.6 Probabilistic Approach to the Bar Straightening

It can be seen that moment and curvature have relationship in reverse kinematic loading for straightening of bar viz. bending moment *M,* initial and final curvatures κ including residual curvatures κ_r are therefore random variables in the event of straightening process which is actually a continuous one. As for continuous variables, probability density function in any arbitrary interval (a,b) or (λ_a , λ_b) or $(\lambda_i , \lambda_{i+1})$ of length segments of bar under reverse kinematic loading is applied [9].

However, values of interval (λ_a , λ_b) or $\mathbf{(\lambda_i , \lambda_{i+1})}$ shall be close to the spacing between set of rolls producing bending moment and not exceeding the length between two rolls. Even if, rolls are somewhat evenly spaced, then too depending on throughput speed and residual stresses and residual curvatures, applied bending moments will be random in nature.

An important addition to make here is that the zero probability of a random variable taking any selected value '*x*' does not imply impossibility for the random variable taking on the value of *x*. Similarly, in the case of continuous assessment, zero probability does not correlate to logical impossibility. Additionally, owing to the practical limitations of our ability to measure and observe the entirety of the generated

results, the study of this field is largely academic by nature and we ideally work within probabilities dealt in defined intervals and not for isolated points by itself.

In the continuous case, probabilities associated with individual points are always zero, and therefore if we deal in the probability associated with the interval present between a and b, the inclusion of the endpoint becomes irrelevant. In the case of continuous intervals, the importance of specifying interval probabilities drops drastically.

As we know, $P(X=x) = 0$ if X is continuous random variable.

Symbolically, it can be written as

$$P(a<X<b) = P(\lambda_a<X<\lambda_b) = P(\lambda_a<X \leq \lambda_b) = P(\lambda_a \leq X<\lambda_b) = P(\lambda_a \leq X \leq \lambda_b) \quad (3.16)$$

Since, this is a continuous case of re-rolling, hence all the parameters figuring in the process will also be continuous random variables. The probability between any intervals, more specifically between the rolls of reverse bending shall be in consideration.

However, certain assumptions can be made which is quite logical and also to make our present case a bit simple. Since all rollers are running by standard commercial motors, revolution of these motors will be nearly constant or with insignificant variation which may be arising out of voltage fluctuation, if any. However, on stabilized power supply, the possibility of variation will actually be insignificant. Hence, throughput speed (v_x) of bars can be treated as constant excepting start and end points. Similarly, average radius of bar can also be treated as constant since dimensional variations will be insignificant and for all practical purpose considering variation is actually not much meaningful. Now, the angle between loading plane and osculating plane (θ) as shown in Figure 3.6 will be indeed varying. Roller positions are by and large fixed and rolling about their fixed axis. Variability aspect of θ can be considered suitably. Hence, at present, we can actually deal primarily with two main variables, i.e. change of bending moment ΔM and final curvature, κ_f.

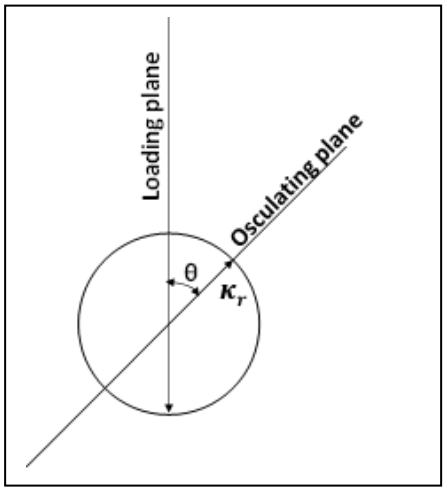

Figure 3.6 Sketch Showing Loading Plane and Osculating Plane Making an Angle θ [15].

Therefore, using equation (3.15), we can say that probability of occurrence of actual loading towards of change in bending moment under straightening process may be defined in Eq.3.17,

$$P(M_{\lambda a} \leq \Delta M \leq M_{\lambda b}) = P(\kappa_{\lambda a} \leq \kappa_f \leq \kappa_{\lambda b}) = \int_{\kappa_{\lambda a}}^{\kappa_{\lambda b}} f_k(\kappa_f)\, d\kappa \qquad (3.17)\ [9]$$

where, $f_\kappa(\kappa_f)$ is the probability density function of final curvature due to change in bending moment on actual loading event during straightening process in the cross-roll arrangement.

Now as the value of mean curvature, μ_κ is available for a process, then by using the equation (3.16) it is possible to ascertain the value of final curvature κ_f at any interval region between a set of rolls causing reverse bending. The probability of any such value for κ_f can also be found out using equations (3.15) and (3.16).

Therefore, the probability or likelihood of falling values of final curvature κ_f within the range of application of reverse bending in the range of any set of rolls (λ_a , λ_b) will be as below:

$$P\,(\kappa_{\lambda a} \leq \kappa_f \leq \kappa_{\lambda b}\,) = \int_{\kappa_{\lambda a}}^{\kappa_{\lambda b}} f_k(\kappa_f)\, d\kappa \qquad (3.18)$$

Probability density function can be evaluated when sufficient amount of experimental data is available. The probability distribution function of the data set will play significant role in ascertaining the probability of occurrence of required straightness between set of rolls under reverse bending. Mean curvature and standard deviation of the bar can also be estimated accordingly. The use of bar straighteners as a valuable preparatory process can be established by comparison between the conventional bar machining process and the use of bar straightening as a preliminary process before the machining stage. This can directly translate into improvements in multiple aspects such as productivity, energy requirements and monetary benefits. The probability of occurrence of final curvature at a point within length segment can be expressed if probability density function is expressed between any two rollers in case of equidistant rollers. For any other arrangement of rollers, limit values of length segment of bar λ_a and λ_b have to be suitably changed and equation shall be changed accordingly. As the mean value of curvature and standard deviation of the bar after straightening process is within acceptable limits, same can be used for commercial purposes. The viability of using this methodology for preparing raw material to produce various components increases as compared to conventional process. Moreover, the concept of statistical consideration has been applied to bar straightening process for estimation of final curvature of line segment of a given bar.

3.2.4 Types of Straighteners

There are various types of rotary straighteners which are based on types of rollers, number of roller and arrangement of rollers. All the rotary straighteners are usually of concave hyperbolic contour. Some of these straighteners are cylindrical or drum type which may be considered as special cases. Lot of advancement has taken place over the time in design and development of straightening machines. Amongst the various types of straighteners, each type has superior advantage in certain specific circumstances. Cross-roll straightening machines are often termed as reeling machine and these machines are most popular in industrial usage. Cross-roll straightening

machines have several combinations driven and of idle roll arrangements. Because of the popularity of cross-roll straightening in industries, its theoretical analysis is separately discussed in detail in section 3.3. Beside these machines there are other types of straightening machines viz. Section straightening machines, Stretch straightening machines, Cluster-roll straighteners, Spinner straighteners, Pulse straightening machines, Parallel Roller straightening machines and Skew roll straightening machines. A brief description of each type of these machines may be considered relevant.

3.2.4.1 Section Straightening Machine

Two-way roller bar section straightening machines are built generally in two separate units, the first unit has two pinch rolls and six straightening rolls and the second unit has eight straightening rolls. This machine is ideally suitable for the straightening of square, hexagon, or round bar in the smaller size ranges from coil, as the machine can be fitted with an uncoiler, flying shear, static shear, or a saw for cutting to the length required.

These machines are designed so that they are adjustable laterally and also vertically, with supplementary adjustments on each roll of both units. Thus, they are easily get up to a very high degree of precision. Inlet and feed guides are fitted to ensure that the material passes easily into the machine and from the leading unit to the trailing unit. The two-way straightener is ideally suited for flats as it can straighten the full plane simultaneously.

Figure 3.7(a) Photograph of Section Straightening Machine, Make: Kabir Section Straightening Machine [76]

Figure 3.7(b) Photograph of Section Straightening Machine, Make: Sohal Machine Tools [77]

Another section straightening machine called the cantilevered section straightening machine is generally used for the straightening of heavier sections used in the constructional industry. Section straightening machines have cantilever design. They are cantilevered rollers similar to that used on the two-way machine, except that they are only straightened in the one plane. Working principle of these machines are based on the process of rotary straightening. **Section Straightening Machine** are robust in construction, have high level resistance and optimum stability. These machines are used to straighten rolled steel sections like rounds, beams, angles and channels etc. Section Straightening Rolls are made according to sections. For materials of rolls, some manufacturers use Adamite (a kind of high carbon steel with carbon percentage ranging from 1.35% to 2%). Figure 3.7(a) & 3.7(b) show the pictures of Section Straightening Machines of two different manufacturers viz. M/s. Kabir Section Straightening Machine and M/s. Sohal Machine Tools respectively.

3.2.4.2 Stretch Straightening Machines

Stretch straightening machines have gripping arrangement at both ends. These machines grip both ends of the bar and exert tension of certain amount to the bar in order to straighten. Extrusion stretch straightening and forming is a fast and economical way to form large extrusions. The process is also quite accurate. It involves stretching an extrusion to yield which is then followed by straightening and forming over a tool. Stretching profiles are made between the two heads, one is fixed and the other is mobile. The movable head is usually set to the length of the expandable profile. Using laser system, the distance between the heads can be controlled. Figure 3.8 shows the photograph of Stretch Straightening Machine.

Figure 3.8 Photograph of Stretch Straightening Machine,
Make: M/s. Cyril Bath Co., North Carolina, USA [78].

3.2.4.3 Spinner Straighteners

Spinner straightening is often carried out as the first process before cross-roll straightening. Spinner straightening is a straightening process for resistant materials which is done mechanically as cold working. A typical application of this machine is in wire production. Wire is pulled through high-speed rotating rollers. These rollers are made of bronze which gives torsional twist resulting into condition of straightness. The

speciality of this machine is that while feeding movement is given to the bar end but rotational movements are given to the dies. The resultant deformation leads to decrease in yield stress value which makes it strained and also softened. Initial curvature can be eliminated by spinner straightening. As wire rods are usually available in coiled form, hence spinner straightening is quite helpful to straighten short-span curvatures which periodically exist. Figures 3.9(a) & 3.9(b) show the schematic diagram and photograph of spinner straightener respectively.

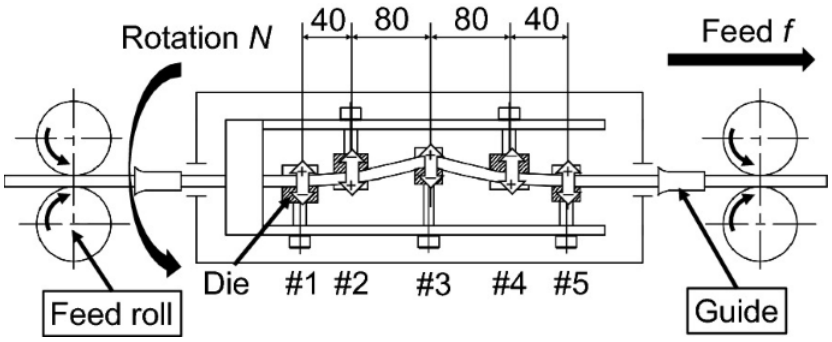

Figure 3.9(a) Schematic Diagram of Spinner Straightener [79].

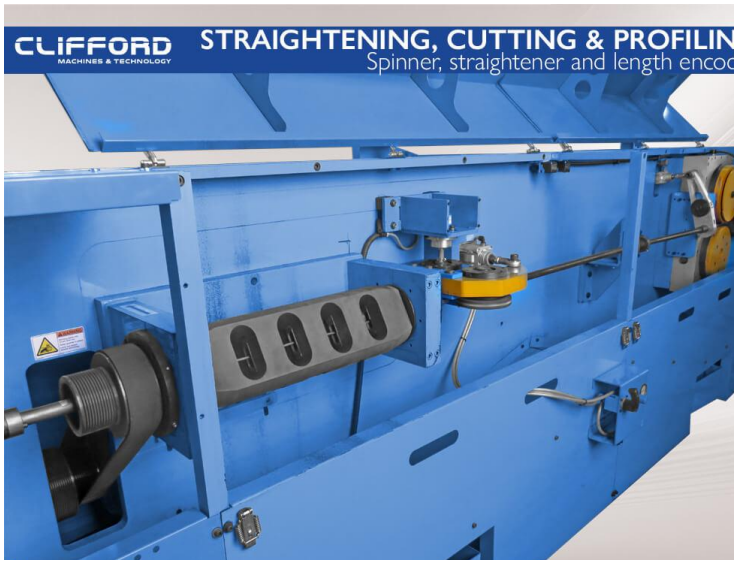

Figure 3.9(b) Photograph of Spinner Straightener.
Make: Clifford Machines & Technology,
South Africa. [80]

3.2.4.4 Pulse Straightening or Magnetic Pulse Straightening

In this machine the effect of hyper plasticity is used. In pulse straightening system, high tensile wire which is to be straightened is pulsed in special machines that give magnetic pulse treatment using hyper plasticity. The specific advantage of this machine is that it permits straightening of highest tensile wire. In this process, tensile yield stress is not altered and results smoother surface of wire, hence less friction. Figure 3.10 shows an experimental set up of Magnetic Pulse Straightening.

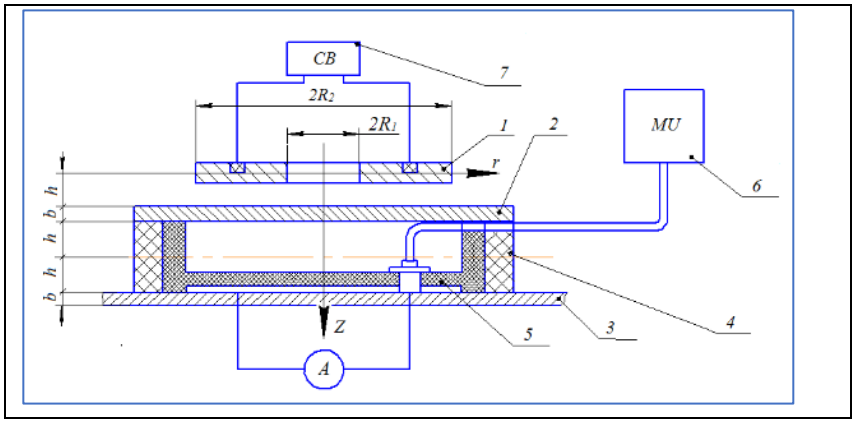

Figure 3.10 Schematic of Experimental Setup of Magnetic Pulse Straightening [81]

Note: 1 – Multi-turn induction coil; 2 – Accessory attracting screen; 3 – Sheet metal blank; 4 – Dielectric intermediate piece; 5 – Spacer with the tensometric linear displacement sensor; 6 – Measuring unit; 7 – Control block.

Beside above types of straightening machines, there are two kinds of internal straightening methods, the first is rotary hub straightening, the other is parallel roller straightening.

3.2.4.5 Rotary Hub-Straightening

In rotary straightening machine it includes a straightening block which is usually installed in the straightening mechanism of the hub. The wire rod is bent many times in the process of moving forward, and gradually tends to be straight when it is through

high-speed rotation and staggered arrangement of straightening blocks. With this straightening method the steel bar is straightened with good straightness and fast speed. But the process also causes damage to the surface of steel bar.

3.2.4.6 Parallel Roller Straightening

The straightening method is parallel roll type roller straightening CNC steel bar straightening machine. The wire rod steel bar meshes through two rows of staggered multi-wheel press roll groups, which directly deforms the steel bar to be straightened, so as to achieve the purpose of straightening. The speed of parallel roller straightening method is slightly slower than that of rotary straightening equipment. However, the straightness of steel bar can meet the construction requirements. Also, this straightening method does not damage the steel bar after straightening process.

3.2.4.7 Skew-Roll Straightening Machine

Very small stainless steel medical tubing often requires straightening. This requirement is fulfilled by Skew-Roll straightening machine which is designed and built to straighten very small stainless-steel tubing. Using identical hyperbolic profiles of rolls, accurate tube can be achieved. These machines are available in 3x3 skew roll designs or 5x5 skew roll designs.

These bar straightening machines described above are individually having certain advantages and disadvantages. In order to make right selection of machine, it is necessary to consider the degree of straightness required, the type of material being fed, machine capacity, surface finish and straightening speeds etc.

Two roll straighteners are used for improving surface finish. The speed at which the process of straightening can be operated depends upon the degree of control that can be applied to the rotating material. All cross-roll straightening machines cause bar material to rotate during straightening operation. Obviously a long badly bent bar cannot be rotated as fast as a short and fairly straight bar.

3.3 Cross-Roll Straightening Machines

These machines are designed for straightening of both bars of circular cross section and tubes. The rolls are mounted at an angle called helix angle to the line of pass. The bar rotates about its axis as it proceeds through the machine. Although several types of straightening machines are available in the market, but generally four basic types of cross-roll machines are in use which may be put as below:

1. Two-roll Straighteners or Reeling machines
2. Six-roll types (six rolls are mounted in a set of three pairs).
3. Multi-staggered roll types having five, seven or even ten rolls
4. Cluster-roll machines having seven rolls. A set of two-clusters each cluster is made of three-rolls and another roll at centre i.e. deflecting roll.

3.3.1 Two-Roll Bar Straighteners or Reeling Machines

Two-Roll Bar Straighteners or Reeling machines comprises of one concave roll and one convex roll. The convex roll can exert reverse load at centre of the bar to be straightened while the ends of concave roll act as horns. The bending of round bar takes place across horns of the concave roll. The Reeling machines are classified further into two types which are as below:

(a) Free-bend straighteners or Air-bend straighteners

(b) Line-contact type rolls straighteners.

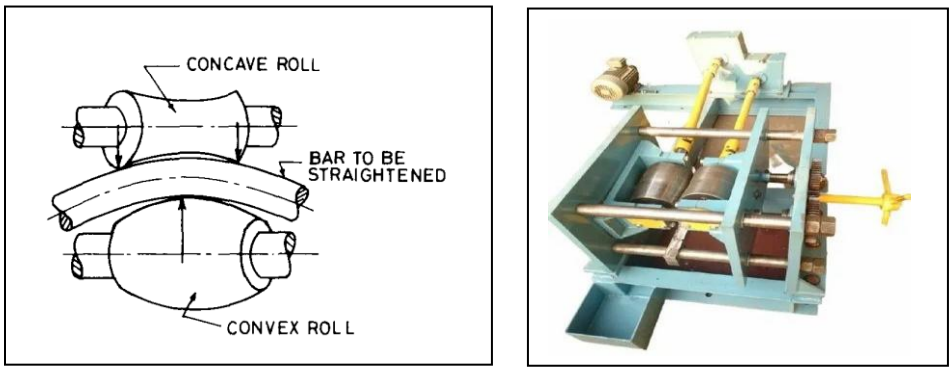

(a) (b)

Figure 3.11(a) Sketch [8] and (b) Photograph of Straightening of Bar in a Two-Roll "Air-Bend" Machine [82].

The application of load is concentrated at a point in free-bend or air-bend straighteners as illustrated in Figure 3.11(a). This loading pattern in this machine is like simply supported beam with a centralised concentrated load. The span of the horns may be considered as beam length.

In line contact roll straighteners, the straightening process takes place by deformation between a set of two rolls. The deformation occurs can be considered as equivalent to conventional simply supported beam which is loaded uniformly over the length or uniformly distributed loading. Loading on the beam is across the span which may be considered as "beam length" of the bar. In cross-roll straighteners rolls are adjusted with a helix angle where angular adjustment of rolls is possible from 5^{o} to 45^{o}.

3.3.2 Six-Roll Straighteners

It is obvious that six-roll straighteners are having six rolls and these rolls are put in a set of three pairs as shown in Figure 3.12. In this system beam-length is also more or larger in comparison to free bend or air-bend straighteners. Loading on bar is distributed but over a small span of length which is a line contact i.e. near mid-span of the bar.

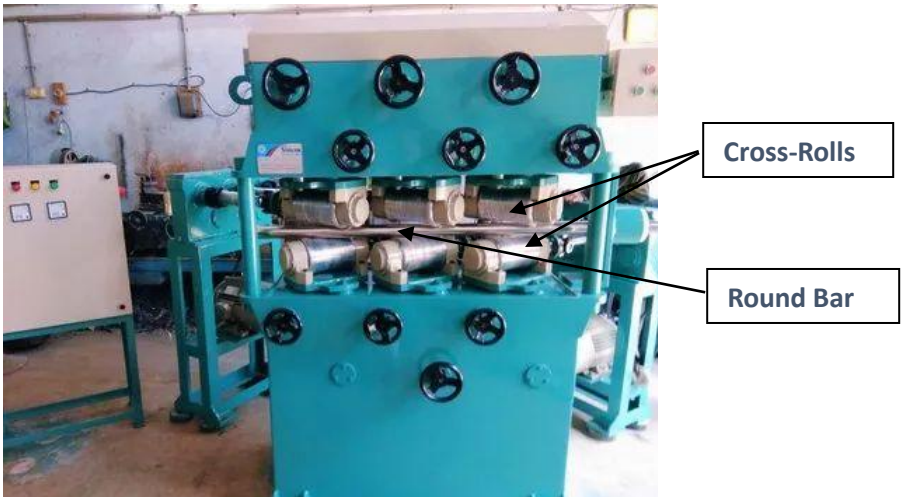

Figure 3.12 Photograph of Six Roll Straightening Machine. Brand: Shivam Engineering [83]

In this case there are support rolls which are at the end and rolls at centre are actually the loading rolls. In this machine, mean value of angular adjustment of rolls is about 30^{o}.

3.3.3 Multi-Staggered Roll Types Having Five, Seven or even Ten Rolls

As the name indicates these machines have staggered rolls and number of rolls vary from five to ten. The rolls are arranged in a manner that it functions like number of "loading bays" and practically at each loading bay beam length is subjected to a concentrated load and acting at opposite directions at consecutive bays as shown in Figure 3.13. Angular adjustment of rolls in this machine is possible up to 35^{o}.

Figure 3.13 Photograph of Multi-Staggered Roller Straightening Machine.[84]

3.3.4 Cluster-Roll Straighteners

In cluster-roll straightening machines, there are seven rolls as shown in Figure 3.14. These rolls are arranged in a set of two-clusters of three-rolls each along with one roll at centre. The centre roll is used for deflecting purpose. The beam length of these machines is considered as simply supported with concentrated point load at mid-span.

Figure 3.14 Photograph of Cluster Roll Straightening Machine [85]

The beam length in this case is as similar as six-roll straighteners. The beam length is comparatively higher than air-bend straighteners or free-bend straightening machines.

3.4 Mechanics of Cross-Roll Straightening

The present investigation is mainly focussed on cross-roll straightening process because of its popularity and extensive use in commercial market and industries. Cross-roll straightening being most popular amongst straightening processes, as already mentioned, it has naturally received most attention in bar straightening world. The straightening process involves certain basic parameters like roller diameter, bar diameter, throughput speed of the bar, rotational motion of bar and roller, angular arrangement of rollers to facilitate progressing of bar as the rollers are in action. Since the bar progresses during straightening, points on the bar surface will face kinematic loading. Moment developed during reverse bending is related to the curvature of the bar. The moment-curvature relationship plays significant characteristics in the entire process of bar straightening, the theory of which is explained earlier. Bar straightening involves plastic deformation The basics of plastic deformation has already been discussed briefly. A systematic presentation on mechanics of cross-roll bar straightening is given below which would give a clear insight as how the process actually works and various factors involved in the straightening process.

The following parameters for mathematical modelling of cross-roll straightening of bars are taken to study its mechanics.

Roller radius = *R,*

Bar radius = *r*

Angular speed of bar = $\dot{\theta}$,

Angular velocity of rollers = ω

Throughput speed of the bar = v_x

Tangential velocity of any point on the surface of the bar = v_t

Cross-roll straighteners are set at an angle to the axis = α

An illustration of bar in motion through cross-rolls in straightening processes has been shown in Figures 3.15(a) and 3.15(b).

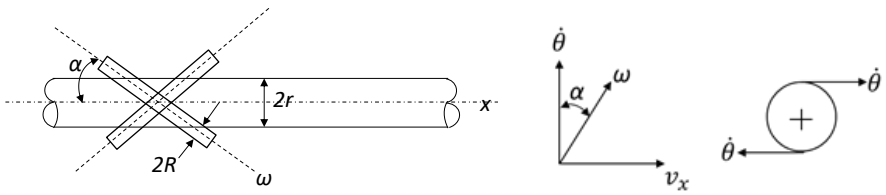

(a) (b)

Figure 3.15(a) Sketch Showing the Angular Arrangement of Rolls [8].

(b) Throughput speed and angular speed of the bar has been shown [8].

Based on above assumption, the we can say that bar's through-put speed along the length, v_x is in the axial direction, while its rotation about its axis with its angular speed $\dot{\theta}$, we can state as below

$$\dot{\theta} = \frac{v_x \cot\alpha}{r} \tag{3.19}$$

The speed of bar can be expressed as

$$v_x = \frac{2\pi NR \sin\alpha}{60}\ , \quad \text{where N is r.p.m. of rollers.} \tag{3.20}$$

Considering any arbitrary point on outer surface of round bar at a distance r from the neutral axis or centre line of bar which moves in a helix angle α, the pitch length, p can be expressed as below.

$$p = 2\pi r \tan\alpha \tag{3.21}$$

The bars while proceeding through rolls rotate about its own longitudinal axis with the initial curvature plane. This plane of initial curvature is osculating plane which makes different angles at various different instants with loading plane as the bar progresses through the rolls. This is well explained in the Figure 3.16.

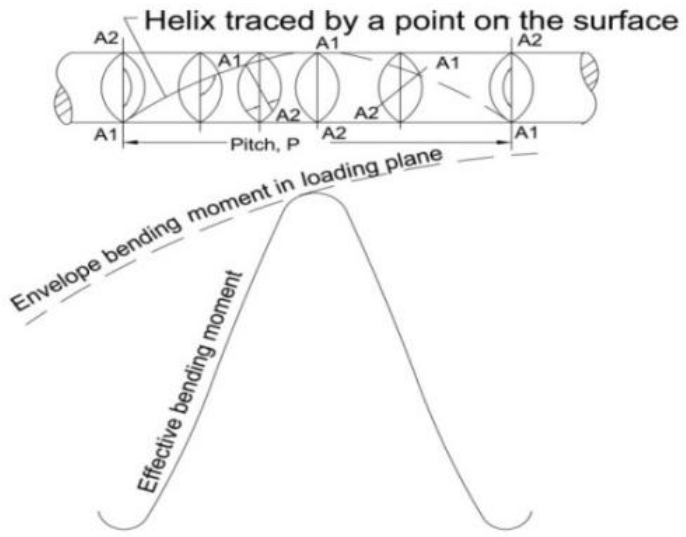

Figure 3.16 Illustration of Variation of Resisting Moment or Effective Bending Moment in Loading Plane and Corresponding Variation of Effective Bending Moment in a Pitch Length as Bar Rotates through 360^{o} in One Cycle [65].

With the progress of bar through the rolls, there will be corresponding variations of resisting moment or effective bending moment. In a span of pitch length, *p* with the rotation of bar, the osculating plane also rotates 360^{o}. Therefore, there is an oscillation of effective bending moment or resisting moment. This effective or resisting bending moment will occur and have variation through one cycle. The effective bending moment will be in its maximum at half the pitch length. Any arbitrary bar section A1-A2 in the Figure 3.16 rotates and position of A1-A2 becomes A2-A1 at half the pitch length and again it becomes A1-A2 at full pitch length. The effective bending moment becomes maximum at half the pitch length.

Considering a simple case, we assume the bar of uniform initial curvature. The curvature change-resisting moment of a bar can be drawn as shown in Figure 3.17.

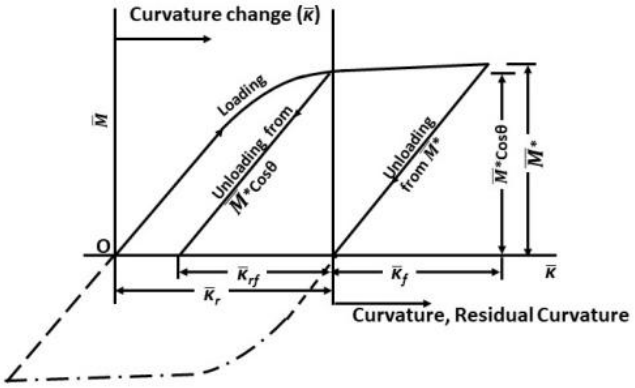

Figure 3.17 Simplified Relationship between Resisting Moment or Effective Bending Moment in the Bar and Change in Curvature [65].

In the arrangement of staggered cross-rolls, maximum loading moment M^* is developed while bar is passing through the rolls and corresponding curvature change is κ^*.

Residual curvature change, $\Delta\kappa_r$ or $\Delta\bar{\kappa}_r$ (in non-dimensional form) can be expressed as

$$\bar{\kappa}_r = \frac{\kappa_r}{\kappa_y}, \quad \text{where } \kappa_y \text{ is the curvature at yield point.} \qquad (3.22)$$

The non-dimensional form of residual curvature to yield curvature is $\bar{\kappa}_r$ which is also equal and opposite to initial curvature.

Non-dimensional form of bending moment, M may be expressed as

$$\bar{M} = \frac{M}{M_y} \qquad (3.23)$$

Based on above diagram, we can say that effective bending moment will be a component of bending moment on loading plane which will be acting on the osculating plane.

Therefore, effective bending moment, $\bar{m}$ in non-dimensional form can be expressed as

$$\bar{m} = \bar{M}\cos\theta. \qquad (3.24)$$

Loading moment is developed at a distance of bar can be expressed as $\left(x - \frac{1}{2}l\right)$.

At an instance, when a bar section approaches the distance at $x = \frac{l}{2}$, the osculating plane and loading plane may not have any angle or zero angle in between.

Effective bending moment in that case of initial curvature will then not be equal to maximum attainable moment M^* at $\theta = 0$. The effective bending moment as described in the diagram, will achieve such value only at a few sections. Such sections will be at pitch length distance, p of the bar.

3.5 Effect of Helix Angle of Cross-Roll in the Process of Bar Straightening

In the process of bar straightening, it has already been highlighted that several parameters play important roles. Out of these parameters it has been found that helix angle of the cross-roll arrangement plays a significant role. Present investigation shows that helix angle has a limiting value beyond which the straightening function would not be possible. Analysis of straightening process pertaining to helix angle will show the relevance of above statement.

Non-dimensional form on the relationship of moment curvature is described as below:

$$\begin{aligned} \bar{M} &= \bar{\kappa} && 0 \leq \bar{M} \leq 1, \\ \bar{M} &= \bar{M}\,(\bar{\kappa}) && 1 \leq \bar{M}, \end{aligned} \qquad (3.25)$$

where, $\bar{M} = M/M_y$, and $\bar{\kappa} = \kappa/\kappa_y$

M_y is the yield moment and κ_y is the yield curvature for a section considered. $\bar{M}(\bar{\kappa})$ is a function of $\bar{\kappa}$, which depends on the stress-strain relationship of the material beyond the yield point. For convenience purpose, Curvature and moment of resistance in reverse loading will be taken as positive. Considering a bar to be straightened is having initial curvature, $-\bar{\kappa}_r$. The length of the bar should be subjected to loading in the reverse direction. The loading should be kinematically either by applying a known moment or a known curvature.

If the loading is kinematic and the curvature to which the bar length is subjected is $\bar{\kappa}_f$, then, in order to leave no final residual curvature on unloading, the curvature change $\Delta\bar{\kappa}$, as illustrated in Figure 3.17.

$$\Delta\bar{\kappa} = \bar{\kappa}_f + \bar{\kappa}_r \tag{3.26}$$

Considering plane of loading as vertical in this analysis, and osculating plane enclosing an angle θ between them, the effective bending moment will be the component of the bending moment in the loading plane, along the osculating plane.

$$\bar{m} = \bar{M}cos\theta \tag{3.27}$$

where $\bar{m}$ is the effective bending moment and $\bar{M}$ is the bending moment in the plane of loading at the section considered.

The component $\bar{M}sin\theta$ of $\bar{M}$ mostly produces elastic deformations, hence of no consequence in the analysis. Therefore, a section which is subjected to curvature $\bar{\kappa}_f$ in the vertical plane and a resisting moment in the loading plane of $\bar{M}$*, the effective resisting moment developed in the section is given by,

$$\bar{m} = \bar{M}^* cos\theta. \tag{3.28}$$

and when unloading takes place from the loading curvature there will remain a final residual curvature in the bar length of $\bar{\kappa}_{rf}$ in Figure 3.17**.**

In the cross-roll straightening machine, the rolls are set at angles $\pm\alpha$ with the axis of the bar of radius *r* as illustrated in Figure 3.15(a). Cross-rolls actually cause bars to rotate about its own axis as the bar progresses forward through the rolls. If ω is the angular velocity of the rolls of radius R, throughput velocity v_x and the tangential velocity is v_t of a point on the surface of the bar Figure 3.15(b) then

$$v_x = \omega R sin\alpha, \text{ and} \tag{3.29}$$

$$v_t = \omega R\, cos\alpha \tag{3.30}$$

The pitch length of the bar can be expressed in terms of helix angle α as below:

$$p = 2\pi r tan\alpha \tag{3.31}$$

In non-dimension form,

$$\bar{p} = \frac{p}{l} = 2\pi\bar{r}tan\alpha, \tag{3.32}$$

where, *l* is the beam length and *r* are the radius of bar and $\bar{r} = \frac{r}{l}$. If moment developed at the mid-section of the of the bar at any instant be $\bar{M}$* in the plane of kinematic loading, then the bending moment $\bar{M}_x$ in the same plane at any other section will depend on the distance of the section from the mid-section and the type of loading. As

a section considered progresses through the rolls, the enclosed angle θ for that section varies continuously due to the rotation of the bar.

Thus, if at a generic section $\bar{x} = x/l$ and $\theta=\theta_x$, then the effective bending moment $\bar{m}_x$ at the section will also vary continuously and will be given by

$$\bar{m}_x = \bar{M}_x cos\theta_x \qquad (3.33)$$

If y is the lateral displacement of the section of the bar then,

$$cos\theta_x = y/r = \bar{y}, \qquad (3.34)$$

From Eq.3.29, we get $x = (\omega R\ sin\alpha).t$

and $y = \omega R\ cos\alpha\ .t \qquad (3.35)$

Also, in non-dimensional form $\bar{x} = x/l$, $\bar{p} = p/l$

Since, pitch length, $p = 2\pi r tan\alpha = 2\pi r\ sin\alpha\ /\cos\alpha$

Therefore, $\cos\alpha = 2\pi r\ sin\alpha/p \qquad (3.36)$

Substituting cosα in Eq.3.35, we get

$$y = \omega R\ cos\alpha.t$$

$$= \omega R(2\pi r\ sin\alpha).t/p \qquad (3.37)$$

Since, $x = (\omega R\ sin\alpha).t,$ then by substituting in Eq.(3.37),

we get $y = 2\pi x\ r/p \qquad (3.38)$

Again, $\bar{y} = y/r$

$$= 2\pi x/p$$

$$= 2\pi\bar{x}/\bar{p} \qquad (3.39)$$

From Eq.3.35, $y = r\ sin\ (t.\omega R\ cos\alpha\ /r)$

therefore, $\bar{y} = sin(2\pi\bar{x}/\bar{p})$

Hence, $\bar{m}_x = \bar{M}_x sin(2\pi\bar{x}/\bar{p}) \qquad (3.40)$

From above equation, it can be seen that $\bar{m}_x$ is an oscillating function of $\bar{x}$ with the curve $\bar{M}_x$ as its envelope.

3.5.1 Criterion for Setting of Helix Angle

The variation of bending moment in the loading plane and the corresponding variation of effective bending (or resisting) moment as the bar progresses through the rolls is illustrated in Figure 3.16. In a pitch length the osculating plane of the bar rotates through 360^o and the effective resisting moment oscillates through one cycle.

However, considering Eq. (3.33)

$$\begin{aligned}\bar{m}_x &= \bar{M}_x \cos\theta_x \\ &= \bar{M}_x (2\pi\bar{x}/\bar{p}) \\ &= \bar{M}_x (2\pi\bar{x}/2\pi\, \bar{r}\, tan\alpha) \\ &= \bar{M}_x \bar{x} cot\alpha\ /\bar{r}\end{aligned}$$

or,
$$\bar{m}_x = \bar{M}_x x\ cot\alpha/r \qquad (3.41)$$

From the above equation, it is clear that theoretically for maximum effective bending moment, helix angle should be kept at lower value *of* α and maximum angle can go up to π/4. Beyond π/4 value starts reducing and value becomes zero at angle π/2. Beyond angle π/2, values are in negative which means helix angle cannot be kept more than π/2. There are practical limitations for setting helix angles since roller diameter itself is a constraint which is due to accommodating required space for roller itself. Roller length and diameter along with bar diameter is a concern for accommodation of roller in the setup.

Considering cotangent graph given in Figure 3.18 [11], appreciable high values are available for above purpose when angle is within π/4 which means helix angle to be kept slightly lower than π/4.

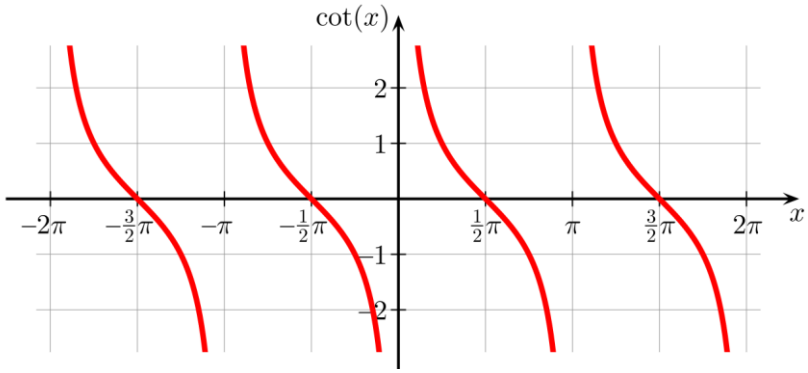

Figure 3.18 Cotangent Graph Showing Values along the Angle From -2π to 2π [11]

Throughput speed of bar is given by

$$\bar{v}_x = v_x/(\omega R)$$
$$= [1+(2\pi\bar{r}/\bar{p})]^{-(1/2)} \qquad (3.42)\ [11]$$

Therefore, it can be seen easily from the above equation that throughput speed of bar can be controlled by controlling helix angle. The bar radius r is constant for a set of bars in a straightening process; hence speed of operation can be controlled by controlling helix angle α. However, if the diameter of bar varies within the length, then throughput speed will change accordingly. It is evident from the above equation that if speed of operation is to be kept high then lower helix angle is essential. However, lower helix angle also means lower pitch length.

The above analysis indicates that helix angle of the bar straightening process is of considerable importance. It is essential to keep lower helix angle for the purpose of workable throughput speed of the bar. Higher throughput speed definitely causes higher production, but a balance is essential. Also, from the cotangent value of helix angle and practicality of roller adjustment in the machine set up, it is prudent to keep the helix angle lower than π/4 [11]. Since helix angle is related to the pitch length of the bar, lowering helix angle also means lowering of pitch length which is a better option considering standard of straightness. However, it is also possible to increase pitch length keeping the same standard of straightness but with a different roll arrangement.

3.6 Application of Straightening in Machines

Now a days, most machines are of automated type performing various functions using motorized power. Power is sometimes transmitted directly or through various mechanical systems, links and mechanisms to perform certain desired operation as per design requirement of the user. Most of the machines and machine tools use straight bars in different forms and sizes to perform automated transmission of motion which may be in any direction. Mechanical shafts, camshafts, links, shafts, driving and driven rollers, support rollers are such mechanical items that require straight bars to support various mechanical functions. Wherever rotational movement is necessary, straight bars are required in the form of power shafts or other transmission shafts. Threaded Rods with square threads are used in lathe machines to assist in sliding of carriage and tool post. The long screws require straight round bars before threading operation. In all polished round sliding system where piston rods are used, straight bar is an essential input.

In general, it can be stated that straight round bars are used extensively in printing machines for various components such as (a) Register pins or Registration Bars (b) Gripper Bars (c) Guide Bars (d) Cutoff Bars and (e) Folding Bars etc.

In Registration Bars, straight round bars are used to ensure accurate registration of paper and alignment during printing. These Bars maintain precise alignment and ensure text and crisp images. In Gripper Bars, straight round bar carries multiple grippers which are controlled by cam and follower to grip and hold paper or material in place during printing and transportation in sheetfed offset presses. Straight round hollow bars are used to guide paper or material through the printing press enabling smooth flow and turnover the web in web offset presses. Cutoff Bars use round straight bars to trim excess paper or material after printing, ensuring precise cutting. After printing operation, it is necessary to do folding of printed materials. Folding Bars are used as to facilitate accurate folding of printed materials, such as brochures or leaflets while. The materials used in these types of bars are usually Steel bars, Aluminium bar, Hardened steel bars, Chrome-plated bars and Ceramic-coated bars. The general benefit of using

such straight round bars in printing is for improved print quality with increased productivity and reduced waste. Also, maintenance is simplified while using straight bars. Straight bars enhance registration accuracy which is essential for quality printing. It has been seen that straight bars are used in different types of printing machines particularly in (i) Offset printing machine (both sheetfed and webfed) (ii) Flexographic printing machine (iii) Screen printing machine (iv) Digital printing machine and (v) Label printing machine etc.

Use of digital printers are extremely popular in printing industry in modern times where usage of highly polished straight bars is essential for smooth travel of printer head as in inkjet printers. Several components are extremely polished straight bar with both ends duly machines for specific purpose.

One example is given here for ready reference where straight polished round bars in the form of shafts have been used as machine part in sheetfed printing machine of type "Super Single Colour Offset Machine (482 mm x 640 mm) 7500 I.P.H. Model No. PO25 Super", Make: Manugraph Industries Ltd. Following round shafts are used in the above printing machine model PO25 Super, [86].

a) Shafts and Cam Shafts have been used in Cam Shaft Separator Mechanism
b) Rods used in Paper Guide Stripper Pipes
c) Shaft in Pile Raising Mechanism and Crank
d) Shaft in Raising Shaft – Pile Board
e) Shaft in Trimming Rack
f) Shaft in Chain Wheels Tension and Shaft Drop Cam
g) Gripper Shaft in Gripper Bars and Chains
h) Shafts in Delivery Pile Lowering Guide Bars and Brackets
i) Shaft in Twin Fork
j) Shaft and Eccentric Shaft in Throw off Mechanism and ECC Shaft
k) Lever Shaft in Stock Register Wall-Connectors
l) Shaft in Trip Throw on Shaft
m) Drum Shaft in Vacuum Belt Drum Shaft
n) Front Lay Shaft in Front Lay Mechanism

o) Shaft in Paper Guide on Belt

p) Paper Guide Shaft in Paper Guide on Belt

q) Plate Cylinder shaft in Plate Cylinder

r) Shafts in Form Roller Throw off

s) Rod in Ink Feed and control

Straight round bars with ends machined have been used in the same machine as

(i) connectors in Brush Photocell and Bushing

(ii) connectors in Paper Guide Stripper Pipes

The different types printing machines also have abundant use of straight bars in the form of various types of power-driven rollers and support rollers. The straightness of different types of rollers and shafts used in the printing machines is required to obtain quality printing.

With the modernization of machineries in various sectors, printing and packaging industries also got modernized and automation became and integral part in printing machines. The automation in printing machines involve conveying system to facilitate automatic packaging. Automatic packaging is also done in pharmaceutical industries where blister packaging in aluminium foils is essential for packaging of tablets and gelatine capsules. In all such machineries where conveying is essential, part of operation need usage of straight rollers which are made of round straight bars. Usually, round straight bars with high accuracy are desired for quality control of all these automated conveying operations. Flex printing machines need extensive use of rollers where straight round bars are essential inputs before manufacturing these rollers including support rollers. Manufacturing of round straight components are thoroughly based on input material that are both round and straight. Bent bars as input material would naturally ask for increased machining time and waste of materials. Hence, industries look for straight bars for higher productivity and overall economic reasons. In paper and pulp industry there are various processing equipment which require straight round bars. Newspaper printing machines mostly include automatic conveying system where precision matters a lot. All conveying rollers are therefore made with high precision requiring straight bars as input materials.

Additive manufacturing or 3D printing has become popular in recent times since many intricate shapes can be made through use of CAD or similar software. Use of straight round bars additive manufacturing machines enables precise movements, stability and structural support which ensures reliable printing. The quality output of these machines largely depends on smooth operation printing head which needs to slide over smooth round straight bars called linear guides and axis rods for allowing precise movement in X, Y and Z axes. Round bars are used as support for making stable platforms where precise and positioning accuracy is prime concern. Straight round bars are also used in frame components, support structure and stability which enables 3D printers for printing of complex geometries.

Straight round bars have some use in spacecrafts, satellite and in defence industry for manufacturing of military equipment. Straight round bars are required in aircraft industry for manufacturing of aircraft parts. Large size earthmoving machines and cement industries require use of straight round bars. In recent Indian Space Mission, Vikram Lander uses several instruments that utilized straight round bars. These instruments include Laser Retroreflector Array (LRA) which is a passive optical instrument, Instrument for Lunar Seismic Activity (ILSA) for measuring seismicity around landing site to understand structure of lunar crust and mantle, Alpha Particle X-Ray Spectrometer (APXS) for measuring chemical composition and mineralogical composition of the lunar surface.

In short, straight round bars have tremendous use in industries. Varied product range in innumerable areas including manufacturing industries, scientific laboratories, defence systems, construction industries, aviation industries and spacecrafts use straight round bars which clearly signifies the importance of study and research in bar straightening.

Rods with threads are significant components in CNC machines and 3D printing machines. Although there are about fifteen different important components in 3D printing machines, but one component i.e. Stud or Threaded Rod play a significant role as accuracy of the threaded rod will decide the quality of the product. Threaded rods are made from round straight bars. High accuracy of both roundness and straightness is extremely desirable in these threaded rods for uninterrupted and smooth movement

of tool and printing heads in all directions. The final outcome of the product accuracy will largely depend on the straightness level of the threaded rods. Figure 3.19 show a photograph of a CNC machine where threaded round rods are components in the system [87].

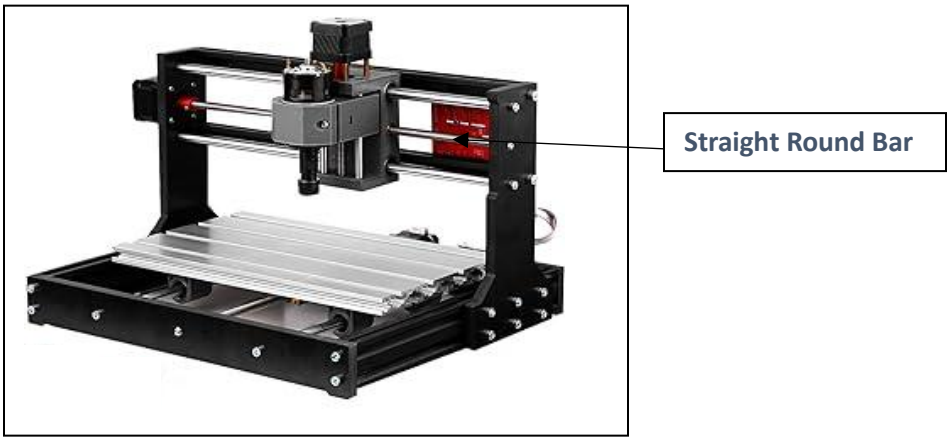

Figure 3.19 5500 mw Upgrade Version CNC 3018 Pro GRBL Control DIY Mini CNC Machine 3 Axis PCB Milling Machine Wood Router Engraver with Offline Controller with ER11 and 5mm Extension Rod Working Area 300*180x40mm [87]

Another model of CNC machine is shown in Figure 3.20 where it is clearly shown that round bars and threaded rods essential components in CNC machine [88].

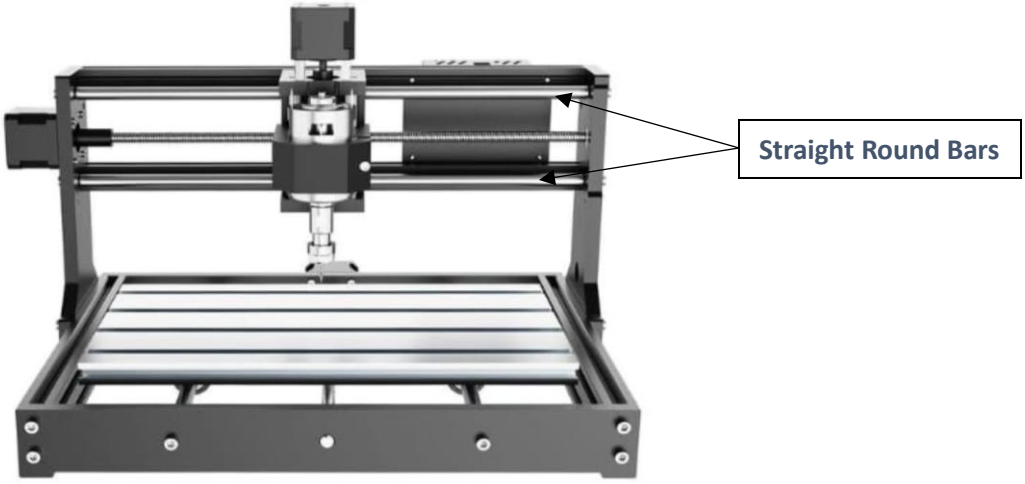

Figure 3.20 Photograph of 3IDEA Two Trees TTC3018S CNC Router Machine with Upgraded CNC Software Including Dust Collection System, End Mills and Router Bits [88]

Hence, it can be stated that there is substantial application of straight round bars in various industrial machines as components. Straightness of round bar used as components is therefore a vulnerable aspect in many industrial machines.

3.7 Discussion

Theoretical aspect being the foundation of any research work has its own importance. In this chapter certain theoretical aspects have been discussed. Basic principle of reverse bending, straightness, working principle and mechanics of bar straightening with certain assumptions have been discussed along with Buaschinger effect. Analysis of bar straightening based on moment-curvature relationship is the gateway of bar straightening. This research has been done keeping statistical aspects in the thought process. Therefore, probabilistic approach to the bar straightening found a place. Since bar straightening is usually a continuous process probability density function has been considered. The salient part of this chapter is discussion on various types of straightening processes and straighteners such as section straightening machine, stretch straightening machine, spinner straighteners, pulse straightening or magnetic pulse straightening, rotary hub-straightening, parallel roller straightening, skew-roll straightening machine and cross-roll straightening machines which includes two-roll straighteners, six-roll straighteners, multi-staggered rolls and cluster-roll straighteners. The mechanics of cross-roll straightening machine has been dealt in detail since most research work is actually centered on this.

A detailed discussion on Helix Angle in cross-roll straightening machine has been made. Effect of Helix Angle in the straightening process is a key parameter that led to develop the criterion for setting helix angle in the cross-roll machine which is one of the key contributions of this research work. The criterion can now be used scientifically as why and how much helix angle should be kept in cross-roll straightening machines. Lastly the chapter indicated applications of straightening in machines and its components that is utility part of the straightening process.

CHAPTER – 4

PROBABILISTIC APPROACH IN STRAIGHTENING PROCESS

4.1 Introduction

Straight bar is extremely useful where some movement of machine parts or components shall take place. Round bars so produced need to meet quality requirements which are sometimes quite stringent based on type of applications. Straight rods are in use as components of machines or as raw materials for manufacturing of components or machinery parts. In wire production industry, straightening of wire is a general requirement after de-coiling. Continuous straightening is a requirement in case of wires. Ferrous and non-ferrous both types of wires require straightening before application.

Bar straightening through cross-roll arrangement enables straightening of bars in continuous manner. However, both the ends still call for further processing since terminal ends usually don't get straightened up easily to acceptable range. Needless to mention that curved bars come with residual curvatures. Even after straightening process elimination of residual curvatures at both ends are extremely difficult. Sometimes, multi-step straightening control system (MSSC) helps in reducing residual curvatures [57].

The round bar chosen for straightening usually has some residual curvature which is actually the final output of previous process. It may be necessary that round bars produced in hot rolling mills would require straightening process depending on nature of applications. Probabilistic approach shall therefore be quite useful in choosing a production lot or a batch of such products which are considered as straight rods. A focus is therefore required on round bars which are subjected in cross roll straightening

machine for straightening purpose under reverse kinematic bending. In cross-roll bar straightening machine, cross rolls are set at an angle called helix angle which actually enables the round bar to move ahead while rotating about its axis in the straightening machine. Since points on the surface is having both axial and rotational movement, it is probabilistic that which point will appear when and what will be the loading condition of the bar at that surface point.

Wherever, bar is not straight it indicates that some amount curvature in a given length segment exists. Therefore, it is important and useful to work on the curvatures of bar in the length segments so that overall process improvement can be done in bar straightening. Since the straightening process will have initially a bar with some curvature called initial curvature will undergo the straightening process to achieve a final curvature, the initial and final residual curvatures will have to be taken into account for overall understanding of the process and its improvement. In the process of bar straightening the bar is actually in rotating motion along with translational motion. Hence, a probabilistic approach on final curvature has been considered for estimation of mean final curvature in any given length segment and standard deviation of the residual curvatures in the length segments of the bars.

4.2 Initial and Final Curvatures of a Round Bar

A round bar which has some initial residual curvature needs to be straightened with a final residual curvature. The desired final curvature value is indeed zero curvature which means bar is completely straight. The bar in the rollers is moving ahead due to cross-rolls set at an angle, α. It cannot be ascertained that which points on the curved surface of the bar will always be subjected to maximum kinematic reverse bending as this event will occur only at a particular situation that maximum curvature point during rotation matches with maximum loading arrangement of cross rolls. It is therefore probabilistic only that to what extent curvature will actually be reduced on each pass of cross-roll arrangement. Various points on outer surface of the rod where curvature actually face different effective reverse bending load. The actual frequency distribution

can be ascertained only after several experiments and data drawn thereof. However, the change in curvature shall indeed be a function of curvature.

The moment-curvature relationship of a round bar during bending operation has already been discussed earlier in Chapter-3. Since the primary concern is about straightness of a bar there is a natural concern on initial residual curvatures, κ_{ri} which after reverse bending will get changed into final residual curvature, κ_{rf}. The process of bar straightening is meaningful only when $\kappa_{rf} < \kappa_{ri}$. Since the round bar in question is under rotation and also progressing through the cross-rolls due to helix angle, it is extremely difficult to say that which section of bar is facing how much reverse kinematic loading due to initial curvature of that section.

If a length of bar with initial curvature -κ_{ri} is to be straightened then bar length should be subjected to loading in the reverse direction either kinematically applying a known moment, or kinematically applying a known curvature causing moment by reverse bending [14]. If the loading is kinematic and the curvature to which the bar length is subjected to final curvature on unloading is κ_{rf}, then the change in residual curvature, $\Delta\kappa_r$ is given by

$$\Delta\kappa_r = \kappa_{rf} - (-\ \kappa_{ri}\ )$$

$$\Delta\kappa_r\ = \kappa_{rf} + \ \kappa_{ri} \qquad (4.1)$$

This curvature change can be expressed as a function of curvature $g(\kappa_r)$. Straightening process involves rotation of bar about its axis, throughput speed, effective bending moment due to kinematic loading. These parameters are visibly observed during complete rotation of the bar. In one complete rotation, the bar will move ahead by its pitch length. Various points of bar's outer surface shall come across different effective bending moment along the bar length. In actual case the bar is continuously in motion and therefore, concept of continuous function is applicable. Final curvature can be evaluated on the basis of initial curvature and expected change in curvature as in Eq.4.1. While the bar is having both rotational and translation motion, it is probabilistic

only that any particular value of final residual curvature will be in the domain of a length segment. A small bar segment at cross-sections between length segment λ_i and λ_{i+1} is subjected to kinematic reverse bending moment M_i. The initial residual curvature of this small segment is considered as κ_{ri} and final residual curvature after straightening process is κ_{rf}.

4.3 Probabilistic Approach in the Analysis of Bar Straightening Process

In article 3.2.3.6, preliminary discussion has been done on the basics of probability with respect to curvature of bar as a variable. Since the process of straightening in cross-roll arrangement is a continuous one, theory of probability has been applied for continuous variable.

A generalized expression given earlier in Eq. (3.18) can be used for probability of occurrence of curvature value at section of any arbitrary cross section of length segment between λ_i and λ_{i+1} or between λ_{i+1} and λ_{i+2} … $\lambda_{i+(n-1)}$ and λ_{i+n} etc. A probability P_i is now considered of occurring maximum reverse bending moment in the length segment λ_i. In case of continuous random variable of residual curvature κ_r for a beam length (a length between the horns of concave roller), probability density function of curvature change is $f_\kappa(\kappa_r)$. Initial residual curvature, κ_{ri} after straightening process will change to final residual curvature κ_{rf}. However, as a generalised case for any length segments λ_i and λ_{i+1}, residual curvatures are $\kappa_{r\lambda i}$ and $\kappa_{r\lambda i+1}$.

In such case, probability of occurring maximum bending moment at length segments λ_i and λ_{i+1} can be expressed in terms of curvatures at these length segments,

$$P(\kappa_{r\lambda i} < \kappa_r < \kappa_{r\lambda i+1}) = \int_{\kappa_{r\lambda i}}^{\kappa_{r\lambda i+1}} f_{\kappa_r}(\kappa_r) d\kappa_r \qquad (4.2)\ [9]$$

It follows then that the corresponding cumulative distribution function (CDF) *of* residual curvature, $F_{\kappa}(\kappa_r)$ can be expressed as below,

$$F_{\kappa}(\kappa_r) = P\,(\kappa_r \leq \kappa_{ri}) = \int_{-\infty}^{\kappa_{ri}} f_{\kappa_r}(\kappa_r) d\kappa_r \qquad (4.3)$$

Accordingly, if $F_{\kappa}(\kappa_r)$ has a first derivative, then from Eq. (4.3)

$$f_{\kappa}(\kappa_r) = \frac{dF_{\kappa}(\kappa_r)}{d\kappa_r} \qquad (4.4)$$

A function being non-negative representing probabilistic distribution of a random variable necessarily satisfy the axioms of probability; the probabilities associated with all possible values of the random variable must add up to unity.

Based on above, it can be stated that, if $F_{\kappa}(\kappa_r)$ is the cumulative distribution function (CDF) of κ_r, then it must have the following properties [75]:

(i) $F_{\kappa}(-\infty) = 0$; $F_{\kappa}(+\infty) = 1$

(ii) $F_{\kappa}(\kappa_r) \geq 0$, and is non-decreasing with κ_r

(iii) It is continuous with κ_r and along the bar length

For any arbitrary segmented length λ_i of bar within cross-roller under reverse kinematic bending,

$$P\,(\kappa_r \leq \kappa_{ri}) = \int_{\lambda_i} f_{\kappa_r}(\kappa_r)\, d\kappa_r \qquad (4.5)$$

In a length segment of λ_i of a bar in process of straightening, P_i, the probability of occurring maximum reduced curvature for a specific pass or final residual curvature κ_{rf} which may be within acceptable range for industrial purpose. This will occur due to maximum effective bending moment or resisting moment arising out of reverse kinematic loading. However, the least curvature is possible only when that particular length segment of rotating bar, λ_i faces an alignment of $\theta=0^{o}$ with loading and osculating plane so that maximum bending moment is available on that segment. If κ_{ri} is the initial residual curvature in the osculating plane, then initial curvature in the loading plane κ_{rl} can be equated as,

$$\kappa = \kappa_{ri} cos\ \theta \qquad (4.6)$$

It is important to note, that both initial residual curvature κ_{ri} and angle θ are certainly random variables as values of these variables at any instances are not known. This is indeed probabilistic that which segment of bar will be subjected to maximum bending moment. This is due to the fact that various parameters are in use in the process i.e. initial residual curvature, κ_{ri}, throughput speed of bar, v_x, radius of bar r, angular speed of bar $\dot{\theta}$ about its longitudinal axis due to cross-roll arrangement of rollers and roller size with radius, R.

As such for mathematical purpose, speed of the motors causing rotation of cross-rolls is assumed to be constant with insignificant variation. In that case throughput speed, i.e. bar speed can also be considered as constant. Roller size and bar size can be considered as constant since variations are insignificant. Therefore, primarily two random variables are in place i.e. initial residual curvature (κ_{ri}) and angle between loading plane and osculating plane (θ).

Considering random bar length segment λ_i with initial residual curvature κ_{ri}, length segment λ_i will come across point of reverse bending under some particular set up of cross-roll arrangements. As the bar is having rotation with angular speed, ω based on r.p.m. of cross-rollers, the particular length segment λ_i with an initial residual curvature κ_{ri} may be at any angle of osculating plane and facing the corresponding kinematic reverse bending load. The situation will certainly occur as a point on bar surface which will be within 0^o to 360^o.

Now, for a length segment of bar, λ_i with initial residual curvature, κ_{ri} shall undergo curvature change, $\Delta\kappa_r$ with effective extra bending moment ΔM required and make new residual curvature or final residual curvature, κ_{rf}. If the probability density functions of the curvature change is $f(\kappa_r)$ or final residual curvature $f_{\kappa_r}(\kappa_{rf})$ for this particular length segment λ_i then, the probability of final residual curvature on that length segment shall be:

$$P(\kappa_{ri} < \kappa_r < \kappa_{rf}) = \int_{\kappa_{ri}}^{\kappa_{rf}} f_{\kappa_r}(\kappa_r) d\kappa_r \quad (4.7)$$

Similar approach can be considered for each small length segment from beginning till end of the bar. Except the terminal ends of the bar, all such length segments will be somewhat subjected to above. It can further be said that, after deformation due to reverse kinematic bending for a length segment of bar region from segment λ_i to segment λ_{i+1}, λ_{i+1} to segment $\lambda_{i+2, \ldots\ldots}$ λ_{n-1} to segment λ_n, probability of occurrence of final residual curvature for entire length of bar can be stated by Eq.(4.8).

$$P(\kappa_{\lambda i} < \kappa_r < \kappa_{\lambda n}) = \int_{\kappa_{\lambda i}}^{\kappa_{\lambda n}} f_{\kappa_r}(\kappa_r) d\kappa_r \quad (4.8)$$

Hence for all practical purposes, it can be stated that probability of final residual curvature of a bar length, L can be put as below as shown in Eq.(4.9).

$$P(\kappa_r) = \int_L f_{\kappa_r}(\kappa_r) d\kappa_r \quad (4.9)$$

Probability density function $f_{\kappa}(\kappa_r)$ can be evaluated by virtue of substantial experimental data of the process. $f(\kappa_r)$ is not a probability; however, $f_{\kappa_r}(\kappa_r)d\kappa_r$ = $P(\kappa_{ri} < \kappa_r < \kappa_{ri} + \Delta\kappa)$ is the probability that values of residual curvature κ_r will be in the interval $(\kappa_r, \kappa_r + \Delta\kappa)$ [9].

It is now possible to calculate probability density function using computer software like Minitab or any other similar software. It may follow some standard distribution. In that case we can straightway deploy that distribution and make estimation of mean value of final curvature.

The expected value of curvature $E(\kappa)$ may be stated by Eq.(4.10):

$$E(\kappa) = \int_{-\infty}^{\infty} \kappa_r f_{\kappa_r}(\kappa_r) d\kappa_r \quad (4.10)$$

It is customary to designate the expected value as mean which is expressed as μ. Hence, for a random continuous variable of residual curvature in a bar, the mean can be expressed by Eq.(4.11).

$$\mu_\kappa = \int_{-\infty}^{\infty} \kappa_r f_{\kappa_r}(\kappa_r)\, d\kappa_r \quad (4.11)$$

Considering residual curvature as a function of residual curvature, then the expected value, *E* of curvature may be estimated by Eq.(4.12)

$$E\,[g(\kappa_r)] = \int_{-\infty}^{\infty} g(\kappa_r)\, f_{\kappa_r}(\kappa_r) d\kappa_r \qquad (4.12)\ [9]$$

where, $g(\kappa_r)$ is a function of residual curvature, κ_r.

Hence, for a random continuous variable of residual curvature in a bar, the mean curvature, μ_κ after the rolling process can be expressed by Eq.(4.13)

$$\mu = \int_{-\infty}^{\infty} g(\kappa_r) f_{\kappa_r}(\kappa_r) d\kappa_r \qquad (4.13)\ [9]$$

In the event, the probability density function of the above equation follows normal distribution then the equation can be expressed by Eq.(4.14)

$$\mu = \int_{-\infty}^{\infty} g(\kappa_r) \frac{1}{\sigma_{\kappa_r}\sqrt{2\pi}} e^{-(\kappa_r-\mu_\kappa)^2/2\sigma_{\kappa_r}^2}\, d\kappa_r \qquad (4.14)\ [9]$$

Here, σ_{κ_r} is the standard deviation of the process. The variance of residual curvature after the rolling process may be expressed as Var (κ_r) and given by Eq. (4.15).

$$\mathrm{Var}(\kappa_r) = \sigma_{\kappa_r}^2 = \int_{-\infty}^{\infty} g(\kappa_r)(\kappa_r-\mu_\kappa)^2 f_{\kappa_r}(\kappa_r) d\kappa_r \qquad (4.15)\ [9]$$

$$= [g(\kappa_r)^2 - \mu_\kappa^2] \qquad (4.16)\ [9]$$

A more convenient measure of dispersion will be standard deviation, σ is given by Eq.(4.17),

$$\sigma_{\kappa_r} = \sqrt{\mathrm{Var}(\kappa_r)} \qquad (4.17)\ [9]$$

Probabilistic approach in the straightening process has led to arrive into the development of mean residual curvature and standard deviation in the continuous process of reduction of residual curvatures in cross-roll arrangement of bar straightening. The usefulness of probability and statistics in the analysis for quality control purposes is well recognized; however, the significance of probabilistic concepts transcends any specific application. Application of probability and statistics, if appropriately used in bar straightening, then it will certainly improve various process parameters. Such probabilistic approach has not been dealt so far in bar straightening process in terms of reduction of residual curvatures.

4.4 Discussion

It is obvious that probabilistic approach has not been practically looked into in earlier researches. With the help of proper database, a more definitive conclusion can be drawn so as to understand the likelihood of reduction of curvatures in cross-roll arrangements, in particular which distribution pattern is exactly followed while reducing the residual curvature in various processes. This probabilistic approach motivates to look into deeply into the process based on statistical approach of residual curvatures. Prediction of number of passes required for reducing the residual curvatures to the desired extent so as to meet the required level of straightness will be possible based on generation of statistical data of the process parameters. Statistical process control can now be considered as scope of present research work in the field of bar straightening which is described in the subsequent chapter.

CHAPTER – 5

STATISTICAL ASPECTS IN BAR STRAIGHTENING

5.1 Introduction

Actual requirement of straightness of round bars depends on deployment of bars either in raw form or after required straightening through kinematic reverse bending with cross-roll straighteners. However, option remains that in precision application, round bars can be machined to required size as per design requirement. Moreover, if material is costly then machining would result in increase of product cost. However, a bent bar can be made straight through reverse kinematic bending either with the help of cross-roll straighteners or by application of load under locking mechanism [63]. The process of bar straightening in cross-roll arrangement essentially begins with the system of cross-rolls with helix angle, α (also termed as roll angle) and roller radius, R or diameter, D which correspond to the equations of throughput speed of bar. A brief discussion on theoretical aspects of bar straightening has been done earlier in Chapter-3.

This chapter deals with statistical aspects of various factors involved in cross-roll straightening and thereupon to look at the significance of experimental design in the process of kinematic reverse bending. Cross-rolls at an angle termed as helix angle is a key parameter in the process. This also causes bars to rotate along the axis and the bar moves forward.

Roller diameter plays another important role in the process. Therefore, roller diameter and helix angle may be considered as two factors and can be employed in experimental design. The present chapter has been focussed on the theoretical aspects of statistical consideration of bar straightening process mainly to understand the significance of

factors like roller diameter, helix angle, bar diameter and modulus of elasticity in the process of straightening. The analysis of variance will show the F-Test value thus enabling to arrive into statistical decision based on the observations. The final residual curvature of bar sections at any segmented length will depend upon roller diameter and helix angle. This chapter specifically deals with statistical approach on Two-Factorial design on residual curvatures. A bar is having an initial residual curvature at various sections of the bar. The final residual curvature will depend upon the bar straightening activity which depends on helix angle and roller diameters. To start with a general arrangement of residual curvatures in factorial design, it is necessary to understand the levels of several factors and replication. An evaluation process of sum of squares has been done considering degrees of freedom on various levels. Further, analysis of variance in tabular form of these factors are done so as to arrive mean squares of the factors like roller diameter, helix angle and their interactions. F-Test is then carried out [10].

Moreover, statistical study of roundness in commercially produced round bars have been done by virtue of experimentation for measurement of roundness of bars. Roundness of all bars is studied for various types of materials and sizes. Analysis of roundness have been done for all these materials with the help of Radar charts. Statistical approach of process control for various types of bars have been looked into. Radar charts prepared for each case of round bars of four different sizes and types of materials to enable understand the variations of deformations present in commercially available bars. All Radar charts also indicate variation of straightness along the length of the bar. Each bar was considered for measurement of diameters at various sections and based on the measured data, statistical process control charts have been prepared. In the statistical process control charts, X-Bar and R charts were considered to check processes followed during production were within lower and upper process control limits.

5.2 Statistical Approach on Two-Factorial Design on Residual Curvature of Cross-Roll Straightening

In the cross-roll straightening process, the rolls are set at angles ±α with the axis of the bar as illustrated in Figure 3.15 [14]. If ω is the angular velocity of the rolls of radius R, throughput velocity v_x and the tangential velocity is v_t of a point on the surface of the bar then it can be said that

$$v_x = \omega R \sin\alpha, \quad \text{and}$$

$$v_t = \omega R \cos\alpha.$$

Based on equations discussed above, it is seen that **helix angle** and **roller diameter** play significant roles in the process of bar straightening. Therefore, helix angle and roller diameters may be considered as factors in factorial design for above process considering one specific bar diameter. However, it is possible to choose bar diameter also as a factor when several bars of various sizes are in consideration. However, at present the focus is on a two-factor factorial design. Through factorial design it may be possible to find a helix angle that is most suitable for the process and can be considered as robust design.

Let us consider the Figure 5.1 below where we have 'a' treatments of roller diameters are to be compared and blocks of helix angles α of 'b' blocks. The randomized complete block design is shown here. There is one observation per treatment in each block, and the order in which the treatments are run within each block is determined randomly.

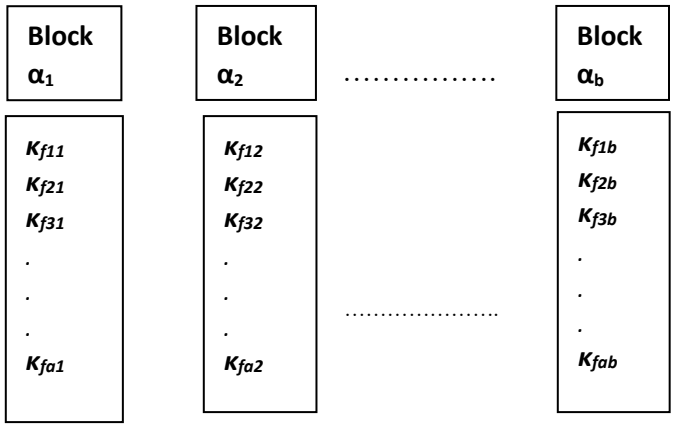

Figure 5.1: Randomised complete block design

The statistical model for the Randomised Complete Block Design (RCBD) can be written in several ways, the traditional model being the effects model. In the present case two factor has been chosen, one being the Roller Diameter (D) and the other being Helix Angle (α). To pass to the general case, let κ_{fijk} be the observed final residual curvature when factor of Roller Diameter (D) is at the ith level (i = 1,2,3, ..a) and factor of Helix Angle (α) is at the jth level (j=1,2,3,…b) for the kth replicate (k= 1,2,3,.. n).

In general, a two-factor factorial experiment has been placed in Table 5.1. The order in which abn observations are taken is selected at random so that this design is a completely randomized design. The observations in a factorial experiment can be described by a model. There are several ways to write the model for a factorial experiment [89].

The effects model for final residual curvature will be,

$$\kappa_{fijk} = \mu + \tau_i + \beta_j + (\tau\beta)_{ij} + \varepsilon_{ijk} \qquad \{i = 1, 2, 3, \ldots, a \quad j = 1,2,3, \ldots.., b \quad k = 1,2,3, \ldots., n\} \qquad (5.1)$$

where μ is the overall mean effect, τ_i is the effect of ith level of the row factor or Roller Diameter (D) factor, β_j is the effect of jth level of the column factor or Helix Angle (α) factor, $(\tau\beta)_{ij}$ is the effect of the interaction between τ_i and β_j, and ε_{ijk} is a random error component.

As a general case, let final residual curvature κ_{fijk} be the observed responses when factor of roller diameter is at i^{th} row (i =1,2,…,a) and factor of helix angle is at j^{th} column (j = 1,2,…,b) for k^{th} replication (k=1,2,…,n).

where,

‘a’ is the level of factor of roller diameter;

‘b’ is the level of factor of helix angle and

‘n’ is the number of replications.

In general, a two-factorial design for helix angle roller diameter can be described as shown in Table 5.1 [10].

Table 5.1 General Arrangement for Final Residual Curvatures in Two-Factor Factorial Design

Factor of Roller Diameter (D_i) for ith level	Factor of Helix Angle for α_j for j^{th} level.			
	α_1	α_2	…	α_b
D_1	$\kappa_{f111}, \kappa_{f112}, \ldots \kappa_{f11n}$	$\kappa_{f121}, \kappa_{f122}, \ldots \kappa_{f12n}$		$\kappa_{f1b1}, \kappa_{f1b2}, \ldots \kappa_{f1bn}$
D_2	$\kappa_{f211}, \kappa_{f212}, \ldots \kappa_{f21n}$	$\kappa_{f221}, \kappa_{f222}, \ldots \kappa_{f22n}$		$\kappa_{f2b1}, \kappa_{f2b2}, \ldots \kappa_{f2bn}$
. . .				
D_a	$\kappa_{fa11}, \kappa_{fa12}, \ldots \kappa_{fa1n}$	$\kappa_{fa21}, \kappa_{fa22}, \ldots \kappa_{fa2n}$		$\kappa_{fab1}, \kappa_{fab2}, \ldots \kappa_{fabn}$

The order in which the abn observations are taken is selected at random so that this design is a completely randomized design. The effects model of the above observations in a factorial experiment can be written by Eq.(5.1).

Both the factors are assumed to be fixed, and the treatment effects are defined as deviations from the overall mean, so that:

for Roller Diameter $\sum_{i=1}^{a} \tau_i = 0$ and (5.2)

for Helix Angle $\sum_{j=1}^{b} \beta_j = 0.$ (5.3)

Similarly, the interaction effects between roller diameter and helix angle are fixed and defined in following way

$$\sum_{i=1}^{a} (\tau\beta)_{ij} = \sum_{j=1}^{b} (\tau\beta)_{ij} = 0. \quad (5.4)$$

If **n** is the number of replications, the number of total observation will be '**abn**'. It is also possible to express factorial experiment through **means model** as below [89].

$$\kappa_{fijk} = \mu_{ij} + \epsilon_{ijk} \quad \{ i = 1,2,\ldots,a \quad \{ j = 1,2,\ldots,b \quad \{ k = 1,2,\ldots,n \quad (5.5)$$

where the mean of the ij^{th} cell is

$$\mu_{ij} = \mu + \tau_i + \beta_j + (\tau\beta)_{ij} \quad (5.6)$$

μ is the overall mean effect of roller diameter and helix angle. In this case two-variable factorial, both variables are of equal interest. Testing hypotheses about the equality of Roller Diameter treatment effects, can be written as

Null Hypothesis $H_0 : \tau_1 = \tau_2 = \ldots. = \tau_a = 0$ (5.7)

Alternate Hypothesis H_1 : at least one $\tau_i \neq 0$ (5.8)

Again, for the equality of helix angle treatment effects, it can be written as

$$H_0 : \beta_1 = \beta_2 = \ldots. = \beta_b = 0 \quad (5.9)$$

$$H_1 : \text{at least one } \beta_j \neq 0 \quad (5.10)$$

In case there is interactions of Roller Diameter and Helix angle, then

$$H_0 : (\tau\beta)_{ij} = 0 \text{ for all } i,j \quad (5.11)$$

$$H_1 : \text{at least one } (\tau\beta)_{ij} \neq 0 \quad (5.12)$$

These hypotheses can be tested using a two-factor analysis of variance.

5.2.1 Statistical Analysis of Roller Diameter and Helix Angle Factors in Cross-Roll Straightening Process

Based on above equations, a statistical analysis is necessary for the final curvatures with respect to both the factors i.e. Roller Diameter and Helix Angle while dealing with bar straightening process [10].

Let $\kappa_{fi..}$ denote the total observations under the i^{th} level of Diameter factor,

$\kappa_{fj.}$ denote the total observations under the j^{th} level of Helix angle factor,

$\kappa_{fij.}$ denote the total of all observations in the ij^{th} cell, and

$\kappa_{f...}$ denote the grand total of all the observations.

It can be defined $\bar{\kappa}_{fi..}$, $\bar{\kappa}_{f.j.}$, $\bar{\kappa}_{fij.}$, and $\bar{\kappa}_{f...}$ as the corresponding row, column, cell and grand averages.

Mathematically we it can be expressed as below:

$$\kappa_{fi\cdot\cdot} = \sum_{j=1}^{b} \sum_{k=1}^{n} \kappa_{fijk} \qquad \bar{\kappa}_{fi\cdot\cdot} = \frac{\kappa_{fi..}}{bn} \qquad i = 1,2,\ldots..,a \qquad (5.13)$$

$$\kappa_{fj\cdot} = \sum_{i=1}^{a} \sum_{k=1}^{n} \kappa_{fijk} \qquad \bar{\kappa}_{fj\cdot} = \frac{\kappa_{f.j.}}{an} \qquad j=1,2,\ldots..,b \qquad (5.14)$$

$$\kappa_{fij\cdot} = \sum_{k=1}^{n} \kappa_{fijk} \qquad \bar{\kappa}_{fij\cdot} = \frac{\kappa_{fij.}}{n} \qquad i = 1,2,\ldots..,a$$

$$j=1,2,\ldots..,b \qquad (5.15)$$

$$\kappa_{f\cdots} = \sum_{i=1}^{a} \sum_{j=1}^{b} \sum_{k=1}^{n} \kappa_{fijk} \qquad \bar{\kappa}_{f\cdot\cdot} = \frac{\kappa_{f...}}{abn} \qquad (5.16)$$

The total corrected sum of squares may be written as

$$\begin{aligned}\sum_{i=1}^{a} \sum_{j=1}^{b} \sum_{k=1}^{n} (\kappa_{fijk} - \bar{\kappa}_{f\cdot\cdot})^2 &= \sum_{i=1}^{a} \sum_{j=1}^{b} \sum_{k=1}^{n} [(\bar{\kappa}_{fi\cdot\cdot} - \bar{\kappa}_{f\cdot\cdot}) + (\bar{\kappa}_{fj\cdot} - \bar{\kappa}_{f\cdot\cdot}) \\ &\quad + (\bar{\kappa}_{fij\cdot} - \bar{\kappa}_{fi\cdot\cdot} - \bar{\kappa}_{fj\cdot} + \bar{\kappa}_{f\cdot\cdot}) + (\kappa_{fijk} - \bar{\kappa}_{fij\cdot})]^2 \\ &= bn \sum_{i=1}^{a} (\bar{\kappa}_{fi\cdot\cdot} - \bar{\kappa}_{f\cdot\cdot})^2 + an \sum_{j=1}^{b} (\bar{\kappa}_{fj\cdot} - \bar{\kappa}_{f\cdot\cdot})^2 \\ &\quad + n \sum_{i=1}^{a} \sum_{j=1}^{b} (\bar{\kappa}_{fij\cdot} - \bar{\kappa}_{fi\cdot\cdot} - \bar{\kappa}_{fj\cdot} + \bar{\kappa}_{f\cdot\cdot})^2 \\ &\quad + \sum_{i=1}^{a} \sum_{j=1}^{b} \sum_{k=1}^{n} (\kappa_{fijk} - \bar{\kappa}_{fij\cdot})^2 \qquad (5.17)\end{aligned}$$

It can be further expressed the above in a simplified manner as below.

Total sum of squares (SS_T) has been partitioned into:

a sum of squares due to factor of Roller Diameter, (SS_{RD});

a sum of squares due to factor of Helix Angle, (SS_{HA});

a sum of squares due to interaction between Roller Diameter and Helix Angle (SS_{RDHA});

a sum of squares due to error (SS_E).

Symbolically, it can be stated as $SS_T = SS_{RD} + SS_{HA} + SS_{RDHA} + SS_E$

The number of degrees of freedom associated with each sum of squares is shown in Table 5.2.

Degree of freedom essentially represents the number of independent pieces of information available for the purpose of estimation of variability of the dataset. It also means that number of free observations that can vary independently. The physical interpretation of degree of freedom in the present case will be based on number of roller sizes, number of helix angles, number of bar sizes or number of types of materials that

are free to vary for which final residual curvatures have been theoretically considered or actually measured as observations. In this case for two-factor factorial design, roller diameters, (a-1) values are free to vary where 'a' is the level of factor of roller diameter. Similarly, for helix angle (b-1) values are free to vary where 'b' is the level factor of helix angle. For combined effect of factors of Roller Diameter and Helix angle degree of freedom will be (a-1)(b-1) and for error degree of freedom is ab(n-1). The total of all these degree of freedom is the summation of all above which is (abn-1) as shown in Table 5.2.

Table 5.2 Table of Effect and Degrees of Freedom for Roller Diameter, Helix Angle and Their Interaction

Effect	Degrees of Freedom
Roller Diameter (RD)	a-1
Helix Angle (HA)	b-1
Roller Diameter & Helix Angle Interaction (RDHA)	(a-1) (b-1)
Error (E)	ab(n-1)
Total	abn-1

Mean Squares (MS) can be evaluated from each sum of squares divided by its degrees of freedom and can be expressed as:

$$MS_{RD} = \frac{SS_{RD}}{a-1}, \quad MS_{HA} = \frac{SS_{HA}}{b-1}, \quad MS_{RDHA} = \frac{SS_{RDHA}}{(a-1)(b-1)}, \quad MS_{E} = \frac{SS_{RD}}{ab(n-1)} \qquad (5.18)$$

Expected values of the mean squares can be evaluated as below:

$$E(MS_{RD}) = E\left(\frac{SS_{RD}}{a-1}\right) = \sigma^2 + \frac{bn\sum_{i=1}^{a}\tau_i^2}{a-1} \qquad (5.19)$$

$$E(MS_{HA}) = E\left(\frac{SS_{HA}}{b-1}\right) = \sigma^2 + \frac{an\sum_{j=1}^{b}\beta_i^2}{b-1} \qquad (5.20)$$

$$E(MS_{RDHA}) = E\left(\frac{SS_{RDHA}}{(a-1)(b-1)}\right) = \sigma^2 + \frac{n\sum_{i=1}^{a}\sum_{j=1}^{b}(\tau\beta)_{ij}^2}{(a-1)(b-1)} \qquad (5.21)$$

and $$E(MS_{E}) = E\left(\frac{SS_{E}}{ab(n-1)}\right) = \sigma^2 \qquad (5.22)$$

If it is assumed that model is adequate and that the error terms ϵ_{ijk} are normally and independently distributed with constant variance σ^2, then each of the ratios of mean squares MS_{RD}/MS_E, MS_{HA}/MS_E, MS_{RDHA}/MS_E is distributed as F with **a-1, b-1 and (a-1)(b-1)** numerators degree of freedom, respectively, and **ab(n-1)** denominator degrees of freedom, and the critical region would be the upper tail of the F distribution.

5.2.2 Analysis of Variance (ANOVA) for Final Residual Curvature

The final residual curvature has been analysed by using ANOVA based on the variables of roller diameter (RD) and helix angle (HA) in the cross-roll bar straightening process. The usual procedure is to employ a statistical software package to conduct an ANOVA. However, mathematical computing of the sums of squares is necessary for developing the software. Analysis of variance (ANOVA) for the two variables RD, HA and its corresponding interaction factor (RDHA) along with its error(e) component is described in Table-5.3. The usual procedure is to employ a statistical software package to conduct an ANOVA. However, computation of the sums of squares is straight forward as shown in Table 5.3 [10].

Table 5.3 ANOVA Table for Roller Diameter and Helix Angle

Source of Variation	Sum of Squares	Degrees of Freedom	Mean Square	F_0
Roller Diameter (RD) Treatments	SS_{RD}	a-1	$MS_{RD} = \frac{SS_{RD}}{a-1}$	$F_0 = \frac{MS_{RD}}{MS_E}$
Helix Angle (HA) Treatments	SS_{HA}	b-1	$MS_{HA} = \frac{SS_{HA}}{b-1}$	$F_0 = \frac{MS_{HA}}{MS_E}$
Interactions between Roller Diameter & Helix Angle	SS_{RDHA}	(a-1) (b-1)	$MS_{RDHA} = \frac{SS_{RDHA}}{(a-1)(b-1)}$	$F_0 = \frac{MS_{RDHA}}{MS_E}$
Error	SS_E	ab(n-1)	$MS_E = \frac{SS_{RD}}{ab(n-1)}$	
Total	SS_T	abn-1		

The total sum of squares is computed as

$$SS_T = \sum_{i=1}^{a} \sum_{j=1}^{b} \sum_{k=1}^{n} \kappa_{fijk}^2 - \frac{\kappa_{f...}^2}{abn} \quad (5.23)$$

The sums of squares for the main effects are

$$SS_{RD} = \frac{1}{bn} \sum_{i=1}^{a} \kappa_{fi..}^2 - \frac{\kappa_{f...}^2}{abn} \quad (5.24)$$

$$SS_{HA} = \frac{1}{an} \sum_{j=1}^{b} \kappa_{f.j.}^2 - \frac{\kappa_{f...}^2}{abn} \quad (5.25)$$

For the purpose of convenience, SS_{RDHA} may be evaluated in two stages. First, computation on the sum of squares between the ab cell totals, which may be termed as sum of squares due to "sub-totals":

$$SS_{Subtotals} = \frac{1}{n} \sum_{i=1}^{a} \sum_{j=1}^{b} \boldsymbol{\kappa_{fij.}^2} - \frac{\kappa_{f...}^2}{abn} \quad (5.26)$$

The sum of squares also contains SS_{RD} and SS_{HA}. Therefore, the second step is to compute SS_{RDHA} as

$$SS_{RDHA} = SS_{Subtotals} - SS_{RD} - SS_{HA} \quad (5.27)$$

We may compute SS_E by subtraction as

$$SS_E = SS_T - SS_{RDHA} - SS_{RD} - SS_{HA} \quad (5.28)$$

or, $$SS_E = SS_T - SS_{Subtotals}$$

The theoretical aspects of bar straightening have been briefly discussed with prime consideration of using statistical theories considering two important process variables i.e. roller diameter and helix angle in the cross-roll bar straightening process. It is pertinent to consider that roller diameter and helix angle of rollers play significant roles in the process which is easily understood from the various equations. Considering variables like Roller diameter and Helix angle as factors, it is essential to understand the significance of the observations of final curvatures based on above under different values of both factors. Statistical aspects have been reasonably detailed like sum of squares and means thereof have been evaluated based on curvature values. A systematic approach conducted earlier [10] has been taken to arrive into mean square values based on factors and their interactions along with error term. The degrees of freedom for both the factors have been taken care of based on their levels.

Application of ANOVA based on two factors of helix angle and roller diameter has become now quite simple. The above process shall hold good by F- Test and compare the value from the F-Table so as to arrive into statistical conclusion for an appropriate hypothesis. Inclusion of other factors like type of material i.e. elastic modulus of bar material and bar diameter have also been taken into consideration. Obviously, considering more factors for ANOVA will make the study more elaborate. This type of investigation may develop useful tool for justification of role and importance on various factors in the process of bar straightening which can certainly form the basis for process improvement.

5.2.2.1 Three and Four Factor Factorial Design in ANOVA

In the two factors consideration, one factor was Roller Diameter while the other factor was Helix Angle. Here an attempt has been made to consider Bar diameter as a factor (B).

Considering the results for the two-factor factorial design may be extended to the general case where there are a levels of Roller Diameter factor D, b levels of Helix Angle factor α, c levels of Bar Diameter factor B arranged in a factorial experiment. In general, there will be $abc\ldots n$ total observations if there are n replicates of the complete experiments [89].

If all factors in the experiments are fixed, we may easily formulate and test hypotheses about the main effects and interactions using ANOVA. For a fixed effects model, test statistics for each main effect and interaction may be constructed by dividing the corresponding mean square for the effect or interaction by the mean square error. All of these F tests will be upper-tail, one-tail tests. The number of degrees of freedom for any main effect is the number of levels of the factor minus one, and the number of degrees of freedom for an interaction is the product of the number of degrees of freedom associated with the individual components of the interaction [89].

Considering the present case of three-factor analysis of variance model of final residual curvatures in bar straightening process:

$$\kappa_{ijkl} = \mu + \tau_i + \beta_j + \gamma_k + (\tau\beta)_{ij} + (\tau\gamma)_{ik} + (\beta\gamma)_{jk} + (\tau\beta\gamma)_{ijk} + \epsilon_{ijkm}$$

$$\{\ i = 1,2,\ldots,a$$

$$\{\ j = 1,2,\ldots,b$$

$$\{\ k = 1,2,\ldots,c$$

$$\{\ m = 1,2,\ldots,n \qquad (5.29)$$

where, μ is the overall mean effect of the roller diameter, helix angle and bar diameter,

τ_i is the effect of the i^{th} level of Roller Diameter (D) factor

β_j is the effect of the j^{th} level of Helix Angle (α) factor

γ_k is the effect of the k^{th} level of Bar Diameter (B) factor

$(\tau\beta)_{ij}$ is the effect of interaction between τ_i and β_j

$(\tau\gamma)_{ik}$ is the effect of interaction between τ_i and γ_k

$(\beta\gamma)_{jk}$ is the effect of interaction between β_j and γ_k

$(\tau\beta\gamma)_{ijk}$ is the effect of interactions among τ_i, β_j and γ_k

ϵ_{ijkm} is the random error component.

All the three factors are assumed to be fixed, and the treatment effects are defined as deviations from overall mean, so that

for Roller Diameter (D), $\sum_i^a \tau_i = 0$ (5.30)

for Helix Angle (α), $\sum_j^b \beta_j = 0$ and (5.31)

for Bar Diameter (B), $\sum_k^c \gamma_k = 0$ (5.32)

Similarly, the interaction effects among roller diameter (D), helix angle (α) and bar diameter (B) are fixed and defined in following way

$$\sum_i^a (\tau\beta)_{ij} = \sum_j^b (\tau\gamma)_{ik} = \sum_k^c (\beta\gamma)_{jk} = 0 \qquad (5.33)$$

Since there are *n* replicates of the experiment, there are *abcn* observations.

Assuming that D, α and B are fixed, the analysis of variance table is shown in Table 5.4.

The *F* tests on main effects and interactions follow directly from the expected mean squares. Usually, the ANOVA computations would be done using statistical software package. However, occasionally manual computing formulas for the sums of squares as in Table 5.4 is useful. The total sum of squares is found in the usual way as

$$SS_T = \sum_{i=1}^a \sum_{j=1}^b \sum_{k=1}^c \sum_{m=1}^n \kappa_{ijkm}^2 - \frac{\kappa_{....}^2}{abcn}$$

The sum of squares for the main effects is found from the totals for factors D($\kappa_{i...}$), α($\kappa_{.j..}$), B($\kappa_{..k.}$) as follows:

$$SS_D = \frac{1}{bcn} \sum_{i=1}^a \kappa_{i...}^2 - \frac{\kappa_{....}^2}{abcn} \qquad (5.34)$$

$$SS_\alpha = \frac{1}{acn} \sum_{j=1}^b \kappa_{.j..}^2 - \frac{\kappa_{....}^2}{abcn} \qquad (5.35)$$

$$SS_B = \frac{1}{abn} \sum_{l=1}^c \kappa_{..k.}^2 - \frac{\kappa_{....}^2}{abcn} \qquad (5.36)$$

To compute the two-factor interaction sums of squares, the totals for the D×α, D×B, and α×B cells are needed. It is frequently helpful to collapse the original data table into three two-way tables to compute these quantities. The sums of squares are found from

$$SS_{D\alpha} = \frac{1}{cn} \sum_{i=1}^a \sum_{j=1}^b \kappa_{ij..}^2 - \frac{\kappa_{....}^2}{abcn} - SS_D - SS_\alpha \qquad (5.37)$$

$$= SS_{Subtotals(D\alpha)} - SS_D - SS_\alpha \qquad (5.38)$$

$$SS_{DB} = \frac{1}{bn} \sum_{i=1}^a \sum_{k=1}^c \kappa_{i.k.}^2 - \frac{\kappa_{....}^2}{abcn} - SS_D - SS_B \qquad (5.39)$$

$$= SS_{Subtotals(DB)} - SS_D - SS_B \qquad (5.40)$$

and

$$SS_{\alpha B} = \frac{1}{an} \sum_{j=1}^b \sum_{l=1}^c \kappa_{.jk.}^2 - \frac{\kappa_{....}^2}{abcn} - SS_\alpha - SS_B \qquad (5.41)$$

$$= SS_{Subtotals(\alpha B)} - SS_\alpha - SS_B \qquad (5.42)$$

$SS_{D\alpha B} = \frac{1}{n}\sum_{i=1}^{a}\ \sum_{j=1}^{b}\ \sum_{k=1}^{c}\ \kappa_{ijk.}^{2} - \frac{\kappa_{....}^{2}}{abcn}$ - SS_D - SS_α - SS_B

- $SS_{D\alpha}$ - SS_{DB} - $SS_{\alpha B}$ (5.43)

$= SS_{Subtotals(D\alpha B)}$ - SS_D - SS_α - SS_B - $SS_{D\alpha}$ - SS_{DB} - $SS_{\alpha B}$ (5.44)

where,

$\kappa_{i...}$ denote the total of all observations under the i^{th} level of Roller Diameter factor (D),

$\kappa_{.j..}$ denote the total of all observations under the j^{th} level of Helix Angle factor (α),

$\kappa_{..k.}$ denote the total of all observations under the k^{th} level of Bar Diameter factor (B),

$\kappa_{....}$ denotes grand total of all observations.

The error sum of squares may be found by subtracting the sum of squares for each main effect and the interaction from the total sum of squares or by

$$SS_\epsilon = SS_T - SS_{Subtotals(D\alpha B)} \quad (5.45)$$

Mean squares of the factors in three-factor factorials and treatments are as below:

$$MS_D = \frac{SS_D}{a-1} \quad (5.46)$$

$$MS_\alpha = \frac{SS_\alpha}{b-1} \quad (5.47)$$

$$MS_B = \frac{SS_\alpha}{c-1} \quad (5.48)$$

$$MS_{D\alpha} = \frac{SS_{D\alpha}}{(a-1)(b-1} \quad (5.49)$$

$$MS_{DB} = \frac{SS_{DB}}{(a-1)(c-1_)} \quad (5.50)$$

$$MS_{\alpha\beta} = \frac{SS_{\alpha\beta}}{(b-1)(c-1)} \quad (5.51)$$

$$MS_{D\alpha\beta} = \frac{SS_{D\alpha\beta}}{(a-1)(b-1)(c-1)} \quad (5.52)$$

$$MS_\epsilon = \frac{SS_\epsilon}{abc(n-1)} \quad (5.53)$$

5.2.2.2 Analysis of Variance (ANOVA) for Final Residual Curvature on Three-Factor Factorial Design

The final residual curvature has been analysed by using ANOVA based on variables of roller diameter (D), helix angle (α) and bar diameter (B) in the cross-roll bar

straightening process. Analysis of variance (ANOVA) for the three variables D, α and B and their corresponding interaction factors Dα, DB, αB and DαB along with its error (ϵ) component is described in Table 5.4.

Table 5.4: The Analysis of Variance Table for the Three-Factor Fixed Effects Model

Source of variation	**Sum of Squares**	**Degrees of Freedom**	**Mean Square**	F_0
Roller Diameter(D)	SS_D	a-1	MS_D	$F_0 = \frac{MS_D}{MS_\epsilon}$
Helix Angle (α)	SS_α	b-1	MS_α	$F_0 = \frac{MS_\alpha}{MS_\epsilon}$
Bar Diameter (B)	SS_B	c-1	MS_B	$F_0 = \frac{MS_B}{MS_\epsilon}$
Dα	$SS_{D\alpha}$	(a-1)(b-1)	$MS_{D\alpha}$	$F_0 = \frac{MS_{D\alpha}}{MS_\epsilon}$
DB	SS_{DB}	(a-1)(c-1)	MS_{DB}	$F_0 = \frac{MS_{DB}}{MS_\epsilon}$
αB	$SS_{\alpha B}$	(b-1)(c-1)	$MS_{\alpha B}$	$F_0 = \frac{MS_{\alpha B}}{MS_\epsilon}$
DαB	$SS_{D\alpha B}$	(a-1)(b-1)(c-1)	$MS_{D\alpha B}$	$F_0 = \frac{MS_{D\alpha B}}{MS_\epsilon}$
Error	SS_ϵ	abc(n-1)	MS_ϵ	
Total	SS_T	$abcn$-1		

5.2.2.3 Four-Factor Factorial Design of Final Residual Curvatures in Bar Straightening

Considering the case of four-factor analysis of variance model of final residual curvatures in bar straightening process:

$$\kappa_{ijkl} = \mu + \tau_i + \beta_j + \gamma_k + d_l + (\tau\beta)_{ij} + (\tau\gamma)_{ik} + (\beta\gamma)_{jk} + (\tau d)_{il} + (\beta d)_{jl} + (\gamma d)_{kl} + (\tau\beta\gamma)_{ijk} + (\tau\beta d)_{ijl} + (\tau\gamma d)_{ikl} + (\beta\gamma d)_{jkl} + (\tau\beta\gamma d)_{ijkl} + \epsilon_{ijklm}$$

$$\begin{aligned} &\{\ i = 1,2,\ldots,a \\ &\{\ j = 1,2,\ldots,b \\ &\{\ k = 1,2,\ldots,c \\ &\{\ l = 1,2,\ldots,d \\ &\{\ m = 1,2,\ \ldots,n \end{aligned} \qquad (5.54)$$

where, μ is the overall mean effect of the roller diameter, helix angle, bar diameter and modulus of elasticity

τ_i is the effect of the i^{th} level of Roller Diameter (D) factor

β_j is the effect of the j^{th} level of Helix Angle (α) factor

γ_k is the effect of the k^{th} level of Bar Diameter (B) factor

d_l is the effect of the l^{th} level of Modulus of Elasticity (E) factor

$(\tau\beta)_{ij}$ is the effect of interaction between τ_i and β_j

$(\tau\gamma)_{ik}$ is the effect of interaction between τ_i and γ_k

$(\beta\gamma)_{jk}$ is the effect of interaction between β_j and γ_k

$(\tau d)_{il}$ is the effect of interaction between β_j and γ_k

$(\beta d)_{jl}$ is the effect of interaction between β_j and d_l

$(\gamma d)_{kl}$ is the effect of interaction between γ_l and d_l

$(\tau\beta\gamma)_{ijk}$ is the effect of interactions among τ_i, β_j and γ_k

$(\tau\beta d)_{ijl}$ is the effect of interactions among τ_i, β_j and d_l

$(\tau\gamma d)_{ikl}$ is the effect of interactions among τ_i, γ_k and d_l

$(\beta\gamma d)_{jkl}$is the effect of interactions among β_j, γ_k and d_l

$(\tau\beta\gamma d)_{ijkl}$ is the effect of interactions among τ_i, β_j, γ_k and d_l

ϵ_{ijkl} is the random error component.

All the three factors are assumed to be fixed, and the treatment effects are defined as deviations from overall mean, so that

for Roller Diameter (D), $\sum_i^a \tau_i = 0$ (5.55)

for Helix Angle (α), $\sum_j^b \beta_j = 0$ (5.56)

for Bar Diameter (B), $\sum_k^c \gamma_k = 0$ and (5.57)

for Modulus of Elasticity (E), $\sum_l^d d_l = 0$ (5.58)

Similarly, the interaction effects among roller diameter (D), helix angle (α), bar diameter (B) and modulus of elasticity (E) are fixed and defined in following way

$$\sum_i^a (\tau\beta)_{ij} = \sum_j^b (\tau\gamma)_{ik} = \sum_k^c (\beta\gamma)_{jk} = \sum_m^d (\tau d)_{il}$$

$$= \sum_m^d (\beta d)_{jl} = \sum_l^d (\gamma d)_{kl} = 0 \quad (5.59)$$

Since there are *n* replicates of the experiment, there are *abcdn* observations.

Assuming that D, α , d and E are fixed, the analysis of variance table is shown in Table 5.5.

The *F* tests on main effects and interactions follow directly from the expected mean squares. Usually, the ANOVA computations would be done using statistical software package. However, occasionally manual computing formulas for the sums of squares as in Table 5.5 is useful. The total sum of squares is found in the usual way as

$$SS_T = \sum_{i=1}^{a} \sum_{j=1}^{b} \sum_{k=1}^{c} \sum_{l=1}^{d} \sum_{m=1}^{n} \kappa_{ijklm}^2 - \frac{\kappa_{.....}^2}{abcdn} \quad (5.60)$$

The sum of squares for the main effects is found from the totals for factors D($\kappa_{i...}$), α($\kappa_{.j..}$), B($\kappa_{..k.}$) and E($\kappa_{...l}$) as follows:

$$SS_D = \frac{1}{bcdn} \sum_{i=1}^{a} \kappa_{i....}^2 - \frac{\kappa_{.....}^2}{abcdn} \quad (5.61)$$

$$SS_\alpha = \frac{1}{acdn} \sum_{j=1}^{b} \kappa_{.j...}^2 - \frac{\kappa_{.....}^2}{abcdn} \quad (5.62)$$

$$SS_B = \frac{1}{abdn} \sum_{k=1}^{c} \kappa_{..k..}^2 - \frac{\kappa_{.....}^2}{abcdn} \quad (5.63)$$

$$SS_E = \frac{1}{abcn} \sum_{l=1}^{d} \kappa_{...l.}^2 - \frac{\kappa_{.....}^2}{abcdn} \quad (5.64)$$

To compute the two-factor interaction sums of squares, the totals for the D×α, D×B, and α×B cells are needed. It is frequently helpful to collapse the original data table into three two-way tables to compute these quantities. The sums of squares are found from

$$SS_{D\alpha} = \frac{1}{cn} \sum_{i=1}^{a} \sum_{j=1}^{b} \kappa_{ij..}^2 - \frac{\kappa_{.....}^2}{abcdn} - SS_D - SS_\alpha \quad (5.65)$$

$$= SS_{Subtotals(D\alpha)} - SS_D - SS_\alpha \quad (5.66)$$

$$SS_{DB} = \frac{1}{bn} \sum_{i=1}^{a} \sum_{k=1}^{c} \kappa_{i.l.}^2 - \frac{\kappa_{.....}^2}{abcdn} - SS_D - SS_B \quad (5.67)$$

$$= SS_{Subtotals(DB)} - SS_D - SS_B \quad \text{and} \quad (5.68)$$

$$SS_{\alpha B} = \frac{1}{an} \sum_{j=1}^{b} \sum_{k=1}^{c} \kappa_{.jk.}^2 - \frac{\kappa_{.....}^2}{abcdn} - SS_\alpha - SS_B \quad (5.69)$$

$$= SS_{Subtotals(\alpha B)} - SS_\alpha - SS_B \quad (5.70)$$

$$SS_{D\alpha B} = \frac{1}{n}\sum_{i=1}^{a}\sum_{j=1}^{b}\sum_{k=1}^{c}\kappa_{ijk.}^{2} - \frac{\kappa_{....}^{2}}{abcdn}$$

$$- SS_D - SS_\alpha - SS_B - SS_{D\alpha} - SS_{DB} - SS_{\alpha B} \quad (5.71)$$

$$= SS_{Subtotals(D\alpha B)} - SS_D - SS_\alpha - SS_B - SS_{D\alpha} - SS_{DB} - SS_{\alpha B} \quad (5.72)$$

$$SS_{D\alpha E} = \frac{1}{n}\sum_{i=1}^{a}\sum_{j=1}^{b}\sum_{l=1}^{d}\kappa_{ijl.}^{2} - \frac{\kappa_{....}^{2}}{abcdn}$$

$$- SS_D - SS_\alpha - SS_B - SS_{D\alpha} - SS_{DB} - SS_{\alpha B} \quad (5.73)$$

$$= SS_{Subtotals(D\alpha B)} - SS_D - SS_\alpha - SS_B - SS_{D\alpha} - SS_{DB} - SS_{\alpha B} \quad (5.74)$$

$$SS_{DBE} = \frac{1}{n}\sum_{i=1}^{a}\sum_{k=1}^{c}\sum_{l=1}^{d}\kappa_{ikl.}^{2} - \frac{\kappa_{....}^{2}}{abcdn}$$

$$- SS_D - SS_B - SS_E - SS_{DB} - SS_{DE} - SS_{BE} \quad (5.75)$$

$$= SS_{Subtotals(DBE)} - SS_D - SS_B - SS_E - SS_{DB} - SS_{DE} - SS_{BE} \quad (5.76)$$

$$SS_{\alpha BE} = \frac{1}{n}\sum_{j=1}^{b}\sum_{k=1}^{c}\sum_{l=1}^{d}\kappa_{jkl.}^{2} - \frac{\kappa_{....}^{2}}{abcdn}$$

$$- SS_D - SS_B - SS_E - SS_{DB} - SS_{DE} - SS_{BE} \quad (5.77)$$

$$= SS_{Subtotals(DBE)} - SS_D - SS_B - SS_E - SS_{DB} - SS_{DE} - SS_{BE} \quad (5.78)$$

The error sum of squares may be found by subtracting the sum of squares for each main effect and the interaction from the total sum of squares or by

$$SS_\epsilon = SS_T - SS_{Subtotals(DBE)} \quad (5.79)$$

where,

$\kappa_{i....}$ denote the total of all observations under the i^{th} level of Roller Diameter factor (D),

$\kappa_{.j...}$ denote the total of all observations under the j^{th} level of Helix Angle factor (α),

$\kappa_{..k..}$ denote the total of all observations under the k^{th} level of Bar Diameter factor (B),

$\kappa_{...l.}$ denote the total of all observations under l^{th} level of Elastic Modulus factor (E),

$\kappa_{.....}$ denotes grand total of all observations.

Mean squares of the factors in four-factor factorials and treatments are as below:

$$MS_D = \frac{SS_D}{a-1} \quad (5.80)$$

$$MS_\alpha = \frac{SS_\alpha}{b-1} \quad (5.81)$$

$$MS_B = \frac{SS_\alpha}{c-1} \quad (5.82)$$

$$MS_{D\alpha} = \frac{SS_{D\alpha}}{(a-1)(b-1} \quad (5.83)$$

$$MS_{DB} = \frac{SS_{DB}}{(a-1)(c-1_)} \quad (5.84)$$

$$MS_{\alpha\beta} = \frac{SS_{\alpha\beta}}{(b-1)(c-1)} \quad (5.85)$$

$$MS_{DE} = \frac{SS_{DE}}{(a-1)(d-1)} \quad (5.86)$$

$$MS_{\alpha E} = \frac{SS_{\alpha E}}{(b-1)(d-1)} \quad (5.87)$$

$$MS_{BE} = \frac{SS_{BE}}{(c-1)(d-1)} \quad (5.88)$$

$$MS_{D\alpha\beta} = \frac{SS_{D\alpha\beta}}{(a-1)(b-1)(c-1)} \quad (5.89)$$

$$MS_{D\alpha E} = \frac{SS_{D\alpha E}}{(a-1)(b-1)(d-1)} \quad (5.90)$$

$$MS_{DBE} = \frac{SS_{DBE}}{(a-1)(c-1)(d-1)} \quad (5.91)$$

$$MS_{\alpha BE} = \frac{SS_{\alpha BE}}{(b-1)(c-1)(d-1)} \quad (5.92)$$

$$MS_{D\alpha BE} = \frac{SS_{D\alpha BE}}{(a-1)(b-1)(c-1)(d-1)} \quad (5.93)$$

$$MS_\epsilon = \frac{SS_\epsilon}{abcd(n-1)} \quad (5.94)$$

Table 5.5: The Analysis of Variance Table for the Four-Factor Fixed Effects Model

Source of variation	Sum of Squares	Degrees of Freedom	Mean Square	F_0
Roller Diameter(D)	SS_D	*a*-1	MS_D	$F_0 = \frac{MS_D}{MS_\epsilon}$
Helix Angle (α)	SS_α	*b-1*	MS_α	$F_0 = \frac{MS_\alpha}{MS_\epsilon}$
Bar Diameter (B)	SS_d	*c-1*	MS_B	$F_0 = \frac{MS_B}{MS_\epsilon}$
Modulus of Elasticity (E)	SS_E	*d-1*	MS_E	$F_0 = \frac{MS_E}{MS_\epsilon}$
Dα	$SS_{D\alpha}$	(*a*-1)(*b*-1)	$MS_{D\alpha}$	$F_0 = \frac{MS_{D\alpha}}{MS_\epsilon}$
DB	SS_{DB}	(*a*-1)(*c*-1)	MS_{DB}	$F_0 = \frac{MS_{DB}}{MS_E}$

αB	$SS_{\alpha B}$	(*b*-1)(*c*-1)	$MS_{\alpha B}$	$F_0 = \frac{MS_{\alpha B}}{MS_\epsilon}$
DE	SS_{DE}	(*a*-1)(*d*-1)	MS_{DE}	$F_0 = \frac{MS_{DE}}{MS_\epsilon}$
αE	$SS_{\alpha E}$	(*b*-1)(*d*-1)	$MS_{\alpha E}$	$F_0 = \frac{MS_{\alpha E}}{MS_\epsilon}$
BE	SS_{BE}	(*c*-1)(*d*-1)	MS_{BE}	$F_0 = \frac{MS_{BE}}{MS_\epsilon}$
DαB	$SS_{D\alpha B}$	(*a*-1)(*b*-1)(*c*-1)	$MS_{D\alpha B}$	$F_0 = \frac{MS_{D\alpha B}}{MS_\epsilon}$
DαE	$SS_{D\alpha E}$	(*a*-1)(*b*-1)(*d*-1)	$MS_{D\alpha E}$	$F_0 = \frac{MS_{D\alpha E}}{MS_\epsilon}$
DBE	SS_{DBE}	(*a*-1)(*c*-1)(*d*-1)	MS_{DBE}	$F_0 = \frac{MS_{DBE}}{MS_\epsilon}$
αBE	$SS_{\alpha BE}$	(*b*-1)(*c*-1)(*d*-1)	$MS_{\alpha BE}$	$F_0 = \frac{MS_{\alpha BE}}{MS_\epsilon}$
DαBE	$SS_{D\alpha BE}$	(*a*-1)(*b*-1)(*c*-1)(*d*-1)	$MS_{D\alpha BE}$	$F_0 = \frac{MS_{D\alpha BE}}{MS_\epsilon}$
Error	SS_ϵ	*abcd*(*n*-1)	MS_ϵ	
Total	SS_T	*abcdn*-1		

5.3 Statistical Approach for Study of Roundness in Commercially Produced Round Metal Bars.

Roundness of bars is a matter of concern which is evident from various research work. Cylindrical components are indispensable part in engineering products. Therefore, roundness may be considered almost fundamental form tolerance for cylindrical components and has direct influence on the product performance [17]. The stability of a measurement system for precision working of ball screw had been investigated by using a Monte Carlo simulation to establish bias, linearity accuracy [90]. A study on optimization of surface roughness and circularity deviation during drilling on CNC machine of different Aluminium alloys was conducted. Waviness measurement of cylindrical surfaces had been conducted by the use of V-block method and the accuracy of the measurements had also been analyzed. Statistical tool ANOVA was used in the design of experiment and presented to predict optimum value of surface roughness and circularity deviation and experimental value [91, 92]. An interesting study by on

circularity or roundness had been investigated by V-Block method during turning of a bar where effect of roundness had been analysed by surface plot [93].

Cuesta et al. [94] investigated dimensional accuracy in precision additive manufacturing for direct metal printing machines. An important investigation had been carried out by Görög [95] by measuring the roundness of cylindrical and conical surface. It had been indicated that measurement accuracy is defined as the closeness of agreement between a measured quantity value and a real quantity value of a measure i.e., the quantity intended to be measured which is often limited by calibration errors.

5.4 Experimentation for Measurement of Deformations

To study and analyse roundness of bars, an experimental study has been conducted by taking sample of such bars. Sample bars are taken one by one and have been placed over V-Blocks. Each bar is then considered for measurement of deflections, if any through dial gauges over small length segments along the bar length. The experimental arrangement for measurement of straightness and roundness of bars is shown in Figure 5.2. Small length segments have been chosen to understand the variation of deviations along the length of rod. The process is repeated throughout each bar at an interval of about 3-mm to 10-mm along the bar length. Readings through dial gauges were taken and data recorded. Four types of round bars are chosen of different diameters. Bar diameters are measured at different positions of a section and mean diameters at each section are evaluated. Materials of bars chosen are Mild steel (MS), Stainless steel (SS), Aluminium (Al) and Copper (Cu). Moreover, it is also assumed that naturally sagging over small length segments are insignificant and can be ignored for present study.

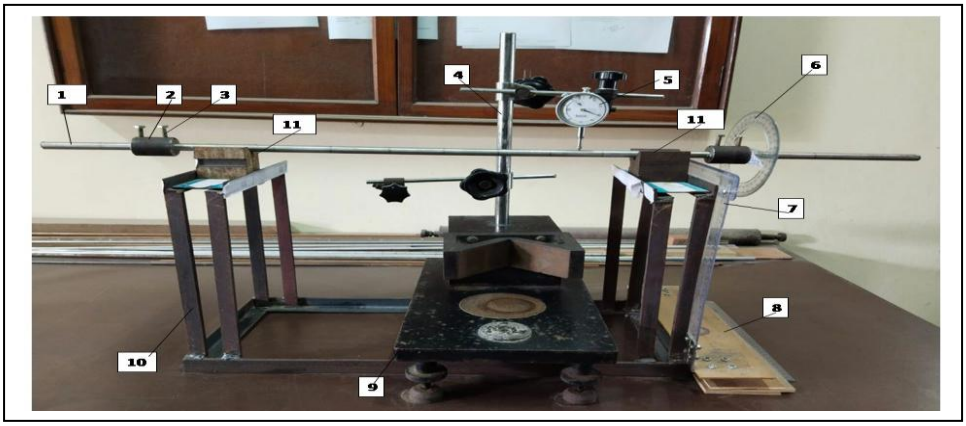

Figure 5.2 Photograph of Experimental Set up for Dial Gauge Measurement of Roundness [12].

[Note: 1-Round Bar, 2-Cylindrical Round Bar Holder, 3-Tightening Screw, 4-Dial Gauge Stand, 5-Dial Gauge, 6-Protractor Screwed with Bar Holder, 7-Horizontal and Vertical Scales for Datum purpose, 8-Levelers, 9-Base of Dial Gauge, 10-Fixture with base, 11-V-Block]

5.4.1 Step by step procedure of recording experimental results

1. Selection of metal round bars. In the present case 6-mm, 8-mm, 10-mm, 12-mm diameter round metal bars of mild steel, stainless steel, aluminium and copper material have been chosen.
2. To consider one round metal bar out of 16 bars, in this case 6-mm diameter Mild Steel (MS) round bar was chosen first. Later, 8-mm, 10-mm, 12-mm bars were taken into consideration one by one.
3. Insertion of round bar in the "Bar Holders" at both ends and tightened by bolts.
4. The round bar with bar holders has been placed over 'V-Blocks' in the experimental set up.
5. Dial Gauge mounted and ensured that gauge head of the dial gauge spindle touches the top surface of the round bar.
6. One end of the bar holder is fitted with a protractor. It is ensured that protractor reading is at zero degree and aligned with bar axis perpendicularly.

7. The distance from one end of bar to the point where dial gauge head of spindle touches on the round bar is recorded.
8. First reading taking at zero degree position. The protractor and round bar is in integrated condition. The protractor has now been rotated by 15^{o} position in counter-clock direction and dial gauge reading recorded. Similarly, the protractor has been rotated again at 30^{o} position and dial gauge reading noted. The process has been continued till 360^{o} rotation is completed at the interval of 15^{o}.
9. After the first set of reading is taken, the round bar is pushed horizontally and now the dial gauge is again at zero degree position at new length segment of the bar. The reading has been noted for 0^{o} position. The process of taking readings at 15^{o} to 360^{o} at the intervals of 15^{o} again carried out for the new position along the length of the bar.
10. The process of measurement continued till the round bar is reached on the other measurable end position. Measurement can not be taken at extreme ends because a small length segment is within the bar holder.
11. This measurement is complete for one dataset. Similar measurements for same length segments for more datasets can be generated. The mean values of each recording dataset to be evaluated and all mean values are to be considered for graphical plots of Radar chart and Surface plot charts. The mean values are considered as final data of measurements.
12. After the complete measurement of one round bar of 6-mm diameter, another round bar, say 8-mm Mild Steel to be taken into consideration. Similar measurement process to be continued and data to be recorded. The process to be continued for 10-mm, 12-mm MS round bars and for round bars of 6-mm, 8-mm, 10-mm and 12-mm Stainless Steel(SS), Aluminium (Al) and Copper(Cu) materials.

13. All these data were recorded for 'Before Straightening'. All sixteen sets of measurements were done systematically.
14. After straightening process, all round bars to be measured in the similar manner and data recordings to be obtained.

    A supplementary video demonstrating the experimental procedure and performance is included in the soft copy for uploading in 'Shodhganga' so that future researchers would be benefitted.

5.5 Results of Roundness of Metal Bars before Straightening.

Round bars of mild steel, stainless steel, aluminium and copper were taken of 6-mm, 8-mm, 10-mm and 12-mm diameters respectively. These bars were placed on two V-Blocks supported in a fixture and deflections were measured by using Dial Gauge as shown in Figure 5.2. Ball of the dial gauge has been so placed that it touches the topmost point on the surface of the round bar. Data have been measured for angles from 0^o to 360^o at an interval angle of 15^o for each length segments of the bars. Dial gauge readings taken at the periphery of the round bar have been noted. For each position, 12 sets of experimental data have been generated by measuring deflections using dial gauge and mean values of each round bar were determined.

Dataset of these mean values before straightening of Mild Steel (MS) round bars of 6-mm, 8-mm, 10-mm and 12-mm diameters are described in detail which are available in corresponding GitHub link [96]. Similarly, the dataset of mean deflection values before straightening of Stainless Steel (SS), Aluminium (Al) and Copper (Cu) for sizes 6-mm, 8-mm, 10-mm and 12-mm diameter round bars are also described in details which are available in the corresponding GitHub links [97], [98], [99].

From these datasets, it is revealed that straightness in the round bar at various sections actually varies and this variation is observed throughout length of the bars**.** It can be said that statistical analysis helps to understand whether a produced lot can be readily accepted or whether calls for further mechanical treatment before actual deployment.

5.5.1 Data Representation

The distribution of numerical data values has been represented by the box plot analysis for comparison of values between multiple graphs. Figures 5.3 to 5.18 show the different kind of box plot analysis of dial gauge deflection values for all the four metal bars under study as an important step of data collection. These are used to interpret in the form of graphical box plot with mean, median, the maximum and minimum observation range, quartile range and outlier points of statistical dataset of each rod, which motivates us to initiate the use of different kinds of statistical analysis to optimise the production process. Though it is demonstrating the comparisons of range and distribution for the large random dataset of a group in a well mannered visual representation system with outlier values but it is not revealing the distribution pattern of deflection values as shown in these figures. However, the variable and continuous collected data of deflection values along the length segment of the bars is summarised and seen that mean, median and outlier values are different for different bar materials of different sizes. To allow the outlier values in box plots, scales on the axes are set in different ranges. The measured data have different representation thus it is not holding any specific pattern of variations in deflection data. So, to understand that pattern it can be further analysed by using statistical process control method and analysis of Radar Charts for optimisation purpose.

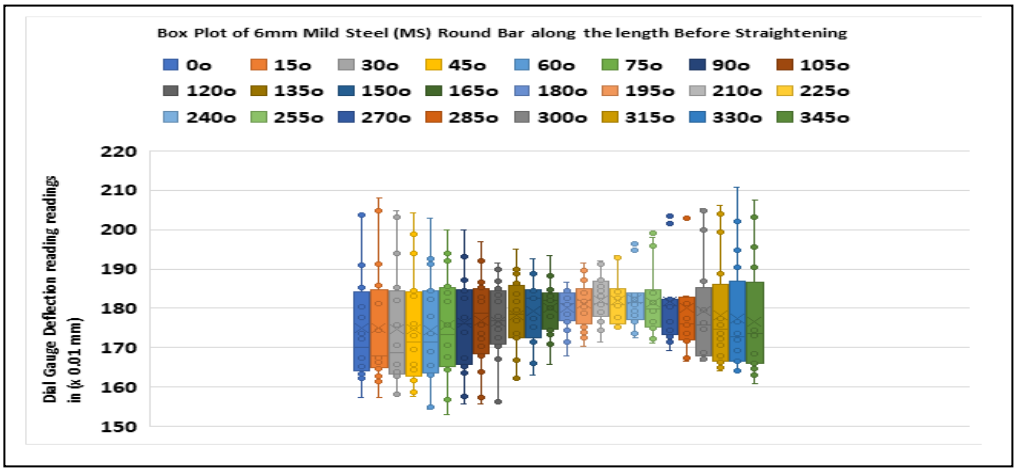

Figure 5.3 Box Plot Analysis of Mean Values of Dial Gauge Deflection Readings of 6-mm Diameter Mild Steel (MS) Round Bar before Straightening.

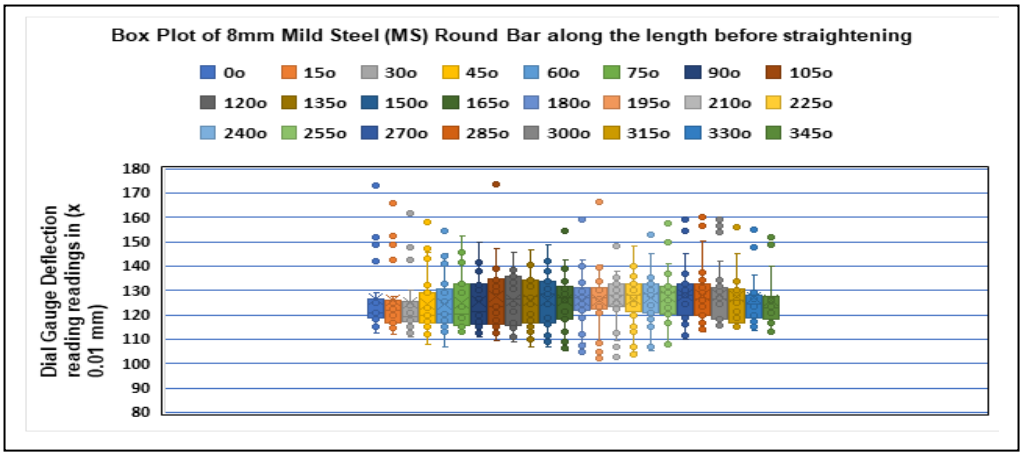

Figure 5.4 Box Plot of Mean Values of Dial Gauge Deflection Readings of 8-mm Diameter Mild Steel (MS) Round Bar before Straightening

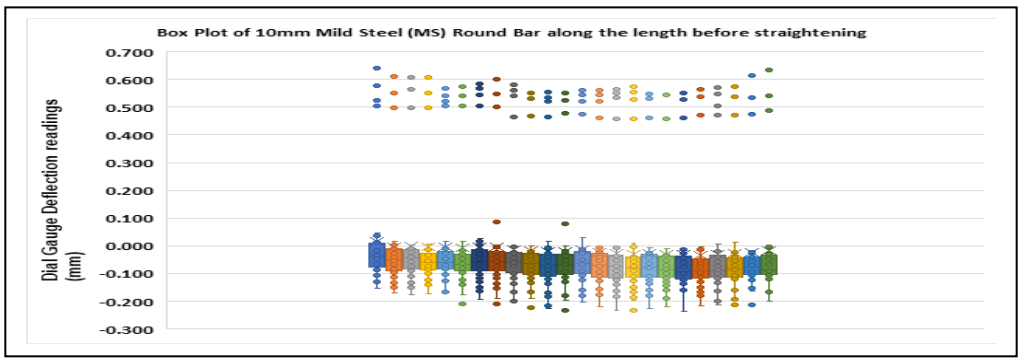

Figure 5.5 Box Plot of Mean Values of Dial Gauge Deflection Readings of 10-mm Diameter Mild Steel (MS) Round Bar before Straightening

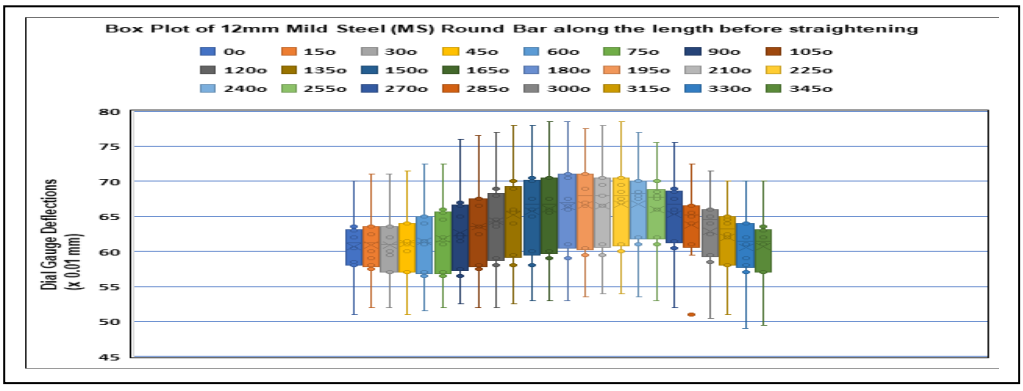

Figure 5.6 Box Plot of Mean Values of Dial Gauge Deflection Readings of 12-mm Diameter Mild Steel (MS) Round Bar before Straightening

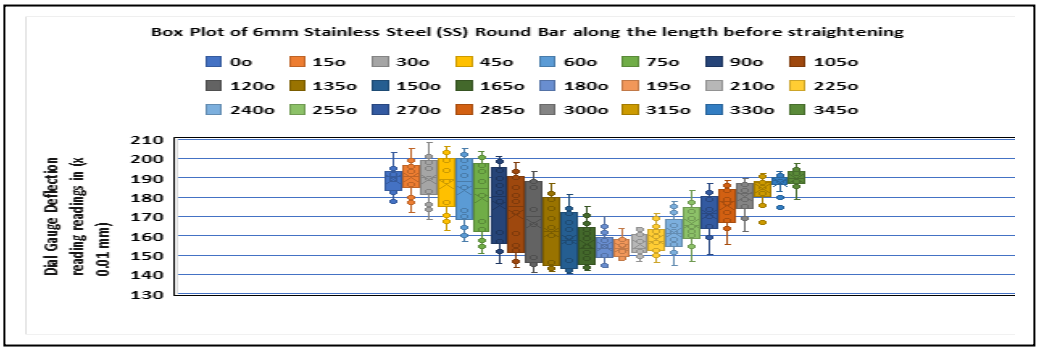

Figure 5.7 Box Plot of Mean Values of Dial Gauge Deflection Readings of 6-mm Diameter Stainless Steel (SS) Round Bar before Straightening.

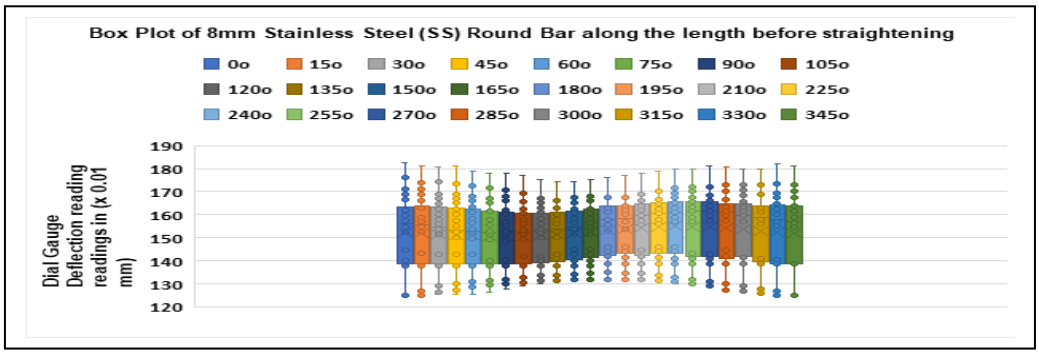

Figure 5.8 Box Plot of Mean Values of Dial Gauge Deflection Readings of 8-mm Diameter Stainless Steel (SS) Round Bar before Straightening

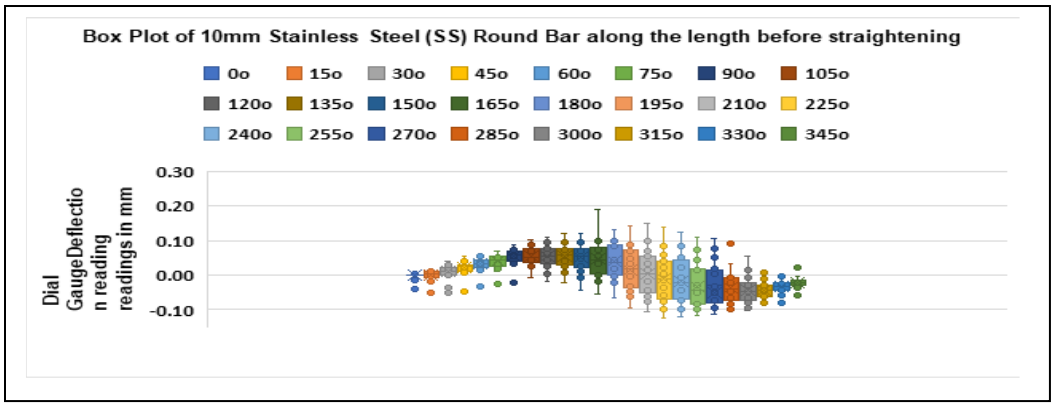

Figure 5.9 Box Plot of Mean Values of Dial Gauge Deflection Readings of 10-mm Diameter Stainless Steel (SS) Round Bar before Straightening

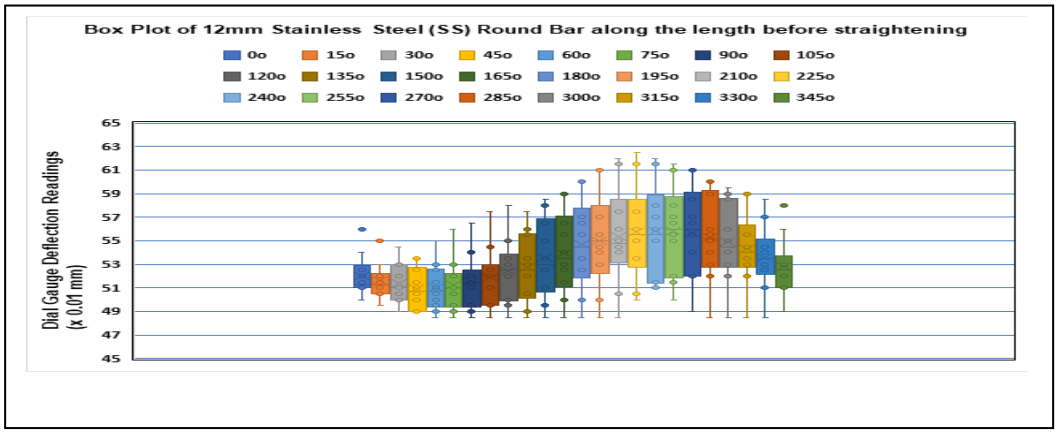

Figure 5.10 Box Plot of Mean Values of Dial Gauge Deflection Readings of 12-mm Diameter Stainless Steel (SS) Round Bar before Straightening

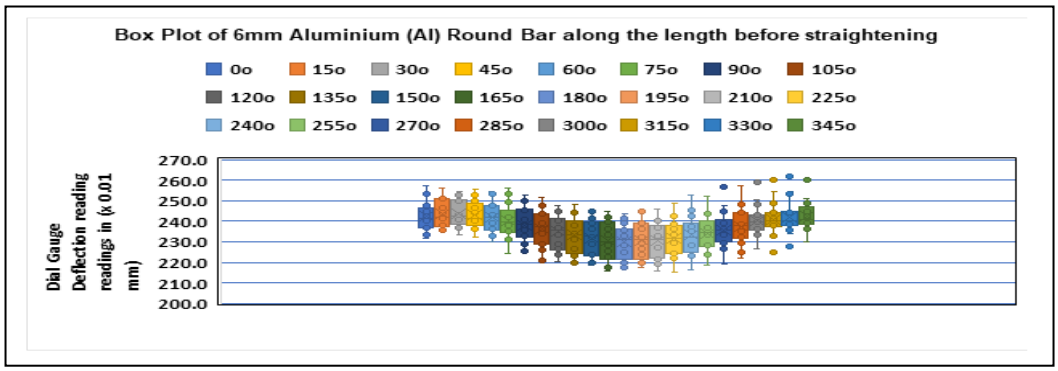

Figure 5.11 Box Plot of Mean Values of Dial Gauge Deflection Readings of 6-mm Diameter Aluminium (Al) Round Bar before Straightening

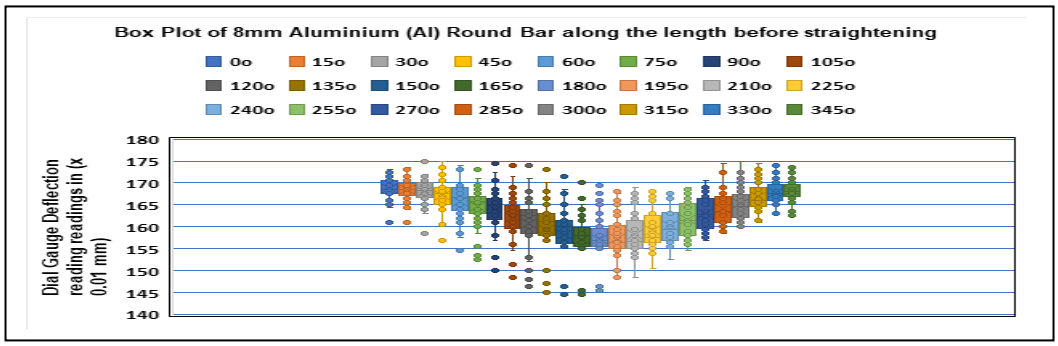

Figure 5.12 Box Plot of Mean Values of Dial Gauge Deflection Readings of 8-mm Diameter Aluminium (Al) Round Bar before Straightening

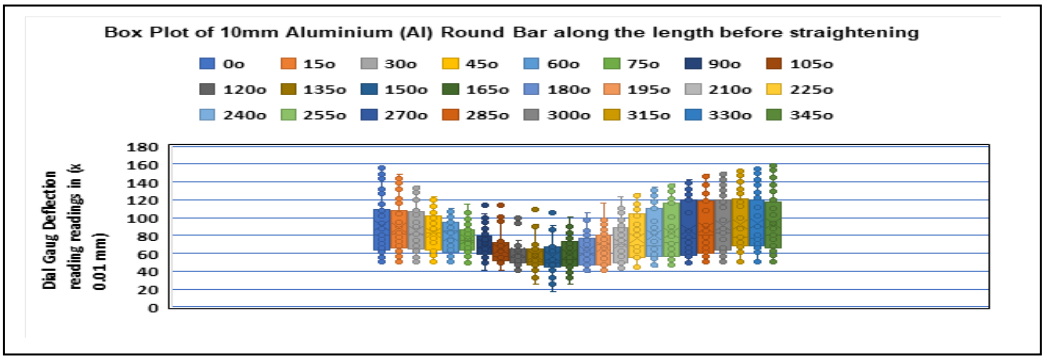

Figure 5.13 Box Plot of Mean Values of Dial Gauge Deflection Readings of 10-mm Diameter Aluminium (Al) Round Bar before Straightening

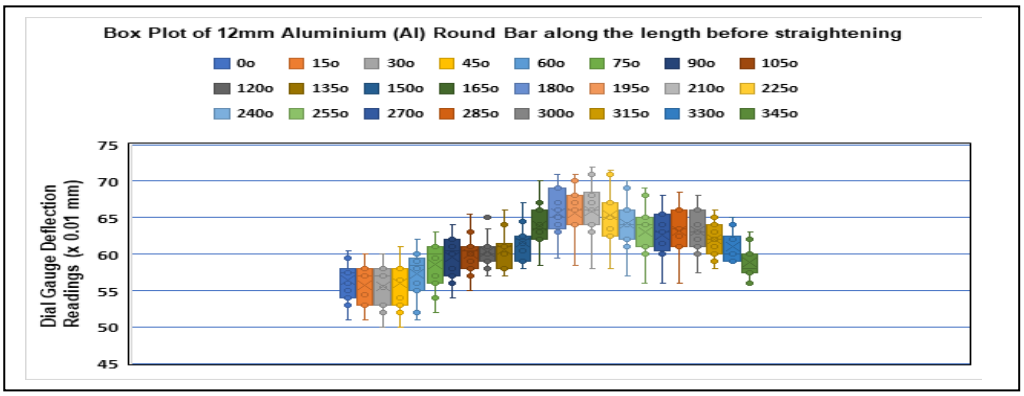

Figure 5.14 Box Plot of Mean Values of Dial Gauge Deflection Readings of 12-mm Diameter Aluminium (Al) Round Bar before Straightening

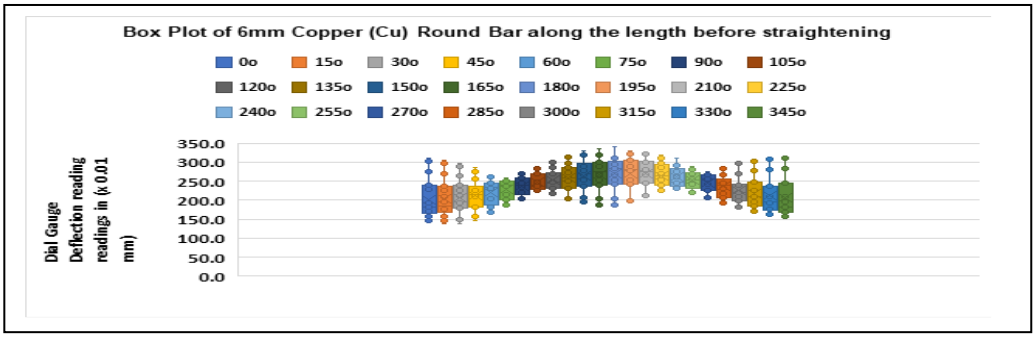

Figure 5.15 Box Plot of Mean Values of Dial Gauge Deflection Readings of 6-mm Diameter Copper (Cu) Round Bar before Straightening

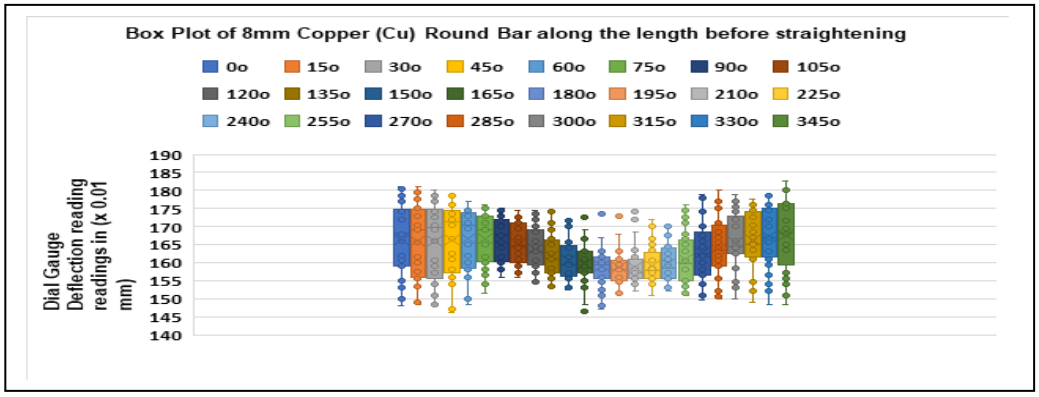

Figure 5.16 Box Plot of Mean Values of Dial Gauge Deflection Readings of 8-mm Diameter Copper (Cu) Round Bar before Straightening.

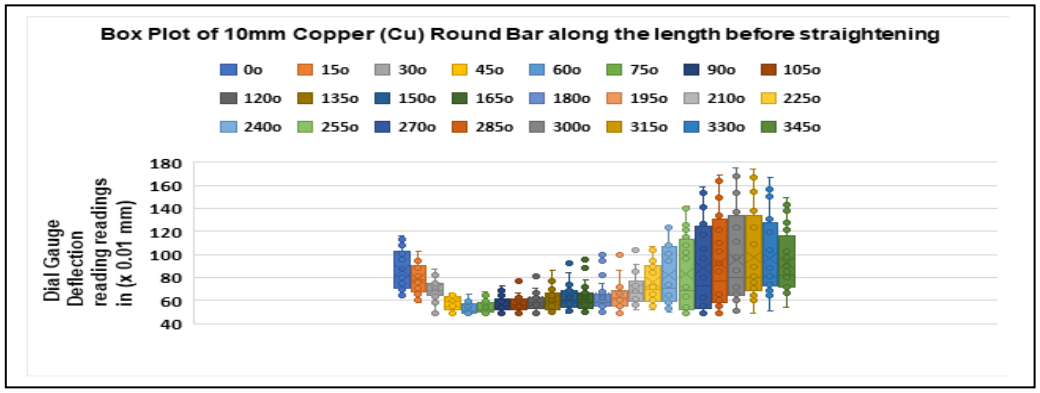

Figure 5.17 Box Plot of Mean Values of Dial Gauge Deflection Readings of 10-mm Diameter Copper (Cu) Round Bar before Straightening

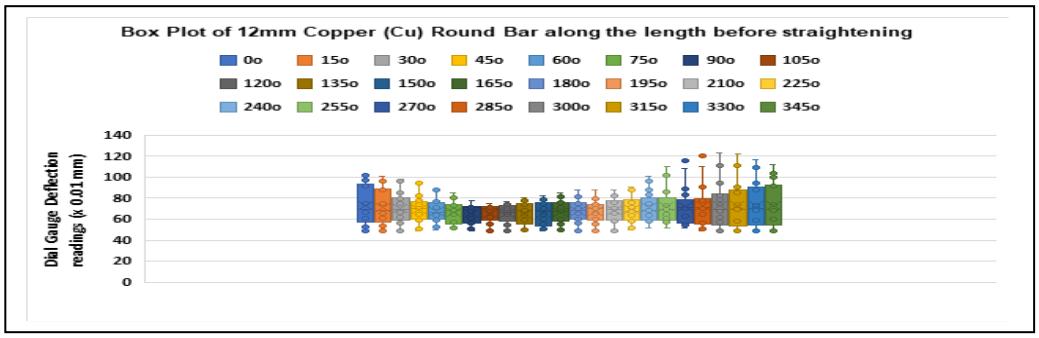

Figure 5.18 Box Plot of Mean Values of Dial Gauge Deflection Readings of 12-mm Diameter Copper (Cu) Round Bar before Straightening

It is known that material strength wise, elastic modulus of Mild Steel (MS) is about 210 GPa. It is seen that variations of deflections not only exist but also not uniform at various sections or length segments of Mild Steel round bars. This indicates that there is a variation in the circularity of the round bar even if the strength of bar is quite high. Although stainless steel bears elastic modulus of about 310 GPa, but it is seen that variations of deflections exist in SS rods also indicating variation in the roundness in case of strong bars too. Like Mild Steel, Stainless Steel round bars, the measurements were taken for Aluminium and Copper rods. Elastic modulus of Aluminium is about 69 GPa while in Copper it is about 120 GPa. It is seen that variations of deflections exist both in Aluminium and Copper rods also which indicates that variation in circularity not only exist in ferrous bars of high strength materials but also in case of relatively less stronger non-ferrous materials of lesser value of modulus of elasticity.

5.6 Analysis of Roundness

Each round bar was measured in several length segments and deflection data was recorded which have been considered for analysis. Circumferential measurement of deflections have been analysed by using Radar charts which have been generated through MS Excel for each of Mild steel, Stainless steel, Aluminium and Copper materials of round bars of sizes 6-mm, 8-mm, 10-mm and 12-mm respectively. These charts are shown in Figures 5.19 to Figure 5.22 based on the datasets. From all the Radar charts in these figures, it is quite clear that variation exist in circularity of round bar of mild steel, stainless steel, aluminium and copper bars.

The overall roundness is observed from the Radar chart at different bar sections. The acceptability of the roundness of such bars in raw state will somewhat depend on the application of raw material and the final product. It is quite possible that such circularity is acceptable for direct application in most of general-purpose work while in precision-based applications such circularity may not be acceptable and further processing like machining or cold working may require before actual application. An

interesting finding from above dataset is that standard deviation for roundness is in general lower both in Mild steel and Stainless steel which indicates better roundness in comparison to Aluminium and Copper bars. This motivated towards statistical analysis of round bars.

5.6.1 Radar Charts of Mild Steel Round Bars Before Straightening

Figure 5.19 shows the Radar chart of 6-mm, 8-mm, 10-mm and 12-mm diameter Mild Steel round bars where deflection data of measurements have been recorded at 15^{o} interval circumferentially and at various sections along the length of the bar before straightening. As stated above 12 sets of measurements data were recorded for one single rod at length segments from one end at distances 16.3 cm, 20 cm, 25 cm, 30 cm, 35 cm, 40 cm, 45 cm, 50 cm, 55 cm, 60 cm, 65 cm, 70 cm, 75 cm, 80 cm, 85 cm and 93 cm of the 6-mm diameter mild steel round bar and mean values of these data at each length segments and angular position were evaluated based on the dataset [96].

12 sets of measurements data were recorded for one single rod at length segments from one end at distances 12 cm, 17 cm, 22 cm, 27 cm, 32 cm, 36 cm, 40 cm, 45 cm, 50 cm, 55 cm, 60 cm, 65 cm, 70 cm, 75 cm, 80 cm, 85 cm, 90 cm, 95 cm, 101.3 cm, 106.3 cm, 111.3 cm, 116.3 cm, 121.3 cm, 126.3 cm, 131.3 cm, 136.3 cm and 141.3 cm of the 8-mm Mild Steel round bar and mean values of these data were evaluated based on dataset [96].

12 sets of measurements data were recorded for one single rod at length segments from one end at distances at 14.5 cm, 17 cm, 20 cm, 23.5 cm, 26 cm, 29 cm, 31.5 cm, 34 cm, 37 cm, 40 cm, 43 cm, 46 cm, 49 cm, 52 cm, 55 cm, 58 cm, 61 cm, 64 cm, 67 cm, 70 cm, 73 cm, 76 cm, 79 cm, 82 cm, 85 cm, 88 cm, 91 cm, 94 cm, 97 cm, 100 cm, 102 cm, 104 cm, 107 cm, 111 cm, 114 cm, 118 cm, 122 cm, 127 cm, 131 cm, 138 cm of the 10-mm Mild Steel round bar and mean values of these data were evaluated based on dataset [96].

12 sets of measurements data were recorded for one single rod at length segments from one end at distances at 12 cm, 22.5 cm, 32.5 cm, 42.5 cm, 52.5 cm, 62.5, 72.5 cm, 82.5 cm, 92.5 cm, 103.5 cm of the 12 mm Mild Steel round bar and mean values of these data were evaluated based on dataset [96].

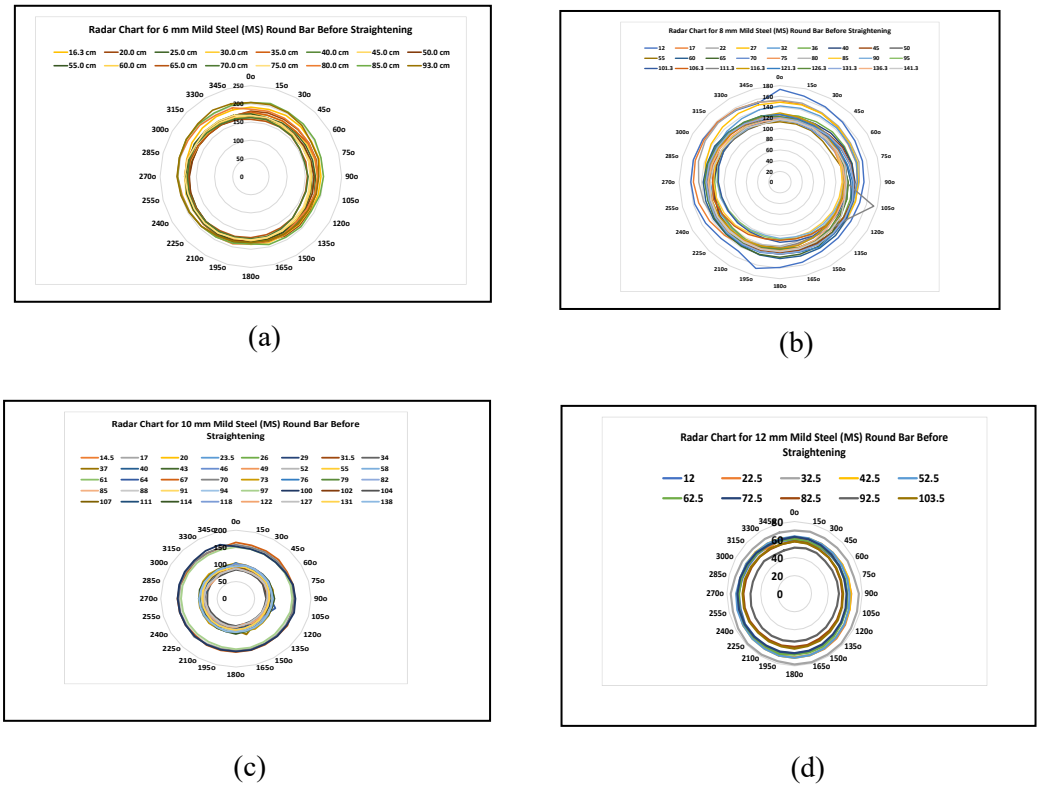

(a) (b)

(c) (d)

Figure 5.19. Radar Charts of (a) 6-mm, (b) 8-mm, (c) 10-mm and (d) 12-mm Diameter Mild Steel (MS) Round Bars

Peripheral lines show the variation of the circularity while variation of straightness is visible from different coloured peripheral lines.

5.6.2 Radar Charts of Stainless Steel Round Bars Before Straightening

Figure 5.20 shows the Radar chart of 6-mm, 8-mm, 10-mm and 12-mm diameter Stainless Steel round bar where deflection data of measurements have been recorded at 15^{o} interval circumferentially and at various sections along the length segments at distances from one end of the bar before straightening. 12 sets of measurements data were recorded for one single rod at length segments from one end at distances at 15 cm, 20 cm, 25 cm, 30 cm, 35 cm, 40 cm, 45 cm, 50 cm, 54 cm, 57.5 cm, 62.5 cm, 66.5 cm, 71.5 cm, 75.3 cm of the 6 mm Stainless Steel round bar and mean values of these data were evaluated based on dataset [97].

12 sets of measurements data were recorded for one single rod at length segments from one end at distances at 11 cm, 14 cm, 18 cm, 21 cm, 24 cm, 28 cm, 32 cm, 35 cm, 38 cm, 41 cm, 44 cm, 47 cm, 50 cm, 53 cm, 57 cm, 61 cm, 65 cm, 69 cm, 73 cm, 77 cm, 80 cm, 84 cm, 88 cm, 92.7 cm, 95.7 cm, 99.7 cm, 103.7 cm, 108.2 cm, 111.7 cm, 114.7 cm, 117.7 cm, 120.7 cm, 120.7 cm, 124.7 cm, 128.7 cm, 132.7 cm, 135.7 cm, 141.7 cm of the 8-mm Stainless Steel round bar and mean values of these data were evaluated based on dataset [97].

12 sets of measurements data were recorded for one single rod at length segments from one end at distances at 11.3 cm, 11.6 cm, 13 cm, 13.7 cm, 15 cm, 15.7 cm, 17 cm, 17.7 cm, 19.7 cm, 20 cm, 21.7 cm, 23 cm, 24.7 cm, 25 cm, 26.7 cm, 27 cm, 29.7 cm, 30 cm, 31.7 cm, 32 cm, 34 cm, 34.7 cm, 36.7 cm, 37.5 cm of the 10-mm Stainless Steel round bar and mean values mean values of these data were evaluated based on dataset [97]. Variation of the circularity and straightness is visible from different coloured peripheral lines.

12 sets of measurements data were recorded for one single rod at length segments from one end at distances at 11 cm, 15 cm, 20 cm, 24.5 cm, 31 cm, 35 cm, 40 cm, 45 cm, 48 cm, 53 cm of the 12-mm Stainless Steel round bar and mean values mean values of these data were evaluated based on dataset [97].

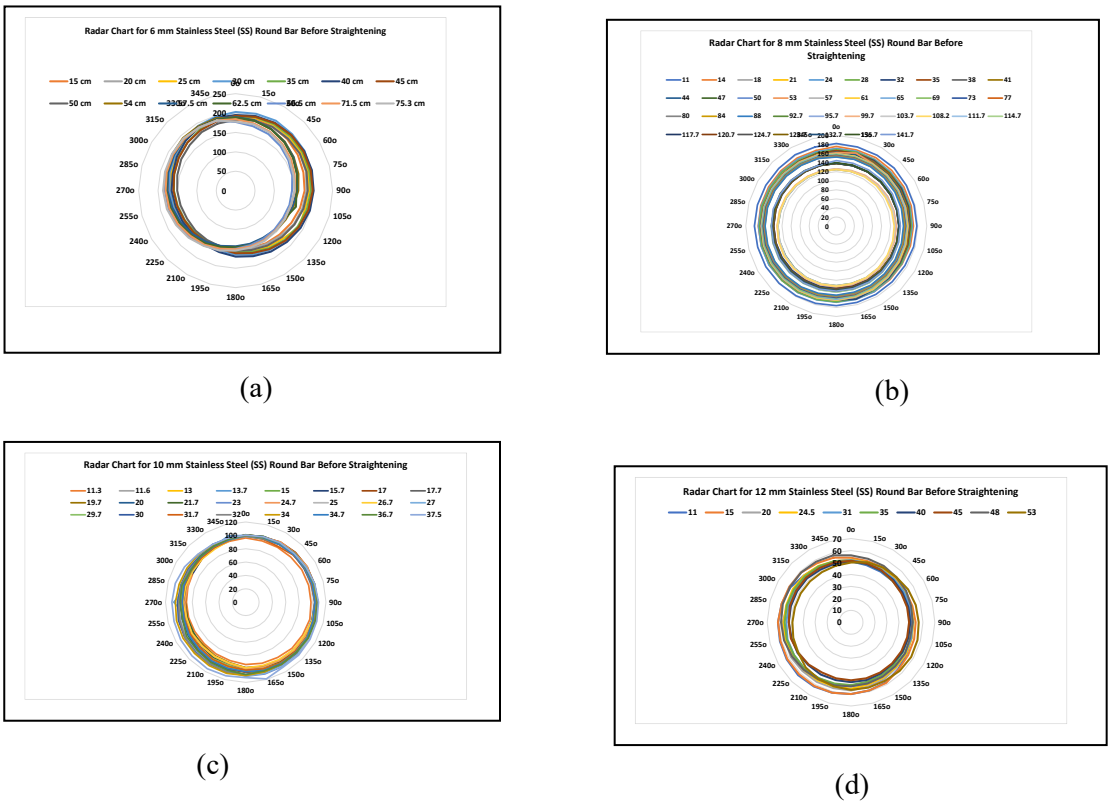

(a) (b)

(c) (d)

Figure 5.20 Radar Charts of (a) 6-mm, (b) 8-mm, (c) 10-mm and (d) 12- mm Diameter Stainless Steel (SS) Round Bar

Peripheral lines show the variation of the circularity while variation of straightness is visible from different coloured peripheral lines.

5.6.3 Radar Charts of Aluminium Round Bars Before Straightening

Figure 5.21 shows the Radar chart of 6-mm, 8-mm, 10-mm and 12-mm diameter Aluminium round bars where deflection data of measurements have been recorded at 15^{o} interval circumferentially and at various sections along the length segments at distances from one end of the bar before straightening. 12 sets of measurements data were recorded for one single rod at length segments from one end at distances at 16.5 cm, 20 cm, 25 cm, 30 cm, 35 cm, 40 cm, 45 cm, 50 cm, 55 cm, 60 cm, 65 cm, 70 cm, 75 cm, 80 cm, 85 cm, 90 cm, 95 cm 100 cm, 105 cm and 109 cm of the 6-mm Aluminium round bar and mean values mean values of these data were evaluated based on dataset [98].

12 sets of measurements data were recorded for one single rod at length segments from one end at distances at 12 cm, 15 cm, 20 cm, 24 cm, 28 cm, 32 cm, 36 cm, 40 cm, 44 cm, 48 cm, 52 cm, 56 cm, 59 cm, 62 cm, 65 cm, 69 cm, 73 cm, 77 cm, 80 cm, 83 cm, 87 cm, 90 cm, 93 cm, 96 cm, 100 cm, 104 cm, 108 cm, 112 cm, 116 cm, 120 cm, 124 cm, 128 cm, 132 cm, 136 cm, 140 cm, 143 cm of the 8-mm Aluminium round bar and mean values mean values of these data were evaluated based on dataset [98].

12 sets of measurements data were recorded for one single rod at length segments from one end at distances at 13 cm, 16 cm, 19 cm, 22 cm, 25 cm, 28 cm, 31 cm, 34 cm, 37 cm, 40 cm, 43 cm, 46 cm, 49 cm, 52 cm, 55 cm, 58 cm, 61 cm, 64 cm, 67 cm, 70 cm, 73 cm, 76 cm, 79 cm, 81 cm, 82 cm, 84 cm, 85 cm, 87 cm, 90 cm, 93 cm, 96 cm, 99 cm, 102 cm, 105 cm, 108 cm, 111 cm, 114 cm, 117 cm, 120 cm, 123 cm, 126 cm, 129 cm, 132 cm, 135 cm, 138 cm and 141 cm of the 10-mm Aluminium round bar and mean values of these data were evaluated based on dataset [98].

12 sets of measurements data were recorded for one single rod at length segments from one end at distances at 11 cm, 20 cm, 30 cm, 40 cm, 50 cm, 60 cm, 70 cm, 80 cm, 90 cm, 100 cm and 109 cm of the 12-mm Aluminium round bar and mean values of these data were evaluated based on dataset [98].

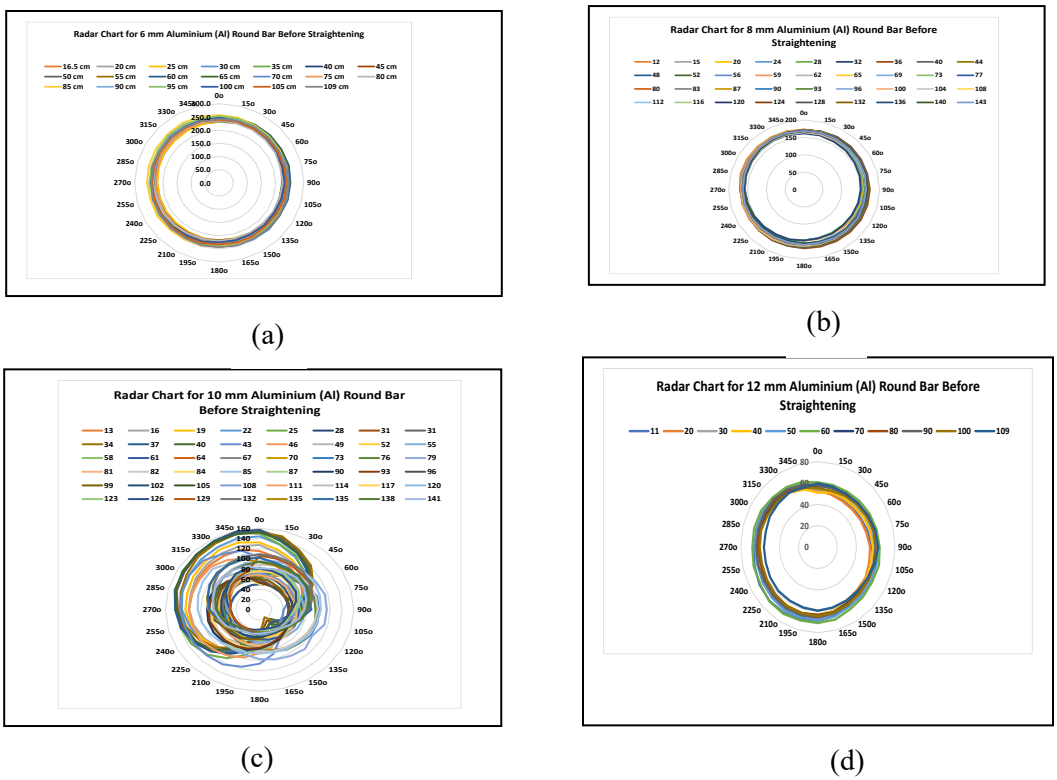

Figure 5.21 Radar Charts of (a) 6-mm, (b) 8-mm, (c) 10-mm and (d) 12-mm Diameter Aluminium (Al) Round Bars

Peripheral lines show the variation of the circularity while variation of straightness is visible from different coloured peripheral lines.

5.6.4 Radar Charts of Copper Round Bars Before Straightening

Figure 5.22 shows the Radar chart of 6-mm, 8-mm, 10-mm and 12-mm diameter Copper round bars where deflection data of measurements have been recorded at 15^{o} interval circumferentially and at various sections along the length segments at distances from one end of the bar before straightening.

12 sets of measurements data were recorded for one single rod at length segments from one end at distances at 16 cm, 18 cm, 20 cm, 22 cm, 25 cm, 30 cm, 35 cm, 40 cm, 45 cm, 50 cm, 55 cm, 60 cm, 62 cm, 65 cm, 68 cm, 70 cm, 75 cm, 80 cm, 86 cm of the 6-mm Copper round bar and mean values of these data were evaluated based on dataset [99].

12 sets of measurements data were recorded for one single rod at length segments from one end at distances at 11.5 cm, 13 cm, 15 cm, 17 cm, 19 cm, 22 cm, 25 cm, 28 cm, 31 cm, 34 cm, 37 cm, 40 cm, 43 cm, 46 cm, 49 cm, 52 cm, 55 cm, 57.5 cm, 61.2 cm, 64.3 cm, 67.5 cm, 70.5 cm, 73.5 cm, 77 cm, 80.2 cm, 83.2 cm, 86.2 cm, 90.2 cm of the 8-mm Copper round bar and mean values of these data were evaluated based on dataset [99].

12 sets of measurements data were recorded for one single rod at length segments from one end at distances at 12.3 cm, 16 cm, 20.5 cm, 25 cm, 28 cm, 31 cm, 35 cm, 40 cm, 45 cm, 48 cm, 51 cm, 54 cm, 57 cm, 60 cm, 63 cm, 66 cm, 69 cm, 72 cm, 75 cm, 78 cm, 81 cm, 85.5 cm of the 10-mm Copper round bar and mean values of these data were evaluated based on dataset [99].

12 sets of measurements data were recorded for one single rod at length segments from one end at distances at 12 cm, 15 cm, 19 cm, 24 cm, 29 cm, 34 cm, 39 cm, 43.5 cm, 49 cm, 56 cm, 59 cm, 62 cm, 67 cm, 72 cm, 77 cm, 82 cm and 87 cm of the 12 mm Copper round bar and mean values of these data were evaluated based on dataset [99].

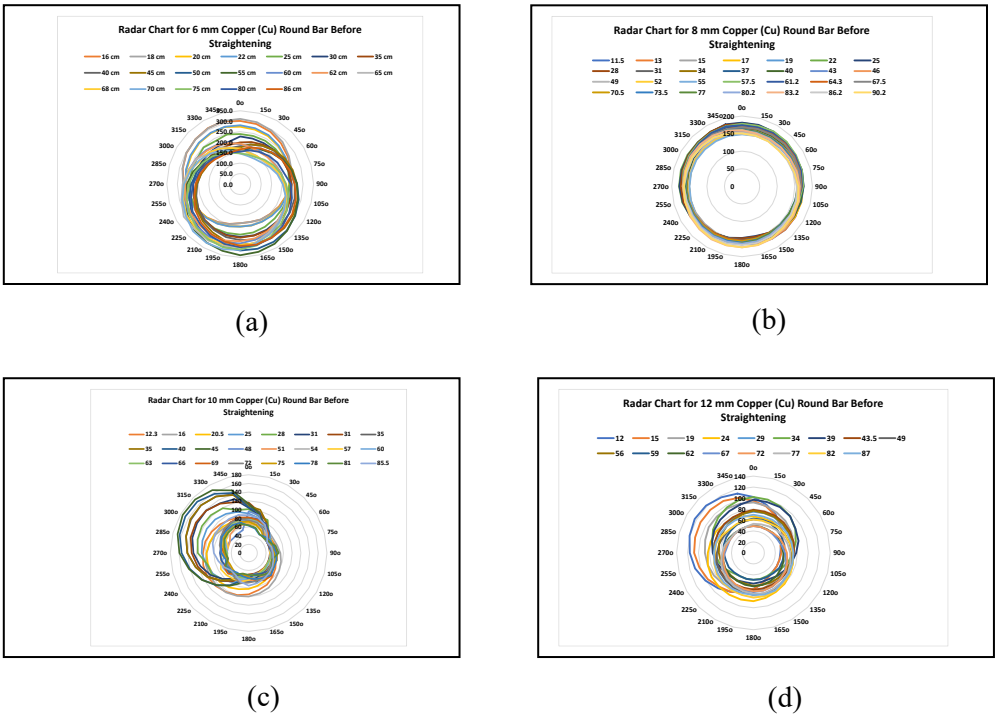

Figure 5.22 Radar Charts of [a] 6-mm, [b] 8-mm, [c] 10-mm and [d] 12-mm Diameter Copper (Cu) Round Bars

Peripheral lines show the variation of the circularity while variation of straightness is visible from different coloured peripheral lines. From the Radar charts as shown in Figure 5.19 to Figure 5.22, it is quite clear that variations exist in circularity in all types and sizes of round bars. The overall roundness is observed from the Radar chart at different bar sections. The acceptability of the roundness of such bars in raw state will somewhat depend on the application of raw material and the final product. It is quite possible that such circularity is acceptable for direct application in most of general-purpose work while in precision-based application such circularity may not be acceptable and further processing like machining or cold working may be required before actual deployment. This has motivated towards the analysis of Statistical Process Control of all these bars which have been discussed in subsequent article 5.7.

5.7 Statistical Process Control Analysis of Round Bars

Statistical process control primarily uses control charts. A control chart is a graphical tool for monitoring the activity of an ongoing process. The values of the quality characteristics are plotted along the vertical axis, and the horizontal axis represents the samples, or subgroups, from which the quality characteristics are found [100].

The sampling method should maximize differences between samples and minimize differences within the samples. Control charts have been used to understand the variability of mean values of subgroups and also the variability of range of values. For this purpose, X-Bar ($\bar{X}$) chart and R chart is quite a reasonable useful tool to understand whether the process is actually within statistical process control limits. Therefore, in the present study, X-Bar and R Chart have been used to understand the variability of deformation value of round bars.

Round bars of small diameters of various sizes and types of materials are considered for the study of actual mean diameters and range as per X-Bar ($\bar{X}$) and R Charts. Nearly 10 to 15 segments of about 3 to 10 cm lengths were measured through micrometre and diameters are noted down at each section at three different angles. It has been found that diameters are actually not uniform at every angle and can be stated that roundness is compromised to some extent along the length of the bars. Average data is calculated for each section and mean values ($\bar{X}$) are plotted along the length segments of the round bars. Average of the mean values, $\bar{\bar{X}}$ was calculated based on average values of mean values ($\bar{X}$) and a centre line $\bar{\bar{X}}$ is plotted along the bar length.

Range of mean values, R at each section is noted and average of the same is considered as centre line, $\bar{R}$. The process has been repeated for round bars of all samples of diameters 6-mm, 8-mm, 10-mm and 12-mm. Upper Control Limit (UCL) and Lower Control Limit (LCL) have been evaluated along with mean values. The evaluations process of control limits is as below:

$$UCL_{\bar{x}} = \bar{\bar{X}} + 3\sigma \quad (5.29)$$

$$LCL_{\bar{x}} = \bar{\bar{X}} - 3\sigma \quad (5.30)$$

$$UCL_R = \bar{R} + 3\sigma \quad (5.31)$$

$$LCL_R = \bar{R} - 3\sigma \quad (5.32)$$

where σ is standard deviation of the set of data of diameter measured at each section. Graphs have been plotted for various types of round bars of diameters 6-mm, 8-mm, 10-mm and 12-mm based on observations and readings noted. Upper Control Limits (UCL) and Lower Control Limits (LCL) have been drawn on each graph along with Mean value data i.e. $\bar{\bar{X}}$ and $\bar{R}$. A brief detail of each case has been published by the author for different bars of 6-mm, 8-mm, 10-mm and 12-mm respectively [12].

Round bars of Mild Steel (MS), Stainless Steel (SS), Aluminium (Al) and Copper (Cu) round bars of 6-mm, 8-mm, 10-mm & 12-mm diameters were first taken for measurement of diameters at various sections at nearly 5 cm intervals. The data set was then evaluated for X-Bar and R-Charts as shown from Figures 5.23 to 5.38.

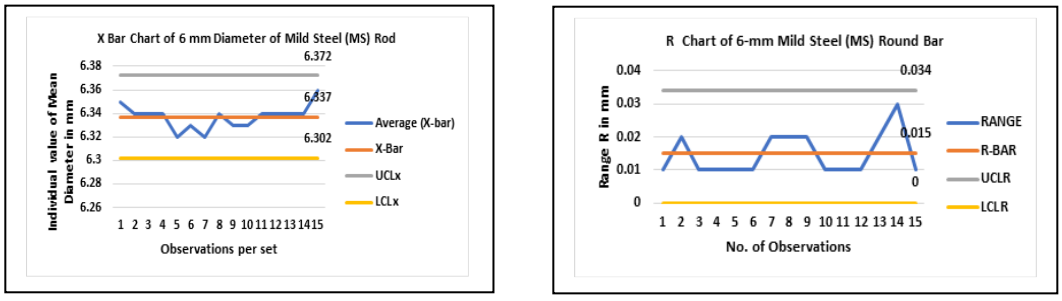

(a) (b)

Figure 5.23 Control Chart for 6-mm Mild Steel (MS) Round Bars (a) X- Bar and (b) R-Chart

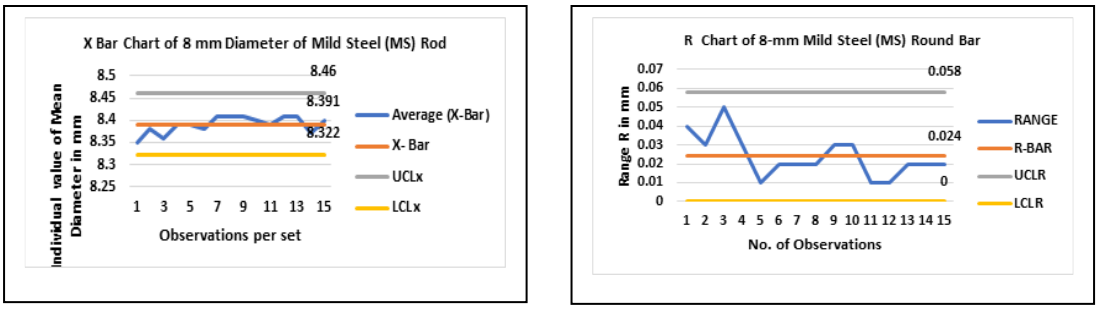

(a) (b)

Figure 5.24 Control Chart for 8-mm Mild Steel (MS) Round Bars (a) X- Bar and (b) R-Chart

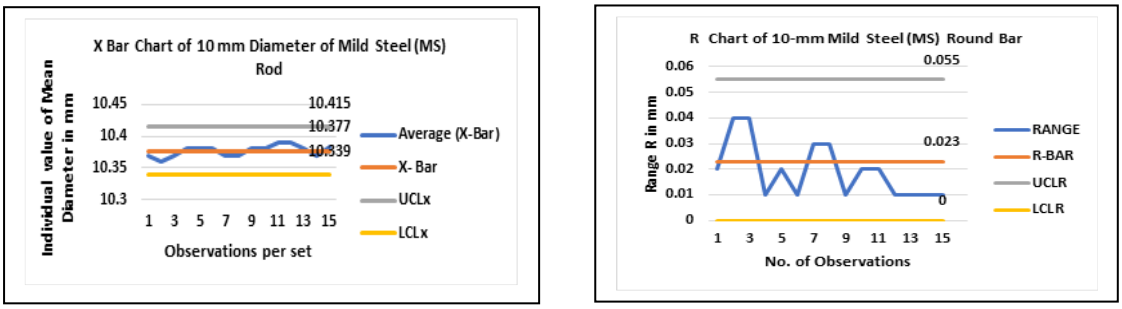

(a) (b)

Figure 5.25 Control Chart for 10-mm Mild Steel (MS) Round Bars (a) X- Bar and (b) R-Chart

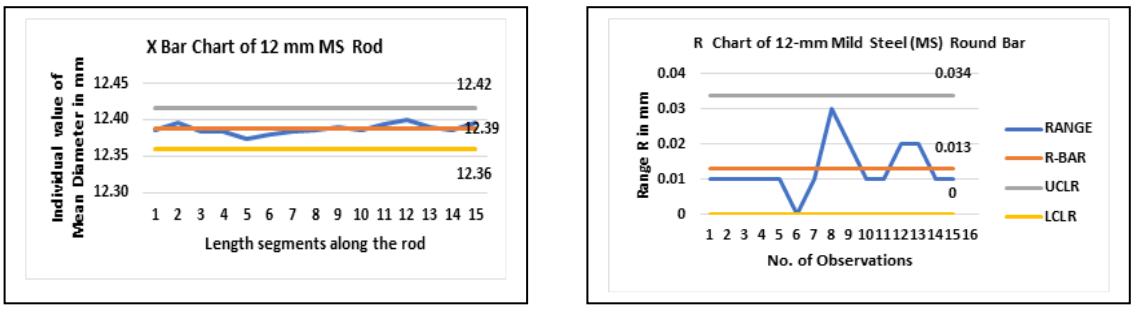

(a) (b)

Figure 5.26 Control Chart for 12-mm Mild Steel (MS) Round Bars (a) X- Bar and (b) R-Chart

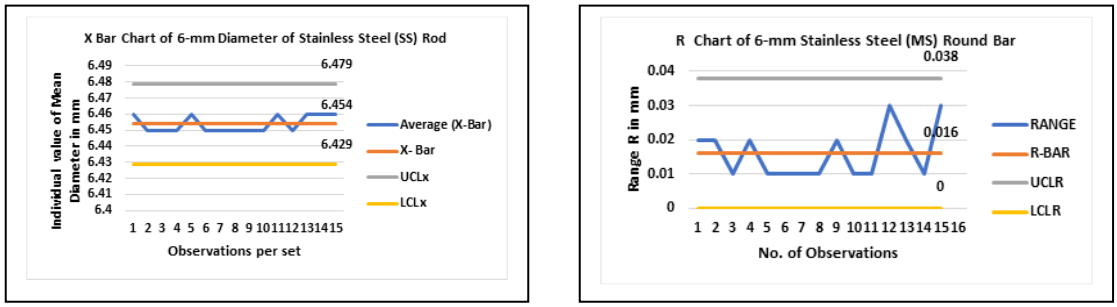

(a) (b)

Figure 5.27 Control Chart for 6-mm Stainless (SS) Round Bars (a) X- Bar and (b) R-Chart

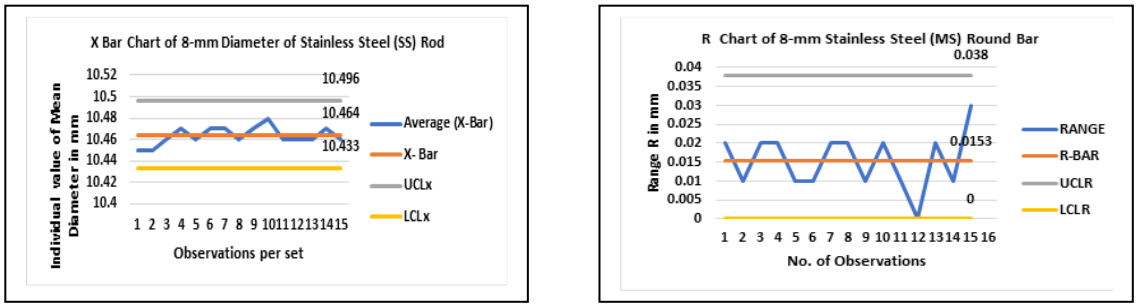

(a) (b)

Figure 5.28 Control Chart for 8-mm Stainless (SS) Round Bars (a) X- Bar and (b) R-Chart

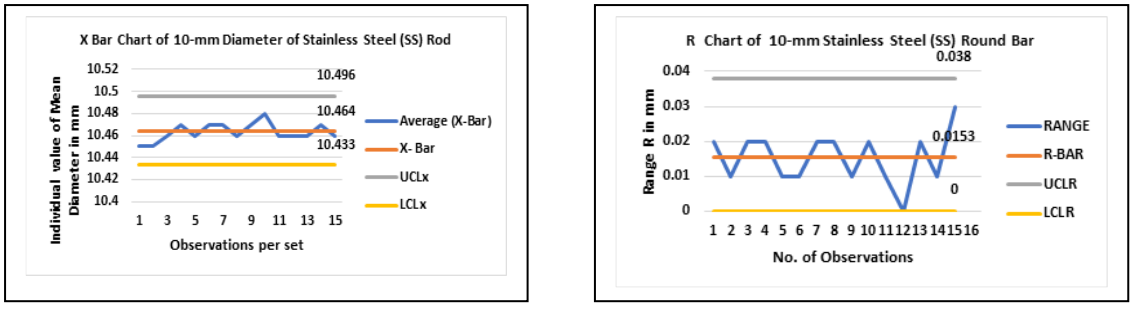

(a) (b)

Figure 5.29 Control Chart for 10-mm Stainless (SS) Round Bars (a) X- Bar and (b) R-Chart

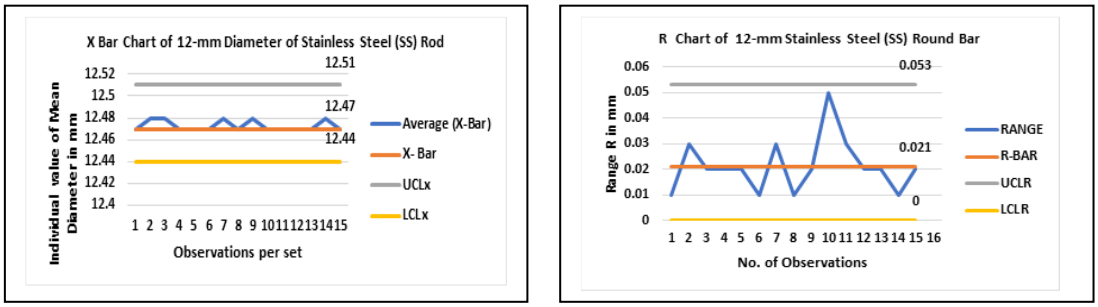

(a) (b)

Figure 5.30 Control Chart for 12-mm Stainless (SS) Round Bars (a) X- Bar and (b) R-Chart

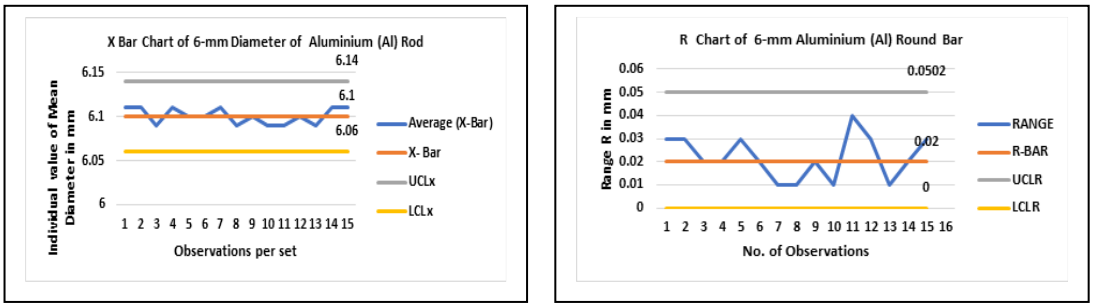

(a) (b)

Figure 5.31 Control Chart for 6-mm Aluminium (Al) Round Bars (a) X- Bar and (b) R-Chart

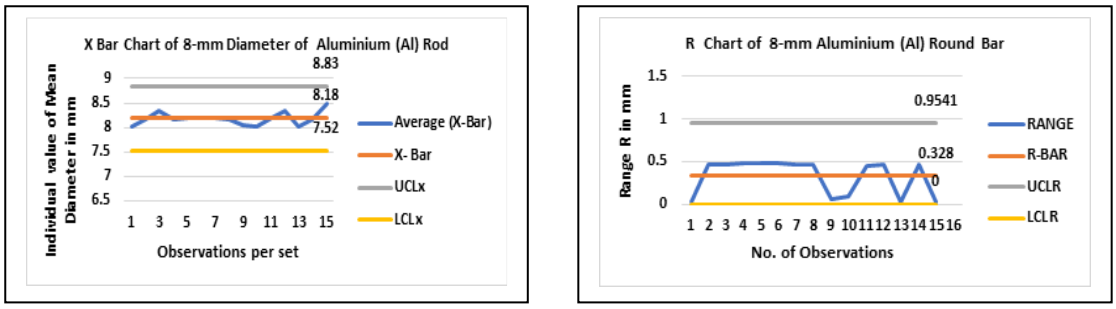

(a) (b)

Figure 5.32 Control Chart for 8-mm Aluminium (Al) Round Bars (a) X- Bar and (b) R-Chart

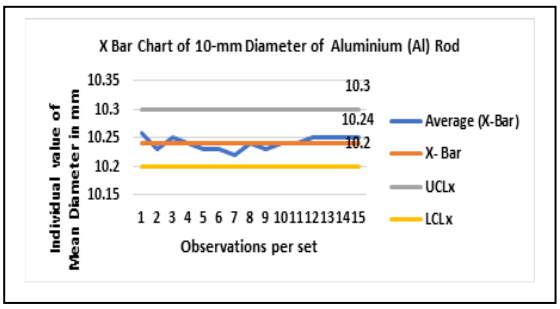

(a)

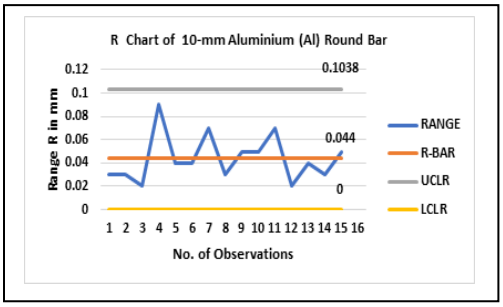

(b)

Figure 5.33 Control Chart for 10-mm Aluminium (Al) Round Bars (a) X- Bar and (b) R-Chart

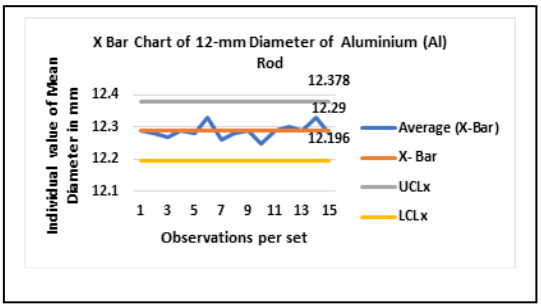

(a)

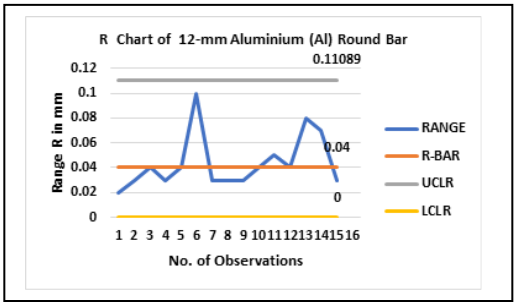

(b)

Figure 5.34 Control Chart for 12-mm Aluminium (Al) Round Bars (a) X- Bar and (b) R-Chart

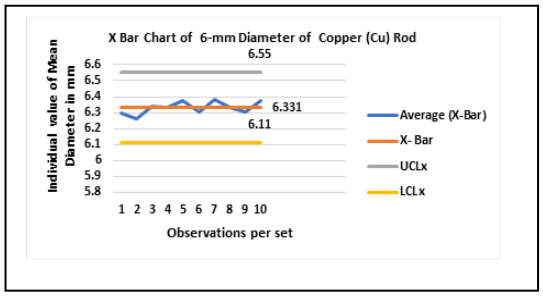

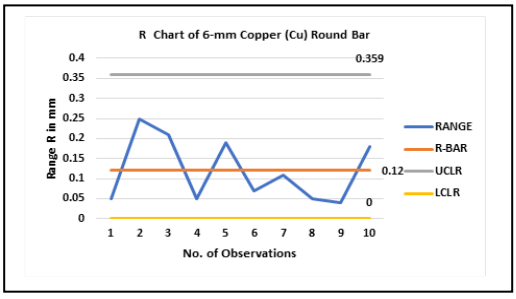

Figure 5.35 Control Chart for 6-mm Copper (Cu) Round Bars (a) X- Bar and (b) R-Chart

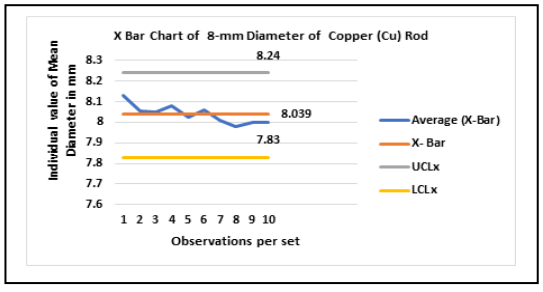

(a)

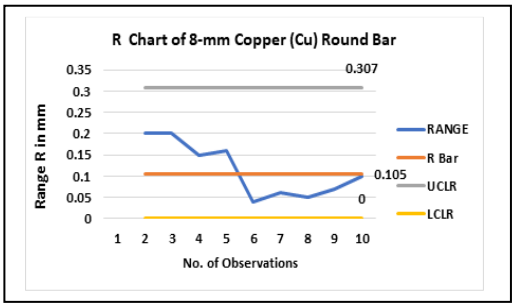

(b)

Figure 5.36 Control Chart for 8-mm Copper (Cu) Round Bars (a) X- Bar and (b) R-Chart

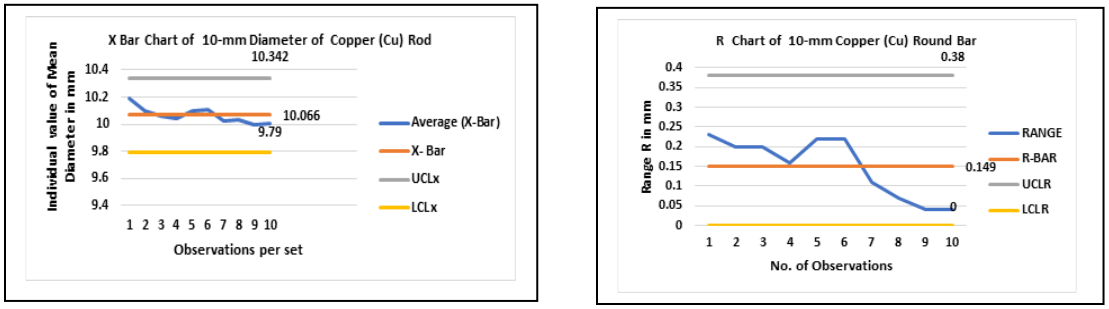

(a) (b)

Figure 5.37 Control Chart for 10-mm Copper (Cu) Round Bars (a) X- Bar and (b) R-Chart

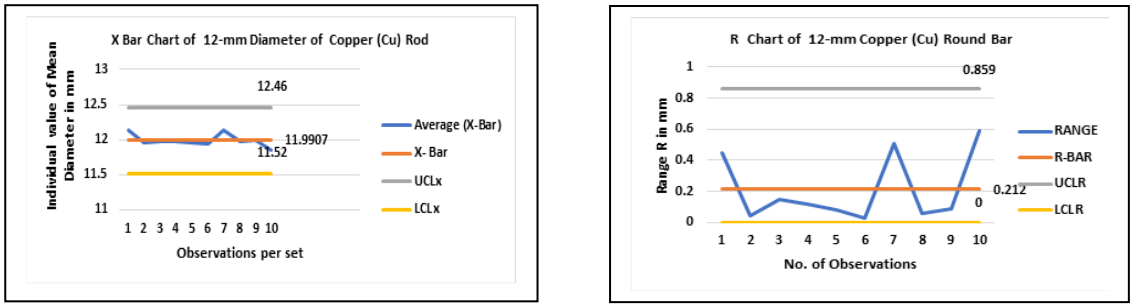

(a) (b)

Figure 5.38 Control Chart for 12-mm Copper (Cu) Round Bars (a) X- Bar and (b) R-Chart

All these control charts clearly indicate that the processes are in control for mild steel, stainless steel, aluminium and copper bars of different sizes as all the data points are within upper and lower control limits of all control charts. Therefore, in most cases these metal round bars are commercially acceptable.

5.8 Deformation Analysis by SPC before Straightening of Bars

Though the previous SPC analysis of diameters shows reasonable results within limit before straightening but SPC analysis of observed deflections before straightening show that there are quite some results which are out of the control limits indicating that the process is out of control. Figure 5.39 to Figure 5.54 illustrate the control charts of observed deflections before straightening for Mild Steel, Stainless Steel, Aluminium and Copper for 6-mm,8-mm,10-mm, & 12-mm respectively. These out-of-control

datapoints of the results indicate that there is necessity for these metal bars to pass through straightening machine.

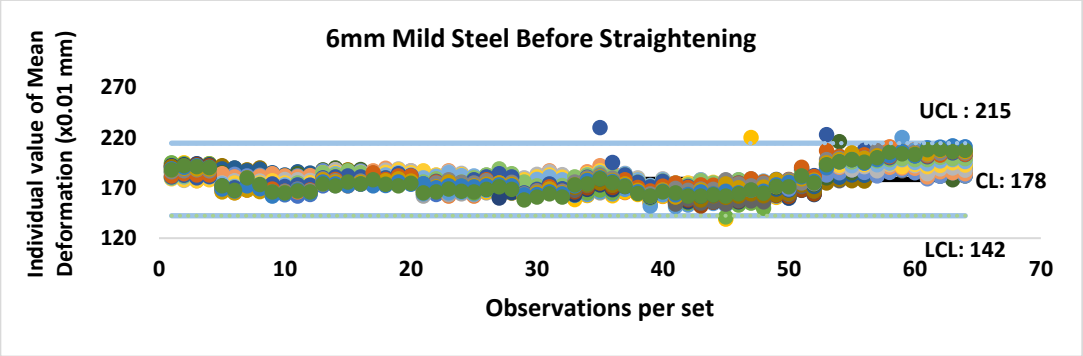

Figure 5.39 Deformation Analysis of 6-mm Mild Steel Round Bar before Straightening Using SPC

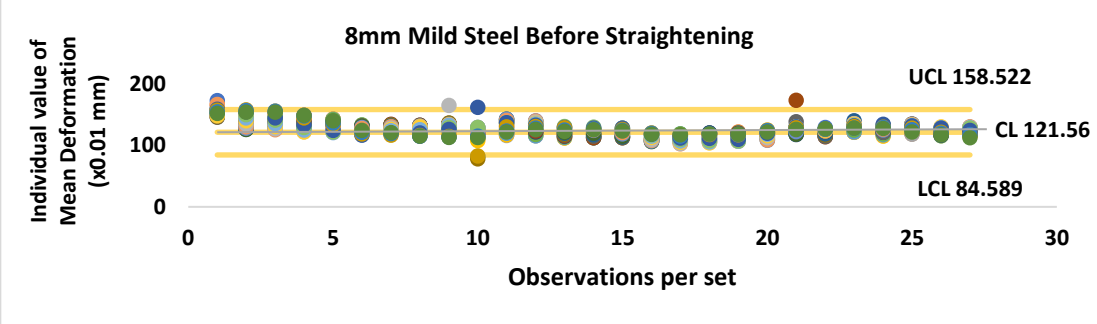

Figure 5.40 Deformation Analysis of 8-mm Mild Steel Round Bar before Straightening Using SPC

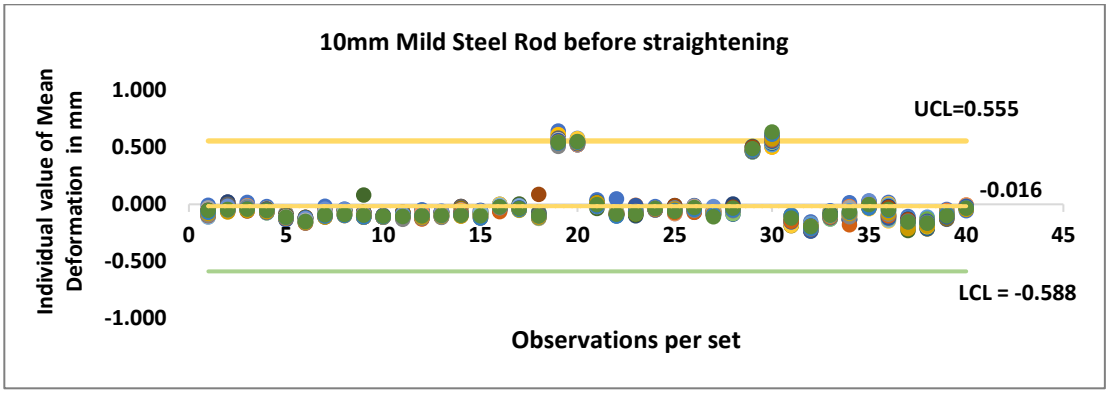

Figure 5.41 Deformation Analysis of 10-mm Mild Steel Round Bar before Straightening Using SPC

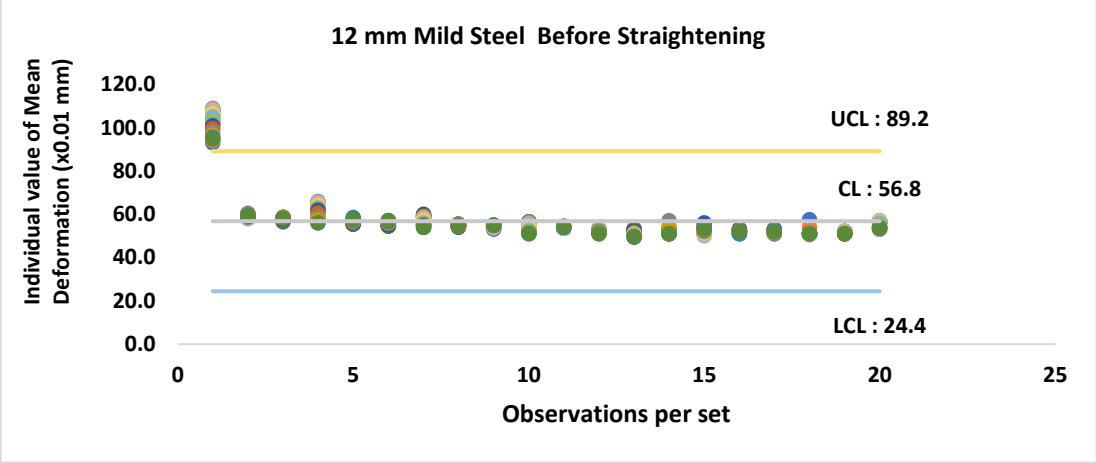

Figure 5.42 Deformation Analysis of 12-mm Mild Steel Round Bar before Straightening Using SPC

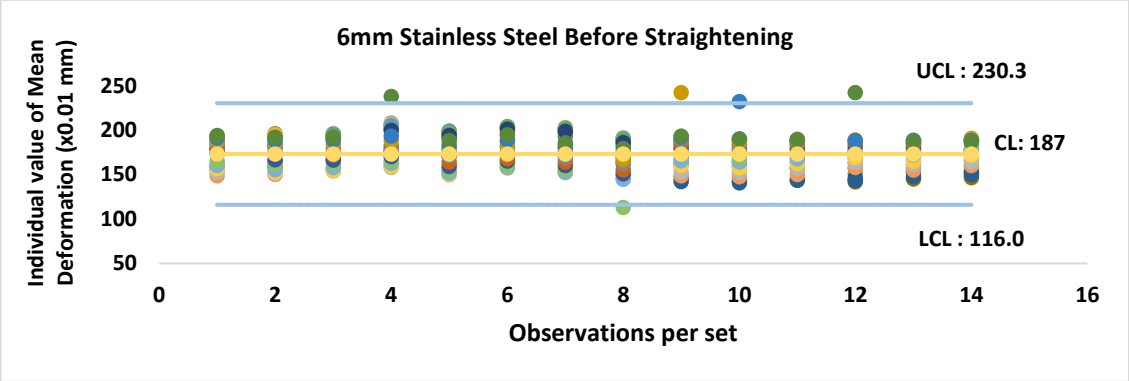

Figure 5.43 Deformation Analysis of 6-mm Stainless Steel Round Bar before Straightening Using SPC

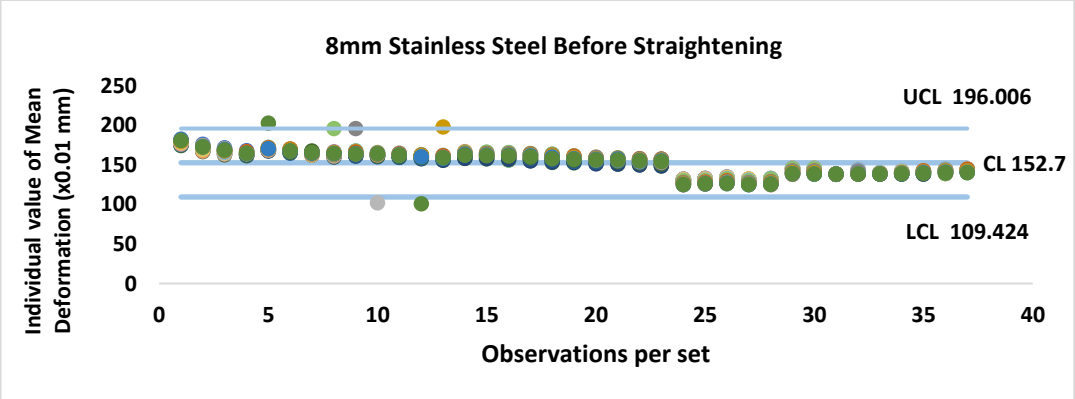

Figure 5.44 Deformation Analysis of 8-mm Stainless Steel Round Bar before Straightening Using SPC

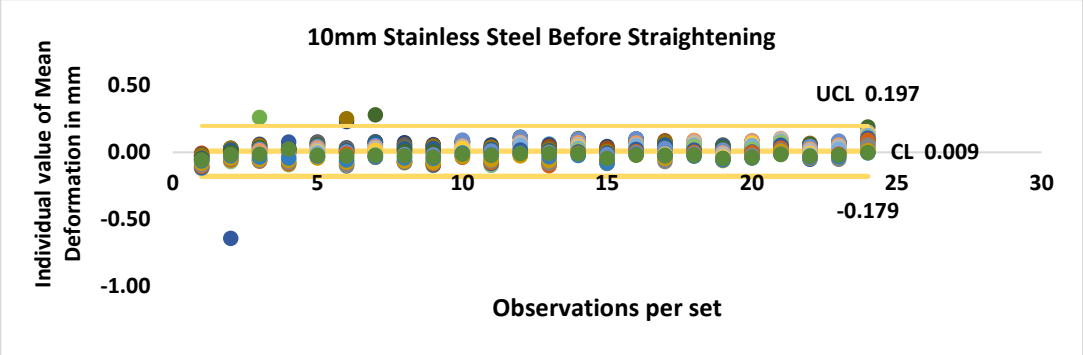

Figure 5.45 Deformation Analysis of 10-mm Stainless Steel Round Bar before Straightening Using SPC

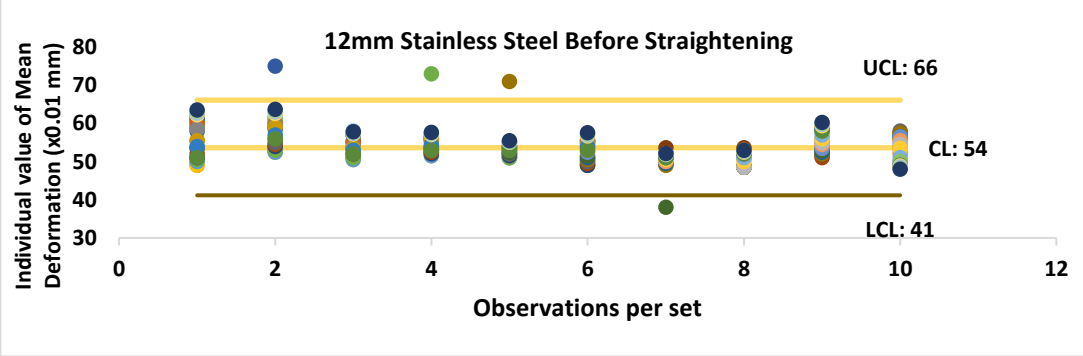

Figure 5.46 Deformation Analysis of 12-mm Stainless Steel Round Bar before Straightening Using SPC

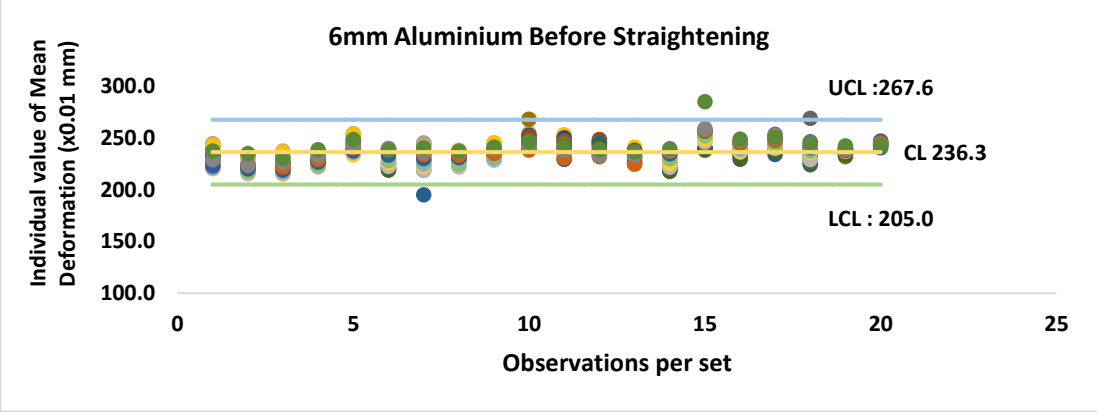

Figure 5.47 Deformation Analysis of 6-mm Aluminium Round Bar Before Straightening Using SPC

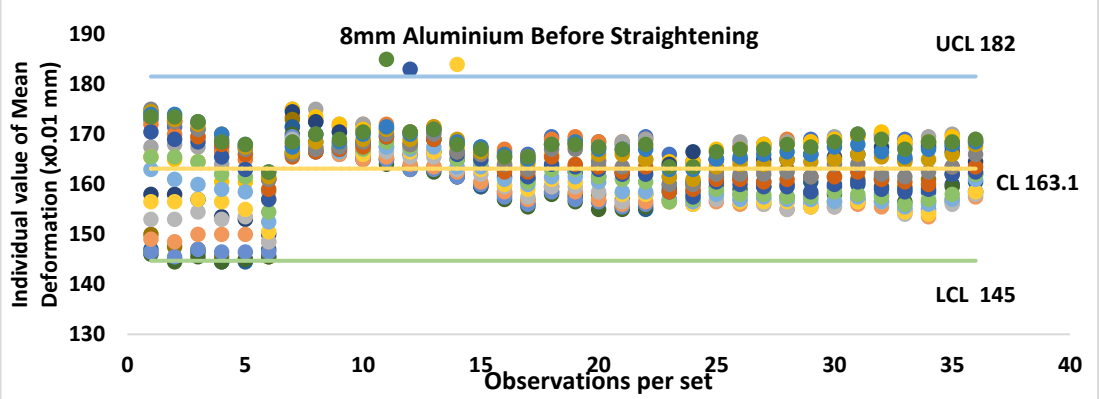

Figure 5.48 Deformation analysis of 8-mm Aluminium Round Bar before Straightening Using SPC

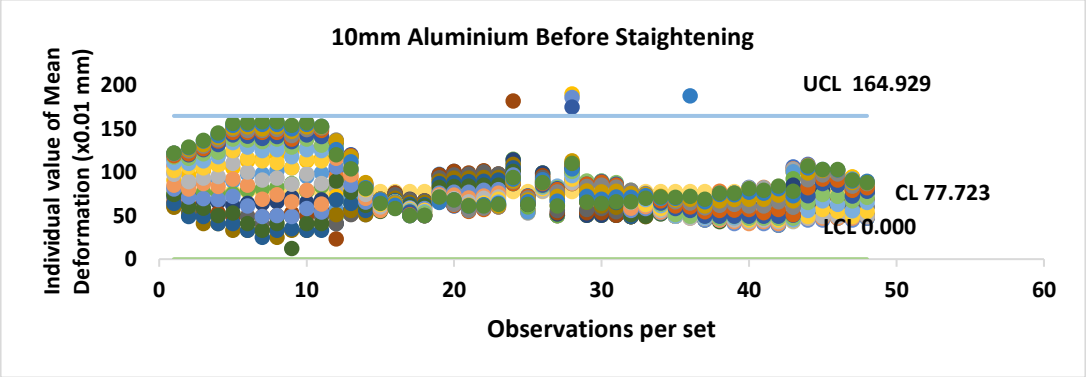

Figure 5.49 Deformation Analysis of 10-mm Aluminium Round Bar before Straightening Using SPC

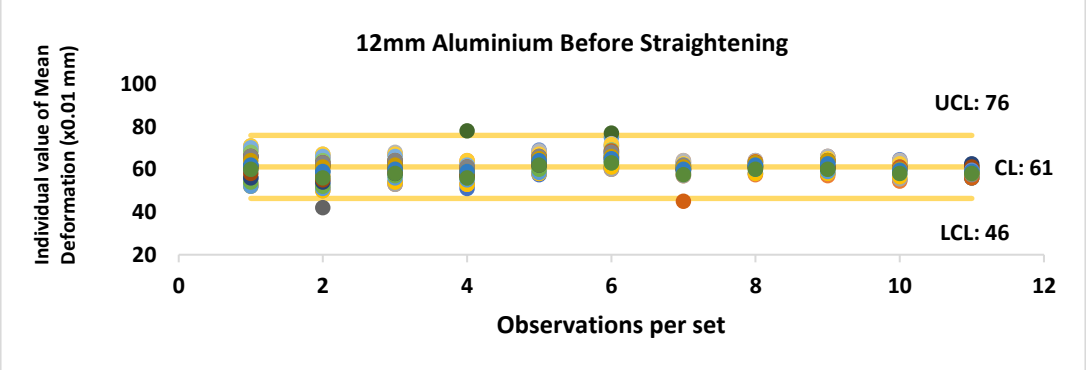

Figure 5.50 Deformation Analysis of 12-mm Aluminium Round Bar before Straightening Using SPC

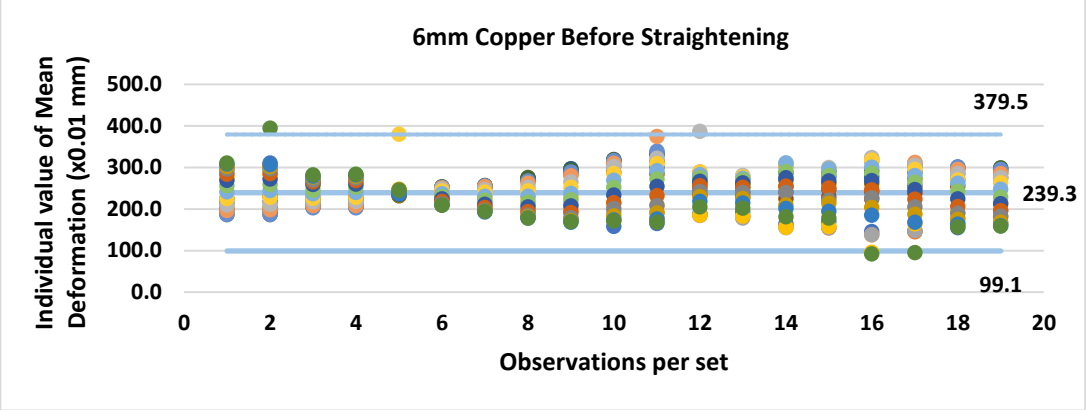

Figure 5.51 Deformation Analysis of 6-mm Copper Round Bar Before Straightening using SPC

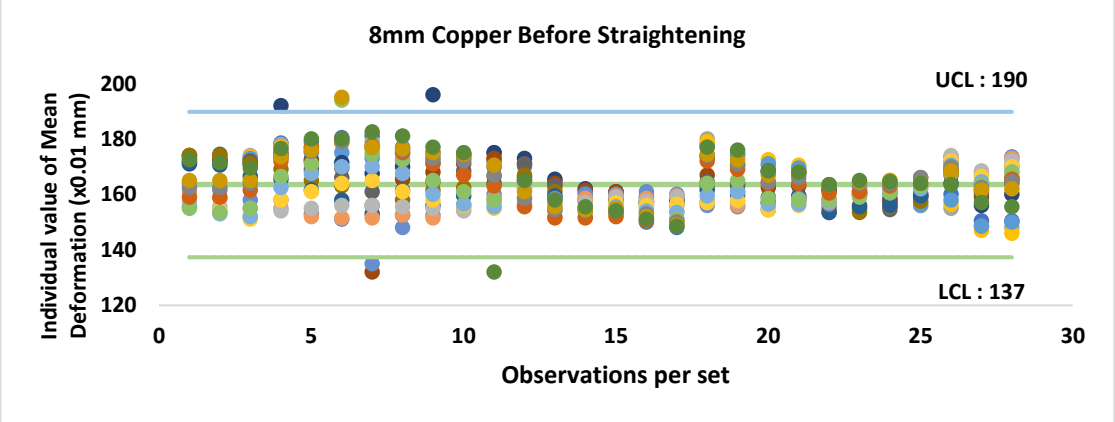

Figure 5.52 Deformation Analysis of 8-mm Copper Round Bar before Straightening Using SPC

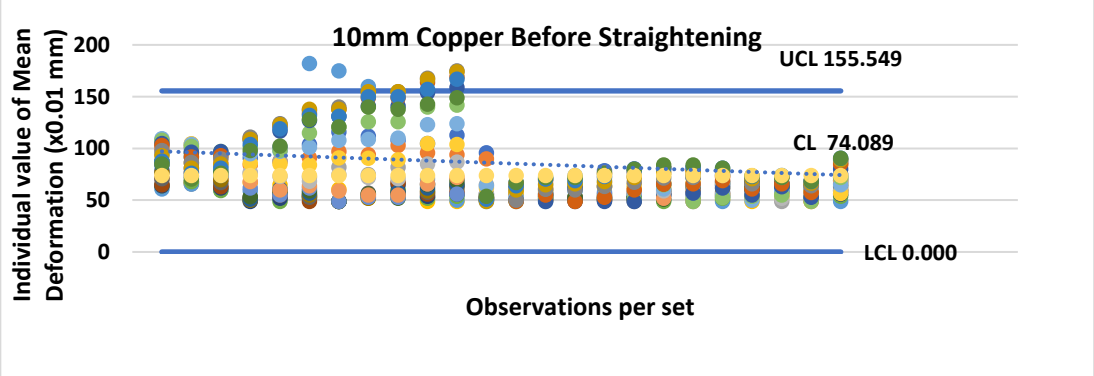

Figure 5.53 Deformation Analysis of 10-mm Copper Round Bar before Straightening Using SPC

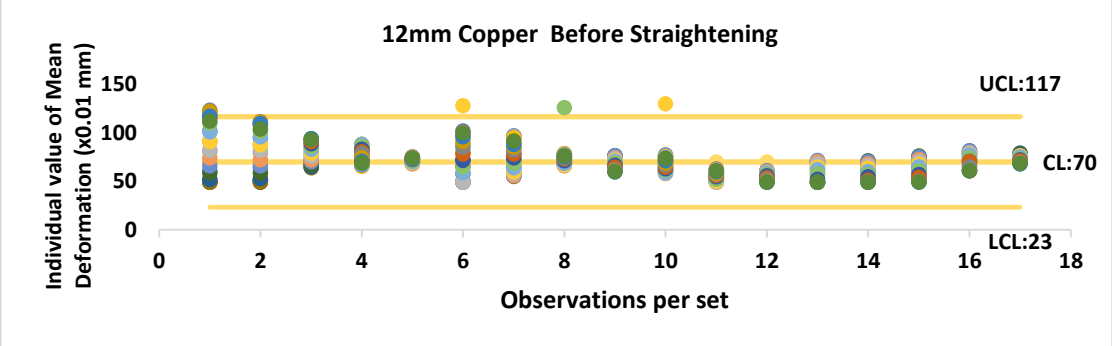

Figure 5.54 Deformation Analysis of 12-mm Copper Round Bar before Straightening Using SPC

5.9 Discussion

The results shown in Figures 5.3 to 5.18 reveal that there is no specific pattern on the observed deviations. Deflections over length segments show that residual curvatures are present along the bar length. The variations of the roundness are clearly visible from the Radar Charts shown in Figures 5.19 to Figures 5.22. Radar charts also indicate straightness aspects to some extent along the bar lengths of through various different coloured lines.

The study on mean diameters based on X-Bar charts and R charts as shown in Figures 5.23 to Figures 5.38 reveal that in all cases diameters measured at various sections are varying to some extent but variations are within control limits. In all the X-Bar charts mean diameters are well within control limits. R charts also show that range variations are also within control limits. The bars which were deployed for experimental data can be considered qualitatively as good enough to assess the overall average diameter of bars.

It is observed that dial gauge readings are varying at specified angles along the bar length in all the data tables. This is a clear indication that bars itself are not straight. This is probably due to residual curvature which got built in during rolling operation and possible material handling. From the database generated of various round bars, it can be postulated that residual curvatures exist even in small length segments. As such our aim was to understand the level of roundness and the variation in circularity and simultaneously straightness of bars. Since residual curvatures are playing a role, the obvious effect finally is on the straightness of the bars which are evident from dial gauge readings. Residual curvatures can be reduced through bar straightening process by cold working, more

specifically by passing the bar in cross roll arrangement. The applied load may be given through reverse kinematic bending or through bending moment at intended sections.

Deformation analyses using SPC have been done for these mild steel, stainless steel, aluminium and copper round bars of sizes 6-mm, 8-mm, 10-mm and 12-mm diameters discussed above and results shown in the graphical plots from Figure 5.39 to Figure 5.54. From these plots it is clearly visible that straightness requirements are actually there as some of the data points are outliers. This is probably due to the fact that the round bars have undergone different situations in terms of rolling and material handling process. Therefore, straightening process through cold working is actually essential requirement and importance of bar straightening plays a significant role in industries.

Theoretical aspect for application of ANOVA based on factors of helix angle and roller diameter has been done for bar straightening process. The above process shall hold good by F-Test and comparing the value with F-Table will lead to statistical conclusion for an appropriate hypothesis. Inclusion of other factors like type of material i.e. elastic/plastic modulus and bar diameter have also been considered. Considering more factors for ANOVA will make the study more elaborate. This type of investigation may develop useful tool for justification of role and importance on various factors in the process of bar straightening which can certainly form the basis for process improvement.

Overall, this study proposes a compact and reasonably accurate method for a straightforward and reliable means of understanding straightness of bars. Surface roughness with those obtained data using Radar charts of the commercially produced bars of different diameters at various angular positions are now available. It can be concluded easily based on samples studied that round bars as produced by industries and available in market are within statistical process control. The above study is on ferrous and non-ferrous materials. In all the samples it has been found that all data are quite in order.

Such round bars can be deployed anywhere as raw materials for the purpose of further production work in industries. So, it can be postulated that the statistical approach proposed for checking the quality of bars in terms of roundness may be considered useful for manufacturing industries.

CHAPTER – 6

DEFORMATION ANALYSIS OF COMMERCIAL BARS

6.1 Introduction

Although straightness measurement system is available with a reflection confocal optical system using He-Ne laser beam but it is costly [101]. Modulation-Based straightness measurement system has been indicated by Egidi et al. [102]. In the present study a simple dial gauge and V-Block arrangement i.e. Total Indicated Reading (TIR) method which is common method of measurement system. In this chapter an attempt has been made to look into the measure of straightness through deflections using dial gauge. Wherever deformations are more, deflection readings will also be more. Four types of materials i.e., mild steel, stainless steel, aluminium and copper have been chosen for this purpose as bar materials for study of deformations through measurement of deflections. In the industries, it is quite usual that after production, round bars undergo several material handlings processes which can cause bending or deformations at various sections of the bar along the axis.

A number of samples of commercially produced metal round bars have been considered for ascertaining production processes particularly after two cross-roll straightening. The effects of circumferential deformations measured by angular rotation of bar at various segmental lengths of round bars for the measurement of roundness and straightness have also been analysed for quality control and straightness improvement on performance metrics.

6.2 Experimental Arrangement

This chapter primarily deals with deformation analysis of round bars of 6-mm, 8-mm, 10-mm and 12-mm diameter of four different materials i.e. mild steel, stainless steel, aluminium and copper. Materials chosen are of both ferrous and non-ferrous type. Experimental set up was made for measurement of deformations before straightening and after straightening. Round bars as measured before straightening have been passed through straightening machine and similar measurements taken after straightening process. Scatter plots done for all the bars before and after straightening to see the variations based on dial gauge readings. Scatter plots were based on dial gauge readings at one plane.

Exhaustive observations were carried out and 12 sets of experimental data were recorded for every single round bar after straightening and mean values of these data were taken for further analysis. 3D Analysis of deformations of round bars before and after straightening has been conducted and surface plots are generated which indicated changes in deformations after straightening. Radar charts have been plotted for all four sets of round bars of four different materials. Radar charts indicate the variations in circularity and also indicate straightness qualitatively. Impact of straightness on overall performance has been looked into.

Deformation study of round bars of different diameters and materials is necessary for two cases that is before straightening and after straightening. In Chapter-5, it has been amply discussed from the dataset [96, 97, 98, 99] that deformation measurements so recorded for round bars are observations before straightening. The dataset described that round bars are primarily commercially available products from rolling industries where various deformations are likely to be present due to industrial processes including material handling. Fast production in the rolling mills would produce long round bars mostly in hot condition where there is every possibility of bending of bars and consequently straightening of round bars is an essential requirement. From the two different arrangement that is measurement of round bars before straightening and

then the same bars are subjected to straightening process. Measurements recorded after straightening process is forming the dataset of post straightening.

6.2.1 Experimental Arrangement for Deformation Measurement

An experimental set up was developed as shown in Figure 6.1. The figure shows the schematic diagram of the arrangement for the study of deformation pattern using dial gauge deflection measurement. The dial gauge was firmly hold in the stand so that readings can be taken properly.

Sample round bars of various sizes of different materials were placed one by one and ensured for clamping of bar with holder arrangement. One of the bar holders is pinned with an angle measuring protractor to ensure angular position of the surface point of the round bar and enable it to measure deflection readings of dial gauge at the desired angle. The protractor and round bar can be rotated together about the bar axis and round bar can be set at any desired or specific angle thus enabling to take measurements at any angular intervals. After dial gauge has been properly set on the surface in the round bar at any point, a linear measurement is also taken on the axial length of the bar i.e. dial gauge deflection measurements were taken at any desired section of the bar. Figure 5.2 in chapter-5 shows the photograph of actual experimental arrangement which is illustrated in schematic as shown in Figure 6.1.

After the experimental set is made ready by inserting one round bar of desired size and material into the bar holder, the protractor is rotated about bar axis and aligned to 0^{o} vertically. After careful observations of dial gauge deflections, readings have been noted for first set of readings. The first set of readings are now recorded. For each mean value data, twelve sets of readings at one section over one surface point has been observed and recorded.

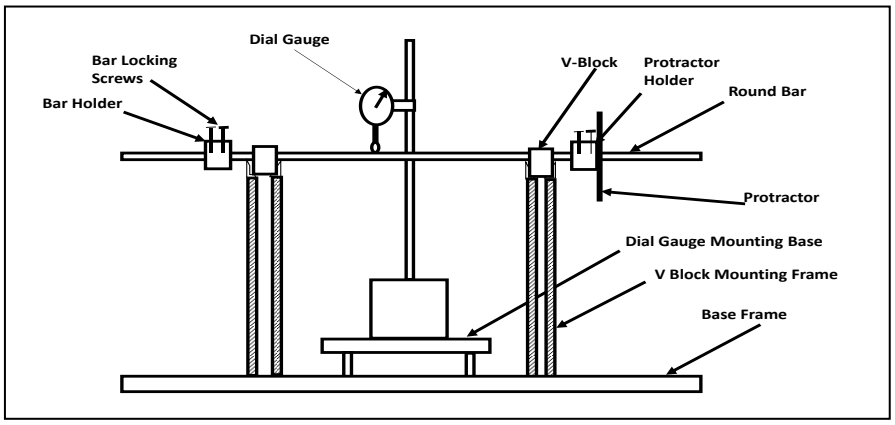

Figure 6.1 Schematic Diagram of Dial Gauge Mounting Arrangement on Experimental Set up for Measurement of Straightness and Roundness of Round Metal Bars [4].

Here it is to be noted that each data set of deflection at one section creates data size of approximately 12x24=288. An average of these data recorded is then evaluated along with maximum and minimum recording for the purpose of error analysis. The mean value of every data set is considered. After one set of observation is completed, the round bar is then rotated at an angle say 15^{o} and then again similar process is followed. Measurements were recorded for every observation at the interval of 15^{o} starting from 0^{o} to 360^{o}. Measurements of data of various sections can now be plotted using Radar chart and surface plot to understand the variational aspect of mean values of the surface points of the round bar in that section. After completion of one complete set of observation at a section from 0^{o} to 360^{o}, the round bar is moved axially at a desired distance interval by sliding from one side and then another set of observations is carried out at that section. The process has been continued till the end of bar except extreme ends since both ends are inside bar holders.

Dial gauge deflection readings have been recorded and mean value of these recorded data were considered for actual evaluation and generation of graphical plots. Error curve for data set has also been generated. Measurements in dial gauge deflections were taken at various sections circumferentially at angular intervals along the axial length at

intermittent spans. Measurements of all the sample bars considered for this purpose were initially done before straightening and again after straightening.

6.2.2 Experimental arrangement of Two Cross-Roll Straightening Machine and Straightening process

All the sample bars were initially studied for deformations and data recorded through observations in the experimental set up as stated above. After recording all these observations, round bar samples were taken to an industry M/s. Bright Bar Industries, Bhandardaha, Domjur, Howrah-711409, West Bengal, India for straightening purpose since cross-roll straightening machines and facilities were not available at university laboratories and workshops. A two-roll cross roll type straightening machine was chosen for straightening purpose. These bars were then passed through this type of straightening machine.

A schematic diagram of experimental set up of Two-Roll Cross Roll Straightening Machines has been shown in Figure 6.2. Primarily the machine comprises of one convex roll and one concave roll which are powered for rotation through electric motors. Arrangement of rollers and power supply through motors may be of different designs as per make and model of the manufacturers of bar straightening machine.

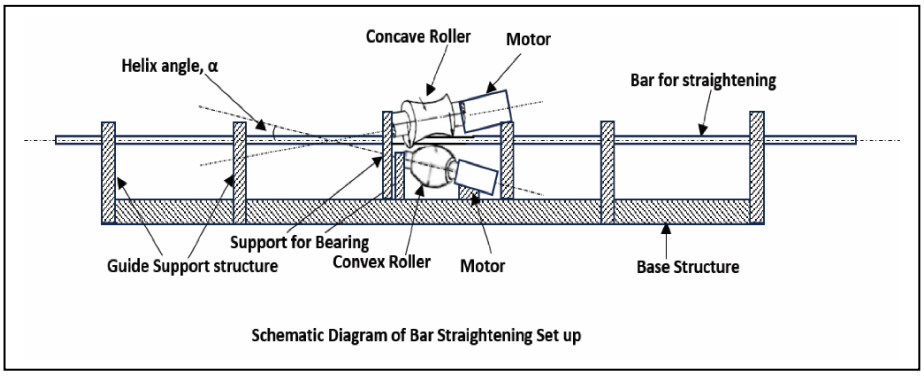

Figure 6.2 Schematic Diagram of Experimental Set up for Straightening Process

In the present case Model no. SMH-25 cross-roll straightening machine was used of Bhambra Engineering Works make where the machine is of single stand of 2 roll type with one convex and one concave roll. The machine was powered by 2 motors of 3.7 kw each. The cross rolls are supported on structural base of the machine with an arrangement of feeding the circular bars from one side and after straightening the bars are moved ahead with spiral motion on the other side. In the process straightening takes place.

The cross-rolls are skewed at an angle which can be varied from 5^{o} to 20^{o}. The diameter of concave roll is 191.60 mm at ends and 177.17 mm at center while convex roll is 177 mm diameter at ends and 192 mm at center. Length of concave and convex rolls are 230 mm and 204 mm respectively. The schematic diagram is a generalized view of the straightening machine and process. Actual machine will have same basic principle with various additional features to facilitate required operation. This cross-roll bar straightening machine of model SMH-25 is capable to adjust gap between the rollers according to the bar size. Specification of this bar straightening machine (Model SMH-25) is given in Table 6.1

Table 6.1 Specification of Rotary Straightener (MODEL: SMH-25)

Type	Single Stand of 2 Roll of High Carbon High Chromium D3 Tool Steel
Round Bar Dimension (Diameter / Length) mm	Diameter up to 25 mm / Length 4500 mm
Roll Diameter, Barrel Length	Concave Roll Dia. 191.60 mm, Centre 177.17 mm, Length 230 mm Convex Roll Dia. 177 mm, Centre 192 mm, Length 204 mm
Profile	One Roll is concave pattern and other Roll is convex pattern
Skew angle range / Degree	$5^{o} – 20^{o}$
Drive Motor	3.7 kW x 2

The model SMH-25 can straighten the round bars up to 25 mm diameter. The helix angle can also be varied according to requirement of user. Based on equations discussed in chapter-3 the throughput speed of the bar depends on roller diameter,

angular speed of roller and helix angle. Figure 6.3 shows a photograph of SMH-25 machine while the bar is in the process of straightening.

For the purpose of clarity on the shape of convex and concave rollers which have been used actually for straightening of round bars have been shown in photograph in Figure 6.4. Dimensional details in millimeter of these rollers are shown in Figure 6.5 and Figure 6.6.

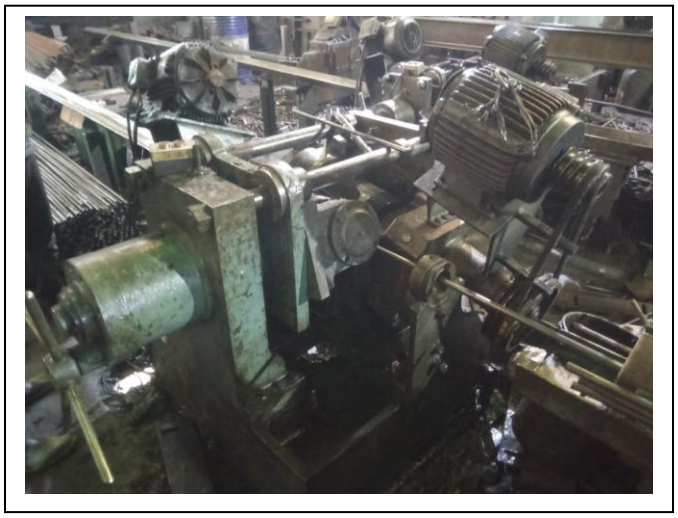

Figure 6.3 Photograph of Experimental Set up of Model SMH-25 Two-Roll Type "Air-Bend" Reeling Machine Used for Cross-Roll Straightening.

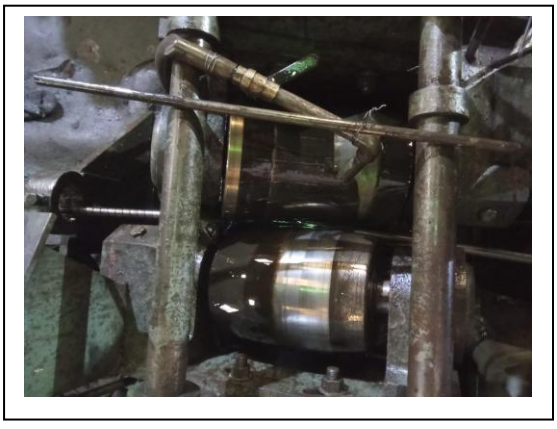

Figure 6.4 Photograph of Cross-Roll Arrangement in SMH-25 Model Showing Convex and Concave Roll and a 12-mm Stainless Steel Round Bar on Actual Straightening Process.

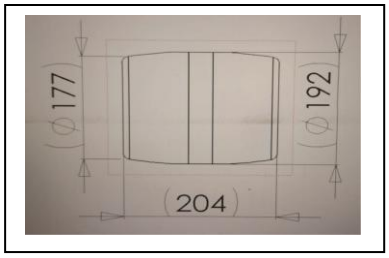

Figure 6.5 Dimensional Sketch of Convex Roller (in mm).

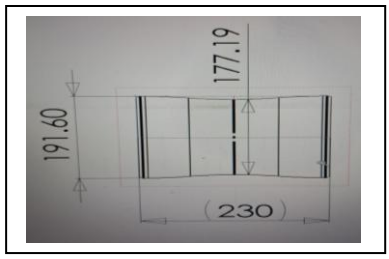

Figure 6.6 Dimensional Sketch of Concave Roller (in mm).

6.3 Results of Measurements of Straightness of Bars through Total Indicated Readings (TIR) before Straightening.

From the experimentation of round bars of various sizes and types of materials, a set of data have been recorded using measurement system through Total Indicated Reading (TIR) using scatter plots before straightening. To study and analyse straightness aspects, experimental set up as shown in Figure 6.1 has been used for measurements before straightening. Experiments have been conducted with sample of round bars of 6-mm, 8-mm, 10-mm and 12-mm diameters of mild steel, stainless steel, aluminium and copper materials respectively before straightening. Sample bars were taken one by one and have been placed over V-Blocks. Each bar is then measured for deflections, if any through dial gauges over small length segments along the bar length. For the purpose of clear understanding of the variations, small length segments have been chosen, otherwise for larger or long segments there would have been natural sagging of simply supported beams. An assumption here is that natural sagging will be insignificant over small length segments and can be ignored for present study. The process was repeated for each bar at intervals of about 6mm to 10mm along the bar lengths shown in Table 6.2, Table 6.3, Table 6.4 and Table 6.5. Readings through dial gauges were taken and data recorded. Graphical representation of these data are given in scatter plots shown in Figure 6.7, Figure 6.8, Figure 6.9 and Figure 6.10 respectively for further analysis. For the purpose of clear understanding of the variation

of deviations, small length segments have been chosen, otherwise for larger or long segments there would have been natural sagging of simply supported beams. An assumption here is that natural sagging will be insignificant over small length segments and can be ignored for present study. The process is repeated at an interval of about 6 mm to 10 mm along the bar length. Dial gauges readings were taken and data recorded. These data have been plotted for graphical representation along the bar axis for further analysis.

6.3.1 Straightness of Mild Steel (MS) Bars before Straightening

Four round bars of ferrous materials i.e. of mild steel were considered for straightness measurement. Diameter of these round bars were chosen as 6-mm, 8-mm, 10-mm and 12-mm respectively. These round bars have been put on two V-Blocks supported in a fixture and deflections through dial gauge readings noted as illustrated in Figure 6.1. Dial gauge readings for each type of MS rod along the length of the bar with an interval of about 10 mm have been taken as shown in Table 6.2.

Table 6.2 Observations of Dial Gauges in Mild Steel Bars of Diameters 6-mm, 8-mm, 10-mm & 12-mm before Straightening.

		Dial Gauge Readings of Mild Steel Rods x 0.01 mm			
Section	Length Segment	Dia. 6 mm	Dia. 8mm	Dia. 10mm	Dia. 12mm
1	30	2	0	0	0
2	40	0	2	1	1
3	50	2	4	1	3
4	60	1	4	0	0
5	70	0	3	2	2
6	80	0	0	2	2
7	90	3	3	3	0
8	100	2	0	0	0
9	110	0	2	0	3
10	120	2	1	0	2

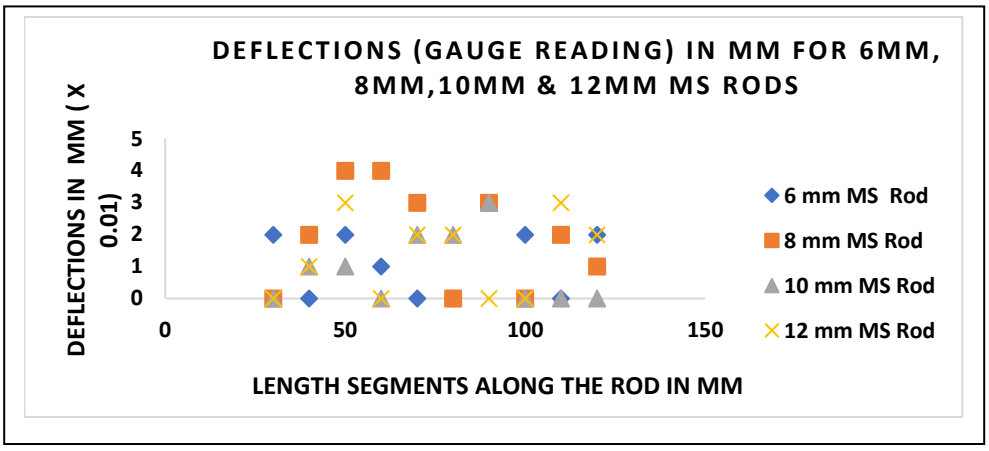

Figure 6.7 Scatter Plot Showing Deflections in Dial Gauges along the Length of 6-mm, 8-mm, 10-mm and 12-mm Mild Steel Bars Respectively before straightening

Variations of deflection readings in dial gauge as observed are shown in Figure 6.7 for four different sizes i.e. 6 mm, 8 mm, 10 mm and 12 mm of bars along the bar lengths. It can be seen from the plot that for each type of round bars, deflection variations are not uniform rather somewhat random in nature. The data shows that there are deflections at many sections in bars which indicates bars are not quite straight. The

scatter plots however show that although straightness is compromised at various sections but for general purpose overall deviations are not very significant. All the four plots of diameters 6-mm, 8-mm, 10-mm & 12-mm of MS bars, it is evident that deflections at various sections along the bar lengths do not follow any specific distribution pattern and hence can be considered as randomly distributed.

6.3.2 Straightness of Stainless Steel (SS) Bars before Straightening

For stainless steel round bars of sizes 6-mm, 8-mm, 10-mm and 12-mm respectively, a similar process has been carried out. Dial gauge readings as tabulated in Table 6.3 have been used against each bar along the length and the corresponding scatter plots shown in Figure 6.8.

Scatter plots of deflections of SS bars along the length at indicated intervals. In this case also, the scatter plot shows that at many sections there are deviations in bars along the length which means residual curvatures are in existence. It can be seen that variations of deflections are again not uniform for each type of round bars. The deviations observed are random in nature.

Table 6.3 Observations of Dial Gauges in Stainless Steel Bars of Diameters 6-mm, 8-mm, 10-mm & 12-mm before Straightening.

		Dial Gauge Readings of Stainless-Steel Rods x 0.01 mm			
Section	Length Segment	Dia. 6 mm	Dia. 8mm	Dia. 10mm	Dia. 12mm
1	18	3	0	0	0
2	24	1	1	2	2
3	30	0	2	0	2
4	36	3	3	0	1
5	42	0	0	0	3
6	48	0	0	2	0
7	54	4	2	3	0
8	60	0	0	5	1
9	66	1	1	0	0
10	72	0	0	0	0

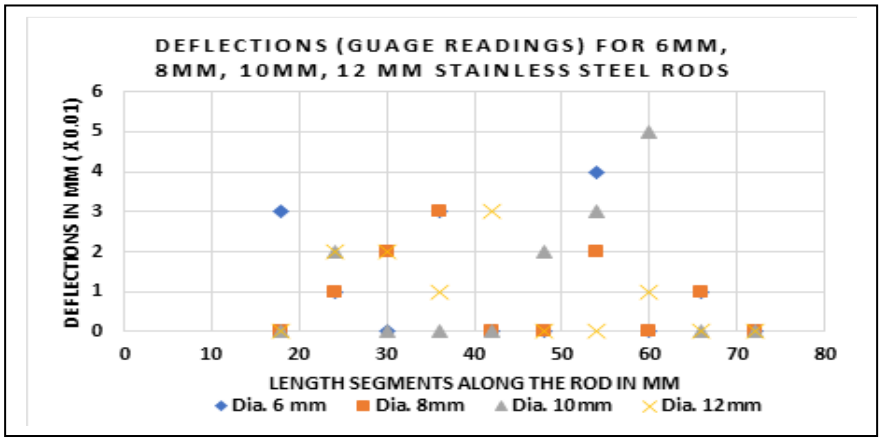

Figure 6.8 Scatter Plot Showing Deflections in Dial Gauges along the Length of 6-mm, 8-mm, 10-mm and 12-mm Stainless Steel Bars respectively before straightening.

However, in many cases deviations are practically zero which means bar is quite straight in these sectional zones. In all the four plots of SS bars of diameters from 6 mm to 12 mm shown in Figure 6.8, it is observed that deflections data along the length as such do not follow any specific distribution pattern and can be considered as random distribution.

6.3.3 Straightness of Aluminium (Al) Bars before Straightening

Four round bars of diameter 6-mm, 8-mm, 10-mm and 12-mm respectively of Aluminum material have been considered for measurement of deflection data using dial gauge as done previously for mild steel and stainless steel round bars. Readings have been noted along bar length at indicated intervals as shown in Table 6.4. From the noted readings, deviations observed at some sections even in small length segments. Scatter plot generated based on these data and shown in Figure 6.9. It has been observed from all the scatter plots of 6mm, 8mm, 10mm and 12mm diameter aluminium round rods that deflections do not follow any specific distribution pattern.

Table 6.4. Observations of Dial Gauges in Aluminium Bars of Diameters 6-mm, 8-mm, 10-mm & 12-mm before Straightening

		Dial Gauge Readings of Aluminium x 0.01 mm			
Section	Length Segment	Dia. 6 mm	Dia. 8mm	Dia. 10mm	Dia. 12mm
1	30	0	0	3	4
2	40	0	3	2	2
3	50	2	0	0	0
4	60	1	2	3	0
5	70	0	5	0	0
6	80	0	3	5	0
7	90	2	0	2	2
8	100	3	0	2	3
9	110	0	4	5	0
10	120	1	0	0	0

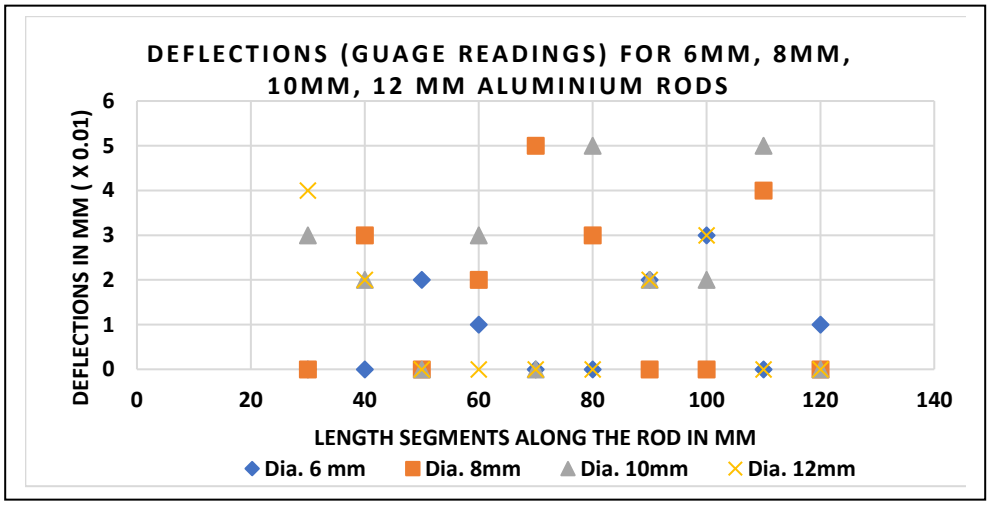

Figure 6.9 Scatter Plot showing Deflections in Dial Gauges along the Length of 6-mm, 8-mm, 10-mm and 12-mm Diameter Aluminium Bars respectively before Straightening.

6.3.4 Straightness of Copper (Cu) Bars before Straightening

In the same process like Mild Steel, Stainless Steel and Aluminium round bars, 6-mm, 8-mm, 10-mm and 12-mm diameter respectively of Copper bars have been chosen for the similar study. Dial gauge readings after measurements have been noted against each bar at intervals and shown in Table 6.5. Scatter plots have been generated based on

these measured data and shown in Figure 6.10. Again, it became quite evident from the scatter plots that there is no specific pattern in the deviations that exist even over small segmented lengths.

Table 6.5 Observations of Dial Gauges in Copper Bars of Diameters 6-mm, 8-mm, 10-mm & 12-mm before Straightening

		Dial Gauge Readings of Copper Rods x 0.01 mm			
Section	Length Segment	Dia. 6 mm	Dia. 8mm	Dia. 10mm	Dia. 12mm
1	20	0	0	0	0
2	30	5	8	2	1
3	40	8	6	7	3
4	50	6	2	10	2
5	60	6	0	8	5
6	70	2	5	2	0
7	80	5	2	0	2
8	90	0	0	0	0

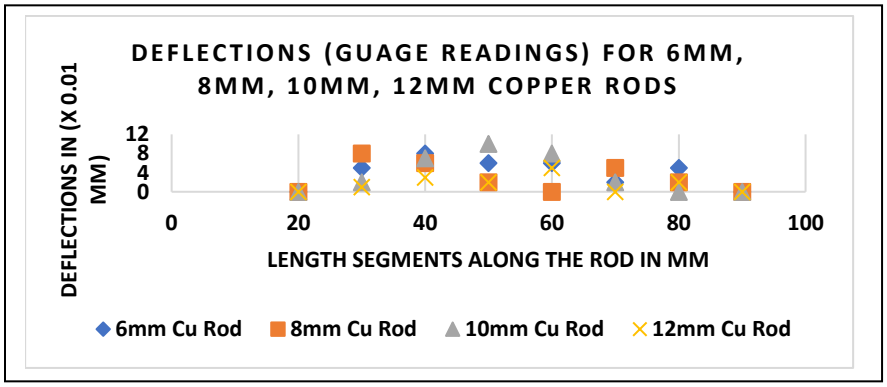

Figure 6.10 Scatter Plot Showing Deflections in Dial Gauges along the Length of 6-mm, 8-mm, 10-mm and 12-mm Copper Bars respectively before straightening

In the manufacturing process of these round bars, several factors seem to be involved viz. rollers speed, rollers adjustments and material handling thereafter at shops. Generally, these bars are usually available in certain standard-length sizes of 6 m length and our samples too have been chosen from cut pieces of such standard size bars. The small length of cut pieces were easy to handle and conduct measurement of required data in the experimental set up of V-Block arrangement as illustrated in Figure 1. Moreover, measurement of dial gauge deflections has also been taken at various length

of segment for different angular positions by rotation of bars (from 0◦ to 360◦) to observe the circularity of outer surface of the bars used in this investigation. Present investigation attempted to show dial gauge deflections based on circumferential deformations into segmental lengths along the bar length with the help of 3D Surface plots and corresponding Radar charts.

6.3.5 Error Analysis of Measurements of Bars before straightening

It is as such well known that performing the experiment and collecting data in only the beginning of the process of completing an experiment. Understanding the results of any given experiment is always the central goal of the experiment. Presenting those results in a clear concise manner completes the experiment. All measurements have errors which may arise from three sources namely Careless Errors, Systematic Errors and lastly Random Errors.

Careless errors are due mistakes in reading scales or careless setting of markers etc. which can be eliminated by repetition of readings by one or two observers. Systematic errors are due to built-in errors in the instrument either in design or calibration. Repetition of observation with the same instrument will not show a spread in the measurements. They are the hardest source of errors to detect. Random errors always lead to a spread or distribution of results on repetition of the particular measurement. They may arise from fluctuations in either the physical parameters due to statistical nature of the particular phenomenon or the judgement of the experimenter, such as variation in response time or estimation in the scale reading. Taking multiple measurements helps reduce uncertainties. In this sub-article error analysis has been done from the dataset shown in previous Chapter-5 for data recorded before straightening process which is basically commercial available round bars.

Error analysis of the dataset given in [96, 97, 98, 99] have been considered here. These dataset are for the measurement of Mild Steel (MS), Stainless Steel (SS), Aluminium (Al) and Copper (Cu) bars of sizes 6-mm, 8-mm, 10-mm and 12-mm diameters respectively. The error plots have been shown in Figure 6.11 to Figure 6.26.

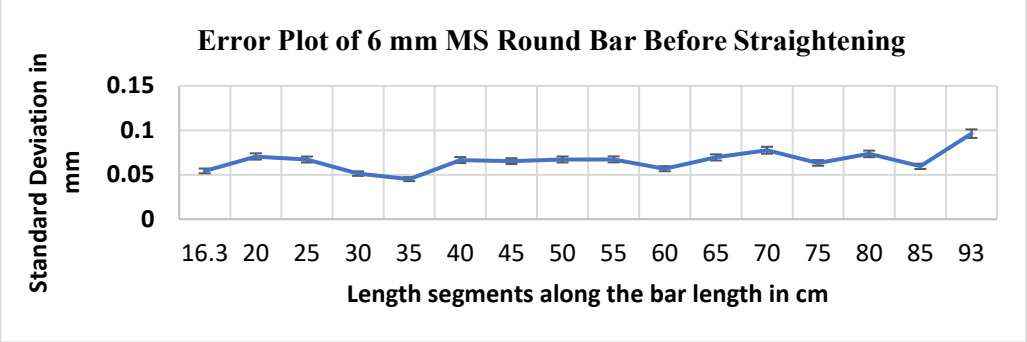

Figure 6.11 Error Plot of 6-mm Mild Steel Round Bar before Straightening

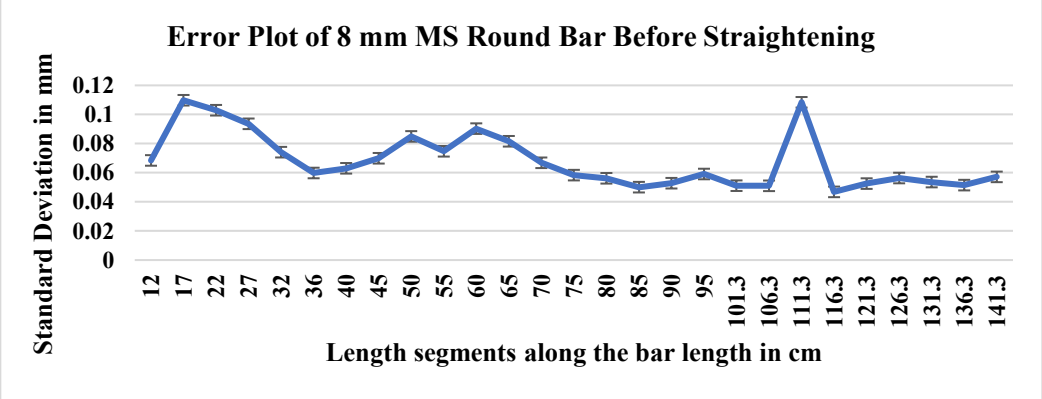

Figure 6.12 Error Plot of 8-mm Mild Steel Round Bar before Straightening

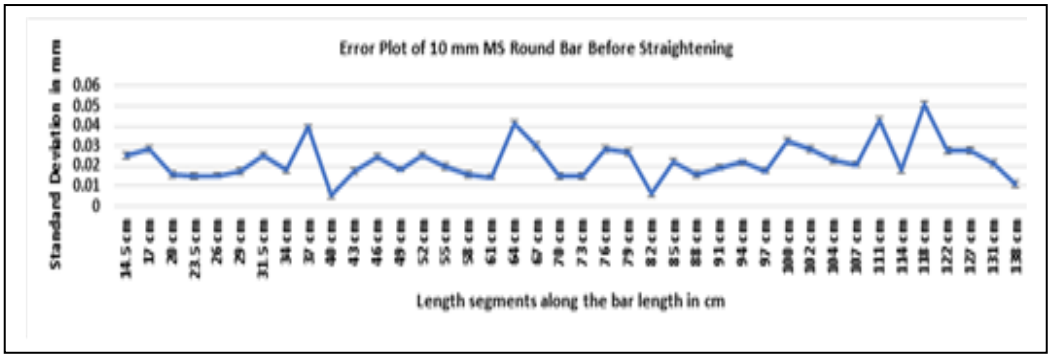

Figure 6.13 Error Plot of 10-mm Mild Steel Round Bar before straightening

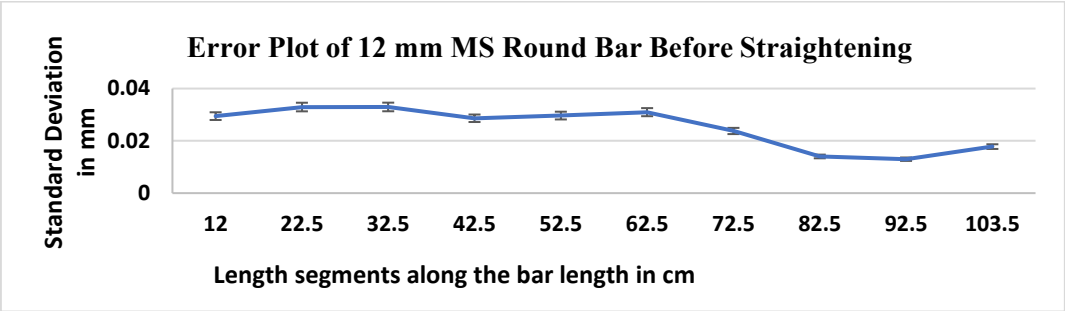

Figure 6.14 Error Plot of 12-mm Mild Steel Round Bar before straightening

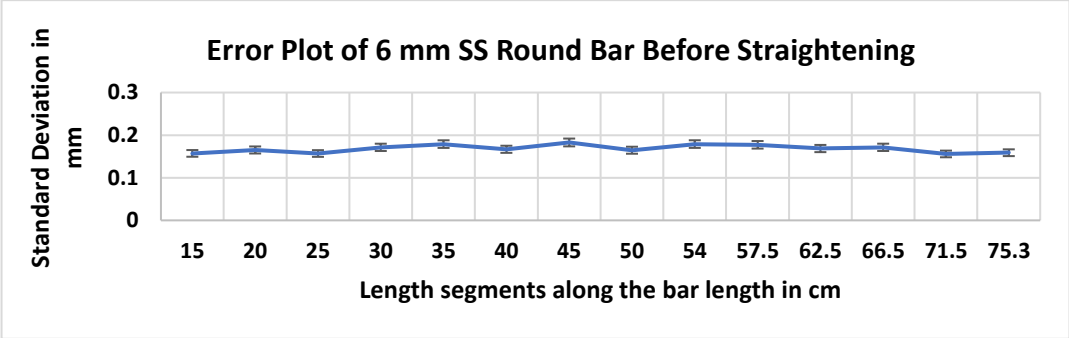

Figure 6.15 Error Plot of 6-mm Stainless Steel Round Bar before straightening

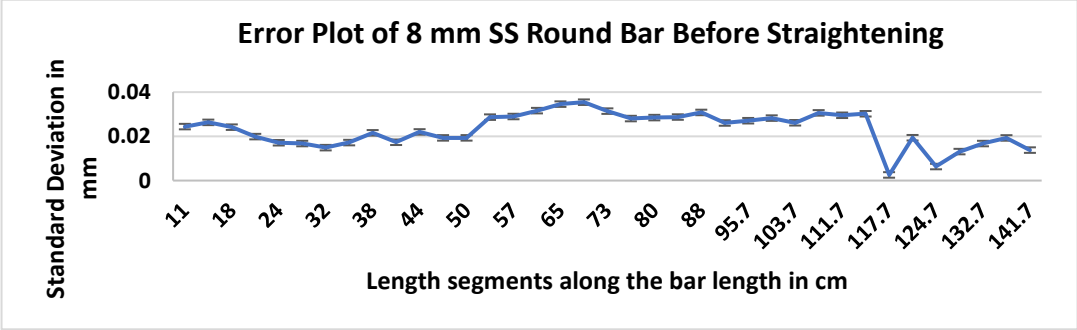

Figure 6.16 Error Plot of 8-mm Stainless Steel Round Bar before straightening

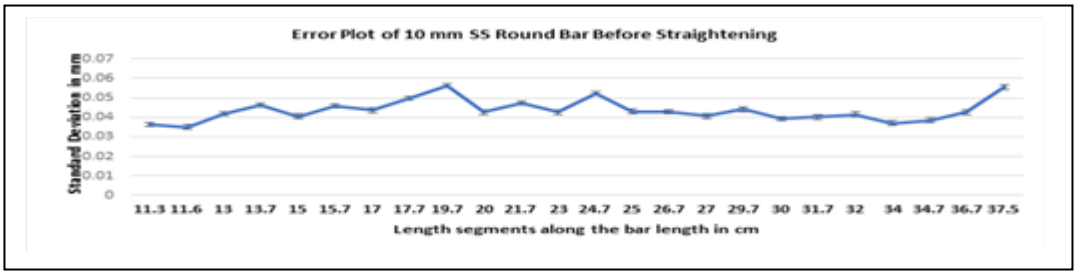

Figure 6.17 Error Plot of 10-mm Stainless Steel Round Bar before straightening

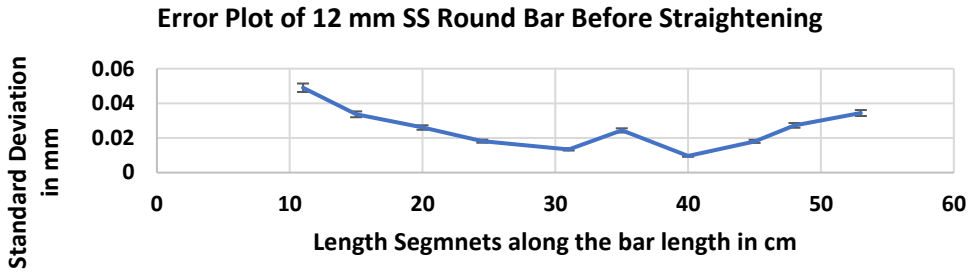

Figure 6.18 Error Plot of 12-mm Stainless Steel Round Bar before straightening

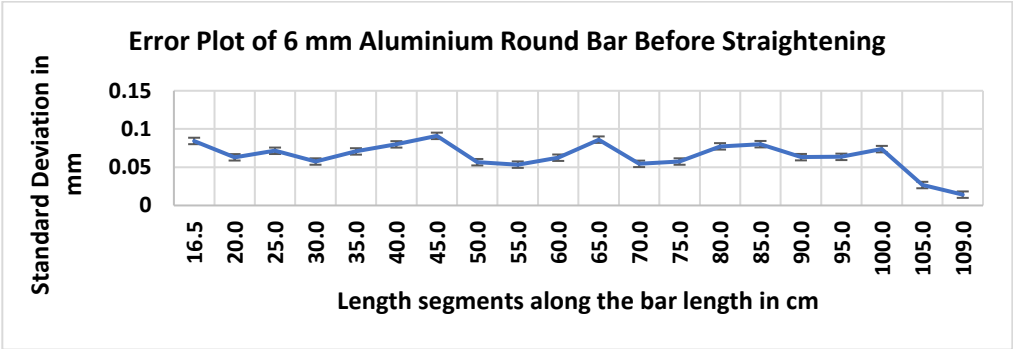

Figure 6.19 Error Plot of 6-mm Aluminium Round Bar before straightening

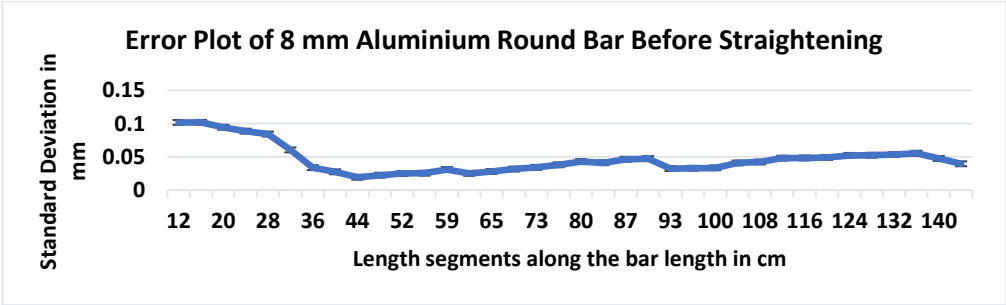

Figure 6.20 Error Plot of 8-mm Aluminium Round Bar before straightening

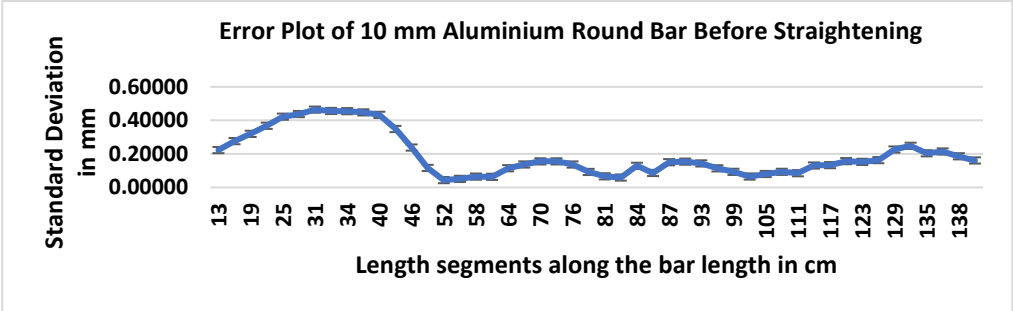

Figure 6.21 Error Plot of 10-mm Aluminium Round Bar before straightening

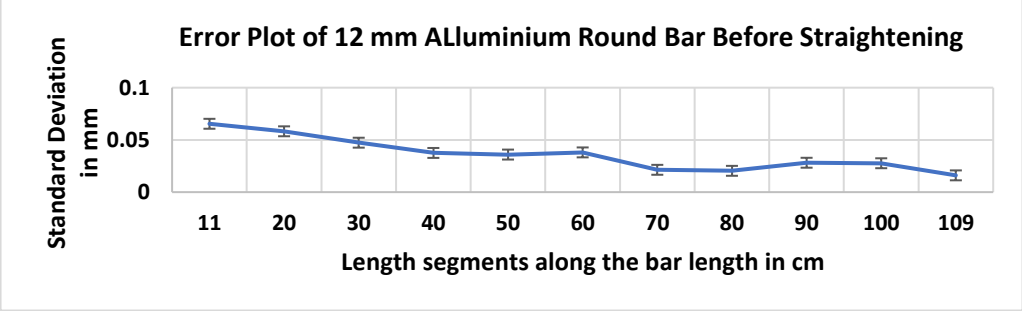

Figure 6.22 Error Plot of 12-mm Aluminium Round Bar before straightening

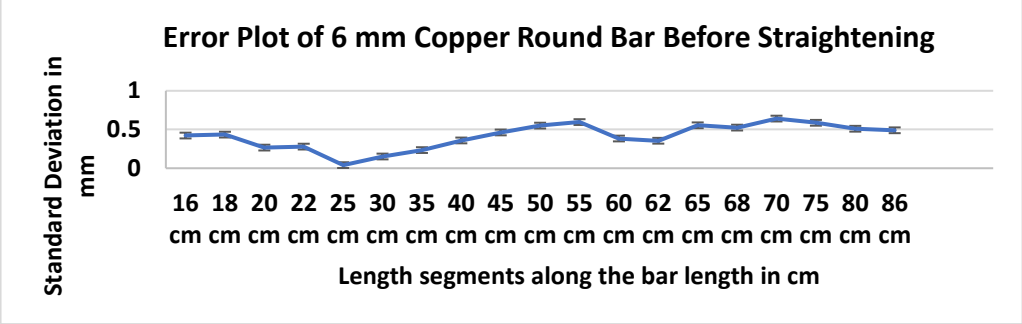

Figure 6.23 Error Plot of 6-mm Copper Round Bar before straightening

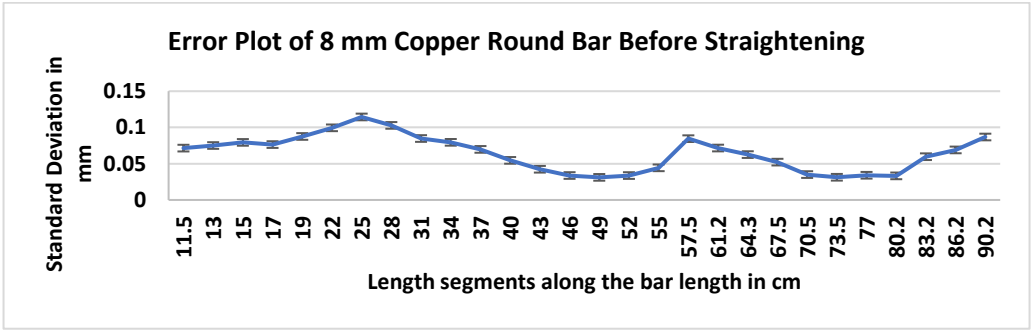

Figure 6.24 Error Plot of 8-mm Copper Round Bar before straightening

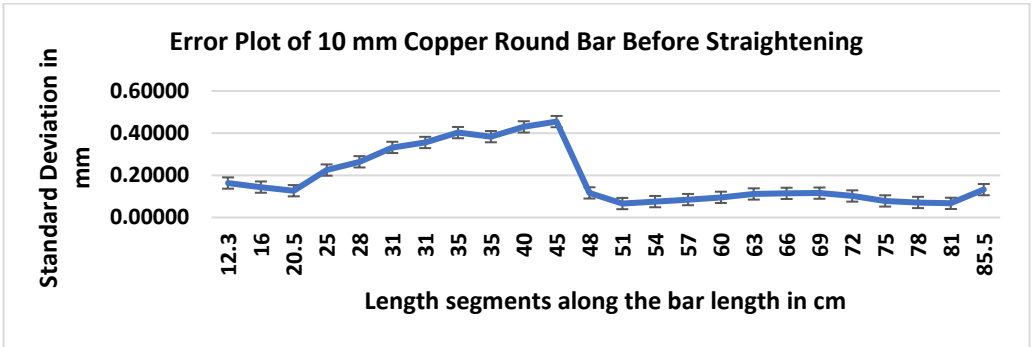

Figure 6.25 Error Plot of 10-mm Copper Round Bar before straightening

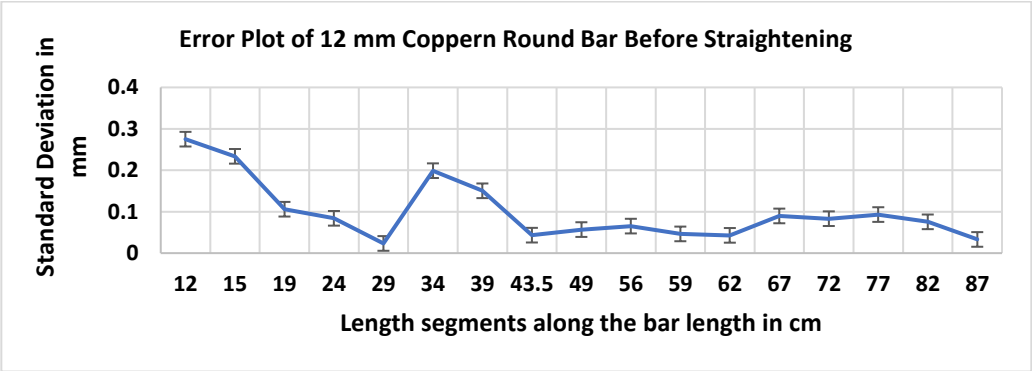

Figure 6.26 Error Plot of 12-mm Copper Round Bar before straightening

The above-mentioned error plots which are based on standard deviations of the dataset measured using the experimental set up reveals that there are variations in the standard deviation itself in all the error plots. There is likelihood of all three kind of errors in the dataset. Although 12x24=288 sets of measurements conducted on every single round bar, but possibility is there that errors exist. It also reveals that the standard deviations in all the above cases lie within a reasonable limit.

6.4 Results of Measurements of Straightness / Roundness of Bars through Total Indicated Readings (TIR) after Straightening

To study and analyse straightness aspect based on TIR system, same experimental set up as shown in Figure 6.1 has been used for measurements after straightening. Experiments have been conducted again with same sample of round bars of 6 mm, 8 mm, 10 mm and 12 mm diameters of mild steel, stainless steel, aluminium and copper materials respectively after straightening. Same sample bars were taken one by one and have been placed over V-Blocks. Each bar is then measured for deflections, if any through dial gauges over small length segments along the bar length.

Same small length segments have been chosen to understand the variation of deviations. The process is repeated throughout each bar at intervals shown in Table 6.6 to Table 6.9 along the bar length. Readings through dial gauges were taken and data are recorded. These data are then plotted along the bar axis for further analysis.

6.4.1 Straightness of Mild Steel (MS) bars after Straightening

Mild Steel round bars of 6mm, 8mm, 10mm and 12mm have been considered one by one in the experimental set up shown in Figure 6.1 and observations have been recorded for analysis of straightness after straightening operation. Table 6.6 shows the data of above mentioned bars taken through dial gauge. The deflection data have been presented in Table 6.6 and scatter plot have been shown in Figure 6.27.

Table 6.6 Observations of Dial Gauges in Mild Steel Bars of Diameters 6-mm, 8-mm, 10-mm & 12-mm after Straightening.

		Dial Gauge Readings of Mild Steel Rods x 0.01 mm			
Section	Length Segment	Dia. 6 mm	Dia. 8mm	Dia. 10mm	Dia. 12mm
1	30	2	0	0	0
2	40	0	1	1	1
3	50	1	3	1	2
4	60	1	3	0	0
5	70	0	2	1	1
6	80	0	0	1	1
7	90	2	2	2	0
8	100	1	0	0	0
9	110	0	1	0	2
10	120	2	1	0	2

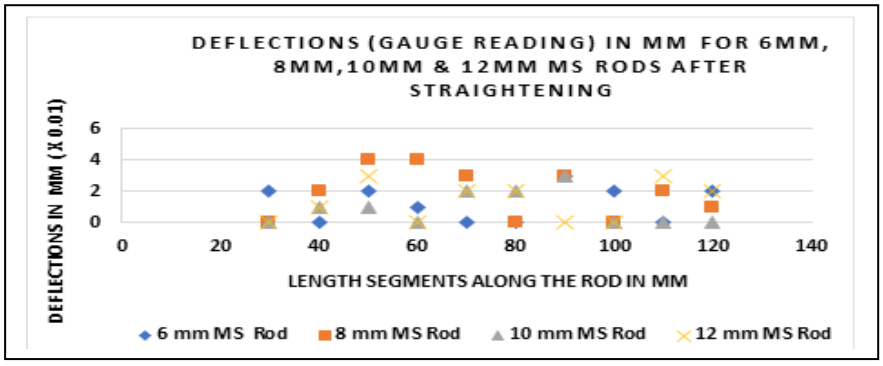

Figure 6.27 Scatter Plot Showing Deflections in Dial Gauges along the Length of 6-mm, 8-mm, 10-mm and 12-mm Mild Steel Bars respectively after straightening

Variations of deflections readings at various sections in dial gauge for four sizes of mild steel bars of 6 mm, 8 mm, 10 mm and 12 mm along the length are shown in Figure 6.27. From the data set it is seen that deflections are not uniform along the length and also random in nature which indicates that straightness in compromised at many sections but for general purpose overall deviations are not very significant. Scatter plots for different sizes indicate maximum and minimum deflections are also random in nature. After straightening some of the deflection values have reduced when compared to data before straightening as shown in Table 6.2 and Figure 6.7.

6.4.2 Straightness of Stainless Steel (SS) Bars after Straightening

Stainless Steel round bars of 6mm, 8mm, 10mm and 12mm have been considered one by one in the experimental set up shown in Figure 6.1 and observations have been recorded for analysis of straightness after straightening operation. Table 6.7 shows the deflection data of above-mentioned bars taken through dial gauge and scatter plot have been shown in Figure 6.28.

Table 6.7 Observations of Dial Gauges in Stainless Steel Bars of Diameters 6-mm, 8-mm, 10-mm & 12-mm after Straightening.

		Dial Gauge Readings of Stainless-Steel Rods x 0.01 mm			
Section	Length Segment	Dia. 6 mm	Dia. 8mm	Dia. 10mm	Dia. 12mm
1	18	2	0	0	0
2	24	1	1	1	1
3	30	0	1	0	1
4	36	2	2	0	0
5	42	0	0	0	2
6	48	0	0	1	0
7	54	3	1	2	0
8	60	0	0	3	1
9	66	1	1	0	0
10	72	0	0	0	0

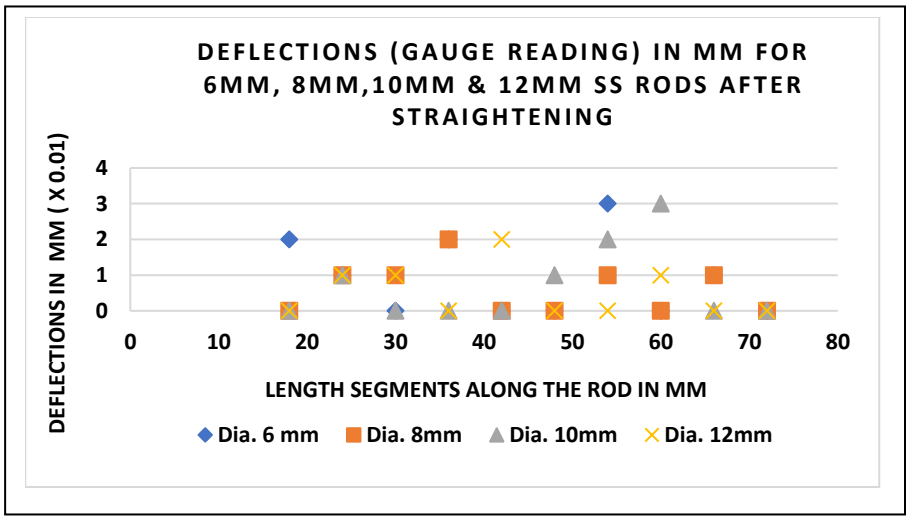

Figure 6.28 Scatter Plot Showing Deflections in Dial Gauges along the Length of 6-mm, 8-mm, 10-mm and 12-mm Stainless Steel Bars respectively after straightening.

Variations of deflections readings at various sections in dial gauge for four sizes of stainless steel bars of 6 mm, 8 mm, 10 mm and 12 mm along the length are shown in Figure 6.28. From the data set it is seen that deflections are not uniform along the length and also random in nature which indicates that straightness in compromised at many sections but for general purpose overall deviations are not very significant. These scatter plots for different sizes of SS bars indicate deflections are also random in nature. After straightening some of the deflection values have reduced when compared to data before straightening as shown in Table 6.3 and Figure 6.8.

6.4.3 Straightness of Aluminium (Al) Bars after Straightening

Aluminium round bars of 6mm, 8mm, 10mm and 12mm have been considered one by one in the experimental set up shown in Figure 6.1 and observations have been recorded for analysis of straightness after straightening operation. Table 6.8 shows the deflection data of above-mentioned bars taken through dial gauge and scatter plot have been shown in Figure 6.29.

Table 6.8 Observations of Dial Gauges in Aluminium Bars of Diameters 6-mm, 8-mm, 10-mm & 12-mm after Straightening.

		Dial Gauge Readings of Stainless-Steel Rods x 0.01 mm			
Section	**Length Segment**	**Dia. 6 mm**	**Dia. 8mm**	**Dia. 10mm**	**Dia. 12mm**
1	30	0	0	2	3
2	40	0	2	1	1
3	50	1	0	0	0
4	60	0	1	2	0
5	70	0	3	0	0
6	80	0	2	3	0
7	90	1	0	1	1
8	100	2	0	1	2
9	110	0	3	4	0
10	120	1	0	0	0

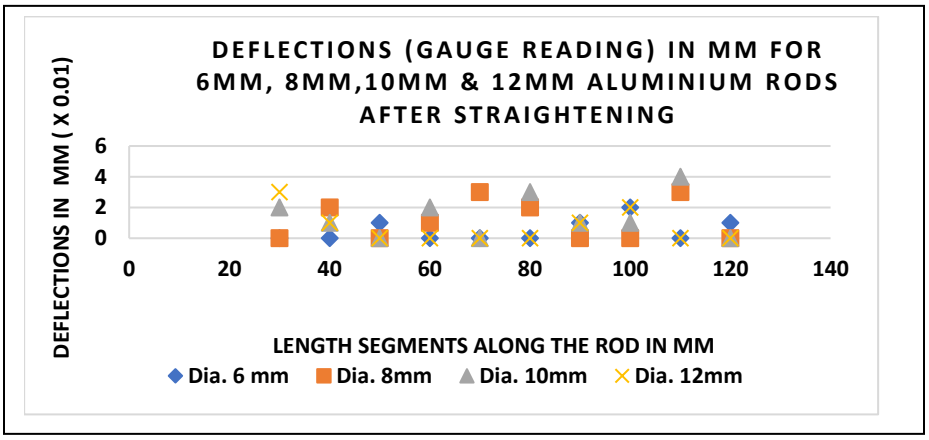

Figure 6.29 Scatter Plot Showing Deflections in Dial Gauges along the Length of 6-mm, 8-mm, 10-mm and 12-mm Aluminium Bars respectively after straightening.

Variations of deflections readings at various sections in dial gauge for four sizes of aluminium bars of 6 mm, 8 mm, 10 mm and 12 mm along the length are shown in Figure 6.29. From the dataset it is seen that deflections are not uniform along the length and also random in nature which indicates that straightness along the round bars is compromised at many sections but for general purpose overall deviations are not very significant. Scatter plots for different sizes indicate maximum and minimum deflections are also random in nature. After straightening some of the deflection values have reduced when compared to data before straightening as shown in Table 6.4 and Figure 6.9.

6.4.4 Straightness of Copper (Cu) Bars after Straightening

Copper round bars of 6-mm, 8-mm, 10-mm and 12-mm have been considered one by one in the experimental set up shown in Figure 6.1 and observations have been recorded for analysis of straightness after straightening operation. Table 6.9 shows the deflection data of above-mentioned bars taken through dial gauge and scatter plot have been shown in Figure 6.30.

Table 6.9 Observations of Dial Gauges in Copper Bars of Diameters 6-mm, 8-mm, 10-mm & 12-mm after Straightening

		Dial Gauge Readings of Copper Rods x 0.01 mm			
Section	Length Segment	Dia. 6 mm	Dia. 8mm	Dia. 10mm	Dia. 12mm
1	20	0	0	0	0
2	30	3	6	1	0
3	40	6	4	5	2
4	50	4	1	7	1
5	60	4	0	6	3
6	70	1	3	1	0
7	80	3	1	0	1
8	90	0	0	0	0

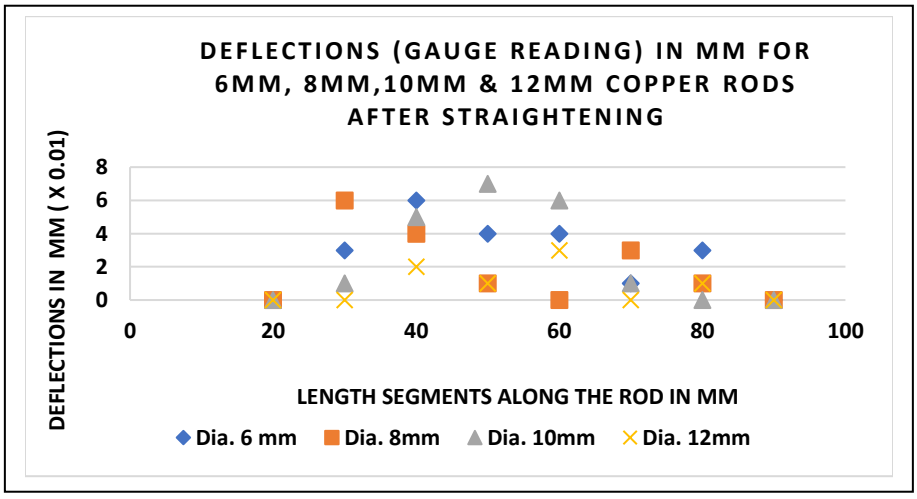

Figure 6.30 Scatter Plot Showing Deflections in Dial Gauges along the Length of 6-mm, 8-mm, 10-mm and 12-mm Copper Bars respectively after straightening

Variations of deflections readings at various sections in dial gauge for four sizes of copper bars of 6 mm, 8 mm, 10 mm and 12 mm along the length are shown in Figure 6.30. From the data set it is seen that deflections are not uniform along the length and also random in nature which indicates that straightness in compromised at many sections but for general purpose overall deviations are not very significant. Scatter plots for different sizes indicate maximum and minimum deflections are also random in nature. After straightening some of the deflection values have reduced when compared to data before straightening as shown in Table 6.5 and Figure 6.10.

6.5 Results of Roundness of Bars after Straightening

From the experimentation of round bars of various sizes and types of materials, a set of data have been recorded using measurement system through Total Indicated Readings (TIR) method before straightening which has been presented in sub-article 6.3. To study and analyse roundness and straightness aspect based on TIR system, same experimental set up as shown in Figure 6.1 has been used for measurements after straightening. Experiments have been conducted again with same sample of round bars of 6 mm, 8 mm, 10 mm and 12 mm diameters of mild steel, stainless steel, aluminium and copper materials respectively after straightening. Same sample of round bars were taken one by one and have been placed over V-Blocks. Each bar is then measured for deflections over small segments along the bar length.

Small length segments have been chosen to understand the variation of deviations. The process is repeated throughout each bar at intervals along the bar length. Readings through dial gauges were taken and data are recorded. These data are then plotted along the bar axis for further analysis.

For each position twelve sets of observations were recorded before straightening and another twelve sets of observations were recorded after straightening. In all the cases measurements have been recorded through dial gauges and deflections have been noted. The details of the observations before straightening process of round bars have been described earlier in Chapter-5. Analysis of roundness before straightening and its variation has already been discussed in Chapter-5. In this chapter, a similar analysis has been done for same set of round bars after straightening.

Observations of deflection values through dial gauge were recorded after straightening processes. Same round bars i.e. of sizes 6-mm, 8-mm, 10-mm and 12-mm of Mild Steel, Stainless Steel, Aluminium and Copper were used respectively for straightening and observations of deflection data noted in the same manner after straightening process. In this manner a possible picture will come out as how straightening have actually occurred in different types of round bars. A brief discussion on each set of observations after straightening is given in the respective sections.

6.5.1 Observations of Mild Steel Round Bars after Straightening

A similar set of observations for 6-mm, 8-mm, 10-mm, 12-mm diameter Mild Steel (MS) round bars respectively were recorded after straightening operation. The observations have been recorded from dial gauge deflections on the outermost profile of the round bar for various cross-sections circumferentially with regular intermittent angles. Mean values of these observations have been considered and described in the dataset which can be available through GitHub link [103]. Graphical representations of dataset have been made by the analysis of box plots given in Figure 6.31 to Figure 6.34. In this manner a possible picture will come out as how straightening has actually occurred in different types of round bars.

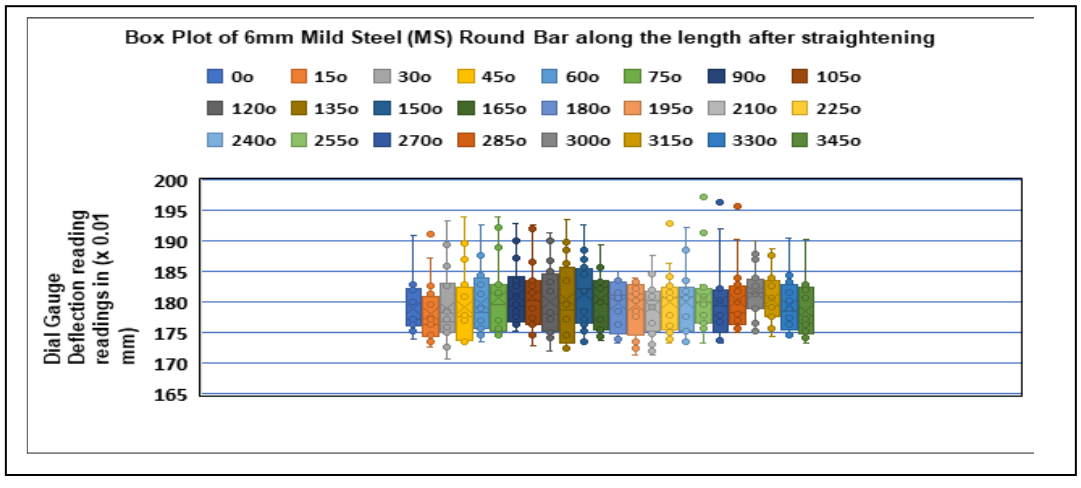

Figure 6.31 Box Plot of Dataset for Mean Values of Dial Gauge Deflection Readings of 6-mm Diameter Mild Steel (MS) Round Bar after straightening

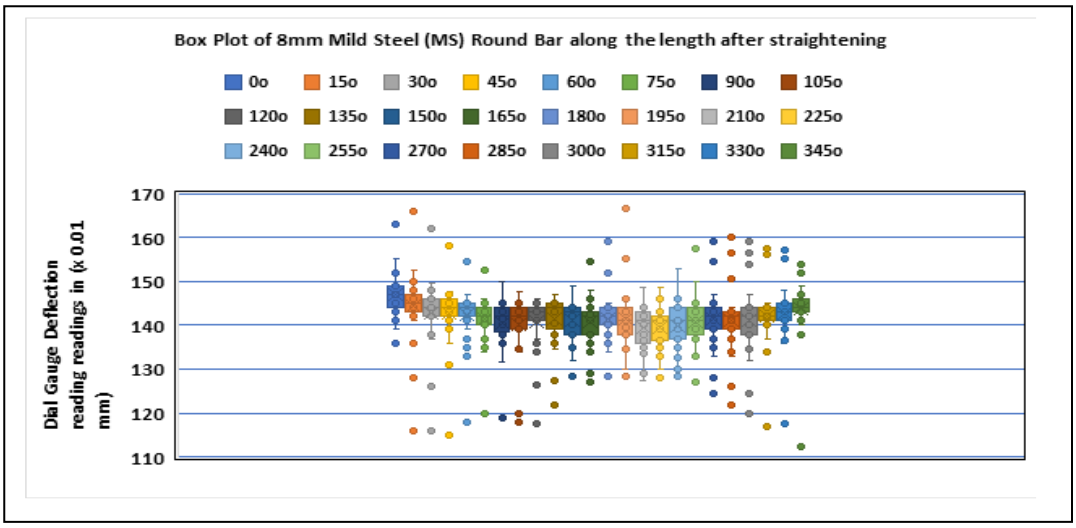

Figure 6.32. Box Plot of Dataset for Mean Values of Dial Gauge Deflection Readings of 8-mm Diameter Mild Steel (MS) Round Bar after Straightening

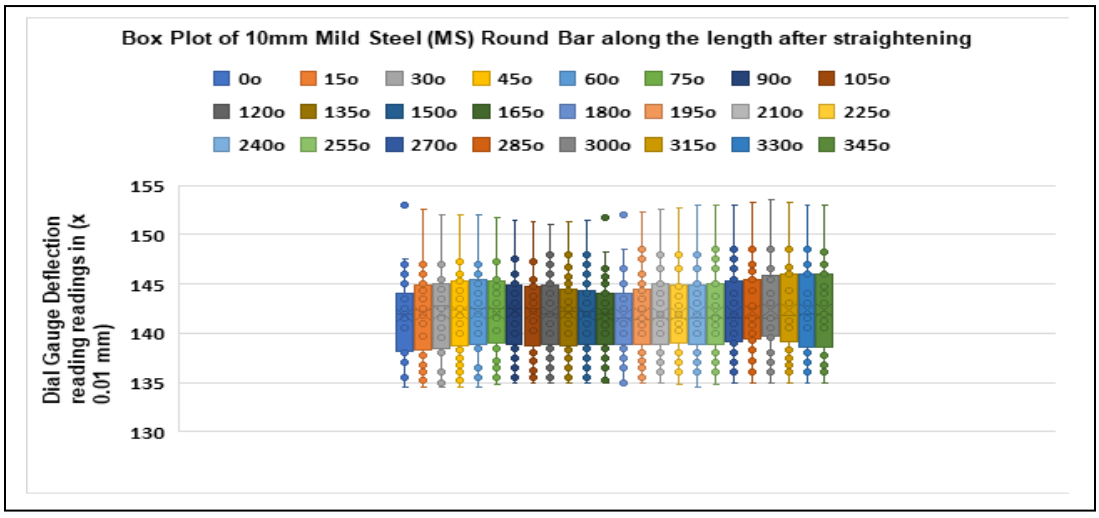

Figure 6.33 Box Plot of Dataset for Mean Values of Dial Gauge Deflection Readings of 10-mm Diameter Mild Steel (MS) Round Bar after straightening

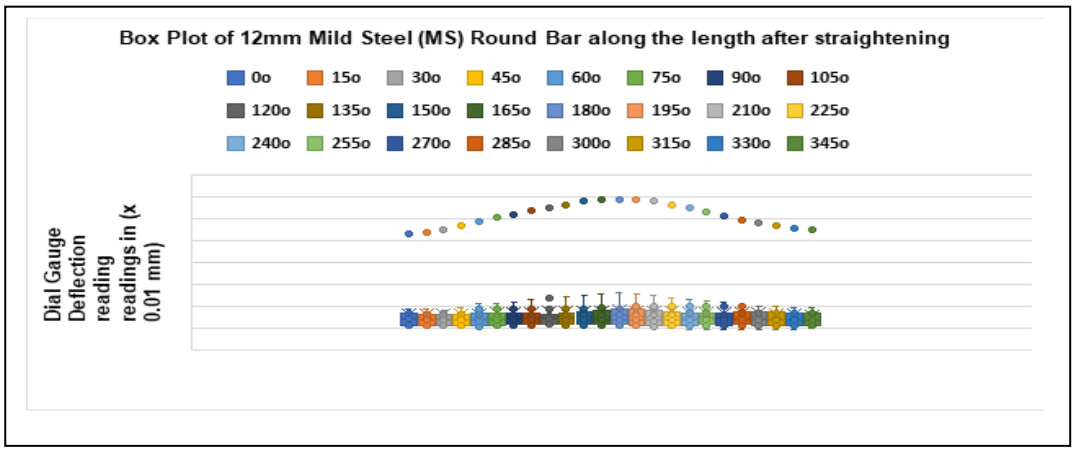

Figure 6.34 Box Plot of Dataset for Mean Values of Dial Gauge Deflection Readings of 12-mm Diameter Mild Steel (MS) Round Bar after straightening

6.5.2 Observations of Stainless Steel Round Bars after Straightening

A set of observations for 6-mm, 8-mm, 10-mm and 12-mm diameter Stainless Steel (SS) round bars were recorded respectively after straightening operation. The observations of deflection values have been recorded from dial gauge on the outermost profile of the round bars for various cross-sections circumferentially with regular intermittent angles of 15º. Mean values of these observations have been considered and given in the dataset which are available **GitHub links** [104] provided in the respective references. These dataset have been represented by the box plot analysis for comparison of values between multiple graphs. Figure 6.35, Figure 6.36, Figure 6.37 and Figure 6.38 show different kinds of box plot analysis of measured deflection values for different sizes of stainless steel round bars.

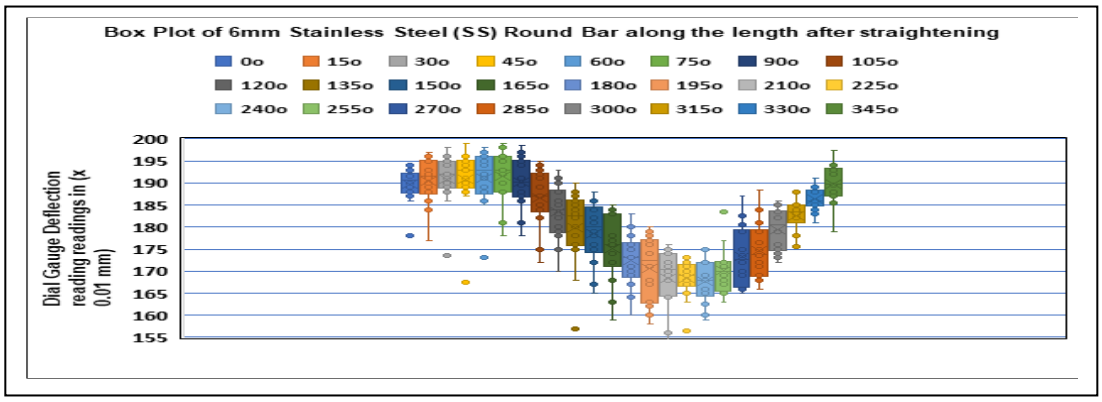

Figure 6.35 Box Plot of Dataset for Mean Values of Dial Gauge Deflection Readings of 6-mm Diameter Stainless (SS) Round Bar after Straightening

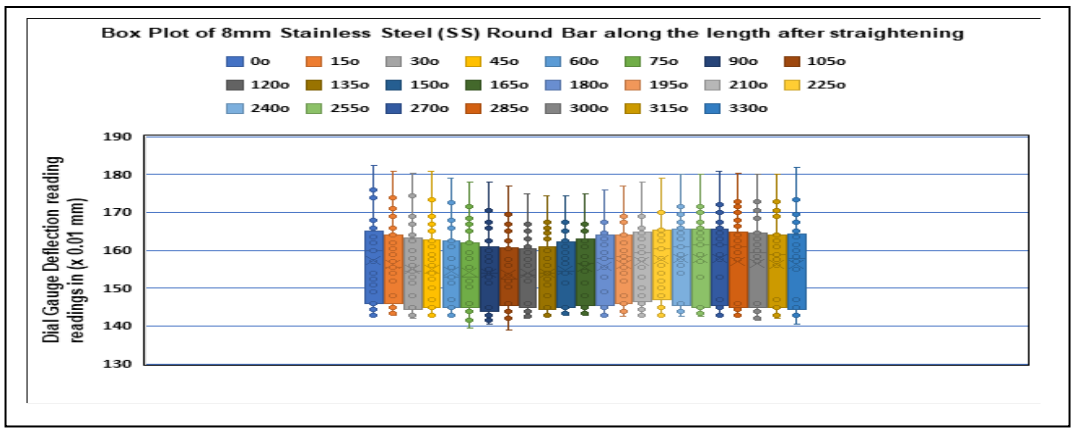

Figure 6.36 Box Plot of Dataset for Mean Values of Dial Gauge Deflection Readings of 8-mm Diameter Stainless (SS) Round Bar after straightening

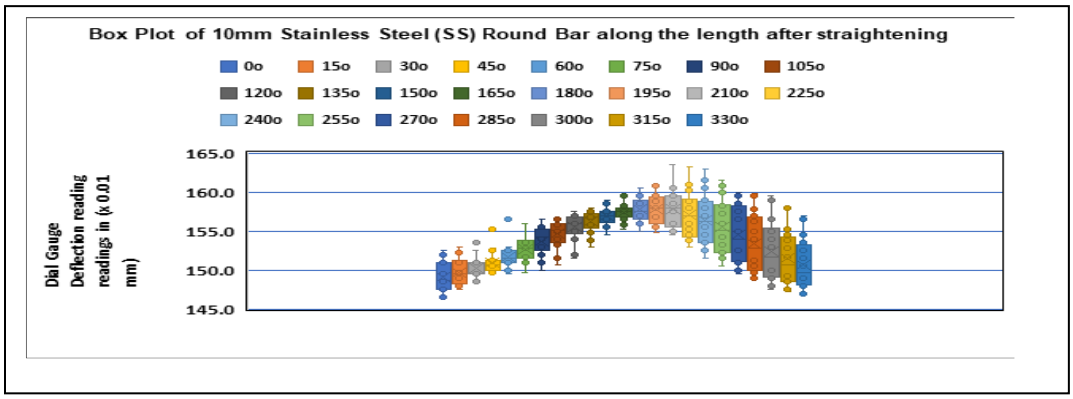

Figure 6.37 Box Plot of Dataset for Mean Values of Dial Gauge Deflection Readings of 10-mm Diameter Stainless (SS) Round Bar after straightening

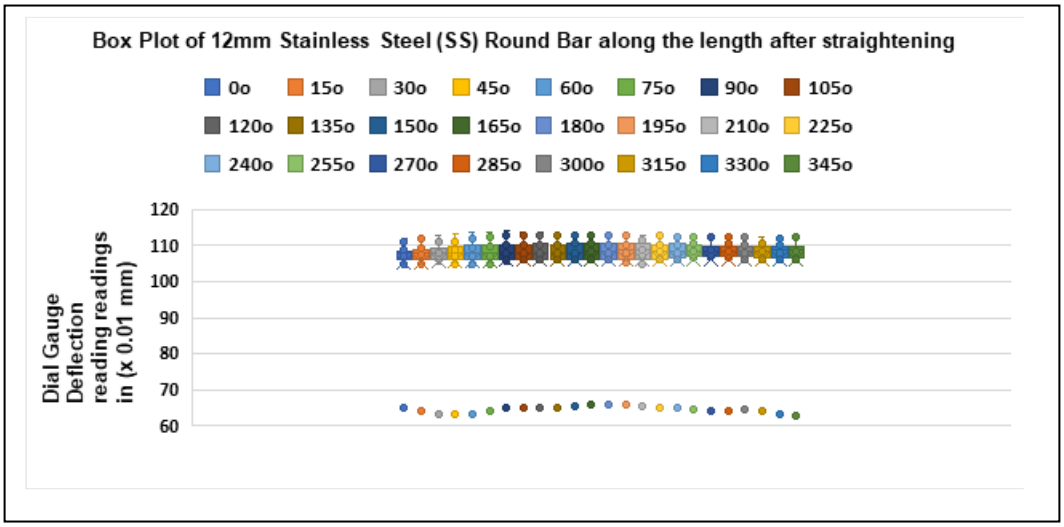

Figure 6.38 Box Plot of Dataset for Mean Values of Dial Gauge Deflection Readings of 12-mm Diameter Stainless (SS) Round Bar after straightening

6.5.3 Observations of Aluminium Round Bars after Straightening

A similar set of observations for 6-mm, 8-mm, 10-mm and 12-mm diameter Aluminium (Al) round bars respectively were recorded after straightening operation. The observations have been recorded from dial gauge deflections on the outermost profile of the round bar for various cross-sections circumferentially with regular intermittent angles of 15º. Mean values of these observations have been considered and given in the dataset which are available in **GitHub links** [105]. These dataset are represented by the analysis of box plot as illustrated in Figure 6.39, Figure 6.40, Figure 6.41 and Figure 6.42 which show the distribution of datapoints across a selected measure. These charts display ranges within variables measured which includes the outliers, the median, the mode, and where the majority of the datapoints lie in the box.

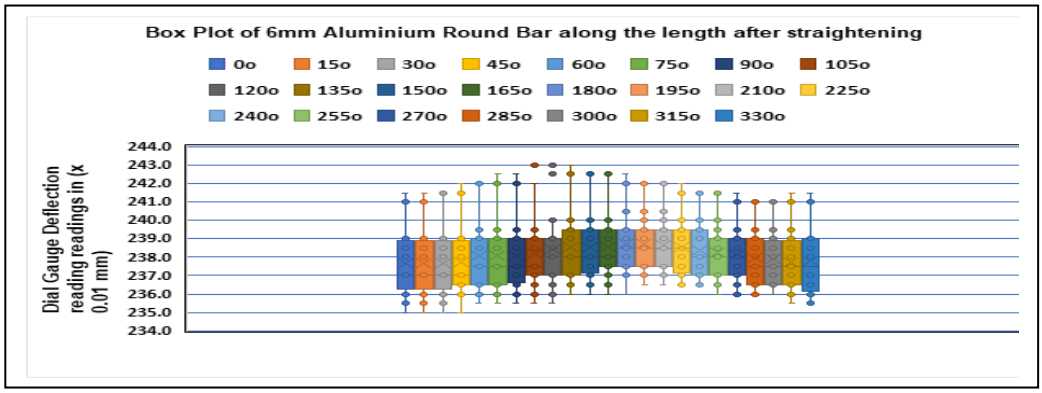

Figure 6.39 Box Plot of Dataset for Mean Values of Dial Gauge Deflection Readings of 6-mm Diameter Aluminium (Al) Round Bar after straightening

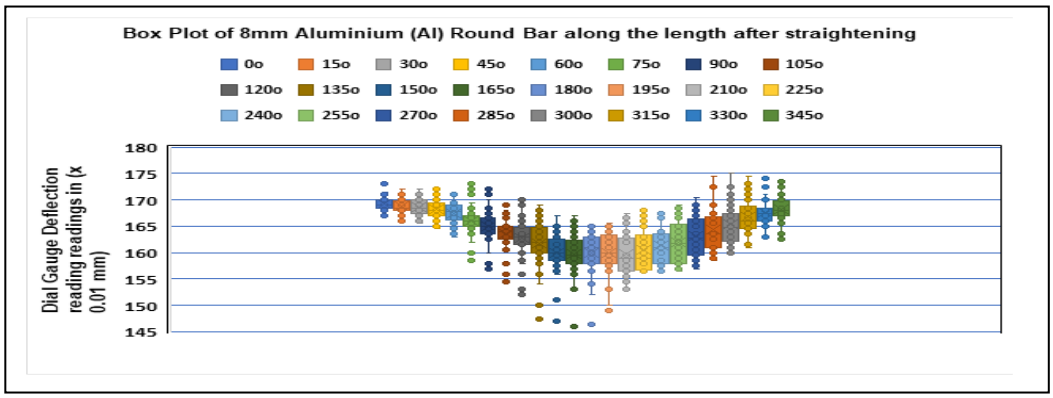

Figure 6.40 Box Plot of Dataset for Mean Values of Dial Gauge Deflection Readings of 8-mm Diameter Aluminium (Al) Round Bar after straightening

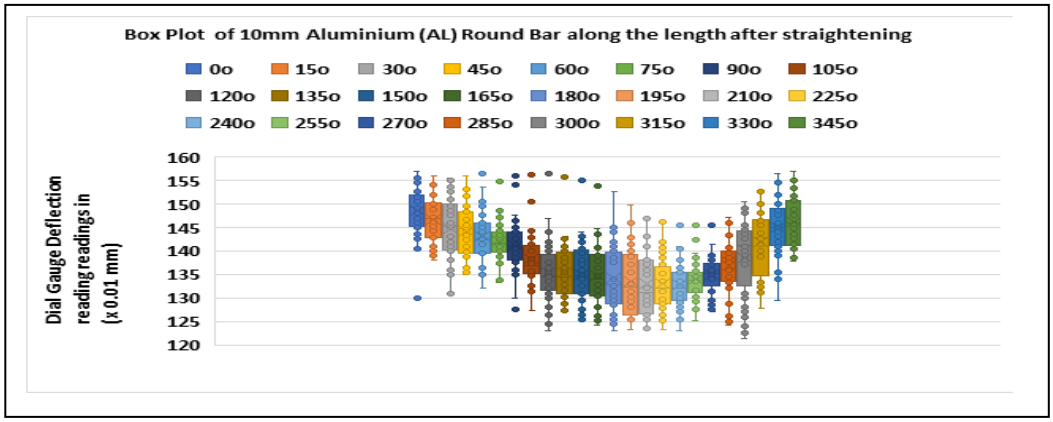

Figure 6.41 Box Plot of Dataset for Mean Values of Dial Gauge Deflection Readings of 10-mm Diameter Aluminium (Al) Round Bar after straightening

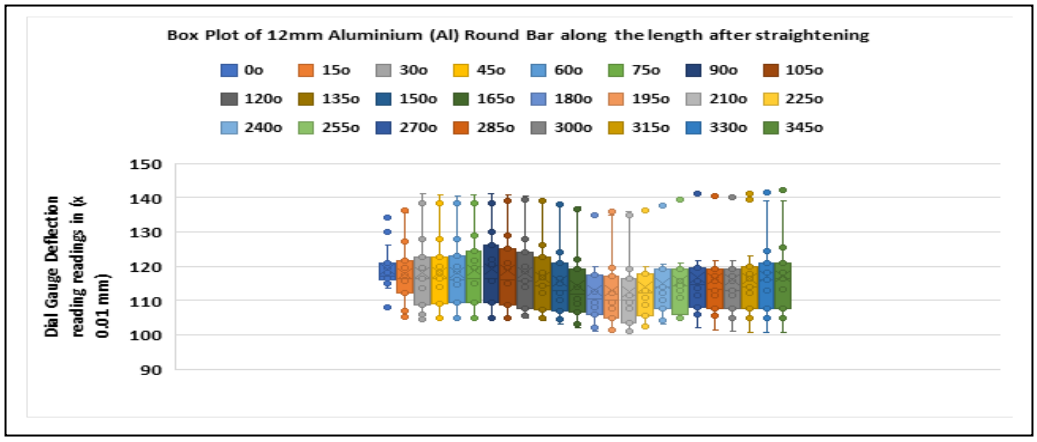

Figure 6.42 Box Plot of Dataset for Mean Values of Dial Gauge Deflection Readings of 12-mm Diameter Aluminium (Al) Round Bar after straightening

6.5.4 Observations of Copper Round Bars after Straightening

A similar set of observations for 6-mm, 8-mm, 10-mm and 12-mm diameter Copper (Cu) round bars respectively were recorded after straightening operation. The observations have been recorded from dial gauge deflections on the outermost profile of the round bar for various cross-sections circumferentially with regular intermittent angles. Mean values of these observations have been considered and given in the dataset which is available **GitHub links** [106]. Box plots are also used here to show distributions of numeric data values for comparison between multiple groups. Figure 6.43 to Figure 6.46 show the corresponding box plots of different sizes of copper round bars. These plots are built to provide high level information at a glance, offering general information about a group of data's symmetry, skew, variance and outliers.

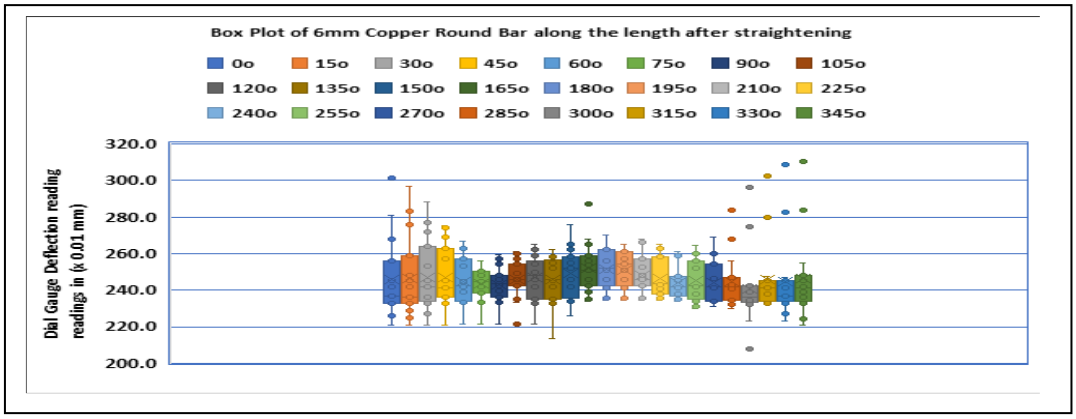

Figure 6.43 Box Plot of Dataset for Mean Values of Dial Gauge Deflection Readings of 6-mm Diameter Copper (Cu) Round Bar after straightening

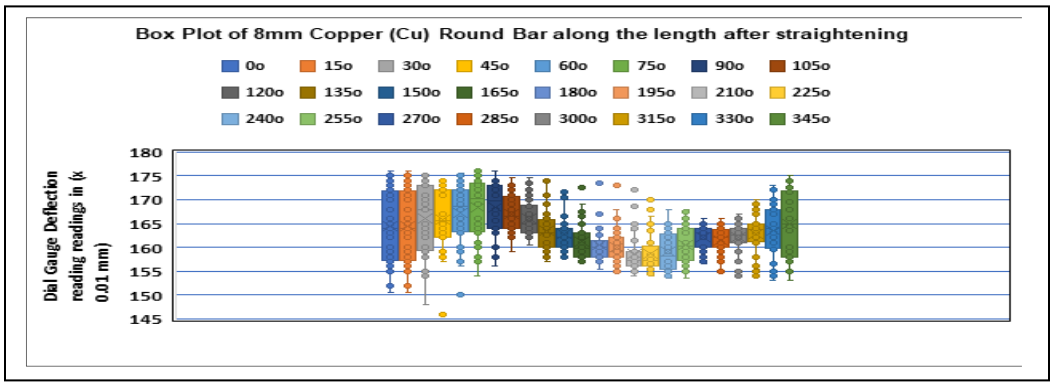

Figure 6.44 Box Plot of Dataset for Mean Values of Dial Gauge Deflection Readings of 8-mm Diameter Copper (Cu) Round Bar after straightening

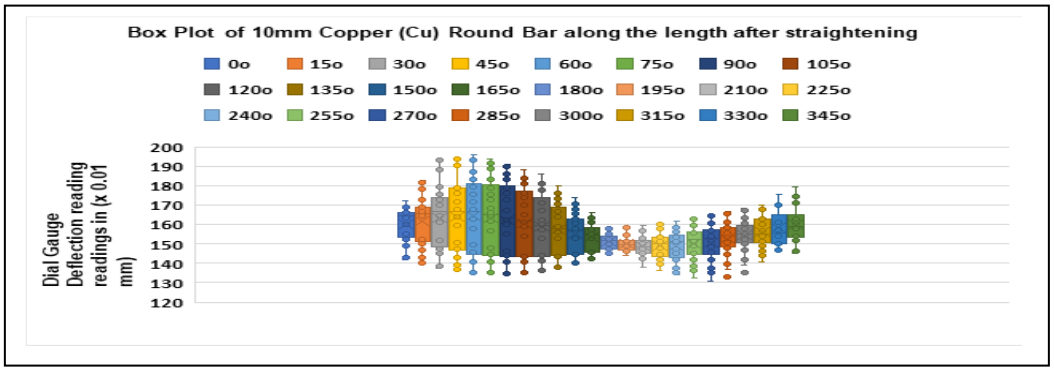

Figure 6.45 Box Plot of Dataset for Mean Values of Dial Gauge Deflection Readings of 10-mm Diameter Copper (Cu) Round Bar after straightening

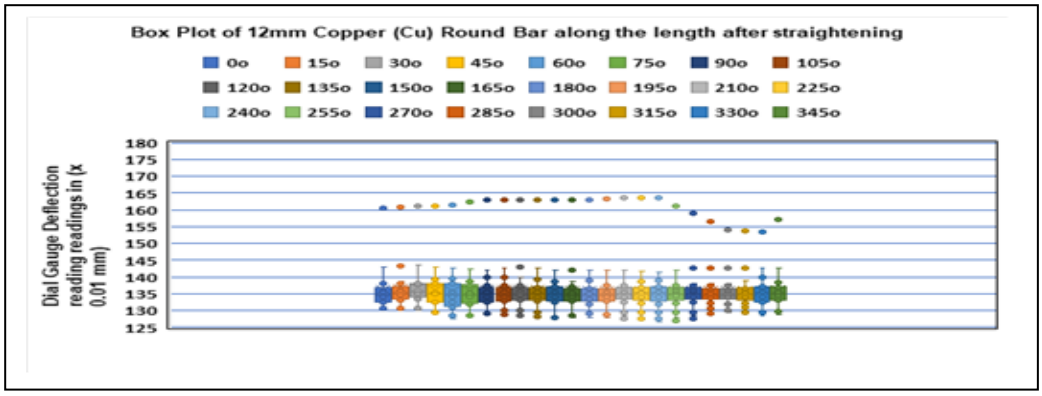

Figure 6.46 Box Plot of Dataset for Mean Values of Dial Gauge Deflection Readings of 12-mm Diameter Copper (Cu) Round Bar after straightening

6.5.5 Error Analysis of Results of Measurements of Bars after Straightening

The basics of error analysis has been described earlier in article 6.3.5. Error analysis of the dataset given in [103, 104, 105, 106] have been considered here. These dataset are for the measurement of Mild Steel (MS), Stainless Steel (SS), Aluminium (Al) and Copper (Cu) bars of sizes 6-mm, 8-mm, 10-mm and 12-mm diameters respectively have been taken into consideration.. The error plots have been shown above in Figure 6.47 to Figure 6.62

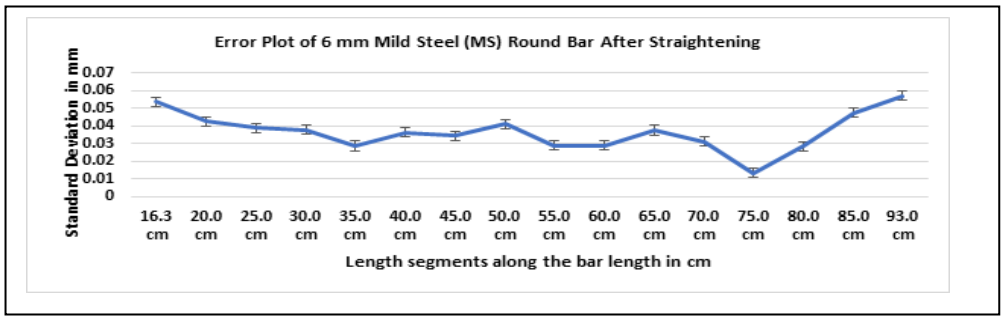

Figure 6.47 Error Plot of Dataset of 6-mm Mild Steel Round Bar after straightening

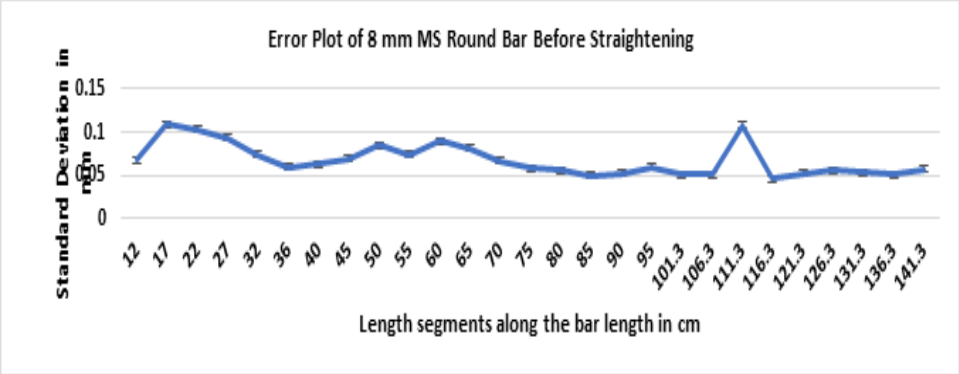

Figure 6.48 Error Plot of Dataset of 8-mm Mild Steel Round Bar after straightening

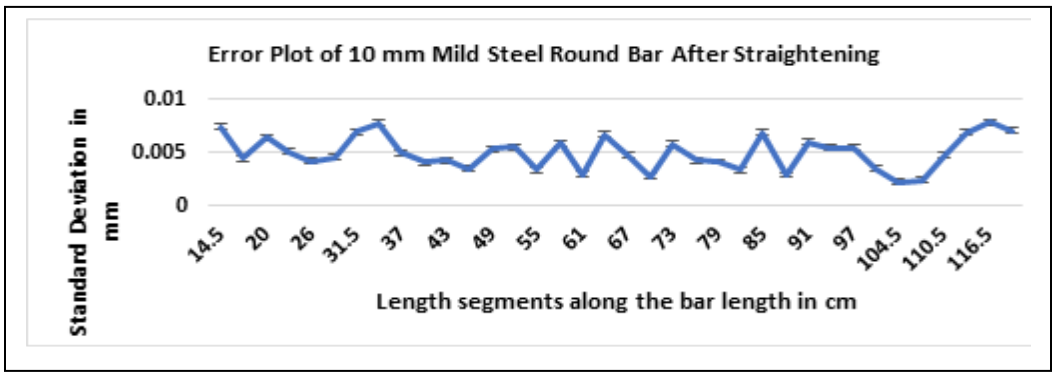

Figure 6.49 Error Plot of Dataset of 10-mm Mild Steel Round Bar after straightening

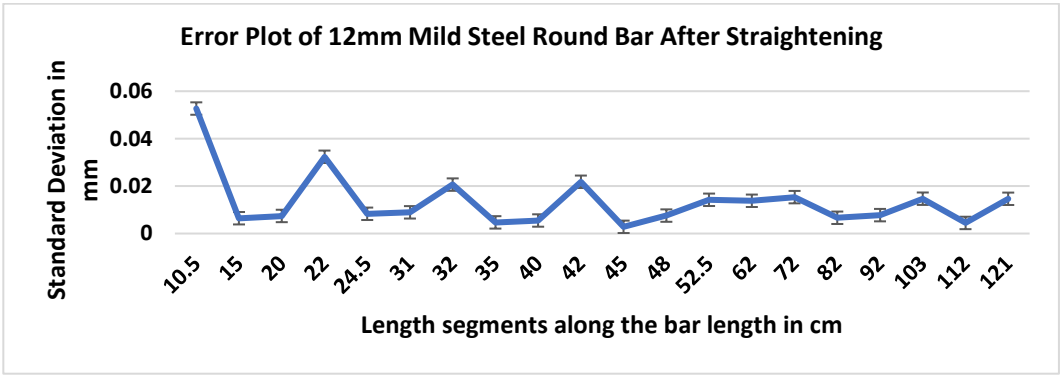

Figure 6.50 Error Plot of Dataset of 12-mm Mild Steel Round Bar after straightening

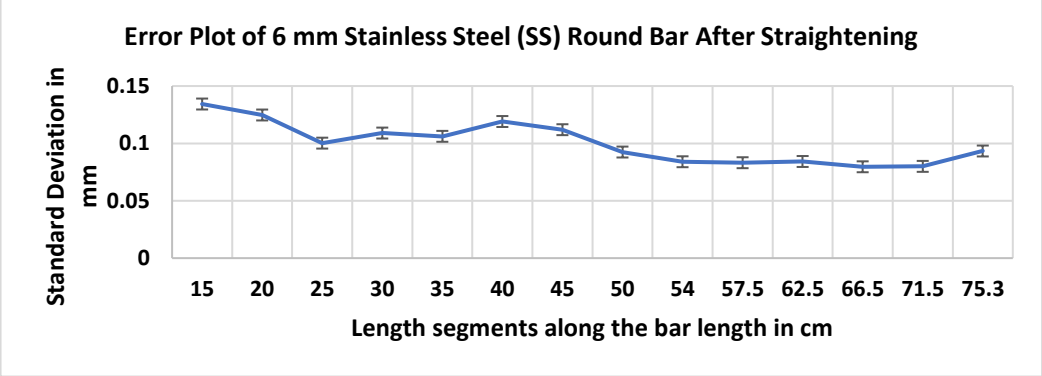

Figure 6.51 Error Plot of Dataset of 6-mm Stainless Steel Round Bar after straightening

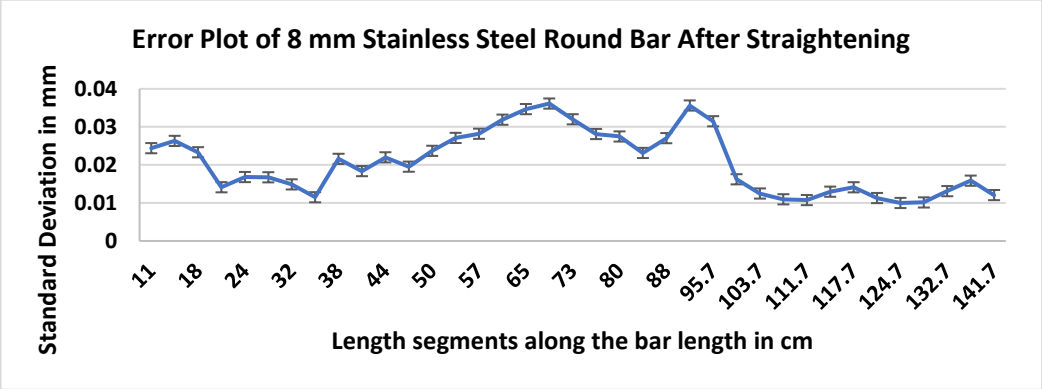

Figure 6.52 Error Plot of Dataset of 8-mm Stainless Steel Round Bar after straightening

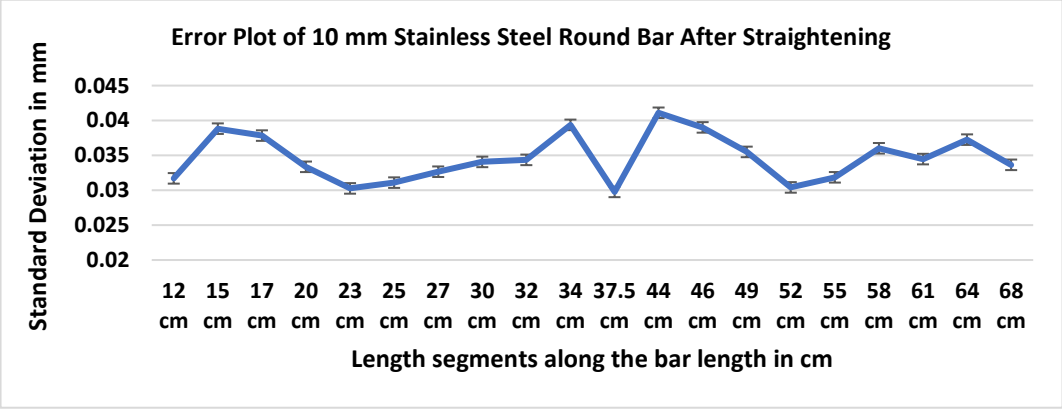

Figure 6.53 Error Plot of Dataset of 10-mm Stainless Steel Round Bar after straightening

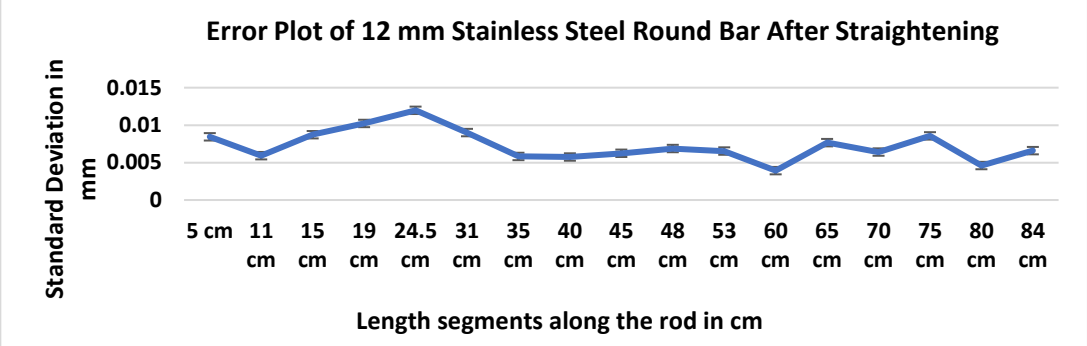

Figure 6.54 Error Plot of Dataset of 12-mm Stainless Steel Round Bar after straightening

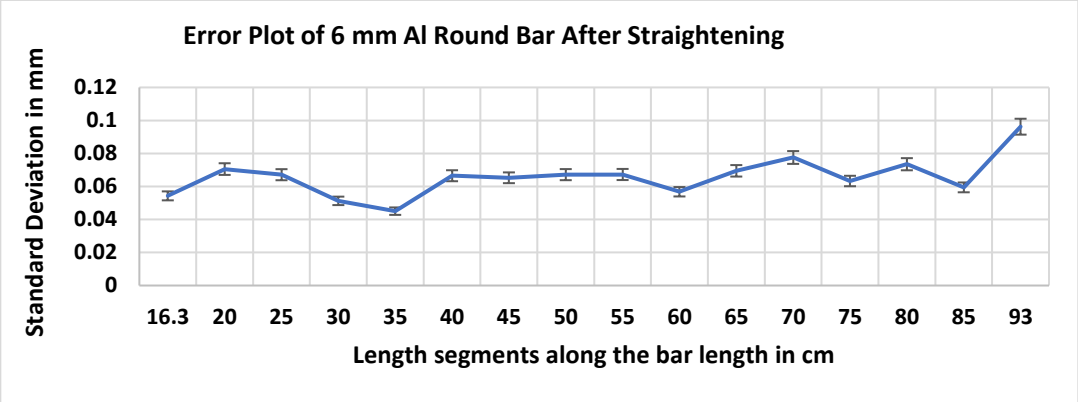

Figure 6.55 Error Plot of dataset of 6-mm Aluminium Round Bar after straightening

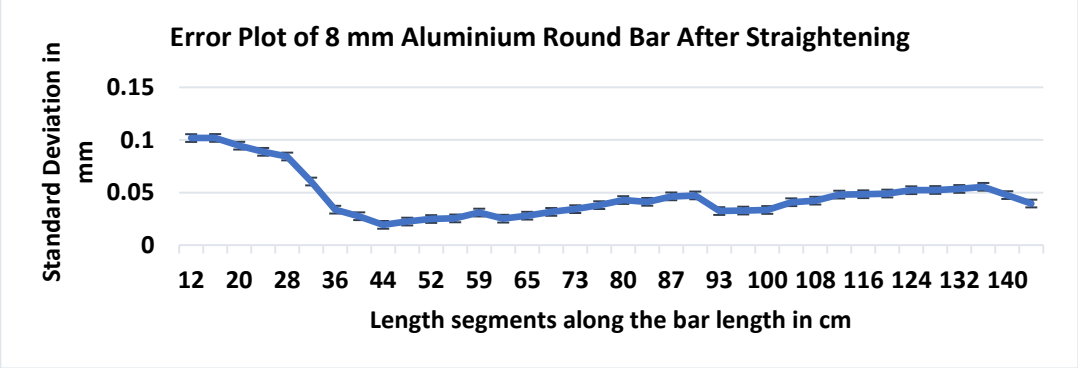

Figure 6.56 Error Plot of Dataset of 8-mm Aluminium Round Bar after straightening

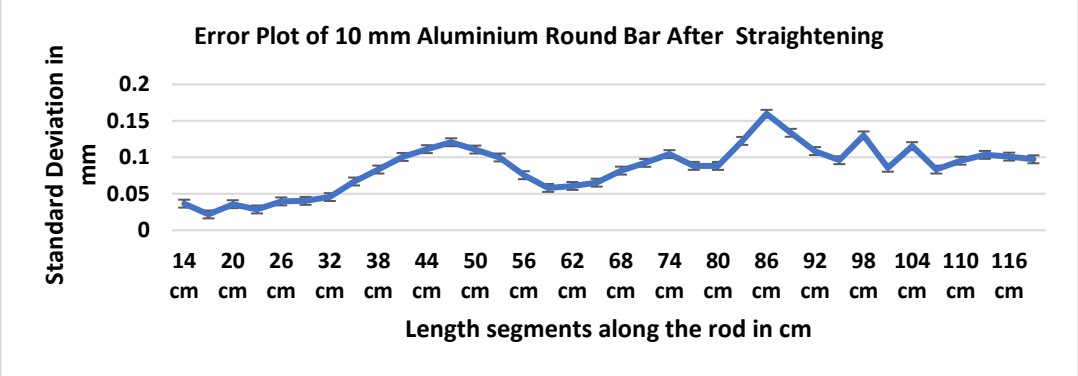

Figure 6.57 Error Plot of Dataset of 10-mm Aluminium Round Bar after straightening

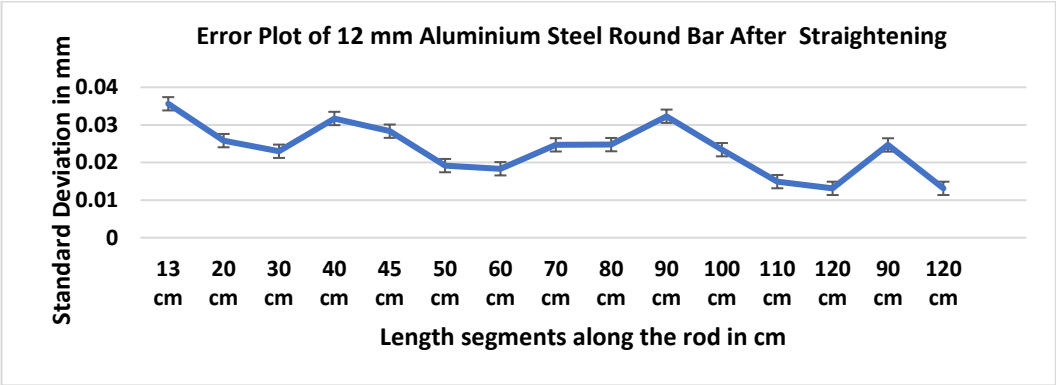

Figure 6.58 Error Plot of Dataset of 12-mm Aluminium Round Bar after straightening

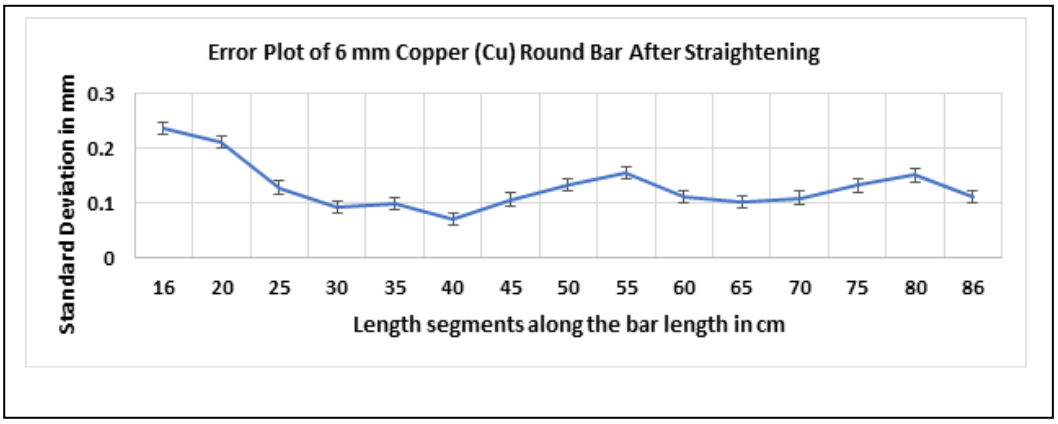

Figure 6.59 Error Plot of Dataset of 6-mm Copper Round Bar after straightening

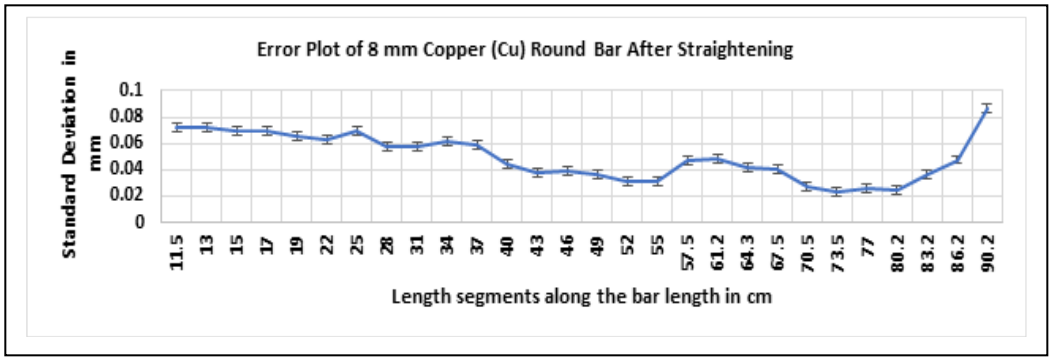

Figure 6.60 Error Plot of dataset of 8-mm Copper Round Bar after straightening

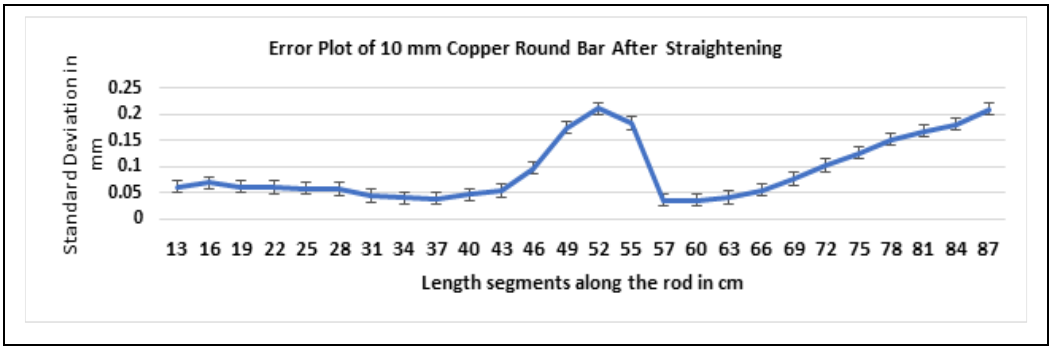

Figure 6.61 Error Plot of Dataset of 10-mm Copper Round Bar after straightening

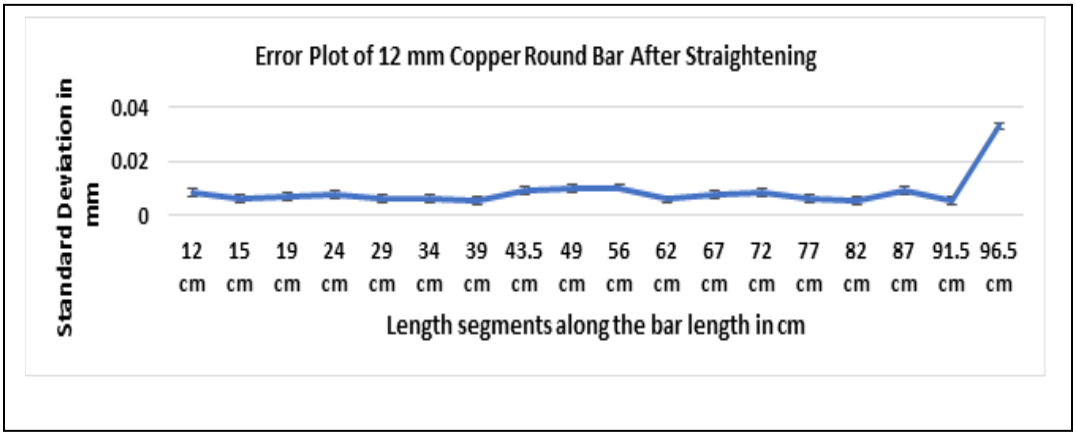

Figure 6.62 Error Plot of Dataset of 12-mm Copper Round Bar after straightening

The above-mentioned error plots which are based on standard deviations of the measured dataset of defections using the experimental set up reveals that there are variations in the standard deviation itself in all the error plots. It is quite likely that all three kinds of errors are present in the dataset. Although (12x24) sets of measurements conducted on every single round bar, but possibility is there that either of the three types of errors exist. The results of error analysis indicate that the standard deviations for all the above cases are falling within a reasonable limit.

6.6 3D Analysis of Deformations of Round Bars before Straightening

It has also been observed that deflections of dial gauge along the segmental length of bar have a strong impetus on the angular rotation (θ) of the circular bar. The observations have been taken for various angular intervals by rotations of bars i.e., θ = 0° to 360° and the resulting deflections show an interesting effect on it. In order to understand the variation of dial gauge deflections at the periphery of round bar with segmental length and angular rotation of the bar, 3D surface plot or analysis is useful for investigating desirable response values with the operating conditions. Operating conditions as predictors are generally on the X and Y axis whereas response values are on Z axis. So, in this case it can be postulated that segmental length and angular rotation of bar are the "operating conditions" and dial gauge deflection is the "Response Value" for the surface plot. Statistical software Minitab 17 is used to generate 3D surface plots.

6.6.1 Analysis of 3D Surface Plots for deformations study of Mild Steel round bars before straightening

Referring to the dataset given in [96] described earlier in Chapter-5, 3D Surface Plots have been generated and shown in Figure 6.63. These 3D Surface Plots for 6-mm, 8-mm, 10-mm and 12-mm round bars of Mild Steel respectively show the deformations already present in the rounds bars.

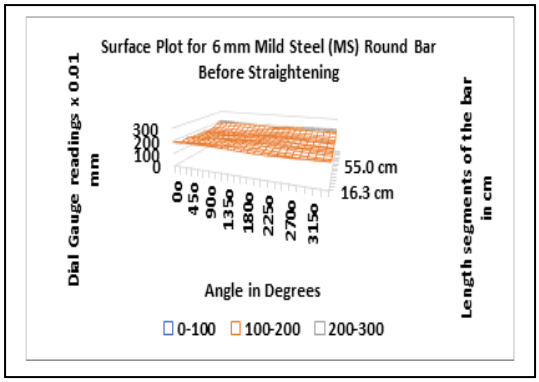

(a)

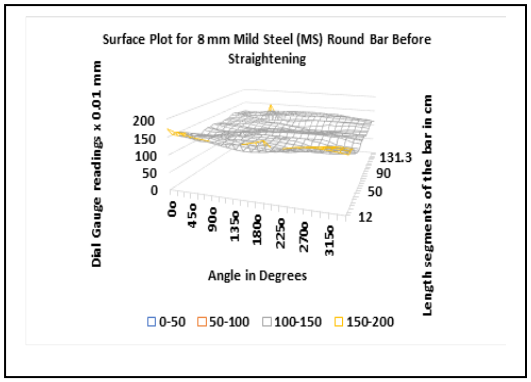

(b)

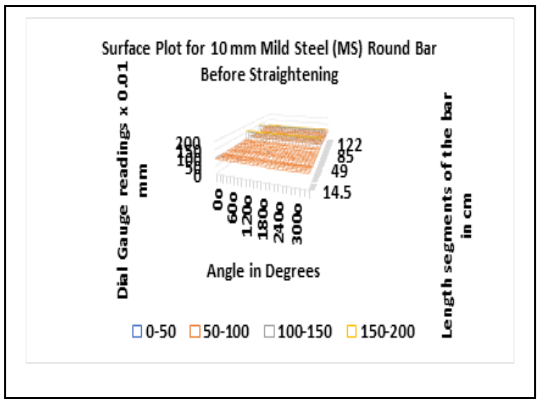

(c)

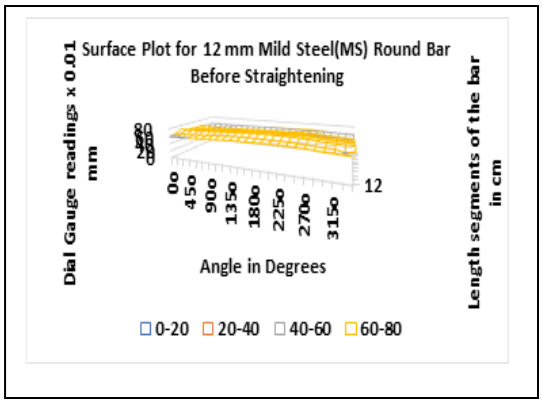

(d)

Figures 6.63 Surface Plot of (a) 6-mm, (b) 8-mm, (c)10-mm and (d) 12-mm Mild Steel Round Bars before straightening

6.6.2 Analysis of 3D Surface Plots for Deformations Study of Stainless Steel Round Bars before Straightening

3D Surface Plots have been generated based on the datasets of stainless steel before straightening [97] and shown in Figures 6.64. These 3D Surface Plots for 6-mm, 8-mm, 10-mm and 12-mm round bars of Stainless Steel materials respectively show the deformations already present in the rounds bars.

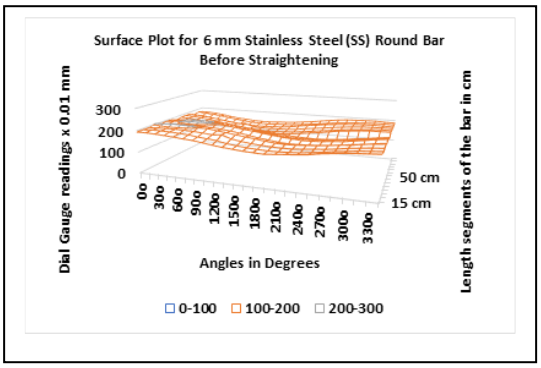

(a)

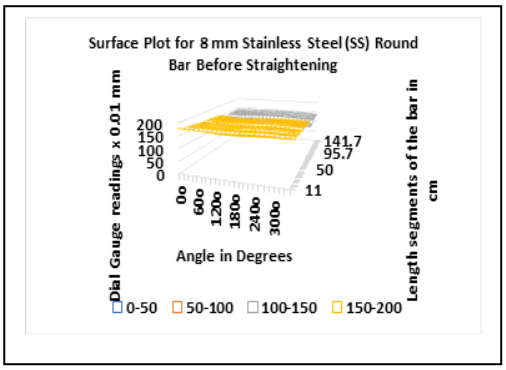

(b)

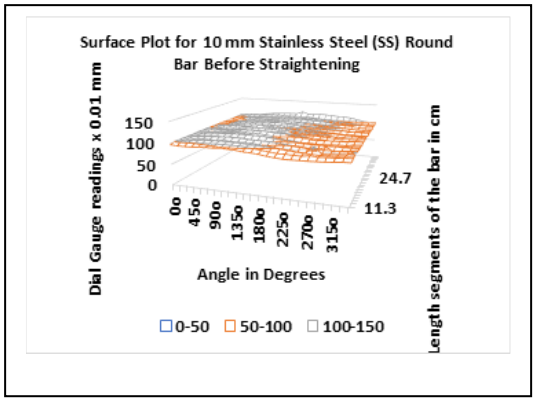

(c)

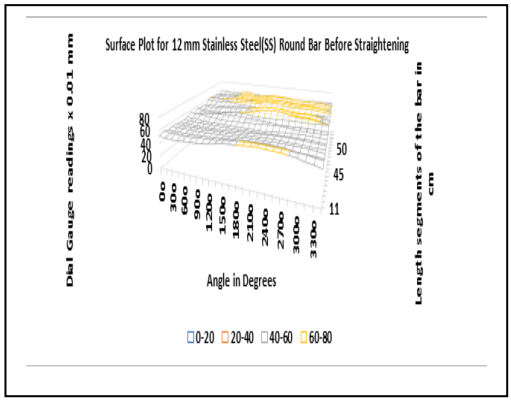

(d)

Figures 6.64 Surface Plot of (a) 6-mm, (b) 8-mm, (c) 10-mm and (d) 12-mm Stainless Steel Round Bars before straightening

6.6.3 Analysis of 3D Surface Plots for Deformations Study of Aluminium Round Bars before Straightening

3D Surface Plots have been generated based on the datasets of aluminium before straightening [98] and shown in Figures 6.64. These 3D Surface Plots for 6-mm, 8-mm, 10-mm and 12-mm round bars of Aluminium materials respectively show the deformations already present in the rounds bars.

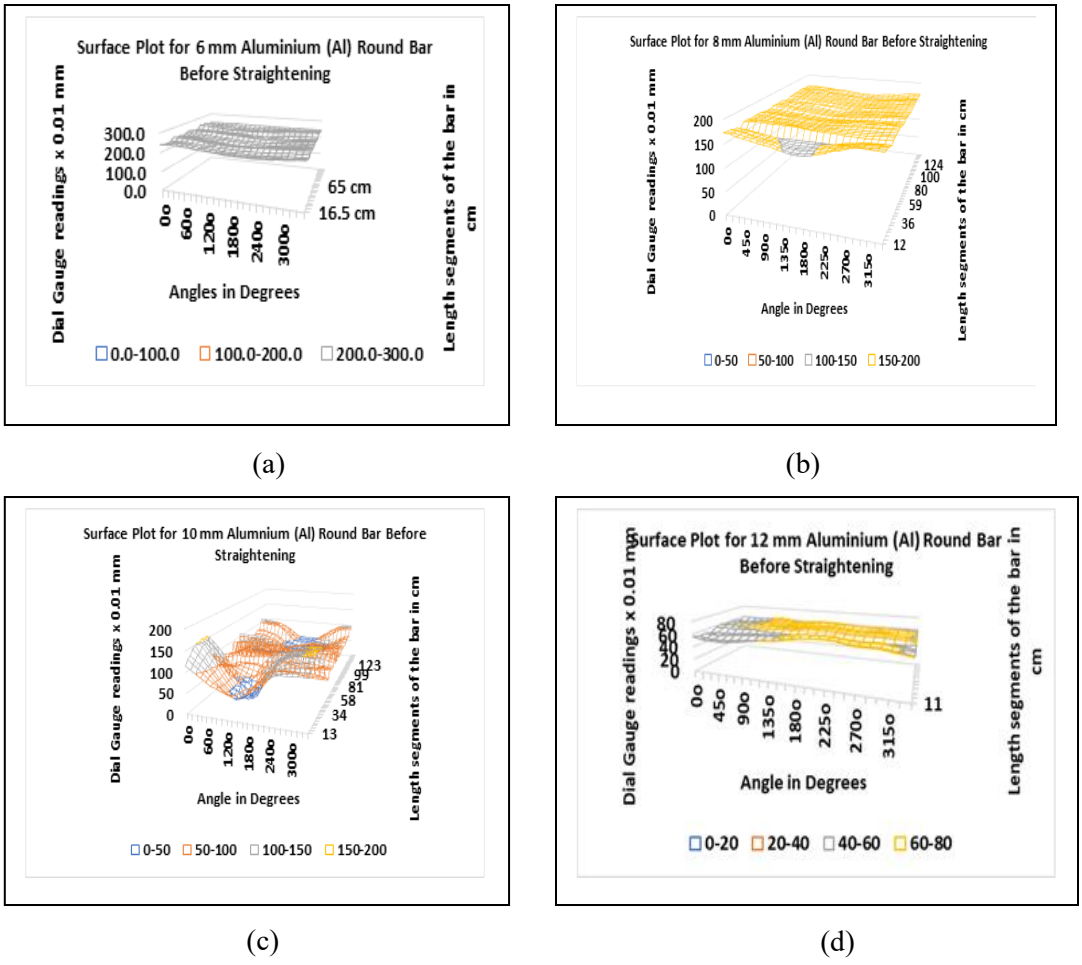

Figures 6.65 Surface Plot of (a) 6-mm, (b) 8-mm, (c) 10-mm and (d) 12-mm Aluminium Round Bars before straightening

6.6.4 Analysis of 3D Surface Plots for Deformations Study of Copper Round Bars before Straightening

3D Surface Plots have been generated based on the datasets of copper round bars before straightening [99] and shown in Figures 6.66. These 3D Surface Plots for 6 mm, 8 mm, 10 mm and 12 mm round bars of Copper materials respectively show the deformations already present in the rounds bars.

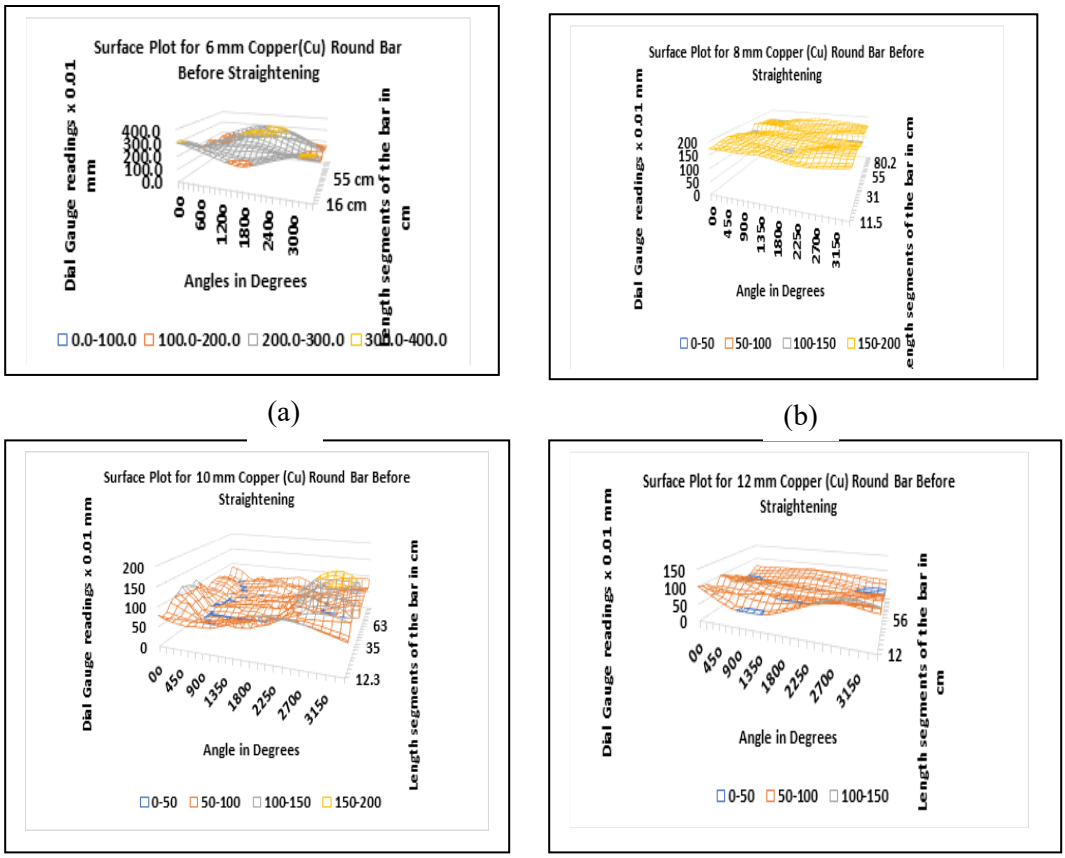

Figures 6.66 Surface Plot of (a) 6-mm, (b) 8-mm, (c) 10-mm and (d) 12-mm Copper Round Bars before straightening

In all the surface plots, the deformations are visible circumferentially and axially along the round bars. These plots reveal that curvatures exist at various sections and not uniform in nature thus curvatures are randomly distributed.

6.7 3D Analysis of Deformations of Round Bars after Straightening

It has been seen in Figures 6.63 to 6.66 i.e. 3D Surface Plots for four types of materials of sizes 6-mm, 8-mm, 10-mm and 12-mm diameters round bars that some deformations are already present at various sections throughout the length before straightening. Some reasons of these deformations have been indicated that possibly deformations have taken place in rolling mills or during materials handling. Now the same round bars have been subjected to two-roll cross-roll straightening machine and thereafter similar study have been conducted again to see the variations of deformations after straightening. In the present case based on datasets [103, 104, 105 and 106], 3D Plots have been considered for analysis using Minitab 17. Operating conditions as predictors are generally on the X and Y axis whereas response values are on Z axis. So, in this case it can be postulated that segmental length and angular rotation of bar are the "operating conditions" and dial gauge deflection is the "Response Value" for the surface plot.

6.7.1 Analysis of 3D Surface Plots for Deformations Study of Mild Steel (MS) Round Bars after Straightening

Referring to the dataset after straightening of round bars given in [103] described earlier, 3D Surface Plots have been generated and shown in Figure 6.67 for 6-mm, 8-mm, 10-mm and 12-mm round bars of Mild Steel respectively.

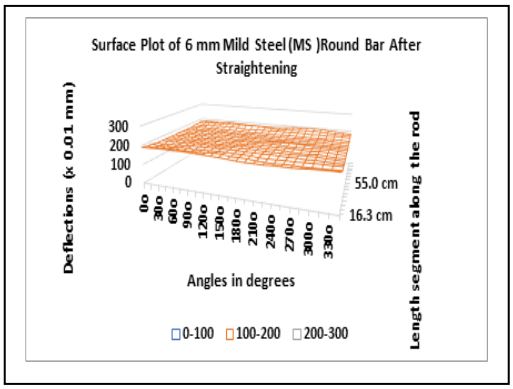

(a)

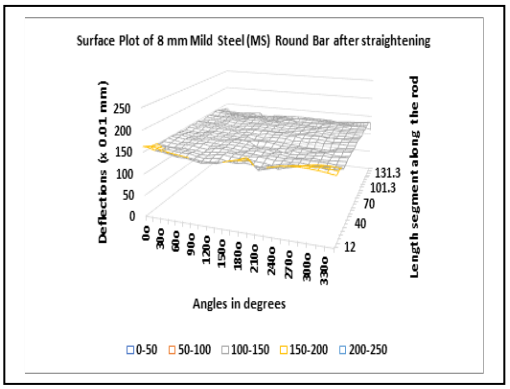

(b)

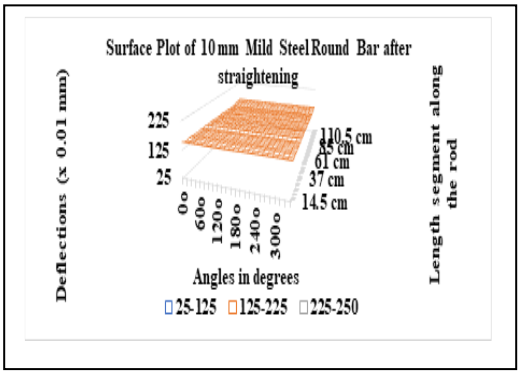

(c)

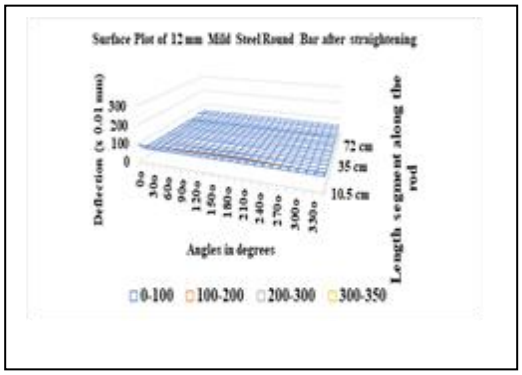

(d)

Figures 6.67 3D Surface Plot of (a) 6-mm, (b) 8-mm, (c) 10-mm and (d) 12-mm Mild Steel Round Bar after straightening

6.7.2 Analysis of 3D Surface Plots for Deformations Study of Stainless Steel (SS) Round Bars after Straightening

3D Surface Plots have been generated based on the datasets of stainless steel round bars after straightening [104] and shown in Figures 6.68 for 6-mm, 8-mm, 10-mm and 12-mm respectively.

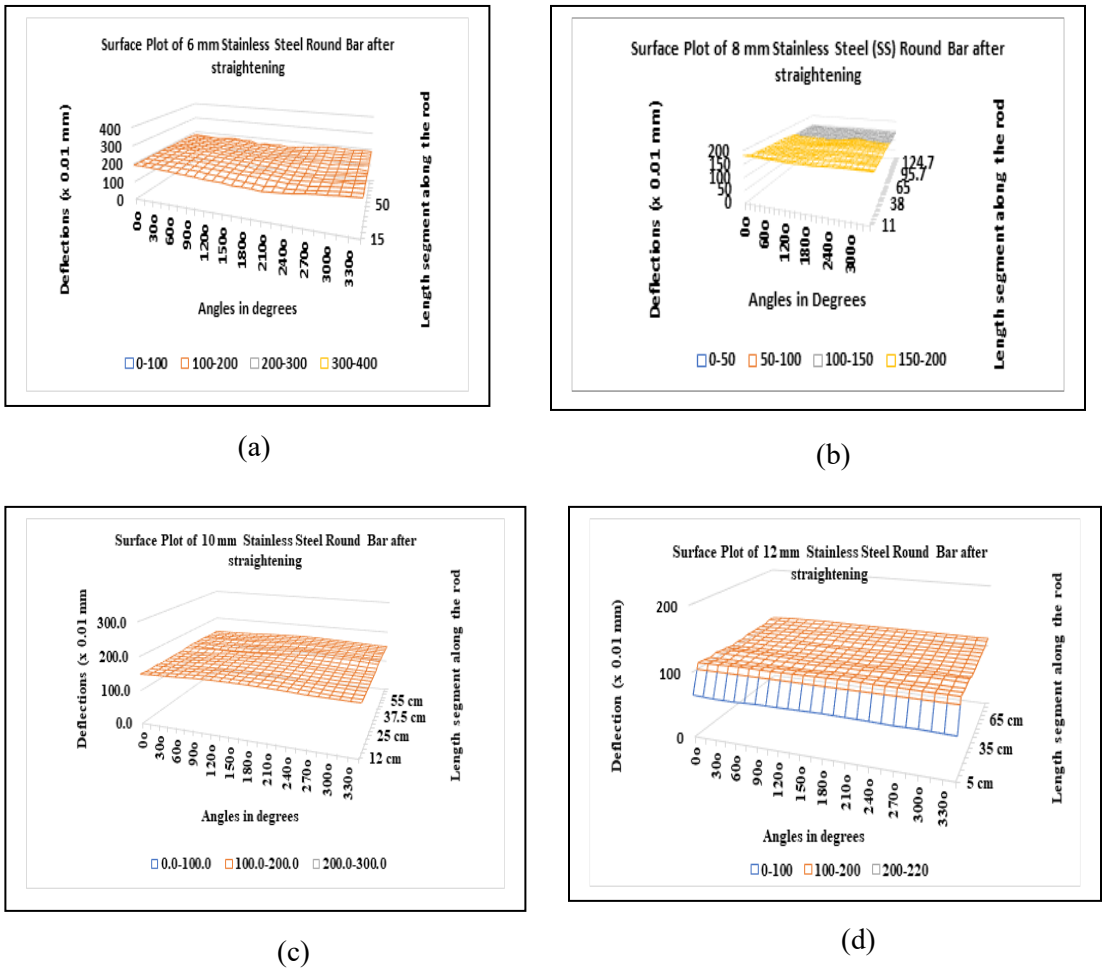

Figures 6.68 3D Surface Plot of (a) 6-mm, (b)8-mm, (c)10-mm and (d)12-mm Stainless Steel Round Bar after straightening

6.7.3 Analysis of 3D Surface Plots for Deformations Study of Aluminium Round Bars after Straightening

3D Surface Plots have been generated based on the datasets of Aluminium round bars after straightening [105] and shown in Figures 6.69 for 6-mm, 8-mm, 10-mm and 12-mm diameters respectively.

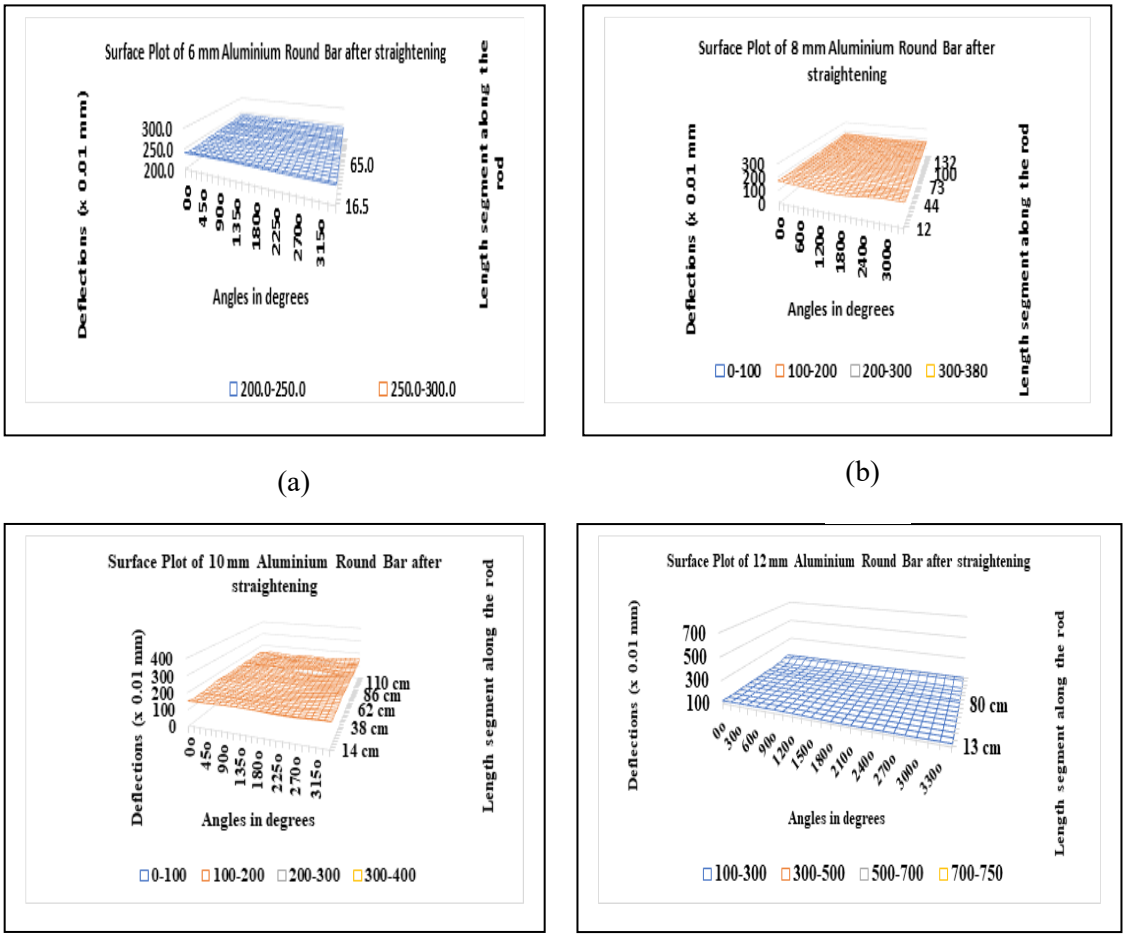

(a) (b)

(c) (d)

Figures 6.69 3D Surface Plot of (a) 6-mm, (b) 8-mm, (c)10-mm, (d) 12-mm Aluminium Round Bar after straightening

6.7.4 Analysis of 3D Surface Plots for Deformations Study of Copper Round Bars after Straightening

3D Surface Plots have been generated based on the datasets of 6-mm, 8-mm, 10-mm and 12-mm diameter of Copper round bars after straightening [106] and shown in Figures 6.70 respectively.

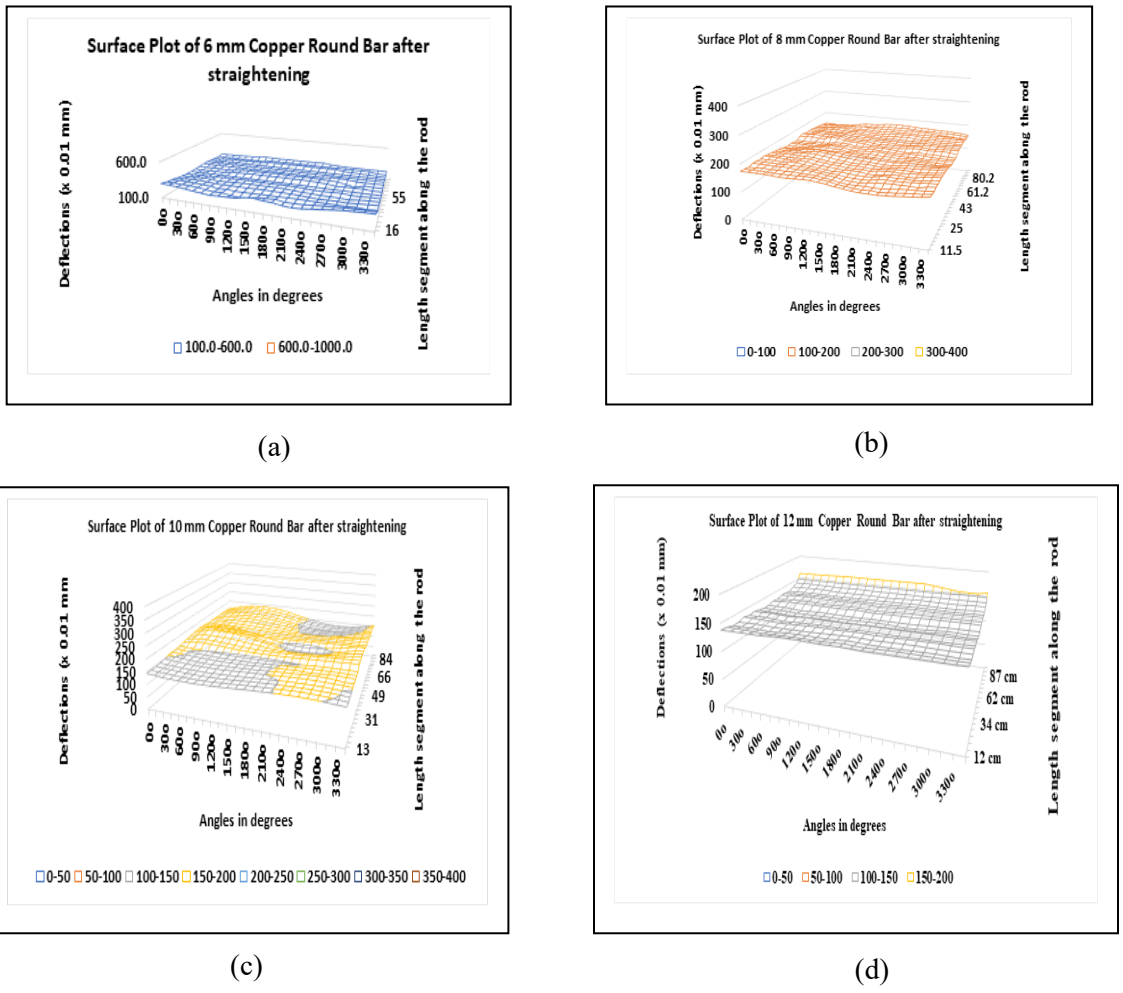

Figures 6.70. 3D Surface Plot of (a) 6-mm, (b) 8-mm, (c) 10-mm, (d) 12-mm Copper Round Bar after straightening

6.8. Analysis of Radar Chart after Straightening

Radar charts have been generated based on the dataset of deformations obtained after straightening of round metal bars. Figure 6.71, Figure 6.72, Figure 6.73 and Figure 6.74 represent the Radar charts of mild steel, stainless steel, aluminium and copper respectively for their different sizes of 6-mm, 8-mm, 10-mm and 12-mm respectively. These charts indicate quite improved roundness and straightness after straightening in comparison with that of before straightening.

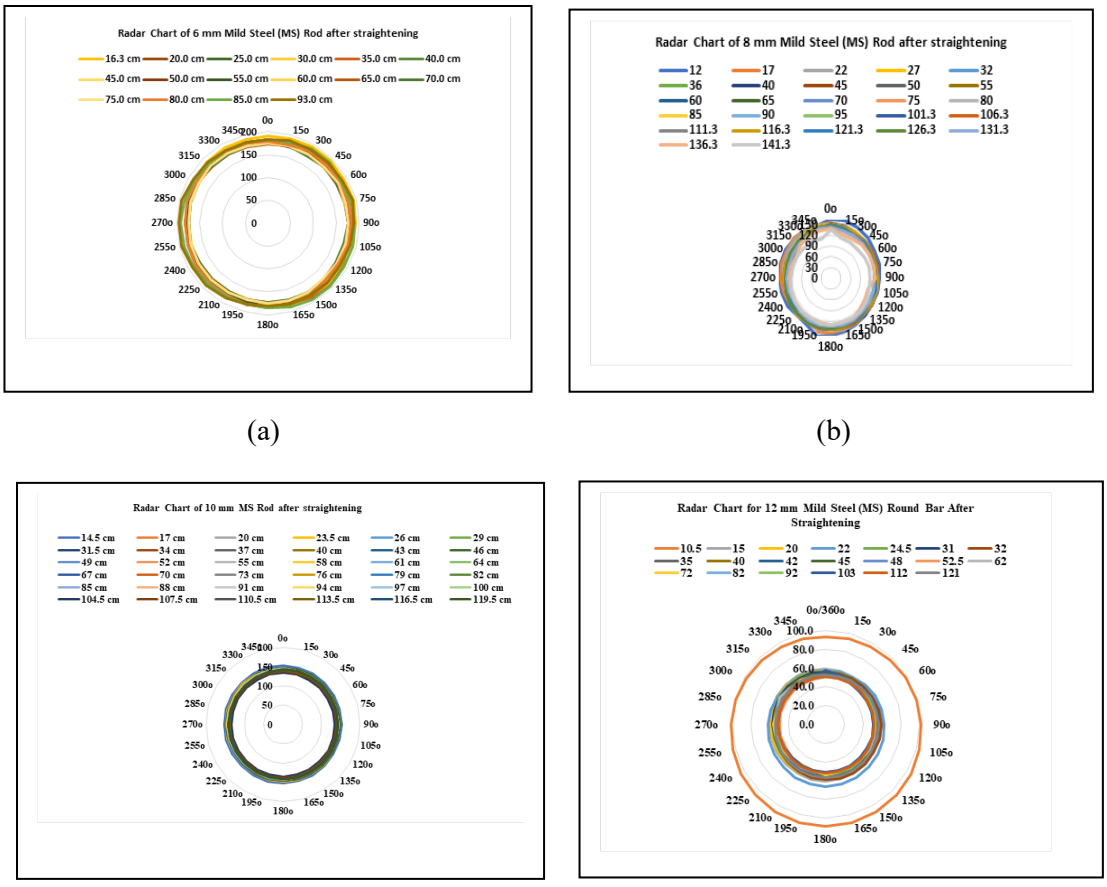

(a) (b)

(c) (d)

Figure 6.71 Radar chart of Mild Steel (MS) Round Bars for (a) 6-mm (b) 8-mm, (c) 10-mm and (d) 12-mm diameters after straightening.

(a) (b)

(c) (d)

Figure 6.72 Radar chart of Stainless Steel (SS) Round Bars for (a) 6-mm (b) 8-mm, (c) 10-mm and (d) 12-mm Diameters after straightening.

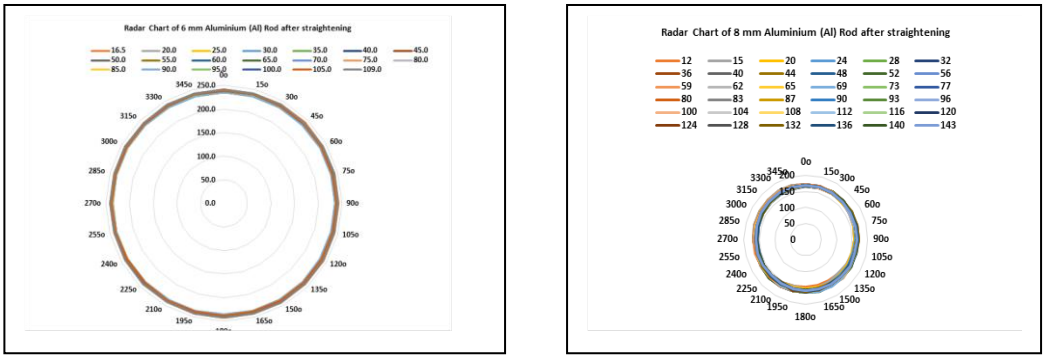

(a) (b)

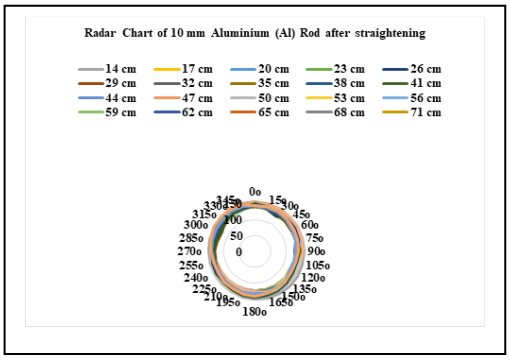

(c)

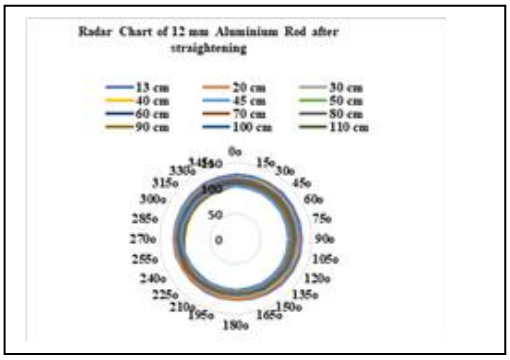

(d)

Figure 6.73 Radar chart of Aluminium (Al) Round Bars for (a) 6-mm (b) 8-mm, (c) 10-mm and (d) 12-mm Diameters after straightening

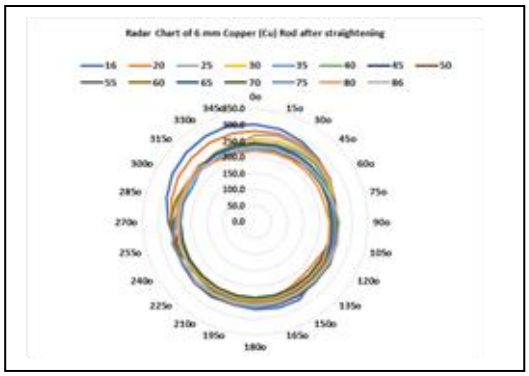

(a)

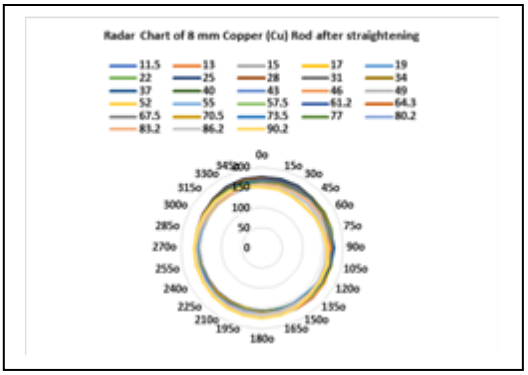

(b)

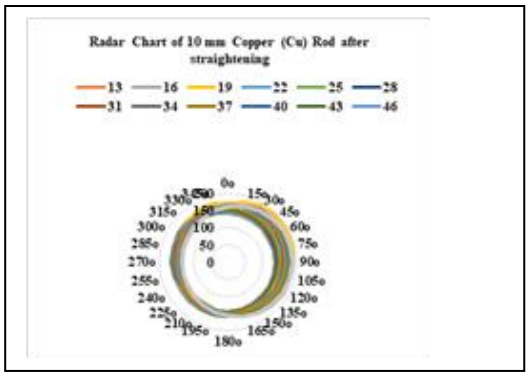

(c)

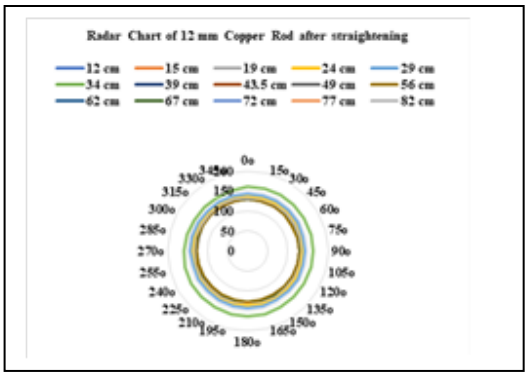

(d)

Figure 6.74 Radar chart of Copper (Cu) Round Bars for (a) 6-mm (b) 8-mm, (c) 10-mm and (d) 12-mm Diameters after straightening.

6.9 SPC analysis of round Metal Bars after straightening

It has been earlier observed that the SPC analyses of diameters for different metal bars show reasonable results within limits before straightening but the analyses of measured deflections before straightening reveals that there are quite some results indicating the processes are out of control. This inspired to examine the SPC analysis of measured deflections after straightening. Figures 6.75 to 6.90 represent the control charts of observed deflections after straightening of the metal round bars of Mild Steel (MS), Stainless Steel (SS), Aluminium (Al) and Copper (Cu) for diameters 6-mm,8-mm, 10-mm & 12-mm respectively. These charts of statistical process control show controlled results after straightening which indicate that straightening process is quite effective for metal bars as deflections obtained after straightening are within control limits. Moreover, it also can be postulated that the deformations of bars after straightening should always be less than that of the deformations obtained before straightening. This postulation is validated by the analysis of finite element method which is described in Chapter 7.

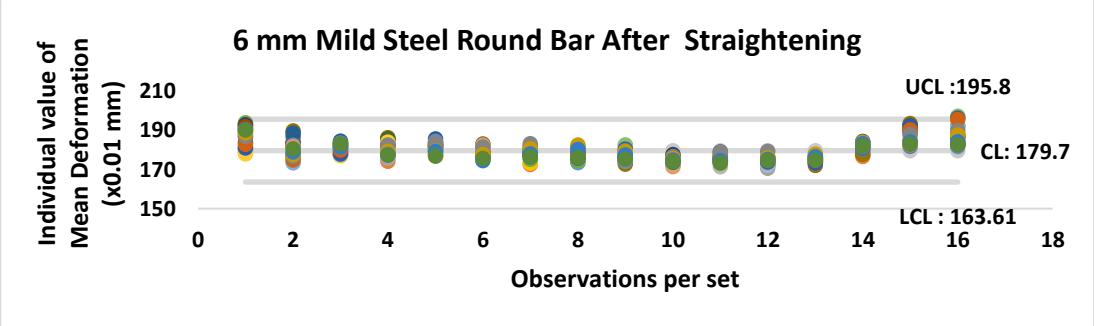

Figure 6.75 Deformation Analysis of 6-mm Mild Steel Round Bar after straightening using SPC

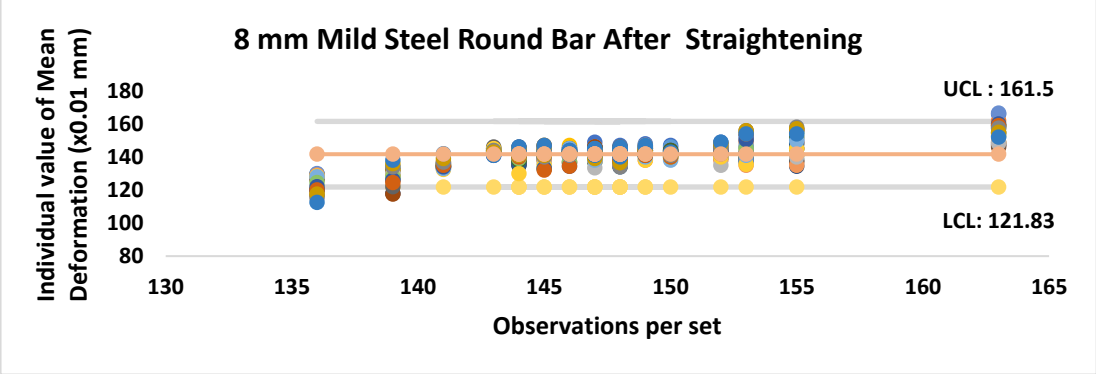

Figure 6.76 Deformation Analysis of 8-mm Mild Steel Round Bar after straightening using SPC

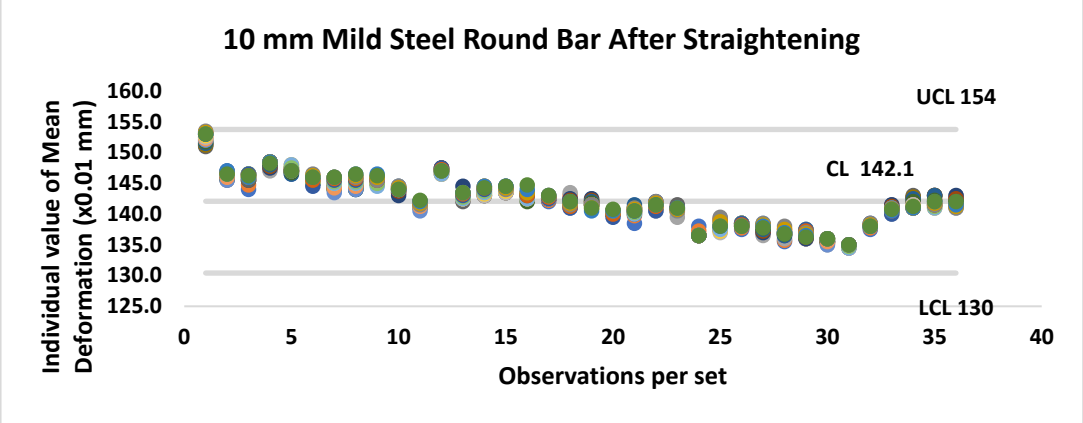

Figure 6.77 Deformation Analysis of 10-mm Mild Steel Round Bar after straightening using SPC

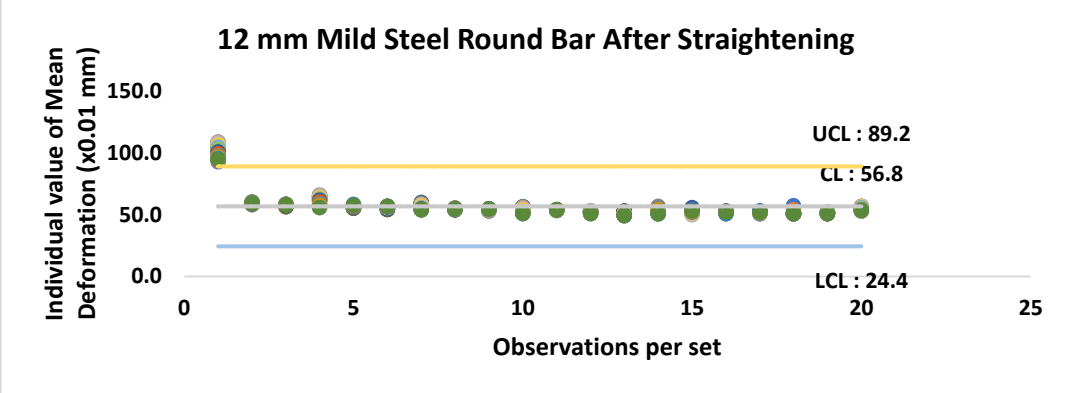

Figure 6.78 Deformation Analysis of 12-mm Mild Steel Round Bar after straightening using SPC

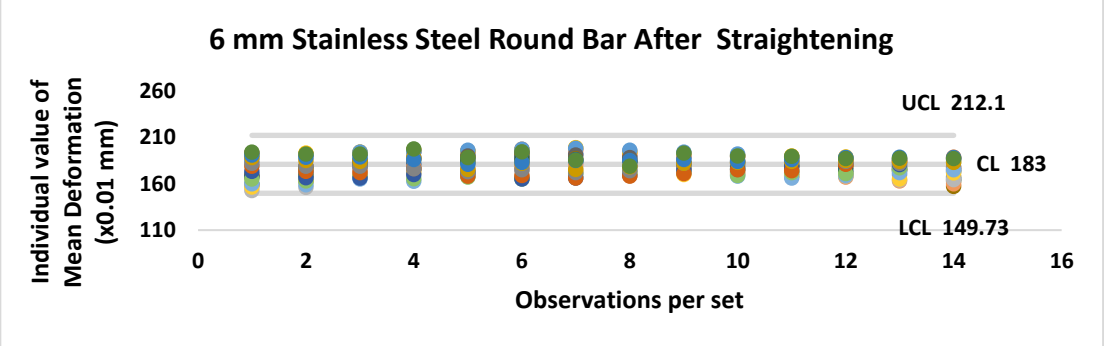

Figure 6.79 Deformation Analysis of 6-mm Stainless Steel Round Bar after straightening using SPC

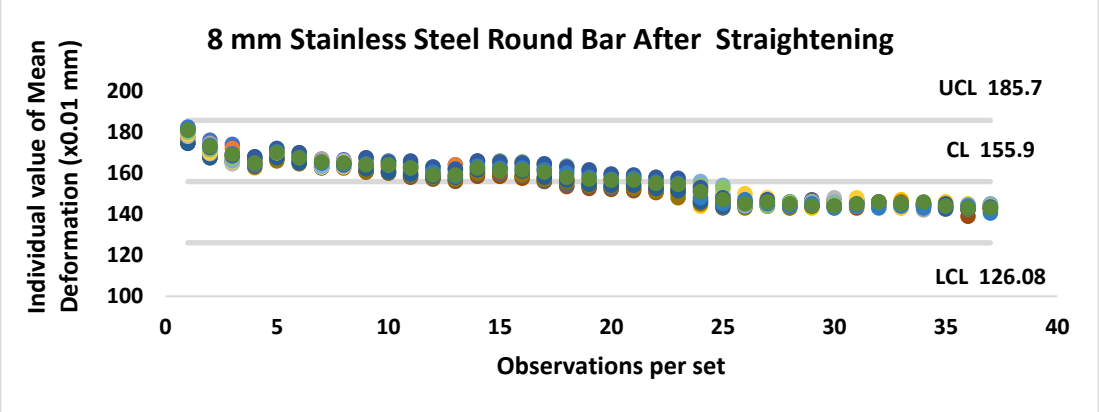

Figure 6.80 Deformation analysis of 8-mm Stainless Steel Round Bar after straightening using SPC

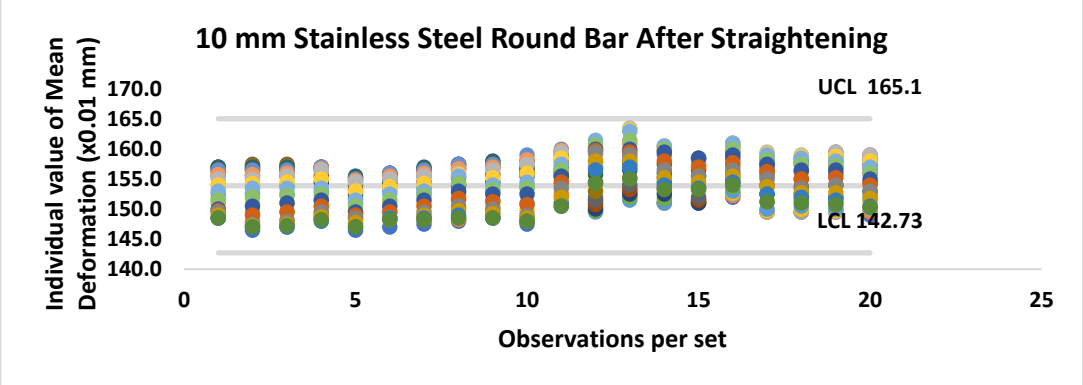

Figure 6.81 Deformation Analysis of 10-mm Stainless Steel Round Bar after straightening using SPC

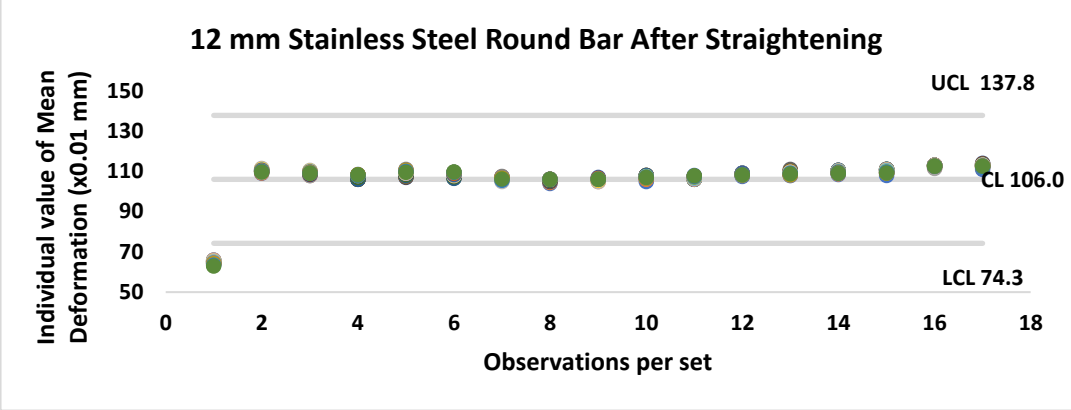

Figure 6.82 Deformation Analysis of 12 mm Stainless Steel Round Bar after straightening using SPC

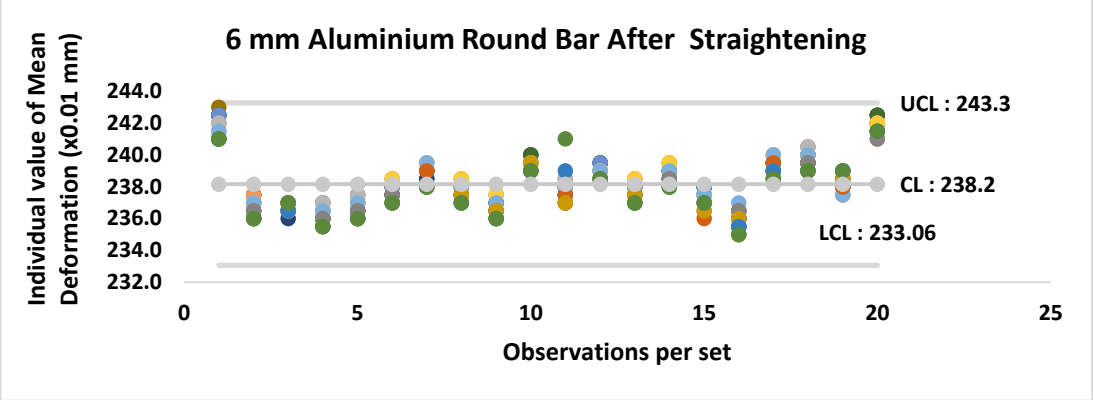

Figure 6.83 Deformation analysis of 6-mm Aluminium Round Bar after straightening using SPC

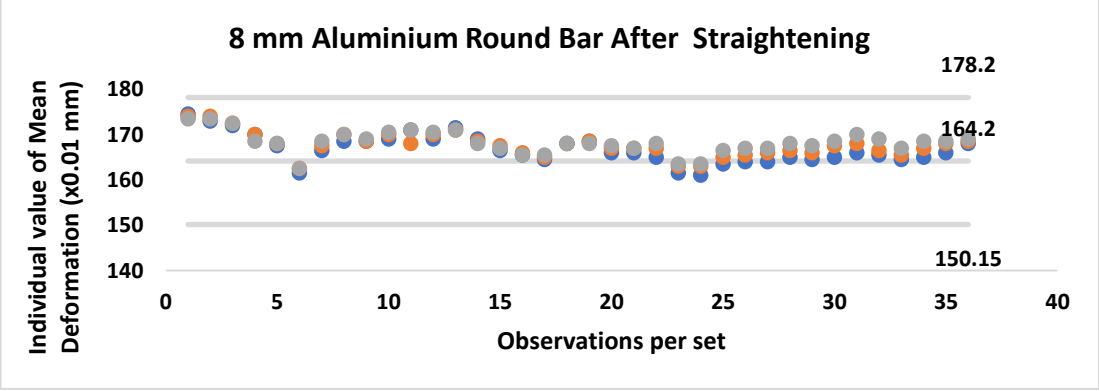

Figure 6.84 Deformation Analysis of 8-mm Aluminium Round Bar after straightening using SPC

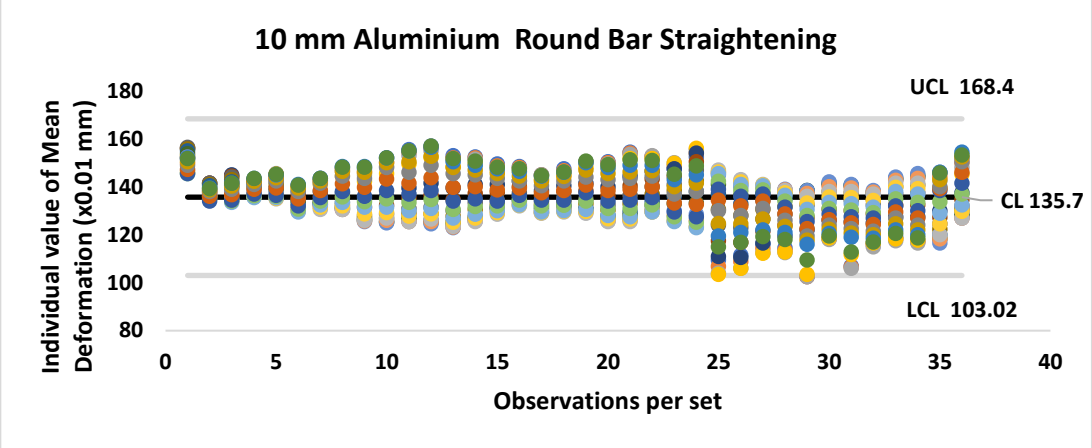

Figure 6.85 Deformation Analysis of 10-mm Aluminium Round Bar after straightening using SPC

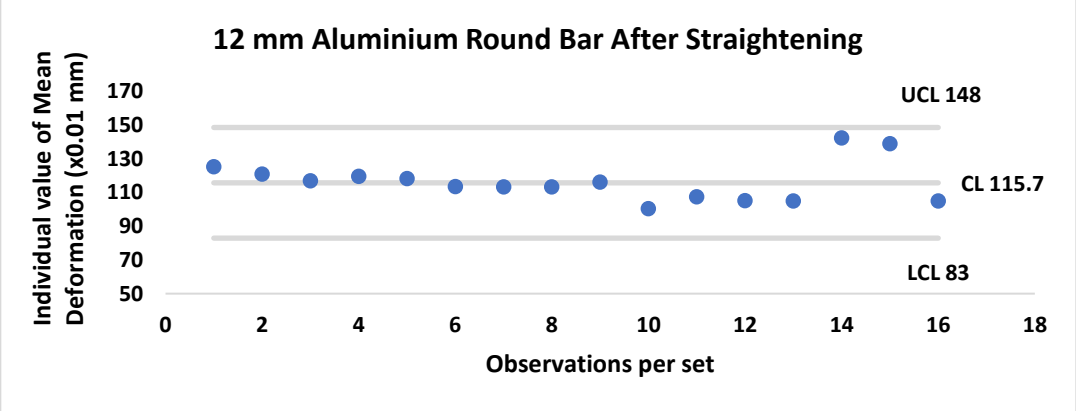

Figure 6.86 Deformation analysis of 12-mm Aluminium Round Bar after straightening using SPC

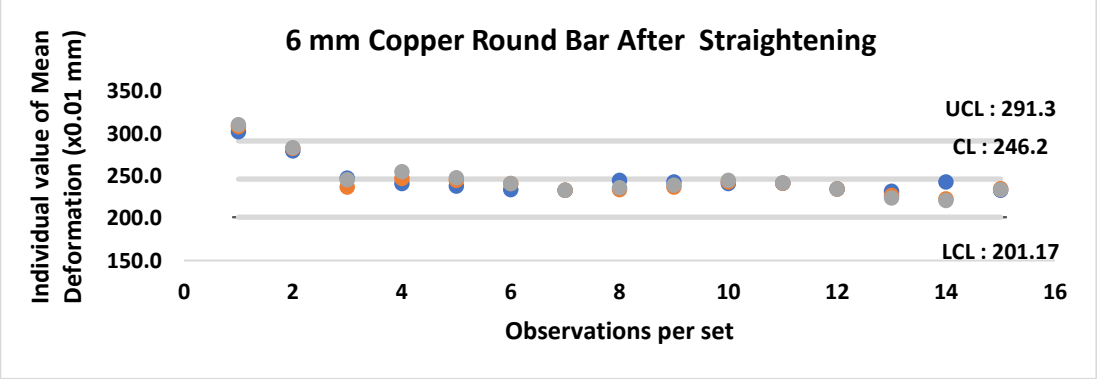

Figure 6.87 Deformation Analysis of 6-mm Copper Round Bar after straightening using SPC

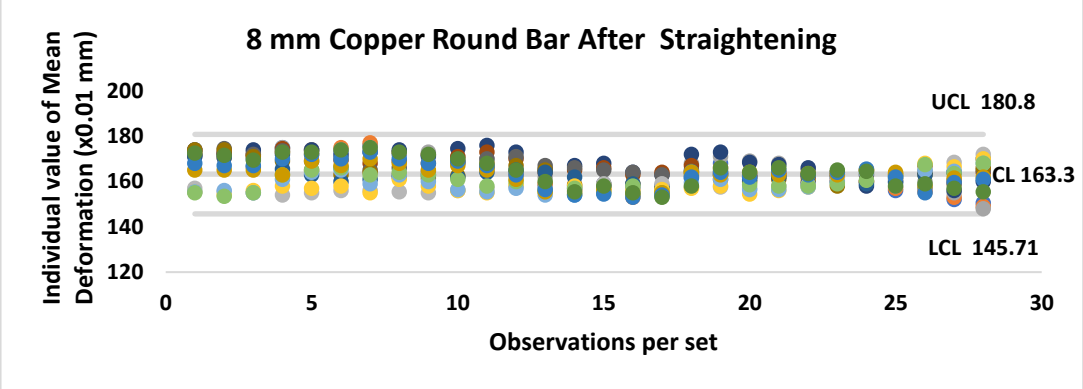

Figure 6.88 Deformation Analysis of 8-mm Copper Round Bar after straightening using SPC

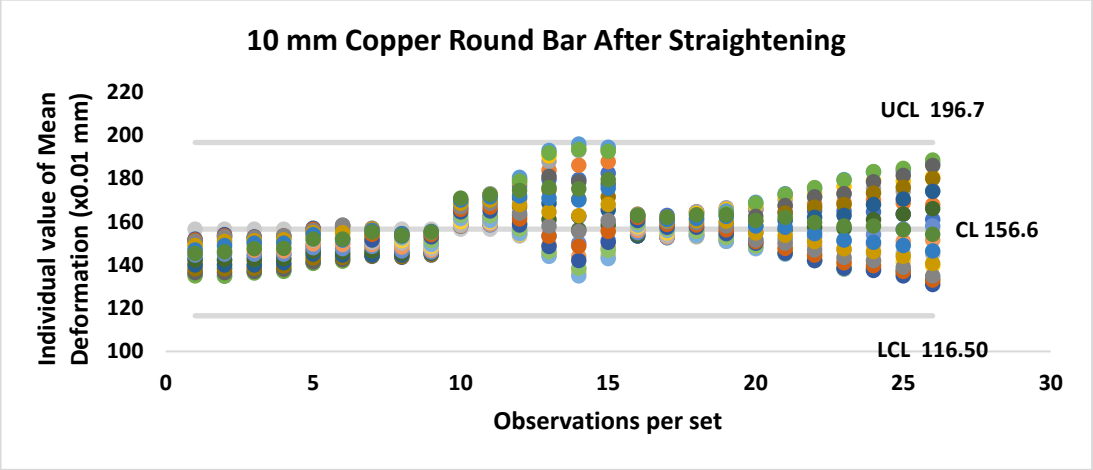

Figure 6.89 Deformation Analysis of 10-mm Copper Round Bar after straightening using SPC

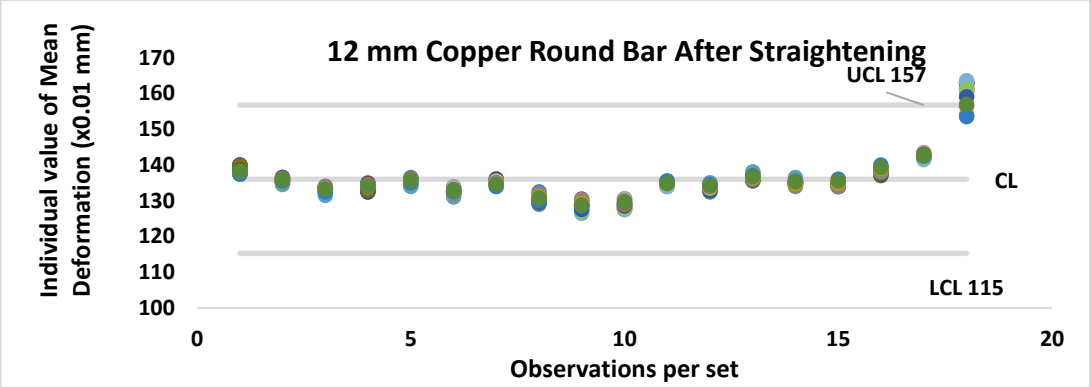

Figure 6.90 Deformation Analysis of 12 mm Copper Round Bar after straightening using SPC

6.10 Impact of Straightness on Overall Performance of Bars

From the various observations, it is amply clear that commercially available round bars evidently not so straight and round. Datasets given in tables and graphical representations thereof reveals the same. It may not be of much concern for general purpose applications but as raw materials when to be deployed for manufacturing of machine parts or machine components then straightness and roundness aspects of these round bars may be of significantly concerned of their roles. Achieving roundness may be somewhat easy through machining processes from higher diameter to lower diameter as desired, but straightness is not at all so easy to achieve economically. If the round bar as raw material is not sufficiently straight then it will obviously call for removal of higher quantity of materials to enable bring out a straight piece out of the work piece. Otherwise straightening of bar will be essential before going ahead with manufacturing process. Material removal leads to higher cost of machining beside wastage. It is imperative that production of large number of machine components demand solid round metal bars as workpiece on a machine and should be reasonably straight before start of manufacturing process. For quality product, straightness is a requirement for overall technical performance. When bars are used for manufacturing of shafts of rotating machines, performance of straightened bar can be seen as in terms of vibrations. Vibration is more if shaft is not straight. Therefore, straightness of bar is a qualitative aspect in manufacturing plant when round bars are raw materials. For final outcome of production system, straight bars have effective impact on overall performance. It can be postulated that deformations in a round bar of solid metals must have some effect on its mechanical properties due to Bauschinger effect [8]. Deformations also cause change in residual stresses. Change in residual stresses are mainly due to change in granular arrangement within the material body i.e solid round metal bars in this case. Mechanical properties may show anisotropic behaviour and become directional. Defects and imperfections in metal bars may affect mechanical strength and other properties of materials.

6.11 Discussion

The measured data used for graphical plots to see the deformations along the length of the bar circumferentially at various angular intervals. Scatter plots show that deformations exist along the length of the round bars and actual straightness of round bars of various diameters like 6 mm, 8 mm, 10 mm and 12 mm respectively are visible through related 3D Surface Plots. All graphs reveal that before straightening small deviations are visibly present at various sections in all types of bars. Graphs also reveal that no specific pattern is observed on the deviations. Deflections over length segments reveal presence of residual curvatures along the bar length. The surface plots have been considered here for Mild steel, Stainless steel, Aluminium and Copper materials of bar diameters 6 mm, 8 mm, 10 mm and 12 mm respectively. Dial gauge measurements of deflection were recorded from 0° to 360° circumferentially at angular interval of 15°. It can be seen from the Radar Charts and 3D Surface Plots shown in various figures that variations of surface smoothness or straightness are visibly observed in the segmental lengths and circumferentially.at angular intervals. The deformations observed in these diagrams reveal that deformations are actually a kind of defects in round metal bars which have possibly occurred during material handling or at production stage. Since deformations are prevailing, bars are not straight at various length segments along the length and curvatures exist in those segments. Although in general curvatures are considered as a deviation along a long length but this is with an assumption that curvature exist only at osculating plane. However, in reality it is seen from Radar Chart and 3D Surface Plots that curvatures also exist in planes other than osculating plane.

The users will have to take a decision on possible acceptance of these defects i.e. round bars with curvatures at various segmental lengths or take a remedial measure accordingly. However, it is as such possible to work on these defects either to nearly eliminate or reduce curvatures with the help of appropriate remedial measures.

Appropriate remedial measures are usually bar straightening process through various types of straighteners which is usually done for reduction of curvatures at various segments along the length of round bars. Straightening of bar is indeed a cold working process with some impact on mechanical properties of the materials as reverse bending is taking place beyond yield point where curvatures will undergo change [8,63].

Based on above, conclusion may be drawn easily that round bars as produced in the industries and as available at market are not necessarily quite round and straight. There is a fair possibility of some residual curvatures at various sections and length segments along the length of the bar. The above study has been conducted for both ferrous and non-ferrous materials which are extensively used for most science and engineering applications. The samples chosen for the above study, reveals that deformations are present in all the round bars throughout the length which indicates that straightness and roundness both are compromised at various sections. This is also evident from various scatter plots. From the scatter plots it is also seen that although variations exist in terms of diameter size at various sections over the entire length of round bars but from X-Bar Chart and R-Chart it is also evident that commercially these variations are within 3σ limits. Therefore, for general purpose most bars can be used. Such commercially available round bars can be deployed as raw materials for the purpose of further production work in industries. It can therefore be postulated that the proposed approach of using different statistical methods for checking the quality of bars in terms of straightness may be considered useful for manufacturing industries. This study proposes an overall accurate and compact method for a reliable and straightforward means of extracting the linear deflections, and thereby straightness with reasonable precision. Validation has been done by analysing the measurement results of experimentation of dial gauge deflections of commercially produced bars of different diameters with those obtained using 3D surface plots. Moreover, approach of finite element method is used further to check the validity of results obtained both experimentally and analytically which is explained in detail in Chapter 7. Finally,

predictive modelling of deformations of round bars obtained after straightening has been performed using different machine learning algorithm based on the datasets acquired experimentally.

CHAPTER – 7

FINITE ELEMENT ANALYSIS OF DEFORMATION OF ROUND BARS BEFORE AND AFTER STRAIGHTENING

7.1 Introduction

Finite element analysis (FEA) is a computing technique that is used to obtain approximate solutions to boundary value problems. It uses numerical method called finite element method (FEM). FEA involves the computer model of a design that is loaded and analysed for specific results, such as stress, deformation, deflection, natural frequencies, mode shapes, temperature distributions, and so on.

The FEA simulates the loading conditions of a design and determines the design response in those conditions. It can be used in new product design as well as in existing product refinement. A model is divided into a finite number of regions/divisions called elements. These elements can be of predefined shapes which helps to define the equations that describe how the element will respond to certain loads. The sum of the responses of all elements in a model gives the total response of the complete model (ANSYS Workbench 14.0 for Engineers and Designers)[107].

This chapter primarily focused on finite element analysis of all types of round bars under consideration for 6-mm, 8-mm, 10-mm and 12-mm diameters. The FEM analyses have been conducted initially with commercially available round bars before straightening and then again after straightening process through a two cross-roll straightening machine which may reflect the effect of changes of deflection behaviour pattern on straightening process.

7.2 FEM Approach using ANSYS Software

As briefly discussed above in introduction that Finite Element is a computing technique which uses numerical method, it is considered very convenient to work on geometrical models and developing a mesh of that model. Geometrical models can be created with features and tools available in software. From one dimensional to three dimensional geometrical models can be created easily. These models can be meshed and with the help of mesh, it is possible to find out various parametric values of nodes and elements using boundary conditions. Since, FEA is capable of simulating an actual situation it is obviously quite convenient to work with a mathematical model. The data generated by models can be compared with experimental data which is a standard practice also as evident from the graphical plots of many publications related to FEM applications. The accuracy of model somewhat depends on size of mesh and also computing. Due to such benefits, FEM is practiced widely for simulation purpose. The advantage of FEA software is to reduce the amount of prototype testing, thereby saving the cost and time beside it offers graphical representation of the result of analysis while the limitations are that it does not provide exact solution and results do not suggest any remedies.

7.3 ANSYS Software

There are a variety of commercial FEA software packages available in the market. Every Computer-Aided Engineering (CAE) software provides various modules for various analysis requirements. Depending on requirement, one can select a required module for the desired analysis. In the present case, ANSYS Workbench 2019 R16.2 software has been used to study commercially available metallic round bars which are extensively used in industries and also in academics for some research purposes. The advantage of this software is that its tutorials are available easily and all operational features are available in drop down menus.

7.4 Procedure Followed for Conducting ANSYS Simulation

To conduct the finite element analysis, following steps are given.

(i) Setting the type of analysis to be used

(ii) Creating a model

(iii) Defining the element type

(iv) Creating mesh of the model

(v) Application of material and other properties

(vi) Interpreting the results

7.4.1 Working on ANSYS Release 16.2

The stages involved in carrying out ANSYS simulation are discussed here with some example snapshots and simulation process visualizations. To simulate how metal round bars deform under both normal and straightened situation, ANSYS simulation has been used to perform deformation behaviour study on different metal rods of different sizes. For the above purpose ANSYS Release 16.2 has been installed in a computer system with configuration of Intel(R) Core (TM) i5-2430M CPU @2.40GHz and installed RAM of 12.0 GB (11.8 GB usable) in 64-bit operating system of x64-based processor in Windows 10 Pro and the software is operated using ANSYS Workbench 16.2 from command prompt with following displays taken by screenshot as shown in Figure 7.1.

Figure 7.1 The Opening Page of ANSYS Workbench 16.2

In the opening page four menu options of "Fluids", "Structures", "Electronics" and "Systems" are displayed as shown in the image. "**Structure**" option has been chosen for our analyses. In the sub-menu option, "**Static Structure**" has been chosen to go further in the finite element analysis as shown by screenshot taken from computer monitor (Figure 7.2).

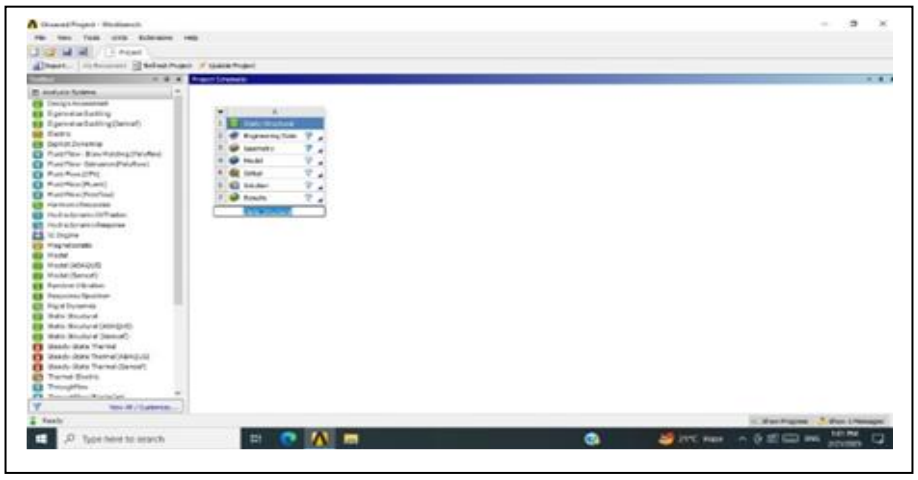

Figure 7.2 Menu of Analysis Systems in the Toolbox

In the "Static Structure" option, a **toolbox** appears with "**Analysis Systems**" showing large number of menu options where "**Static Structural**" is the required option to choose for the present case. After selecting 'Static Structural' a sub-menu appears with

"**Engineering Data**" where options are available to select materials and add its properties. The related screenshot of the menu is shown in Figure 7.3 as below.

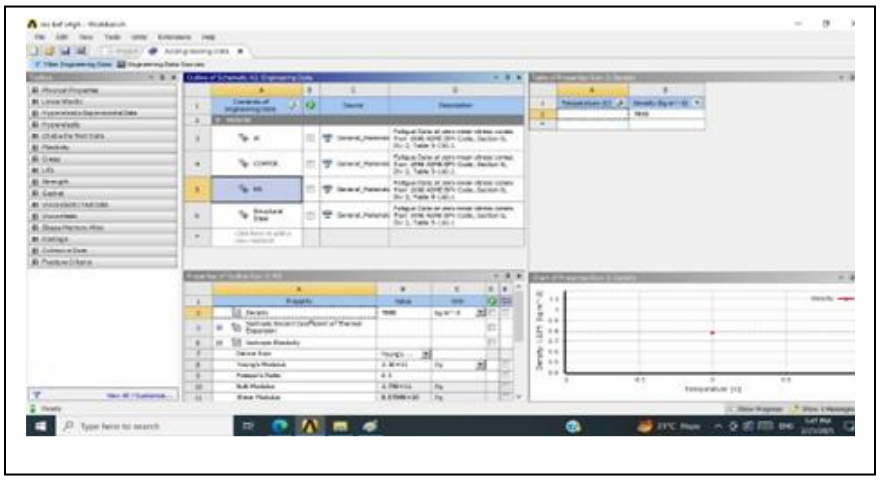

Figure 7.3 Menu of Engineering Data in the Toolbox

After selecting all engineering data of the materials and its properties, there is a need to invoke "DM Geometry" which is '**Design Modeler**" showing a page where geometry of required model can be made using XY plane, ZX Plane and YZ plane. With the selection of XY Plane, a 3D axis system appears for creating the model geometry. With this "Setting the type of analysis to be used" as first step is over.

The seconds step includes "**Creating a model**" which begins with selecting "**Geometry**" menu and choosing a plane. Another menu appears where a "**Tree Outline**" is displayed with two tabs "**Sketching**" and "**Modeling**". By selecting "**Sketching**", and then in "**Draw**" sub-menu, a blank graphic page is opened where a sketch can be generated using various sketching tools from the draw menu. In the present system, a sketch of circle has been made in XY Plane as shown by screenshot from computer monitor (Figure 7.4).

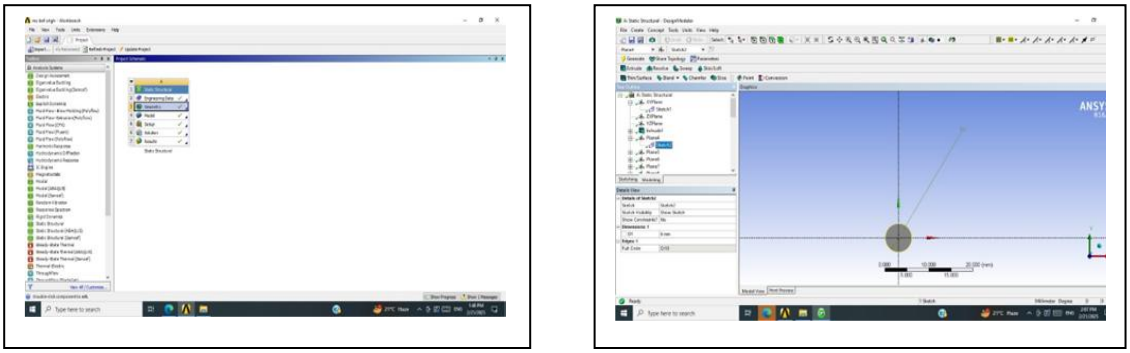

(a) (b)

Figure 7.4 Diagrams Showing (a) Geometry and (b) Sketch Menu in Design Modeler

Dimensional details of the sketch is required in the chosen plane and then extruded up to a required length. The process is continued from same plane to another plane. Consequently, a circular bar is created as shown by screenshot from computer monitor (Figure 7.5).

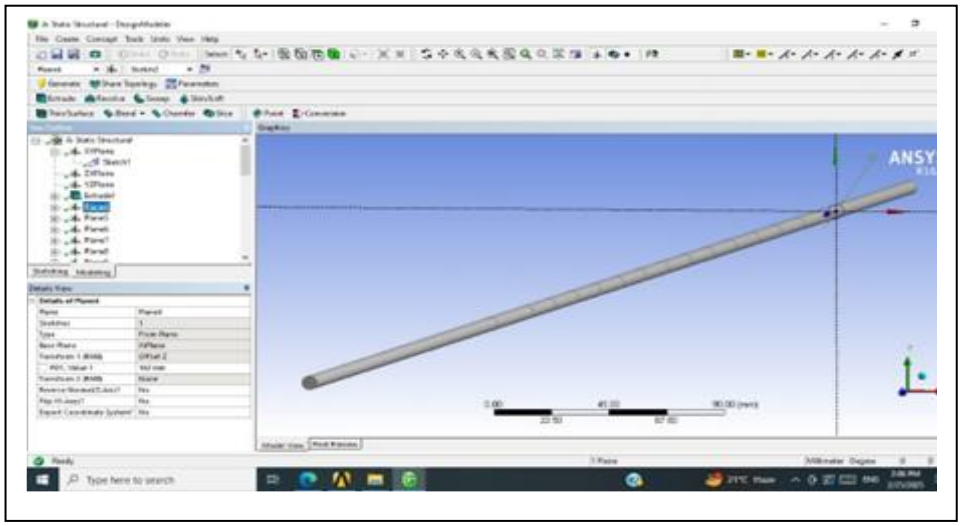

Figure 7.5 Diagram of Circular Bar using "**Sketching**" Menu

Upon going through all above steps, there is a necessity of "**Creating mesh of the model**" and "**Application of material and other properties**". The screenshot taken from computer monitor (Figure 7.6) shows the representation of image of the process of mesh generation with ANSYS as the starting point for the simulation model.

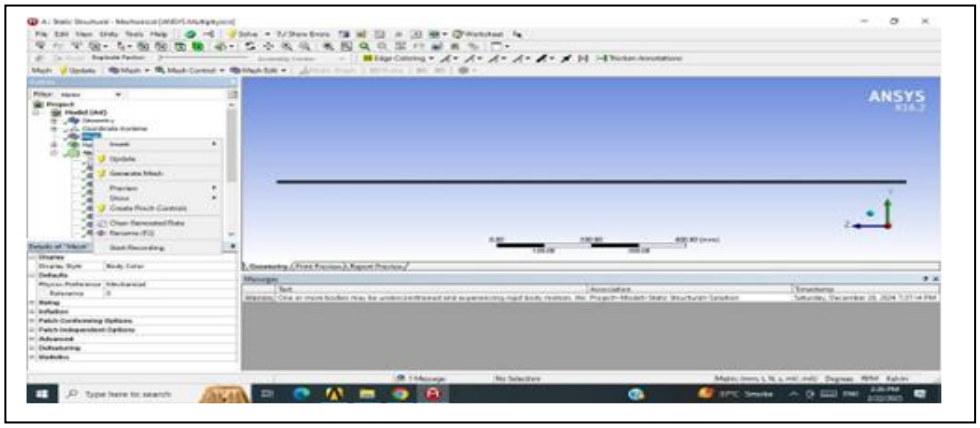

Figure 7.6 Diagram of "Generate Mesh" Menu and Generated Mesh.

Nodal displacements are shown in Figure 7.7 using a specific case of 6-mm MS round bar before straightening which has also been separately displayed and discussed later in subsequent article. Screenshot shown in Figure 7.7 provides a thorough overview of the procedure and the data gathered during the study, making it easier to understand the work flow and simulation results.

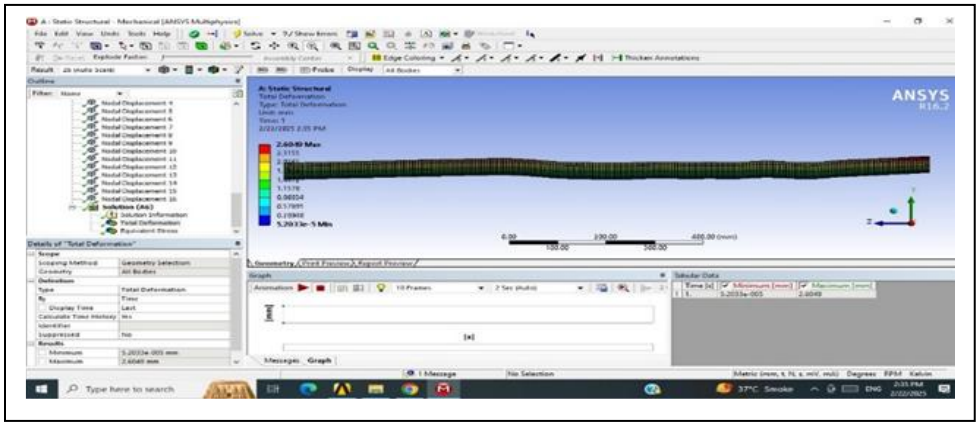

Figure 7.7 Menu Showing Nodal Displacements and Mesh Generated for 6-mm Round Bar using "Mesh" Generation"

With these above pictures in the figures all steps are completed except last step that is "**Interpreting the results**". Results are generated in the form of pdf files where all details like dimensional aspects, number of nodes, number of elements with total deformation values at various nodes are available. A short summary report includes the

minimum and maximum values of total deformations of the round bar along the length. Individual cases of mild steel, stainless steel, aluminium and copper of 6-mm, 8-mm, 10-mm and 12-mm respectively are presented sequentially in the subsequent articles for before and after straightening.

7.5 Finite Element Analysis of Metal Round Bars before Straightening

For in-depth study of deformation behaviour of straight round metal bars, finite element analysis (FEA) is carried out with the help of ANSYS R16.2 simulation software. Results obtained from the ANSYS based finite element model of straight round bars are presented and analysed in this section.

Finite Element analysis has been carried out for 6-mm,8-mm,10-mm and 12-mm Mild Steel round bar with mean values data available from observations. The relevant output data is given in Table 7.1 to Table 7.4 for different sizes. Also, the elements formed after meshing by considering deflections of round bars before straightening process using ANSYS R16.2 are given in Figure 7.8 to Figure 7.11 for different sizes of mild steel round bars. These mesh diagrams are generated after execution of measured dataset of deflections of bars before straightening.

Similarly for Stainless Steel round bars of same sizes, FEA has been carried out for mean values of observed data and relevant output is given in Table 7.5 to Table 7.8 with corresponding mesh diagrams in Figure 7.12 to Figure 7.15.

Likewise, the process of FEA has been carried out for 6-mm, 8-mm, 10-mm and 12-mm diameter Aluminium round bars with relevant output data given in Table 7.9 to Table 7.12 and corresponding mesh diagrams shown in Figure 7.16 to Figure 7.19.

Lastly, FEA has also been carried out for Copper round bars of same sizes as done previously for mild steel, stainless steel and aluminium bars. The relevant output data is given in Table 7.13 to Table 7.16 and mesh diagrams in Figure 7.20 to Figure 7.23. All these tables and figures are presented below sequentially.

Table 7.1 FEM Output Data for 6-mm Mild Steel Round Bar before straightening

Statistics	
Nodes	33450
Elements	6336
Maximum Total Deformation	2.6049 mm
Minimum Total Deformation	5.2033e-005 mm

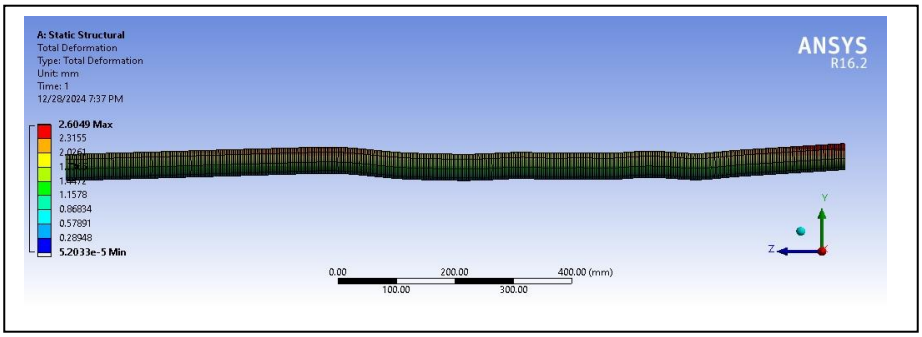

Figure 7.8 Deformation Analysis of 6-mm Mild Steel Round Bar before straightening

Table 7.2 FEM Output Data for 8-mm Mild Steel Round Bar before straightening

Statistics	
Nodes	28578
Elements	5412
Maximum Total Deformation	2.5265 mm
Minimum Total Deformation	1.0589 mm

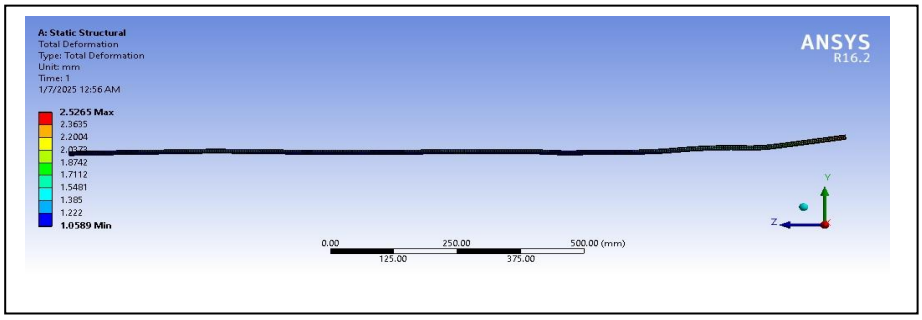

Figure 7.9 Deformation Analysis of 8-mm Mild Steel Round Bar before straightening.

Table 7.3 FEM Output Data for 10-mm Mild Steel Round Bar before straightening

Statistics	
Nodes	23706
Elements	4488
Maximum Total Deformation	3.8764 mm
Minimum Total Deformation	1.258e-003 mm

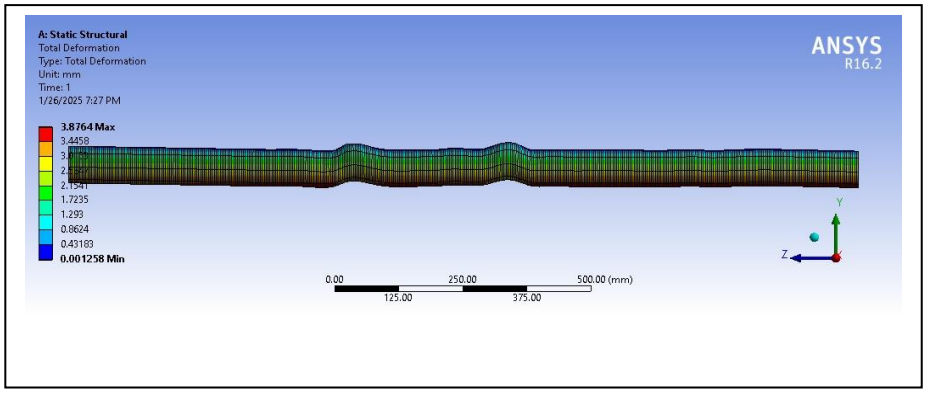

Figure 7.10 Deformation Analysis of 10-mm Mild Steel Round Bar before straightening

Table 7.4 FEM Output Data for 12-mm Mild Steel Round Bar before straightening

Statistics	
Nodes	18950
Elements	3586
Maximum Total Deformation	0.45477 mm
Minimum Total Deformation	6.5554e-004 mm

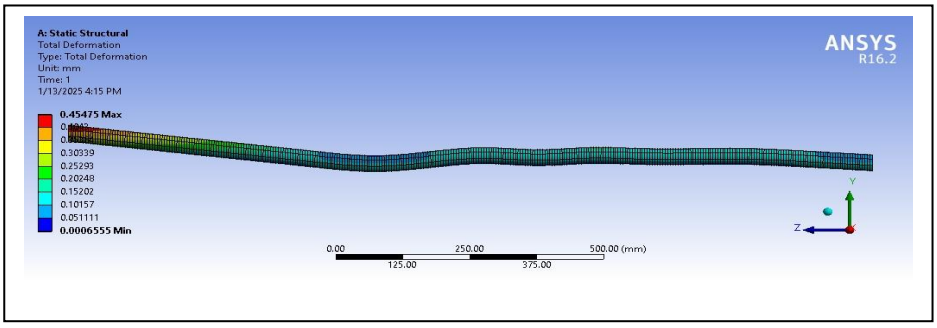

Figure 7.11 Deformation Analysis of 12-mm MS Round Bar before straightening

Table 7.5 FEM Output Data for 6-mm Stainless Steel Round Bar before straightening

Statistics	
Nodes	23184
Elements	4389
Maximum Total Deformation	2.2553 mm
Minimum Total Deformation	5.2997e-002 mm

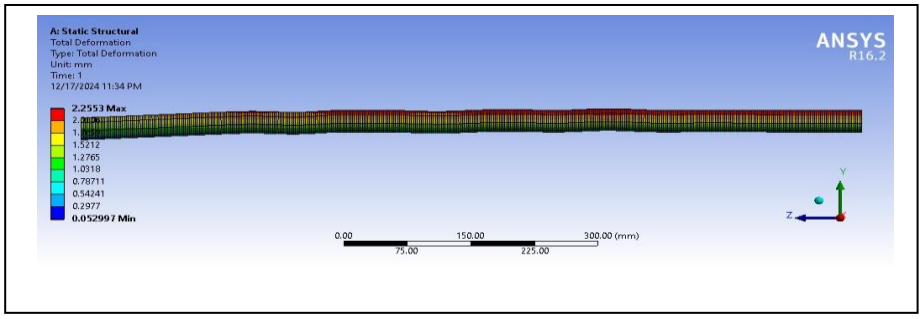

Figure 7.12 Deformation Analysis of 6-mm Stainless Steel Round Bar before straightening

Table 7.6 FEM Output Data for 8-mm Stainless Steel Round Bar before straightening

Statistics	
Nodes	29158
Elements	5522
Maximum Total Deformation	2.1294 mm
Minimum Total Deformation	1.2011 mm

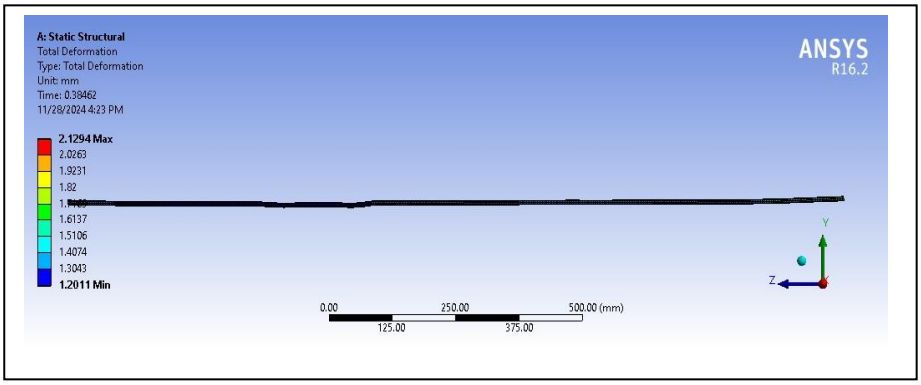

Figure 7.13 Deformation Analysis of 8-mm Stainless Steel Round Bar before straightening.

Table 7.7 FEM Output Data for 10-mm Stainless Steel Round Bar before straightening

Statistics	
Nodes	12686
Elements	2398
Maximum Total Deformation	0.29641 mm
Minimum Total Deformation	1.8505e-004 mm

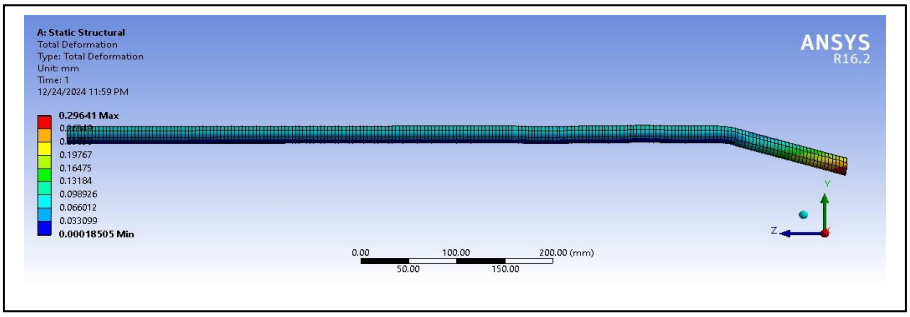

Figure 7.14 Deformation Analysis of 10 mm Stainless Steel Round Bar before straightening.

Table 7.8 FEM Output Data for 12-mm Stainless Steel before straightening

Statistics	
Nodes	18776
Elements	3553
Maximum Total Deformation	1.6373 mm
Minimum Total Deformation	3.1794e-004 mm

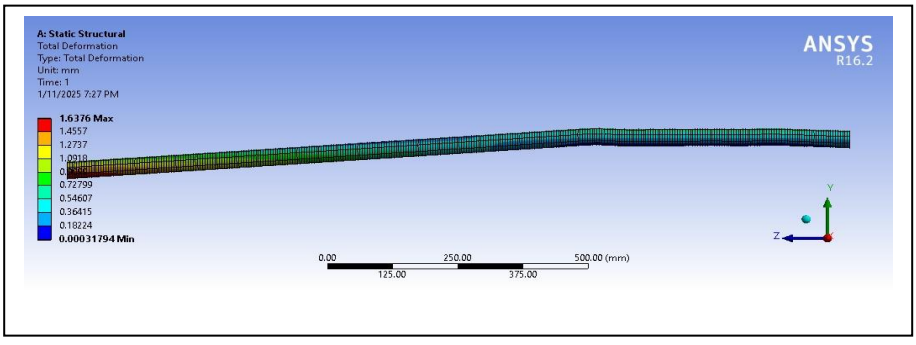

Figure 7.15 Deformation Analysis of 12-mm Stainless Steel Round Bar before straightening

Table 7.9. FEM Output Data for 6-mm Aluminium Round Bar before straightening

Statistics	
Nodes	31188
Elements	5907
Maximum Total Deformation	3.3662 mm
Minimum Total Deformation	5.1433e-002 mm

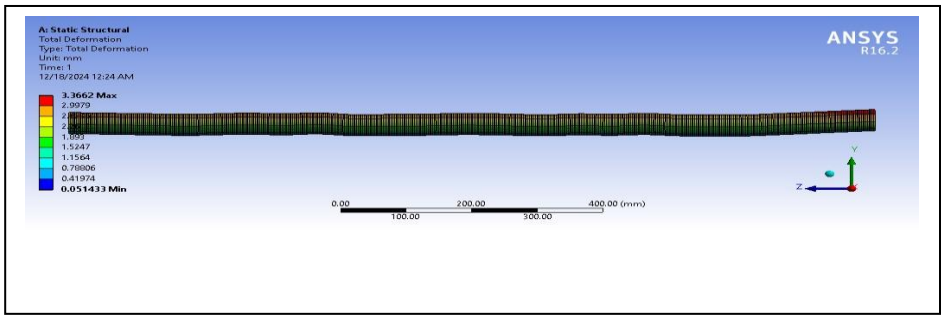

Figure 7.16 Deformation Analysis of 6-mm Aluminium Round Bar before straightening

Table 7.10 FEM Output Data for 8-mm Aluminium Round Bar before straightening

Statistics	
Nodes	28984
Elements	5489
Maximum Total Deformation	2.0168 mm
Minimum Total Deformation	0.2087 mm

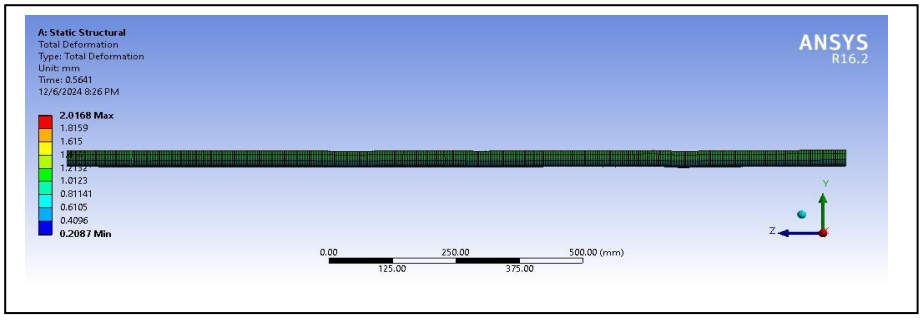

Figure 7.17 Deformation Analysis of 8-mm Aluminium Round Bar before straightening

Table 7.11 FEM Output Data for 10-mm Aluminium Round Bar before straightening

Statistics	
Nodes	23300
Elements	4411
Maximum Total Deformation	1.777 mm
Minimum Total Deformation	7.7548e-002 mm

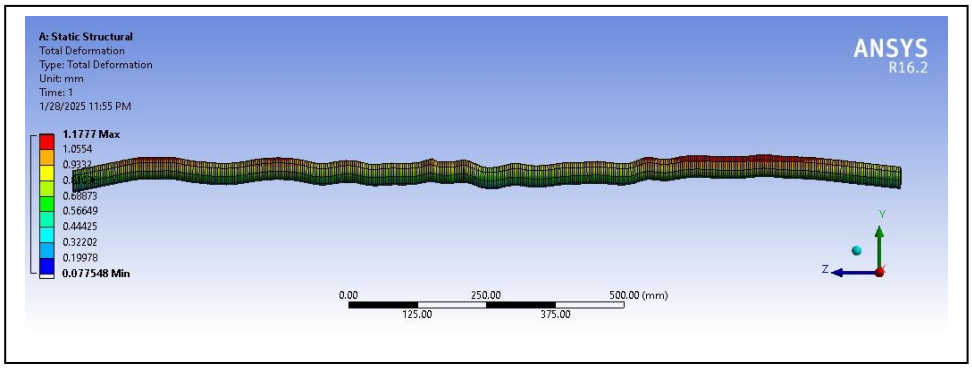

Figure 7.18 Deformation Analysis of 10-mm Aluminium Round Bar before straightening

Table 7.12 FEM Output Data for 12-mm Aluminium Round Bar before straightening

Statistics	
Nodes	19066
Elements	3608
Maximum Total Deformation	0.4052 mm
Minimum Total Deformation	4.183e-004 mm

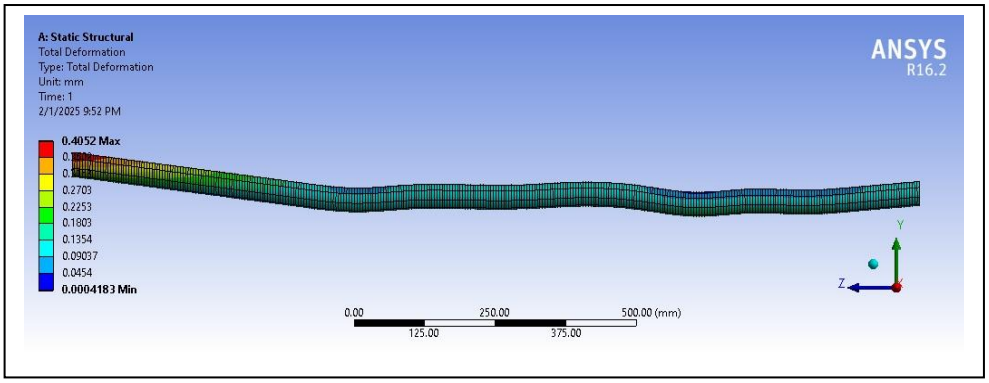

Figure 7.19 Deformation Analysis of 12-mm Aluminium Round Bar before straightening.

Table 7.13 FEM Output Data for 6-mm Copper Round Bar before straightening

Statistics	
Nodes	25504
Elements	4829
Maximum Total Deformation	3.3588 mm
Minimum Total Deformation	1.754e-004 mm

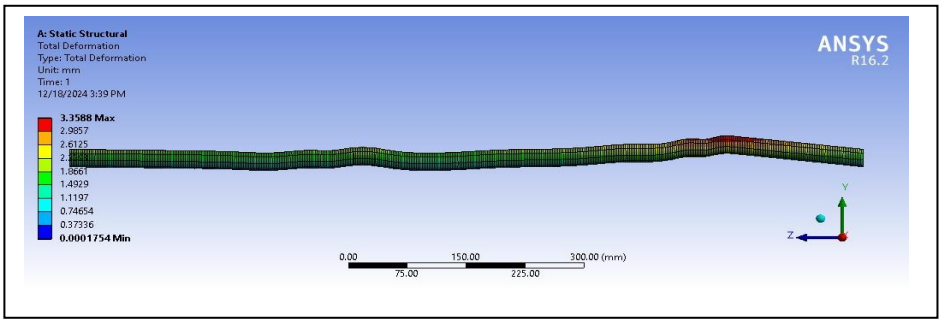

Figure 7.20 Deformation Analysis of 6-mm Copper Round Bar before straightening

Table 7.14 FEM Output Data for 8-mm Copper Round Bar before Straightening

Statistics	
Nodes	19646
Elements	3718
Maximum Total Deformation	1.8402 mm
Minimum Total Deformation	1.4568 mm

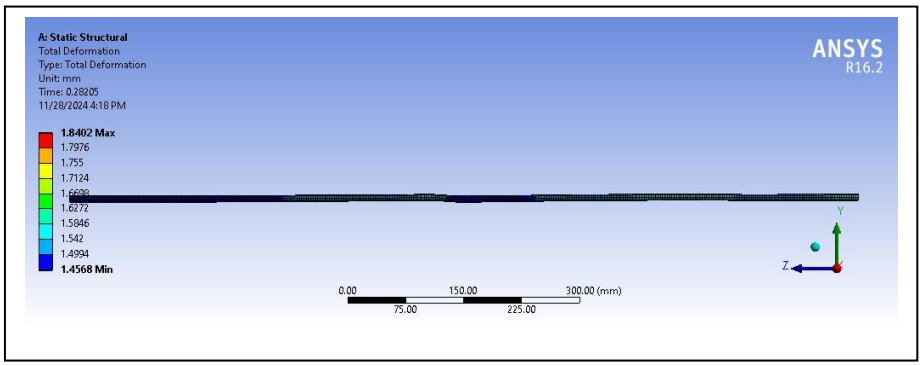

Figure 7.21 Deformation Analysis of 8-mm Copper Round Bar before straightening

Table 7.15 FEM Output Data for 10-mm Copper Round Bar before straightening

Statistics	
Nodes	23416
Elements	4433
Maximum Total Deformation	1.8467 mm
Minimum Total Deformation	1.1819 mm

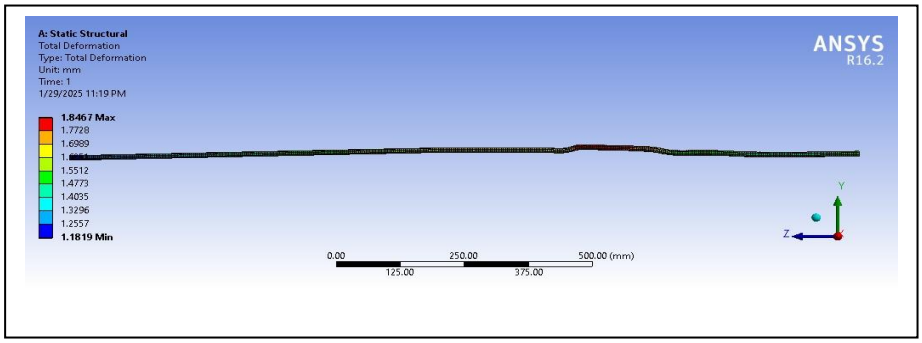

Figure 7.22 Deformation Analysis of 10-mm Copper Round Bar before straightening

Table 7.16 FEM Output Data for 12-mm Copper Round Bar before Straightening

Statistics	
Nodes	19472
Elements	3685
Maximum Total Deformation	3.3534 mm
Minimum Total Deformation	1.5069e-003

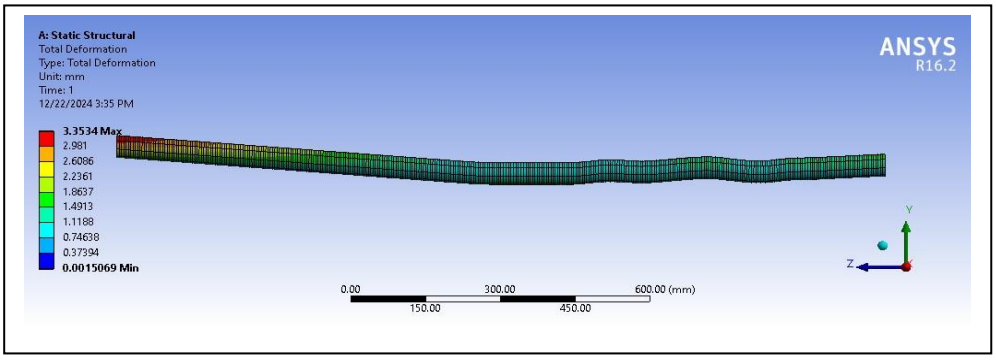

Figure 7.23 Deformation Analysis of 12-mm Copper Round Bar before straightening

7.6 Finite Element Analysis of Round Metal Bars after Straightening

The previous analyses have been discussed for round bars before straightening which is actually for the round bars available commercially. The results thereof reveal that deformations are already existing in the round bars. The same round bars have been used for straightening purpose in a two cross-roll straightening machine. The deflection readings of these bars were then recorded again and data thereof used for FE analysis.

Finite Element analysis has been carried out for 6-mm, 8-mm, 10-mm and 12-mm **Mild Steel (MS)** round bars with mean values of observed dataset after straightening. The relevant output data is given in Table 7.17 to Table 7.32 and with nodes and elements formed after meshing by considering the corresponding deflections of round bars under study using ANSYS R16.2 is given in Figure 7.24 to Figure 7.27 respectively. Similarly, as FEA analysis done earlier for mild steel round bars, same has been done for 6-mm, 8-mm, 10-mm and 12-mm diameters **Stainless Steel (SS)** round bars after straightening considering the mean values of observed dataset. The nodes, elements and deformation results from output results is given in Table 7.21 to Table 7.24 and relevant mesh diagrams shown in Figure 7.28 to Figure 7.31.

In a similar manner, Finite Element analysis has been carried out for 6-mm, 8-mm, 10-mm and 12 mm diameter **Aluminium (Al)** round bars with mean values of observed dataset and relevant output data is given in Table 7.25 to Table 7.28 along with corresponding mesh diagram shown in Figure 7.32 to Figure 7.35. Lastly, FEA has been also been done for 6-mm, 8-mm, 10-mm and 12-mm diameter **Copper (Cu)** round bars with mean values of observed dataset. The relevant output data of nodes, elements and total deformations is tabulated in Table 7.29 to Table 7.32 and corresponding mesh diagrams displayed in Figure 7.36 to Figure 7.39.

Table 7.17 FEM Output Data for 6-mm Mild Steel Round Bar after straightening

Statistics	
Nodes	33450
Elements	6336
Maximum Total Deformation	2.4277 mm
Minimum Total Deformation	4.709e-005 mm

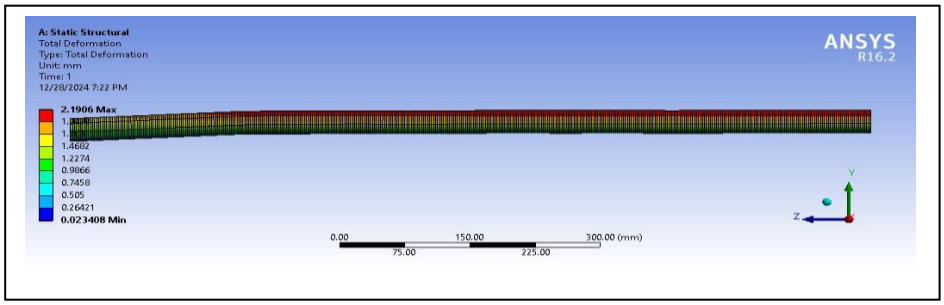

Figure 7.24 Deformation Analysis of 6-mm Mild Steel Round Bar after straightening

Table 7.18 FEM Output Data for 8-mm Mild Steel Round Bar after straightening

Statistics	
Nodes	25878
Elements	5412
Maximum Total Deformation	1.8483 mm
Minimum Total Deformation	0.99844 mm

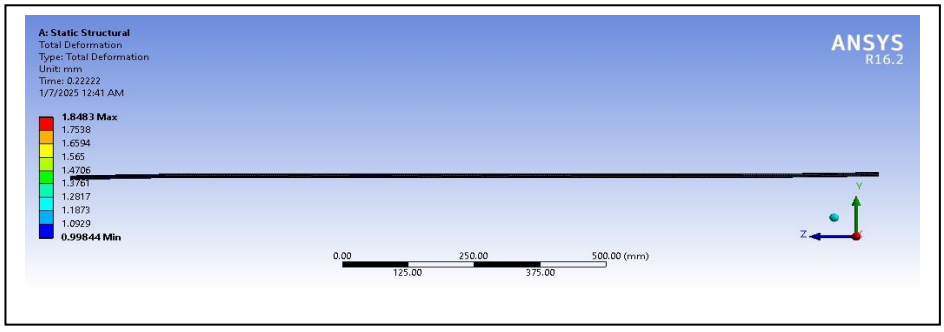

Figure 7.25. Deformation Analysis of 8-mm Mild Steel Round Bar after straightening

Table 7.19 FEM Output Data for 10-mm Mild Steel Round Bar after straightening

Statistics	
Nodes	23590
Elements	4466
Maximum Total Deformation	0.49691 mm
Minimum Total Deformation	5.2072e-005 mm

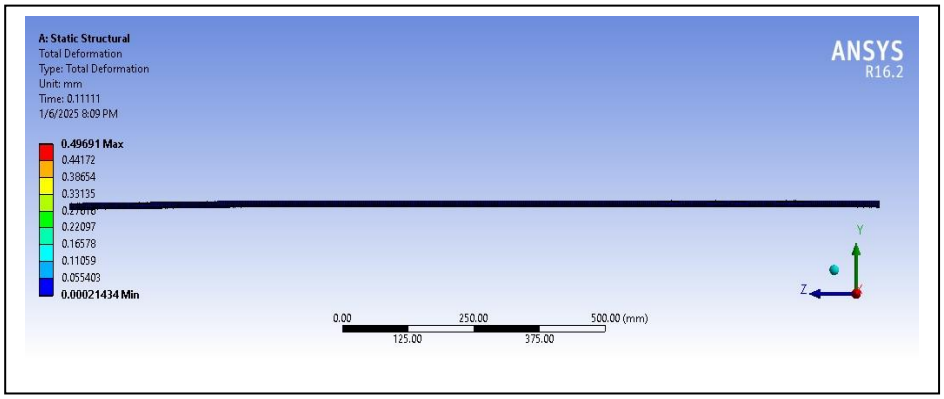

Figure 7.26 Deformation Analysis of 10 mm Mild Steel Round Bar after straightening

Table 7.20 FEM Output Data for 12-mm Mild Steel Round Bar after Straightening

Statistics	
Nodes	17094
Elements	3234
Maximum Total Deformation	0.28152 mm
Minimum Total Deformation	7.8433e-005 mm

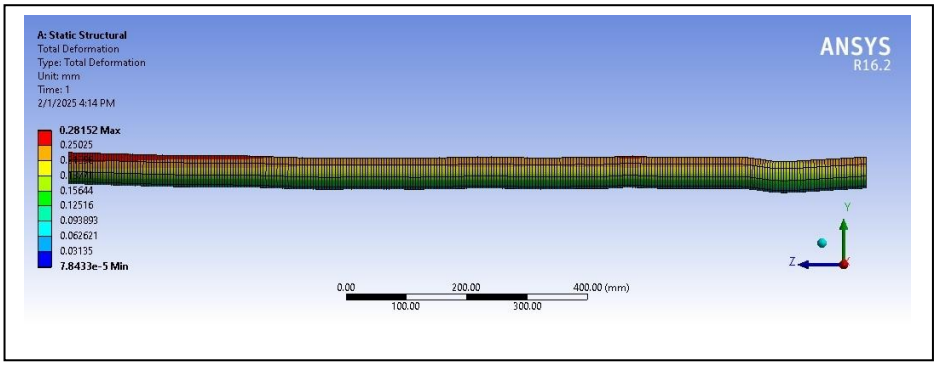

Figure 7.27 Deformation Analysis of 12-mm Mild Steel Round Bar after straightening

Table 7.21 FEM Output Data for 6-mm Stainless Steel Round Bar after straightening

Statistics	
Nodes	23184
Elements	4389
Maximum Total Deformation	2.1906 mm
Minimum Total Deformation	2.3408e-002 mm

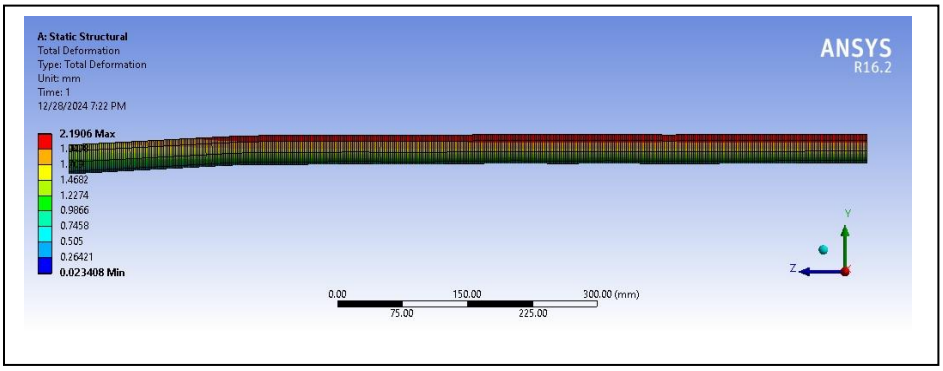

Figure 7.28 Deformation Analysis of 6-mm Stainless Steel Round Bar after straightening

Table 7.22 FEM output data for 8-mm Stainless Steel round bar after straightening

Statistics	
Nodes	29158
Elements	5522
Maximum Total Deformation	1.7206 mm
Minimum Total Deformation	1.1146 mm

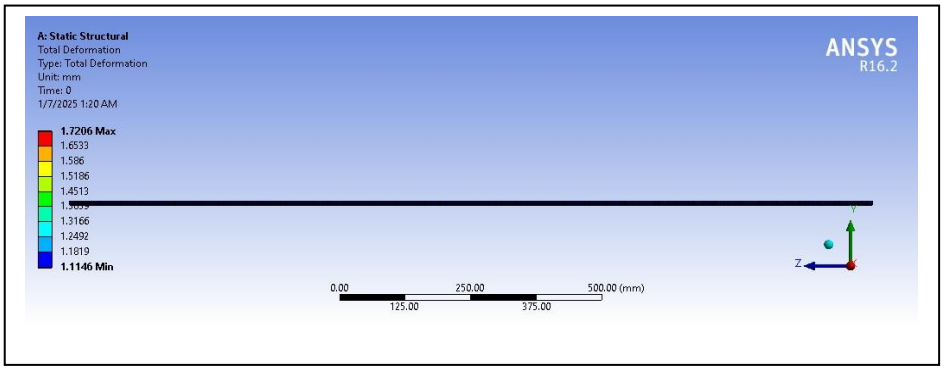

Figure 7.29 Deformation analysis of 8-mm Stainless Steel Round Bar after straightening.

Table 7.23 FEM Output Data for 10-mm Stainless Steel Round Bar after straightening

Statistics	
Nodes	12628
Elements	2387
Maximum Total Deformation	0.23411 mm
Minimum Total Deformation	1.3269e-004 mm

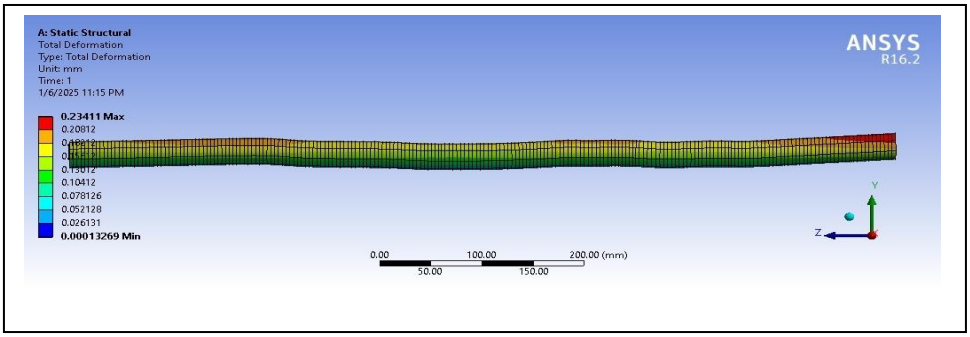

Figure 7.30 Deformation analysis of 10-mm Stainless Steel Round Bar after straightening.

Table 7.24 FEM Output Data for 12-mm Stainless Steel Round Bar after straightening

Statistics	
Nodes	18950
Elements	3586
Maximum Total Deformation	1.1662 mm
Minimum Total Deformation	1.5937e-004

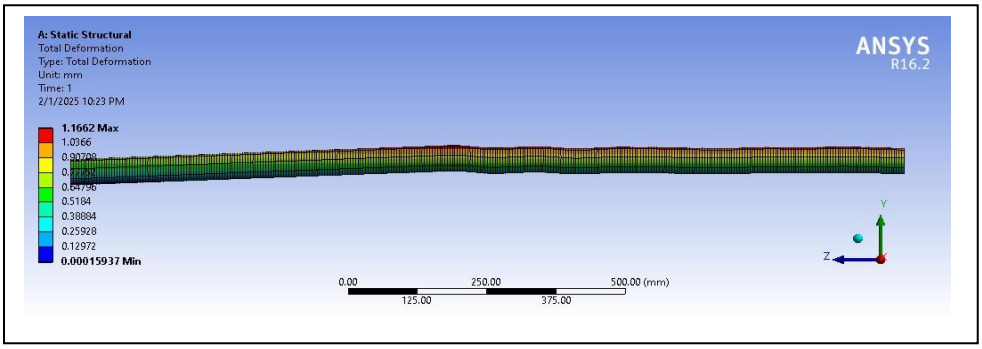

Figure 7.31 Deformation Analysis of 12-mm Stainless Steel Round Bar after straightening

Table 7.25 FEM Output Data for 6-mm Aluminium Round Bar after straightening

Statistics	
Nodes	31188
Elements	5907
Maximum Total Deformation	0.6587 mm
Minimum Total Deformation	4.6952e-002 mm

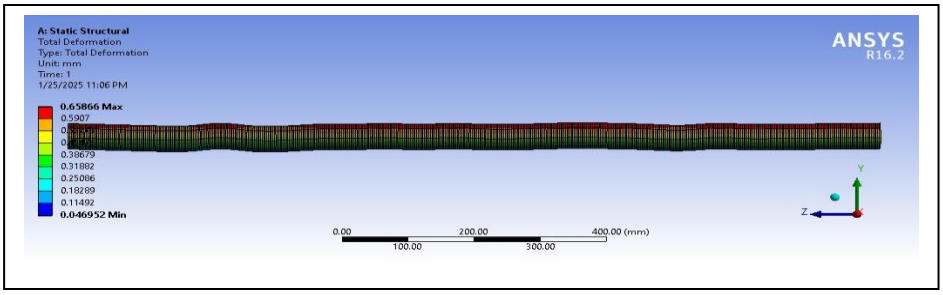

Figure 7.32 Deformation Analysis of 6-mm Aluminium Round Bar after straightening

Table 7.26 FEM Output Data for 8-mm Aluminium Round Bar after straightening

Statistics	
Nodes	28984
Elements	5489
Maximum Total Deformation	0.59651 mm
Minimum Total Deformation	4.0654e-002 mm

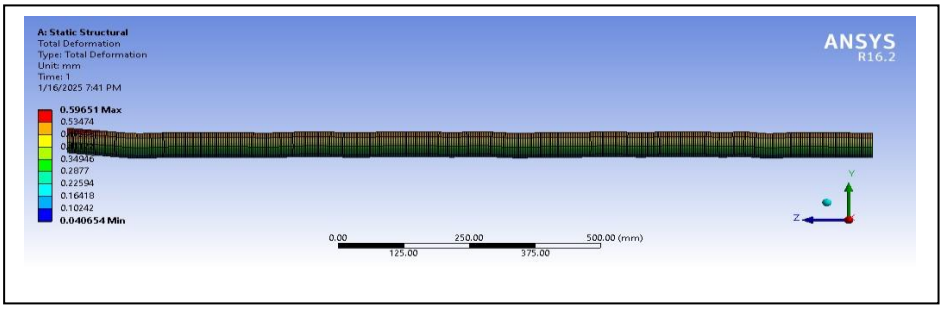

Figure 7.33 Deformation Analysis of 8-mm Aluminium Round Bar after straightening

Table 7.27 FEM Output Data for 10-mm Aluminium Round Bar after straightening

Statistics	
Nodes	22952
Elements	4345
Maximum Total Deformation	0.49444 mm
Minimum Total Deformation	1.991e-002

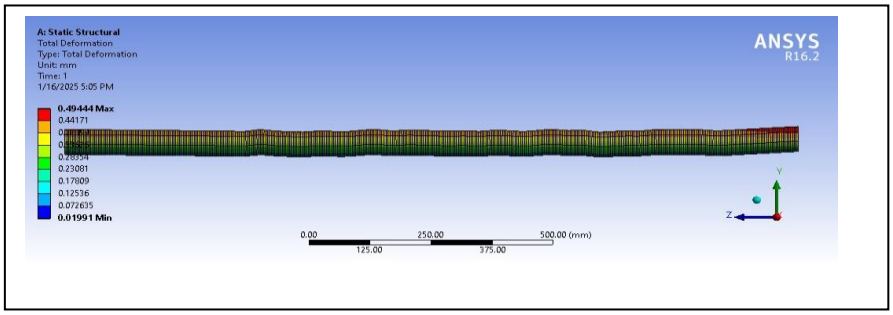

Figure 7.34 Deformation Analysis of 10-mm Aluminium Round Bar after straightening.

Table 7.28 FEM Output Data for 12-mm Aluminium Round Bar after straightening

Statistics	
Nodes	19066
Elements	3608
Maximum Total Deformation	0.1075 mm
Minimum Total Deformation	3.821e-005

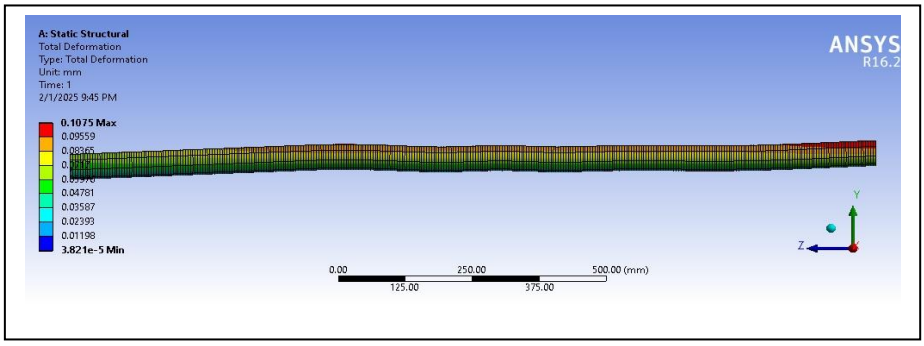

Figure 7.35 Deformation Analysis of 12 mm Aluminium Round Bar after straightening

Table 7.29 FEM Output Data for 6-mm Copper Round Bar after straightening

Statistics	
Nodes	25504
Elements	4829
Maximum Total Deformation	0.99293 mm
Minimum Total Deformation	1.0853e-004 mm

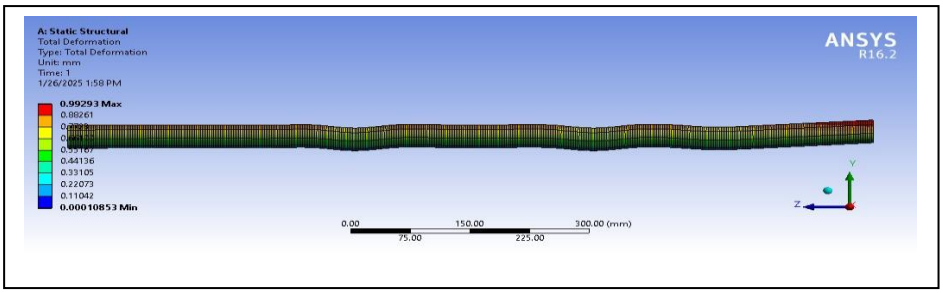

Figure 7.36. Deformation Analysis of 6-mm Copper Round Bar after straightening.

Table 7.30 FEM Output Data for 8-mm Copper Round Bar after Straightening

Statistics	
Nodes	19646
Elements	3718
Maximum Total Deformation	0.98615 mm
Minimum Total Deformation	0.6429 mm

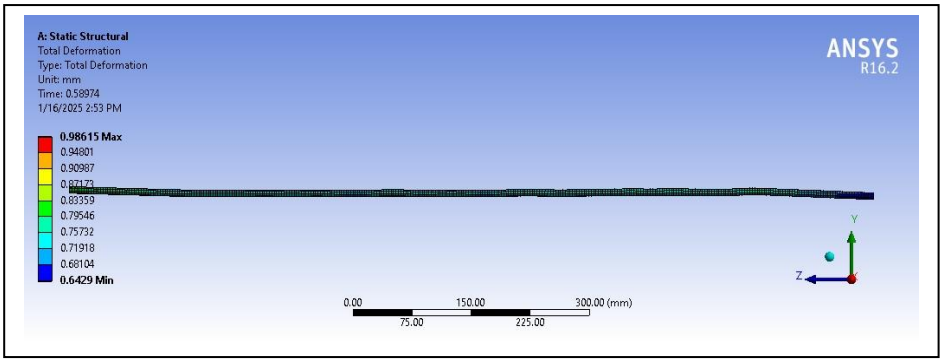

Figure 7.37 Deformation Analysis of 8-mm Copper Round Bar after straightening.

Table 7.31 FEM Output Data for 10-mm Copper Round Bar after straightening

Statistics	
Nodes	23416
Elements	4433
Maximum Total Deformation	0.97444 mm
Minimum Total Deformation	0.81556 mm

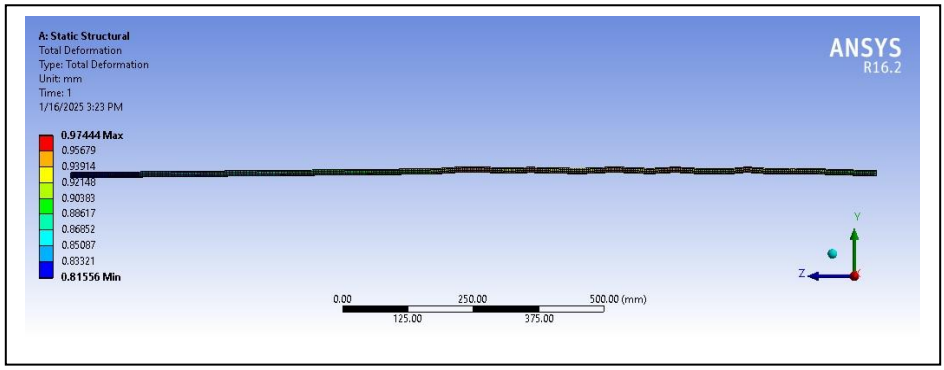

Figure 7.38 Deformation Analysis of 10 mm Copper Round Bar after straightening.

Table 7.32 FEM Output Data for 12-mm Copper Round Bar after straightening

Statistics	
Nodes	13034
Elements	2464
Maximum Total Deformation	0.91741 mm
Minimum Total Deformation	9.765e-5 mm

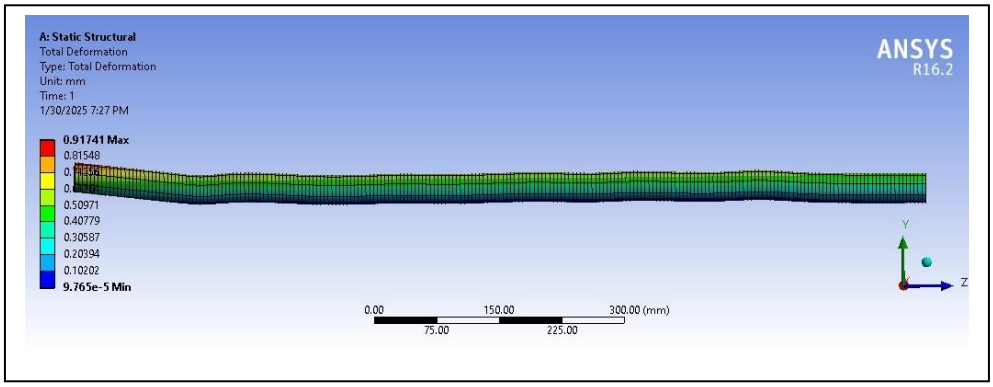

Figure 7.39 Deformation Analysis of 12 mm Copper Round Bar after straightening.

7.7 Discussions

The impact of straightness on overall performance of metal bars before and after straightening is discussed here. The observations from the data recorded from the experiments and finite element analysis thereafter reveal that although commercially available bars before straightening are actually not so straight but after straightening process there is visible improvement in straightness. Table 7.33 illustrates the comparative results of deformation values obtained from finite element meshing of metal bars before and after straightening.

Table 7.33. Comparison of Results Obtained from Finite Element Analysis of Metal Round Bars before and after Straightening

SN	Material Type	Bar dia. (mm)	Deformation Values in mm			
			Before Straightening		After Straightening	
			Max	Min	Max	Min
1	Mild Steel	6	2.6049	5.2033e-005	2.4277	4.709e-005
2	Mild Steel	8	2.5265	1.0589	1.8483	0.99844
3	Mild Steel	10	3.8764	1.258e-003	0.49987	5.2072e-004
4	Mild Steel	12	0.4547	6.5554e-004	0.28152	7.8433e-005
5	Stainless Steel	6	2.2553	5.2997e-002	2.1906	2.3408e-002
6	Stainless Steel	8	2.1294	1.2011	1.7206	1.1146
7	Stainless Steel	10	0.29641	1.8505e-004	0.23411	1.3269e-004
8	Stainless Steel	12	1.6376	3.1794e-004	1.1662	1.5937e-004
9	Aluminium	6	3.3662	5.1433e-002	0.65866	4.6952e-002
10	Aluminium	8	2.0168	0.2087	0.59651	4.0654e-002
11	Aluminium	10	1.777	7.7548e-002	0.49444	1.991e-002
12	Aluminium	12	0.40522	4.1828e-004	0.1075	3.821e-005
13	Copper	6	3.3588	1.754e-004	0.99293	1.0853e-004
14	Copper	8	1.8402	1.4568	0.98615	0.6429
15	Copper	10	1.8467	1.1819	0.97444	0.81556
16	Copper	12	3.3534	1.5069e-003	0.91741	9.765e-005

By comparing both datasets and results of finite element analysis it can be postulated that straightness at various length segments of metal bars have improved significantly after straightening process. It has also been observed that the effect of straightening is

more significant for non-ferrous materials than ferrous materials while passing through hardened chromium steel cross-rolls. Since the process involves elasto-plastic bending, deformation would be comparatively more in case of relatively softer material under same loading condition. Moreover, modulus of elasticity in non-ferrous material are much lower than that of ferrous materials. Therefore, under the same loading condition, straightening process will be more significant for non-ferrous materials in comparison with ferrous materials. It can be stated that there is a direct impact of reverse bending during transit of round bars of various materials through straightening rollers. This experiment has used one set of concave roller and convex roller which caused straightness of bars after having passed through the rotary straighteners which led to improved quality level of the bars. After straightening metal removal rate will be much lesser compared to earlier condition that is before straightening. The effect of straightening on commercially produced bars of both ferrous and non-ferrous materials will give an overall improved straightness and round metal bars would have otherwise been rejected from quality point of view. Now these can be successfully be accommodated in the lot and be used for the production of many items.

7.8 Inference

Based on the results obtained from finite element analyses of deformations of round bars after cross-roll straightening process, it has been observed that straightness has been improved quite significantly after straightening. Reasonable improvement of straightness has been observed in case of non-ferrous materials i.e. aluminium and copper. The reason could be low modulus of elasticity of the materials which probably causes less deformation after straightening during reverse bending. Experimental results of dial gauge deflections of commercially produced bars of different materials and sizes have been validated by the analysis of finite element method. The main contribution of this chapter is that FEM analysis of the round metal bars after cross-roll straightening show a significant achievement. Finally, it can be concluded that effect of cross-roll straightening process is more significant for non-ferrous materials than ferrous materials.

This type of study can be extended in the emerging field of cross-roll straightening process by analysing the radius of curvatures and corresponding residual stresses of the bars with the help of finite element approach. Moreover, the scope of this study can be expanded to predict the improved straightness of metal bars by using machine learning approach which is explained in detail in Chapter-8.

CHAPTER – 8

PREDICTIVE MODELING OF STRAIGHTNESS USING MACHINE LEARNING

8.1 Introduction

From the point of view of production and manufacturing process, issues related to straightness are very important. The straightness after straightening of any round bar is significantly influenced by its uniformity of sectional roundness, length of the bar and material properties such as elastic modulus. In this chapter, datasets obtained from experimental study carried out on samples of round bars of various types of materials of same size have been studied. This is followed by predictive modelling of straightness using machine algorithms. The problem is formulated based on design of experiments for the measurement of straightness of mild steel, stainless steel, aluminium and copper round bars of different sizes. Experiments are conducted with four input variables. As a part of developing a predictive model, machine learning algorithms namely linear regression, random forest regression, support vector regression, XgBoost and decision tree have been applied to the experimentally acquired data. Computed metrics such as R squared value, mean absolute error, root mean square error and prediction time resulted in random forest regression better than all the other methods. Using this random forest regression model, deformation values are predicted as a measure of straightness.

In manufacturing process ensuring the perfect straightness of round bars or shafts is of chief importance. The current development of machining techniques makes it possible to conduct subtractive machining processes with high efficiency. The main and most visible effect of the machining process is the machined surface condition. Not only

does this affect the visual aspect of the component, but also its operating properties. It is therefore necessary to obtain a surface with the most favourable structure, which is usually evaluated based on straightness but this requires conducting prior experimental studies. Researches have been done by the authors [4] so as to show the surface irregularity and existence of curvatures at various section of normally available commercial bars using statistical analysis and finite element analysis on deformation behaviour before any kind of straightening process. The earlier experimental investigation shows an attempt to understand the straightness achieved after single pass straightening process by measuring deflections circumferentially at various points of the surface of the metal round bars at various length segments with the help of dial gauge readings. One of the greatest challenges in dealing with straightness of commercially available round bars is to generate the dataset that is systematic and authentic. Here artificial intelligence plays an important role wherein the use of correct data is essential to make suitable decisions. Several researches on this topic carried out recently are illustrated in Table 8.1 representing a comparative overview of the approaches towards straightening process. Though all of these studies related to straightness have been of incredible significance, the present investigation focusses some research gap and brings a new perspective on how deformations after straightening process are predicted by using machine learning algorithms at least as a first approximation. Hence, predictive modelling of machine learning algorithms is highly required to obtain precise information about straightness as well as surface roughness.

Table 8.1 Comparison of the Present Investigation with Some Recent Works

Literature Review on Bar Straightening	Research Area and Problem Addressed	Method and Tools used	Significant Features	Research Gap
Wu et al. (2000) [38]	Precision modelling of round bars	Theoretical formulation and experimental approach	Geometry of axis of bar in straightening	Statistical aspect and Modelling not addressed
Marcos-Barcena et al. (2005) [18]	Roundness of precision elements Aluminium-Copper alloyed cylindrical bars.	Experimental set up for measurement of roundness	- Surface plot generated with roundness as response variable. - Result shows improved roundness at lower cutting speed.	Statistical measure on overall straightness not addressed.

Kalos et al. (2007) [19]	Control of roundness. Feed and roundness were studied.	Artificial Neural Network and MATLAB	- Algorithm developed. - 3D plot for prediction of roundness	Straightness not addressed
Mutrux et al. (2008) [41]	Simulation of straightening process	LS-DYNA (FEM Software)	Bending can be controlled by changing helix angle.	Statistical aspect not addressed
Tian et al. (2010) [42]	Numerical analysis and simulation for straightening force	FEM, DEFORM-3D software	Best straightening force and curvature is determined	Statistical aspect not addressed
Yali & Herong (2012) [44]	Straightening of bars	FEM and Standstill Locking mechanism	Roll-layout of equivalent curvature and straightening mechanism.	Statistical aspect not addressed
Huang et al. (2012) [45]	Simulation analysis of straightening	FEM on platform MSC.MARC	-Maximum straightening force -Simulation of equivalent stress and strain.	Statistical aspect not addressed
Raab & Hynek (2012) [46]	Simulation analysis of cross roll straightening processes	FEM on platform MSC.MARC	-Maximum straightening force -Simulation of equivalent stress and strain.	Statistical aspect not addressed
Navrat & Petruska (2014) [50]	Roller straightening of Rails	FEM & MATLAB	Numerical analysis of roller straightening process	Statistical aspects not considered
Yu et al. (2017) [54]	Straightening process mechanism	Theoretical analysis & FEM	Numerical simulation	Statistical consideration not addressed
Lidong Ma et al. (2019) [30]	Surface quality and high straightness precision	Design method of continuous curvature and FEM	Application of variable curvature, surface stress profile	Statistical aspect not addressed
Gribkov et al. (2023) [108]	Computer modelling on six roll straightening	FEM	Application on pipe straightening	Statistical aspect not addressed
Xing, S. (2023) [109]	Analytical Modelling	Mechanical Straightening Process	Case hardened circular shafts	Statistical aspect not addressed
This study	Prediction of Straightening in terms of deflection	Machine Learning algorithms	Circumferential deformation of round metal (ferrous and non-ferrous) bars	Predicting Modelling of straightness using Machine Learning algorithm.

Considering the research gaps addressed, this chapter primarily deals with a novel methodology of predictive modelling of the straightness of metal bars of both ferrous and non-ferrous materials with the help of machine learning algorithms namely Linear Regression (LR), Support Vector Regression (SVR), Random Forest Regression (RFR), Extreme Gradient Boost (XGBoost) and Decision Tree (DT). These regression algorithms have been applied to the experimentally acquired data. The results of the analysis show that RFR model fits more accurately for prediction of straightness of metal bars in terms of lower mean absolute error (MAE) and root mean square error (RMSE), along with higher R-Squared (R^2) values. In this study different sizes of metal

bars of four types of materials have been considered after single pass of two cross-roll straightening machine and predictive modelling of straightness of metal bars has been developed on the basis of variation of circumferential deformations with respect to length of the bars and different angular positions of the bars. This modelling will allow proper forecasting of straightness after straightening process and can be implemented in manufacturing process.

8.2 Predictive Model Characteristics

For prediction modelling, machine learning makes use of computation methods to extract information from varieties of dataset. In this work five regression model namely Linear Regression (LR), Support Vector Regressor (SVR), Random Forest Regressor (RFR), XgBoost and Decision Tree (DT) regression have been explored. The choice of these five regression models is due to their different conceptual foundation which in turn enable them to solve regression problem of varying complexity. For instance, LR is comparatively simpler for finding the coefficient values to the most optimized linear functions which can be used for prediction on dataset. SVR can address problems with higher complexity due to the dynamics of support vectors driven hyperplane. RFR on the other hand is conceptually different from many other regression algorithms and falls under the ensemble learning category where the final prediction is the outcome from many binary predictors. Decision trees (DT) are an approach used in supervised machine learning, a technique which uses a tree like model of decisions and their possible consequences and simplifies the decision making process by breaking down the different paths of available action. The main advantage of DT is its potential to visualise how a supervised learning algorithm leads to specific outcomes. All these models have been briefly described below for ready reference; however, readers are encouraged to go through different repositories for needed details. Moreover, these regressors are operated by their computational simplicity and considerable amount of high accuracy in predicting non-linear data set. Now, it can be stated that since the work includes four types of materials which are totally different

in their compositions, a single prediction model may not be suitable. Therefore, different prediction models under each of the algorithm are developed here for experimentation.

8.2.1 Linear Regression

Linear regression is a fundamental machine learning algorithm used for predicting modelling based on the concept of learning under supervision. It assumes a linear relationship between the input features and the target variable. The model learns the coefficients that best fit the data and can make predictions for new inputs. Machine learning regression models generally vary depending on the relationships between different types of independent variables under consideration.

8.2.2 Support Vector Regression

Support Vector Regression (SVR) is considered as a type of support vector machine (SVM) that is used for regression tasks. It attempts to find a function that best predicts the continuous output value for a given input value. SVR can use both linear and non-linear kernels which are functions that determine the similarity between input vectors. Kernel functions can be quadratic, radial basis function (RBF) and sigmoid to handle non-linear relationships in data.

In the classification problem dealt by Awad & Khanna in 2015 [110], the regression problem is a generalization of it in which the model returns a continuous-valued output, as opposed to an output from a finite set. The root of support vector regression is certainly in statistical learning. As far as classification is concerned, support vector regression (SVR) is characterized by use of kernels, sparse solution, and Vapnil-Chervonenkis (VC) control of the margin and the number of support vectors. SVR has been proven to be an effective tool in real-value function estimation. Considering SVR is advantageous as its computational complexity does not depend on the dimensionality

of the input space. SVR has excellent generalization capability with high prediction accuracy.

Considering the data non-linearity the Support Vector Regression (SVR) transforms the problem to a higher dimensional space using kernel transforms as shown in Eq. (8.1) [111] where φ(.) is the kernel function, $x \in R^n$ and $y \in R$ are n dimensional features and predicted results respectively. w and b are the normal direction of the hyperplane and a kind of threshold value for class belongingness. Radial basis function (RBF) is one of the popular kernels commons used for SVR due to its lower parameter tuning complexity compared to polynomial kernel. The regularization parameter 'C' is used to control the trade-off between achieving a low training error and low testing error. In our work the default value of 'C' is taken as 1.0. In SVR epsilon is a hyper parameter that controls the width of the margin of tolerance around the regression line. The default value of epsilon is taken as 0.1. Moreover, the gamma parameter defines how far the single training example reaches.

$$y(x) = \bar{\omega}^T + \varphi(x) + b \tag{8.1}$$

8.2.3 Random Forest Regression

RFR is a supervised ensemble learning algorithm that uses numbers of decision trees which are binary predictors. Ensemble learning being a method or a technique which combines the predictions from multiple machine learning algorithms together to make more accurate predictions than any individual model. Random forest is to be considered as a bagging technique and not a boosting technique. Boosting refers to a group of algorithms that utilize weighted averages to make weak learners into strong learners. In boosting each model that runs, dictates the features on which the next model will focus. Boosting here means that one is learning from another which in turn boosts the learning. Bagging or Bootstrap Aggregation refers to random sampling with replacement. Bootstrap allows us to better understand the bias and variance within the dataset. Bootstrapping involves a random sampling of a small subset of data from the dataset. Bagging is a general procedure that can be used to reduce the variance for

those algorithms that have high variance, typically decision tress. Bagging makes each model run independently and then aggregates the outputs at the end without preference to any model.

The trees in Random Forest run in parallel indicating that random forests run in parallel which essentially indicates that there is no interaction between the trees while building the trees [112]. A random forest is a meta-estimator which means it combines the result of multiple predictions that aggregates many decisions tress with some helpful modifications. These modifications help prevent the trees from being too highly correlated.

- The number of features that can be split at each node is limited to some percentage of the total namely hyper-parameter. This being a limitation also ensures that the ensemble model does not rely too much on any individual feature and therefore makes a fair use of all potentially predictive features.
- Each tree draws a random sample from the original dataset when generating its splits and adding a further element of randomness that prevents overfitting.

  During training stage each of the trees optimize to reduce the error between the target result and predicted result calculated as an error described in Eq.(8.2) where φl denotes the model of each tree with learning dynamics l. A majority voting strategy is adopted for the final decision from the model based on the decision received from different trees. A random forest is a meta-estimator meaning that it combines the result of multiple predictions which aggregates many decision trees with some modifications. RFR is particularly advantageous for its potential to avoid overfitting even with small dataset and lower number of tuneable parameters. In our work 200 estimators (trees) are used for accurate prediction.

$$Err(\varphi l) = \mathrm{E}_{\mathrm{X,Y}}\{L(Y, \varphi l(X))\} \tag{8.2}$$

Random forests regressions have certain disadvantages also. Random forests have been observed to overfit for some datasets with noisy classification / regression tasks. For data including categorical variables with different numbers of levels, random forests are biased in favour of those attributes with more levels. Therefore, the variable importance scores from random forest are not reliable.

8.2.4 Extreme Gradient Boosting (XgBoost) Regression

Extreme gradient boosting known as XgBoost is a popular supervised machine learning method used for regression problems where the intent is to predict continuous numerical values. This type of regressor generally classifies the order of importance of each feature used in the prediction. Benefit of using gradient boosting is that, after the boosted trees are constructed, it is relatively straight forward to retrieve importance of scores for each attribute.

8.2.5 Decision Tree Regression

Decision tree is a classic supervised learning algorithm that uses a tree like graph to represent a flow chart like structure. It has a hierarchical, tree structure, which consist of a root node, branches, internal nodes and leaf nodes. It is commonly used in operation research specifically in decision analysis. Interpretability, less data preparation, versatility and non-linearity are the main advantages of decision tree, whereas overfitting, feature reduction and data resampling are its disadvantages. This type of algorithm generates decision trees with the whole dataset as the root node. It then repeats the instructions on each attribute and uses metrics like entropy or information gain to divide the information into subsets.

Decision trees are sensitive to the specific data on which they are trained. If the training data is changed, the resulting decision tree can be quite different and, in turn the predictions can be distinct. Decision trees are also computationally expensive to train, carry a big risk of overfitting and tend to find local optima because they can't go back after they have made a split.

8.3 Hyperparameter Tuning

Hyperparameter tuning is the process of choosing a set of optimal hyperparameters for any machine learning model. In this present investigation a traditional grid search method is used as the metric to measure the performance of each selected

hyperparameter. Table 8.2 shows the examined settings of various hyperparameters fed into the grid search method for these algorithms under considerations.

Table 8.2. Parameter setting for prediction models

Models	Parameter settings
LR	fit_intercept=True, copy_X=True, n_jobs=None
SVR	C=1.0, epsilon=0.1, kernel='rbf', gamma='scale'
RFR	max_depth = 10, min_samples_leaf = 1, min_samples_split = 2, n_estimators = 200
XGB	max_depth=5, learning_rate=0.1, n_estimators=200, gamma=0, subsample=0.8, colsample_bytree=0.8, reg_alpha=0.1, reg_lambda=1, n_jobs=-1
DT	max_depth=5, min_samples_split=2, min_samples_leaf=1

8.4 Experimental Procedures

Experiments have been carried out on a setup of two cross-roller straightening machine as shown earlier in Figure 6.2 given in Chapter-6. The schematic diagram of two cross-roller straightening machine explains basic function of straightening process in simplified form. Two cross-rolls i.e. one concave roll and one convex roll are powered by electric motors usually associated with a gear box assembly. Round metallic bars are fed from one side through guides in the space between two cross-rolls which are at helix angle about 18º considering the theoretical approach for the effect of helix angle in this process with kinematic reverse bending.

8.4.1 Deflection Measurement using Dial Gauge Method

Round bars of sizes 6-mm, 8-mm, 10-mm and 12-mm diameter of various materials such as mild steel (MS), stainless steel (SS), aluminium (Al) and copper (Cu) have been chosen which were passed through the above type of two cross-rolls straightening machine. Before straightening these bars were studied earlier with deflection measurement method using dial gauge the results and analyses of which is

given earlier in detail in Chapter-5. Deflection measurements of these round bars after straightening process are recorded again after passing through two-roll straightening machine and for which the schematic diagram of experimental arrangement for measurement of straightness is shown earlier in Figure 6.1 given in Chapter-6.

8.5 Proposed Framework

The architecture of proposed framework for prediction modelling using machine learning algorithms has been illustrated in Figure 8.1 which is self-explanatory. The choice of algorithms in proposed research is based on the need of detailed analysis of machine learning techniques for accurate prediction of straightness of round metal bars for different materials under study. These algorithms are carefully examined by addressing the challenges inherent to straightness forecasting. Linear regression serves as a foundational algorithm providing a clear understanding the linear relationships between deformation and length of the bar for its various angular rotation. Random forest being an ensemble method is chosen for its capacity in capturing complex, non-linear relationships in the data and for its ability to handle a multitude of features effectively. Decision Tree regression offers simplicity and interpretability which allows the performance of the models and identifies important features influencing deformation. Lastly gradient boosting regression being another ensemble method allows to focus on increasing predictive accuracy by iteratively improving model performance. This diverse selection of algorithms helps to examine the comparative performance of models in the context of straightness prediction which finally contributes in depth analysis of machine learning algorithms for prediction of straightness of round metal bars.

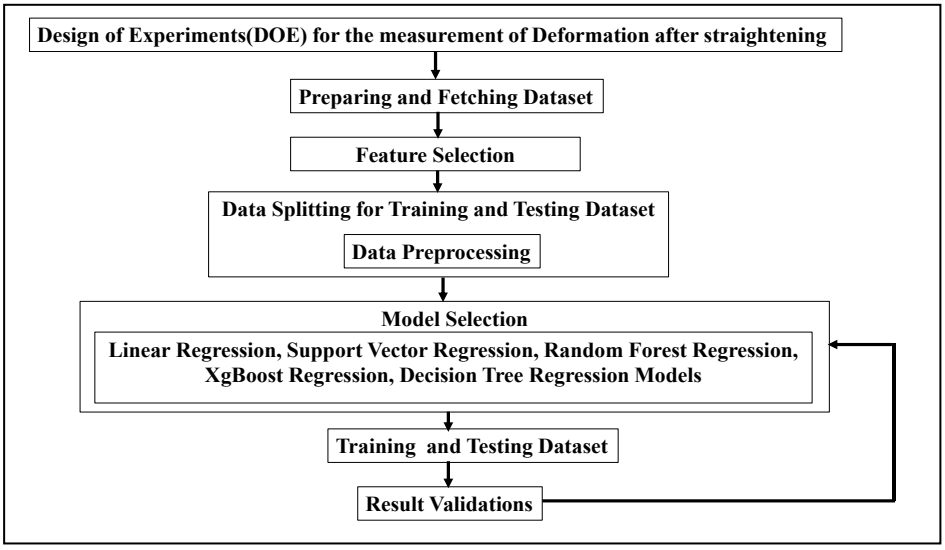

Figure 8.1. Architecture of Proposed Framework

8.6 Evaluation Metrics

Evaluation metrics are quantitative measures that assess the performance of machine learning regression models. They help to compare the performance of different algorithm models. In this work three such metrics, namely coefficient of determination (R^2), mean absolute error (MEA) and root mean squared error (RMSE) as detailed by Sharma, et al. in 2024 [113] have been used towards evaluation of the prediction results. It is hereby important to note three of the majorly utilized parameters for the precision measurement of continuous variables, i.e. MAE, RMSE and R^2 -Score.

a) Mean Absolute Error (MAE)

It is the condition that enables the measurement of an average value of errors in a data set of predictions, while being heedless of directions. MAE is the average distance between predicted value (y) and actual value ($\hat{y}$) as shown in Eq. 8.1 where n is the number of observations or data points. As MAE is error based metric, hence lower values are desired.

$$\text{MAE} = \frac{\Sigma(y-\hat{y})^2}{n} \tag{8.3}$$

(b) Root mean squared error (RMSE)

RMSE is additionally put to use, so that the average value of the errors can be inferred. To obtain this, one takes the average of the square of the numerical variations within the real and the prediction values, and finds the square root of the final output as well. RMSE is generally calculated by taking square root of mean squared error (MSE) as shown in Eq.(8.2) while MSE is the average squared difference between predicted values and actual values that are used to avoid negative or positive values. This metric give higher weightage to the large errors in predictions.

$$\text{RMSE} = \sqrt{\frac{\sum (y - \hat{y})^2}{n}} \tag{8.4}$$

(c) R-Squared (R^2)

The performance of any linear regression model is measured through the coefficient of determination R-Squared (R^2) score. It can be defined as the quantity of differences in the outcome dependent attribute, predicted using the variables indifferent to the value of input. The precision and quality of observations of the results as given out by the model are checked using the criterion. The R^2 value score compares of association between dependent predictable variable (y) and actual variable ($\hat{y}$) as shown in Eq.8.3 where SS_{res} and SS_{tot} are residual sum of squares of residual errors and total sum of squares of errors respectively and $\bar{y}$ is the mean of actual variable. The model will best fit when the predicted value will only be same to actual value resulting R^2 value of 1. Hence, higher R^2 values are desired for a good prediction model.

$$R^2 = 1 - \frac{SS_{res}}{SS_{tot}} = 1 - \frac{\sum(\hat{y} - y)^2}{\sum(\hat{y} - \bar{y})^2} \tag{8.5}$$

8.7 Algorithm used

Algorithms used in this work are Linear Regression (LR), Support Vector Regression (SVR), Random Forest Regression (RFR), Extreme Gradient Boost (XgBoost) and Decision Tree (DT) which have been briefly discussed in article in 8.2.1 through 8.2.5. The workflow used for generating the necessary coding for getting prediction results in terms of prediction plots, residual plots and different types of computational metrices is illustrated in Figure 8.2.

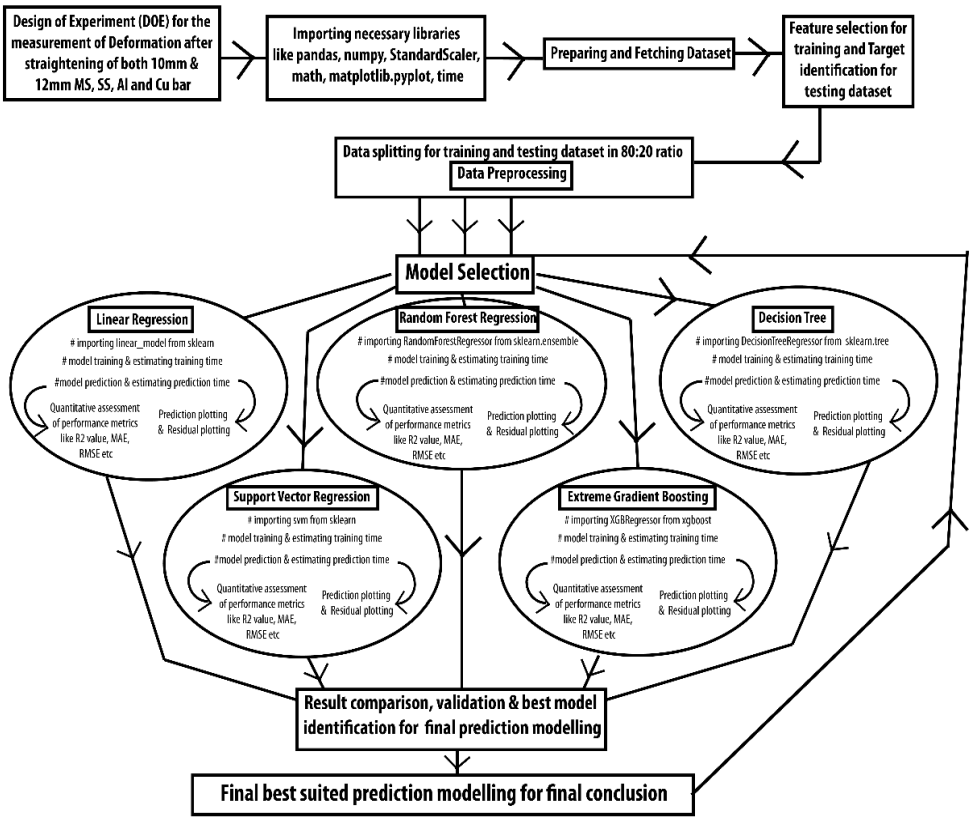

Figure 8.2 Algorithm for the Coding

8.8 System Configurations used

The model analyses and comparison of different learning models have been performed in an environment with a system of following configuration of AMD A8-7410 APU with AMD Radeon R5 Graphics 2.20 GHz, CPU, Windows 10 Pro (64 bit) machine with RAM of 8 GB.

8.9 Details of Coding

Each and every prediction models are executed for prediction plots along with residual plots and for measuring performance metrics with the assistance of python, Jupyter Network and Anaconda prompt environment. The Sklearn, Numpy & Pandas library etc. are utilsed to achieve accurate prediction. The coding generated for getting prediction results is available in detail in GitHub [114] where the coding can be viewed.

8.10 Results and Analysis

The experimental datasets as generated from the observations and measurements using experimental set up have been considered for the purpose of machine learning. These data need to be explored using scatter diagrams, box plots and machine learning algorithms for various predictive and residual regression plots namely Linear Regression, Support Vector Regression, Random Forest Regression, Extreme Gradient Boosting and Decision Tree.

8.10.1 Data Exploration

The dataset used in this work had four columns i.e. material, deformation (mm), length of the rod (cm) and circumferential rotation of bar (degrees). These dataset of deformations obtained after single pass of cross-roll straightening can be observed in the corresponding box plots for all the materials under study as shown from Figures 6.31 to 6.46 for 6-mm, 8-mm, 10-mm and 12-mm diameter round bars respectively. These experimental dataset for MS, SS, Al and Cu round bars of 6-mm, 8-mm, 10-mm and 12-mm diameters respectively after single pass of two cross-roll straightening machine have been extracted from datasets given in GitHub links [103], [104], [105] and [106] and shown in Chapter-6. It is seen that non-linearity in the data set is observed on the box plots where the median line within the box is not centered in most of the cases indicating a skewed distribution, where one side of the box is significantly longer than the others signifying a disproportionate spread of data points towards one extreme of the distribution. Therefore, the degree of non-linearity of the dataset has been studied which provides a valuable resource for studying and monitoring straightness of round metal bars of different materials after cross-roll straightening. The summary statistics reveal extensive information about the experimental dataset describing mean values, standard deviations, and quartile ranges for each parameter illustrated in Table 8.3.

Table 8.3 Dataset Parameters

Mild Steel Bar

	Position in length (in mm)				Angular position (in degree)				Deflection (x 0.01 mm)				Position in length (in mm)				Angular position (in degree)				Deflection (x 0.01 mm)			
Diameter	6mm	8mm	10mm	12mm	6mm	8mm	10mm	12mm	6mm	8mm	10mm	12mm	6mm	8mm	10mm	12mm	6mm	8mm	10mm	12mm	6mm	8mm	10mm	12mm
count	368	624	828	391	368	624	828	391	368	624	828	391	322	851	460	368	322	851	460	368	322	851	460	368
mean	52.77	73.9	65.958	59.765	165	172.5	165	165	180	126.7	142.09	54.032	46.236	74.008	38.47	47.22	165	165	165	165	180.6	156	154.1	108.6
std	23.27	38.36	31.25	30.75	99.63	103.92	99.56	99.63	5.285	11.93	3.898	3.002	18.746	38.736	17.06	22.89	99.65	99.5	99.607	99.63	10.40	9.99	3.685	2.245
min	16.30	12	14.5	22	0	0	0	0	170.6	103.0	134.5	49.5	15	11	12	11	0	0	0	0	152.5	139	146.5	104
25%	33.75	40	39.25	35	75	86.250	75	75	176.0	118.0	139.45	52	30	41	24.5	29.37	75	75	75	75	172	145	151	107
50%	52.50	72.5	65.5	48	165	172.50	165	165	179.2	126	142	54	47.5	73	35.75	46.5	165	165	165	165	182	158	154.25	108.5
75%	71.25	106.3	91.75	82	255	258.75	255	255	183	133	145	55.625	62.5	108.2	52.75	66.25	255	255	255	255	189	164	157	110
max	93.00	141.3	119.5	121	330	345	330	330	197	174	153.5	66	75.3	141.7	68	84	330	330	330	330	199	183	163.5	114

Aluminium Bar

	Position in length (in mm)				Angular position (in degree)				Deflection (x 0.01 mm)				Position in length (in mm)				Angular position (in degree)				Deflection (x 0.01 mm)			
Diameter	6mm	8mm	10mm	12mm	6mm	8mm	10mm	12mm	6mm	8mm	10mm	12mm	6mm	8mm	10mm	12mm	6mm	8mm	10mm	12mm	6mm	8mm	10mm	12mm
count	460	828	828	299	460	828	828	299	460	828	828	299	345	644	598	414	345	644	598	414	345	644	598	414
mean	62.525	77.9	66.5	63.69	165	165	165	165	238.17	164.17	135.53	113.04	50.13	48.17	50.08	53.08	165	165	165	165	246.2	163.3	156.4	136.0
std	28.658	38.3	31.184	33.288	99.607	99.56	99.56	99.67	1.69	4.666	10.667	6.642	21.64	24.103	22.09	26.86	99.64	99.6	99.58	99.62	14.63	5.79	13.48	6.95
min	16.5	12	14	13	0	0	0	0	235	146	102.5	100.5	16	11.5	13	12	0	0	0	0	208	146	131	126.5
25%	38.75	47	40.25	40	75	75	75	75	237	161	129.19	107.5	30	27.25	31	29	75	75	75	75	235.	159	146.5	133
50%	62.50	78.5	66.5	60	165	165	165	165	238	165	136.5	113.5	50	47.5	50.5	52.5	165	165	165	165	243	163	154	135
75%	86.25	109	92.75	90	255	255	255	255	239	168	143	117.5	70	68.25	69	77	255	255	255	255	255	167	164.5	136.5
max	109	143	119	120	330	330	330	330	243	175	157	130	86	90.2	87	96.5	330	330	330	330	308.5	177	196	163.5

Stainless Steel Bar

Copper Bar

8.10.2 Performance of Machine Learning Models

The dataset has been divided in such a way that testing can take place once the model has been trained. In our experiment, 80% of the data was used for training and the remaining 20% data are used to test the utility and effectiveness of the respective model. The training of the dataset has been performed by using five algorithms namely LR, SVR, RFR, XgBoost and DT. The comparative performance analysis of the models has also been carried out. The accuracies of the individual models with different cases have been measured using percentage residual plots and different computational metrices.

The prediction results of 6-mm, 8-mm, 10-mm and 12-mm round bars of MS for the testing set are presented in Figures 8.3 to 8.6. Similarly Figures to 8.7 to 8.10 represent the prediction results of 6-mm, 8-mm, 10-mm and 12-mm round bars of SS for the above four sizes respectively. Whereas Figures 8.11 to 8.14 represents prediction plots of Aluminum Bars and Figures 8.15 to 8.18 represents prediction plots of Copper bars for 6-mm, 8-mm, 10-mm and 12-mm round bars respectively. In these prediction plots index is represented in x-axis and deformation is represented in y-axis. The index in the x-axis identifies the element of the array that is addressed by two variables namely length and angular rotation of bar. In these plots actual and predicted values are shown in blue and red dots respectively. Completely and partially overlapped blue and red dots thus reflect accurate and near accurate predictions while far points reflect inaccurate ones. As it can be seen in all the cases prediction of aluminium and copper bars is better than that of mild steel and stainless steel for most of the sizes. The reason may be due to the comparatively lower value of modulus of elasticity being non-ferrous material aluminium and copper. Among the different regression model the overall performance of RFR is significantly better than others. It can be seen that in some of the points where the prediction values are far away from the actual values with LR, SVR, XgBoost and DT, RFR has performed much closer prediction. The same can be further observed that in the residual plots where the residual values between actual and prediction are plotted against fitted value.

The residual plots for 6-mm, 8-mm, 10-mm and 12-mm round bars of Mild Steel, Stainless Steel, Aluminium and Copper are shown in Figures 8.19 to 8.34 respectively where reference line is shown as 0. This line is helpful to assess the deviation of the predicted values from the actual ones. The residual plots clearly show that the RFR can outperform the other regression models under consideration in most cases. The residual values for RFR are in the close proximity of the reference line. The numbers of outliers are also very less in RFR. Nevertheless, XgBoost had also performed well in terms of residual values within close band of reference line and lower number of outliers. But LR, SVR and DT could not perform reasonably due to the high degree of non-linearity present in the data as revealed in box plot analysis.

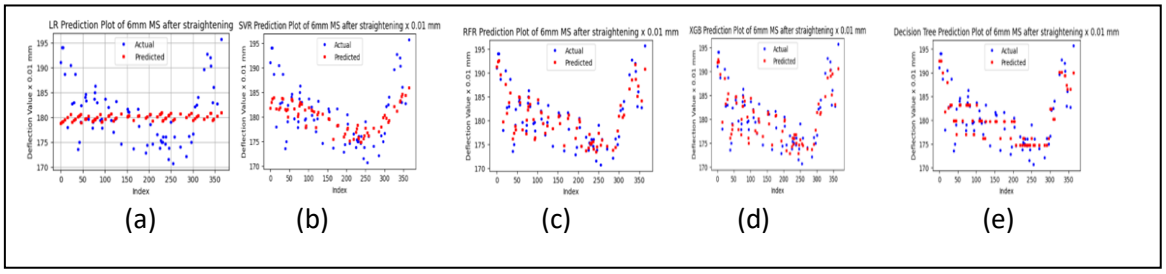

Figure 8.3 Prediction Plots of 6-mm Mild Steel Round Bar after Straightening using (a) LR, (b) SVR, (c) RFR, (d) XGB and (e) DT

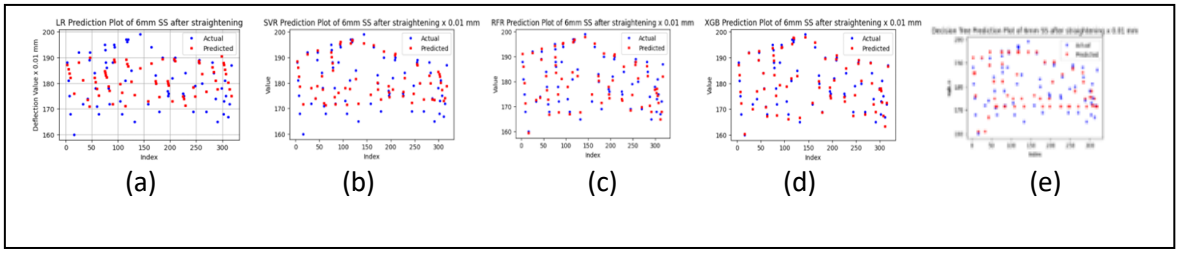

Figure 8.4 Prediction Plots of 6-mm Stainless Steel Round Bar after Straightening using (a) LR, (b) SVR, (c) RFR, (d) XGB and (e) DT

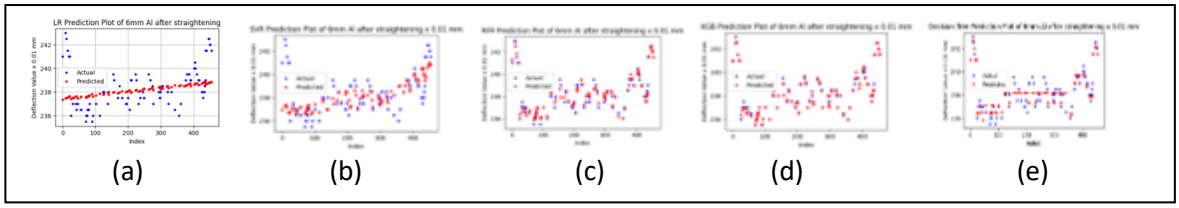

Figure 8.5 Prediction Plots of 6-mm Aluminium Round Bar after Straightening using (a) LR, (b) SVR, (c) RFR, (d) XGB and (e) DT

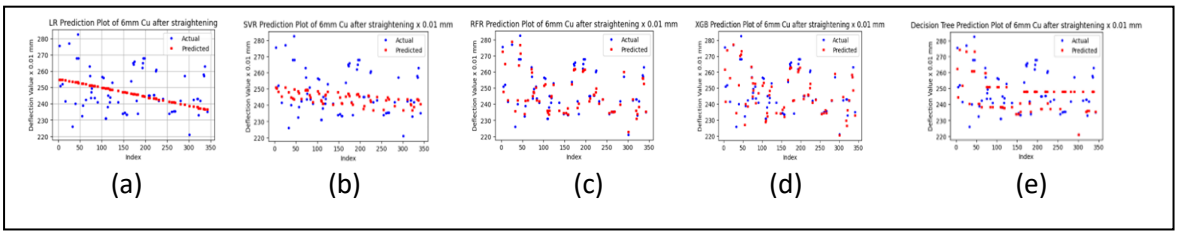

Figure 8.6 Prediction Plots of 6-mm Copper Round Bar after Straightening using (a) LR, (b) SVR, (c) RFR, (d) XGB and (e) DT

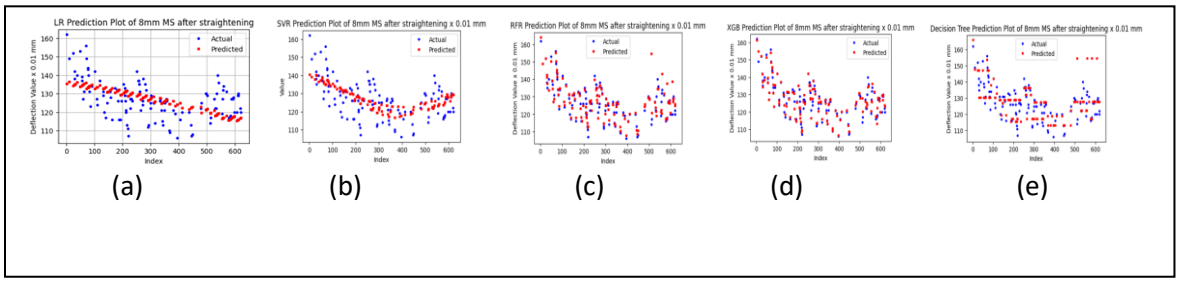

Figure 8.7 Prediction Plots of 8-mm Mild Steel Round Bar after Straightening using (a) LR, (b) SVR, (c) RFR, (d) XGB and (e) DT

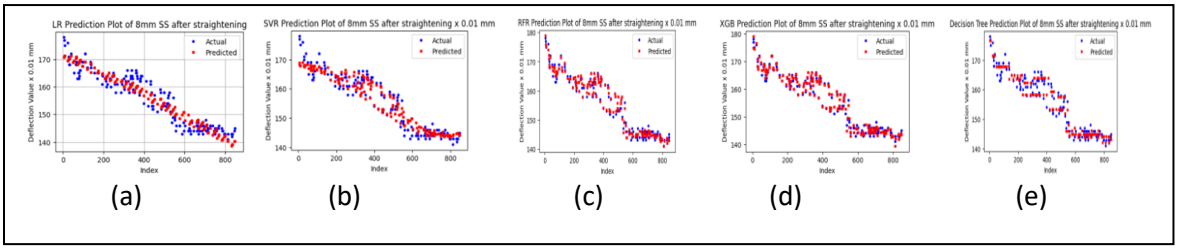

Figure 8.8 Prediction Plots of 8-mm Stainless Steel Round Bar after Straightening using (a) LR, (b) SVR, (c) RFR, (d) XGB and (e) DT

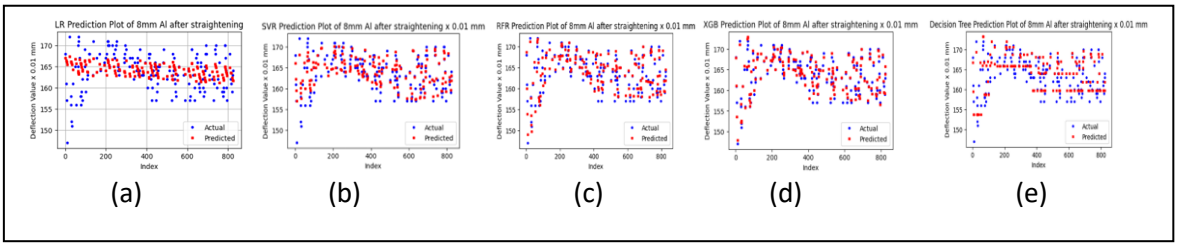

Figure 8.9 Prediction Plots of 8-mm Aluminium Round Bar after Straightening using (a) LR, (b) SVR, (c) RFR, (d) XGB and (e) DT

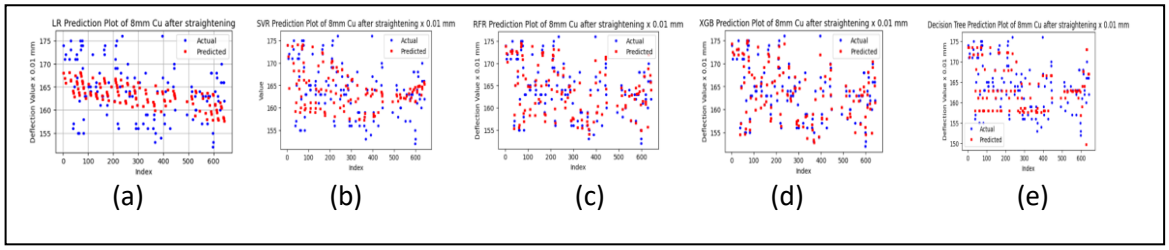

Figure 8.10 Prediction Plots of 8-mm Copper Round Bar after Straightening using (a) LR, (b) SVR, (c) RFR, (d) XGB and (e) DT

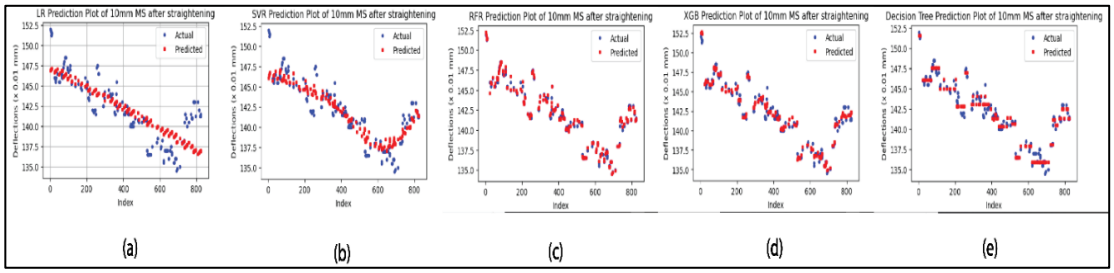

Figure 8.11 Prediction Plots of 10-mm Mild Steel Round Bar after Straightening using (a) LR, (b) SVR, (c) RFR, (d) XGB and (e) DT

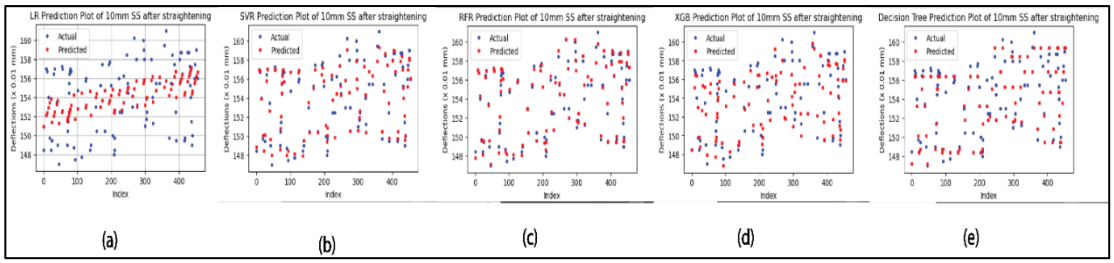

Figure 8.12 Prediction Plots of 10-mm Stainless Steel Round Bar after Straightening using (a) LR, (b) SVR, (c) RFR, (d) XGB and (e) DT

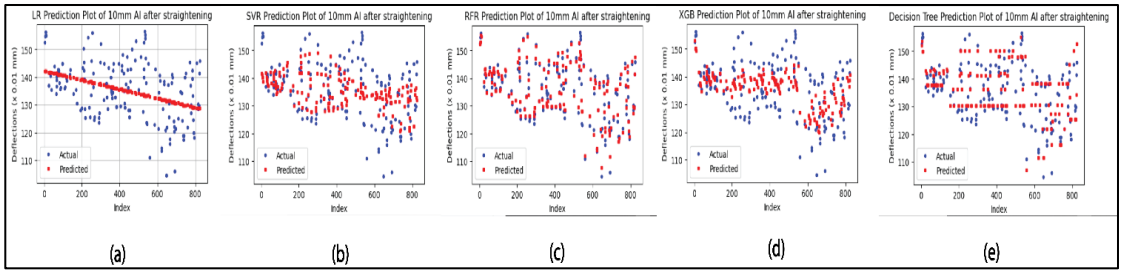

Figure 8.13 Prediction Plots of 10-mm Aluminium Round Bar after Straightening using (a) LR, (b) SVR, (c) RFR, (d) XGB and (e) DT

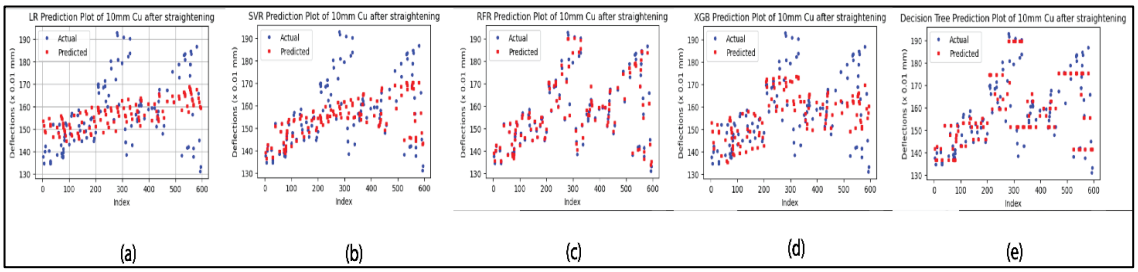

Figure 8.14 Prediction Plots of 10-mm Copper Round Bar after Straightening using (a) LR, (b) SVR, (c) RFR, (d) XGB and (e) DT

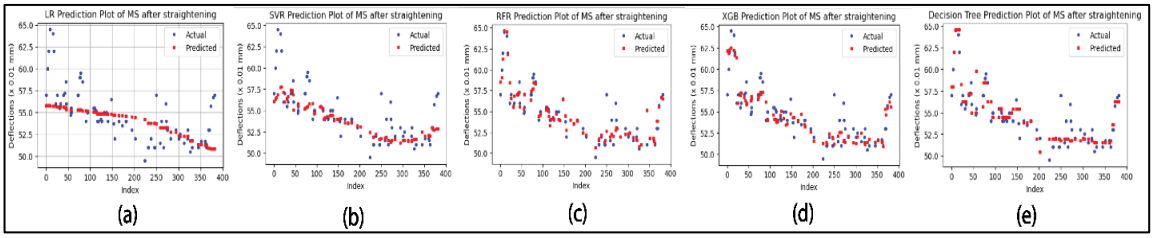

Figure 8.15. Prediction Plots of 12-mm Mild Steel Round Bar after Straightening using (a) LR, (b) SVR, (c) RFR, (d) XGB and (e) DT

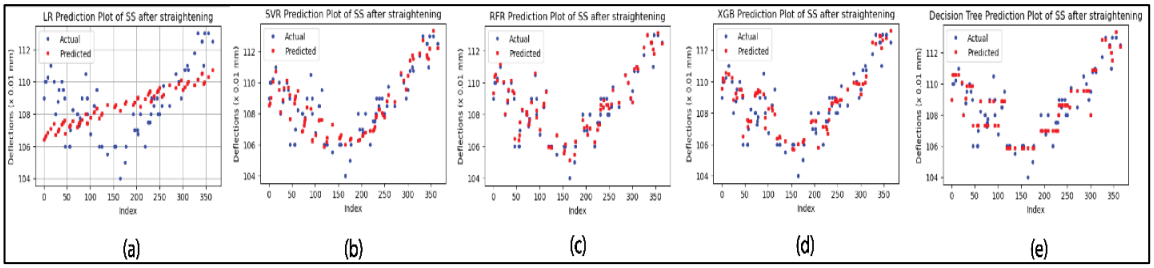

Figure 8.16 Prediction Plots of 12-mm Stainless Steel Round Bar after Straightening using (a) LR, (b) SVR, (c) RFR, (d) XGB and (e) DT

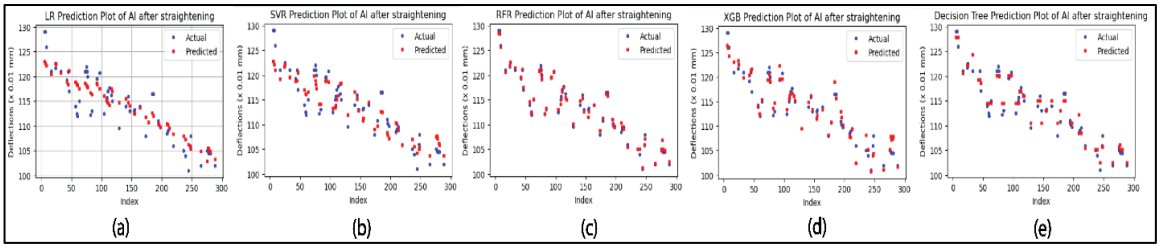

Figure 8.17 Prediction Plots of 12-mm Aluminium Round Bar after Straightening using (a) LR, (b) SVR, (c) RFR, (d) XGB and (e) DT

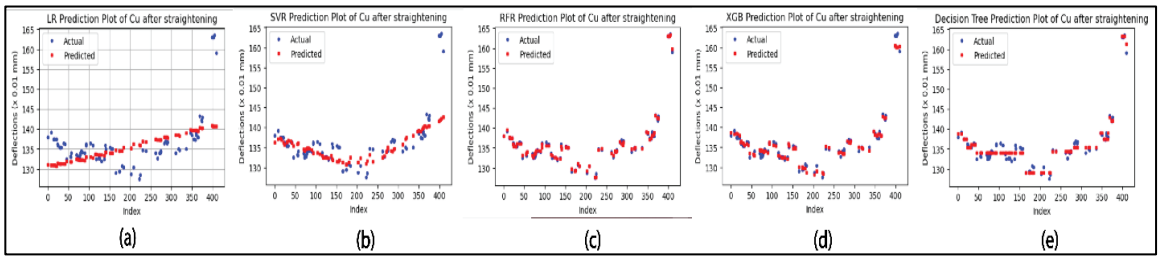

Figure 8.18 Prediction Plots of 12-mm Copper Round Bar after Straightening using (a) LR, (b) SVR, (c) RFR, (d) XGB and (e) DT

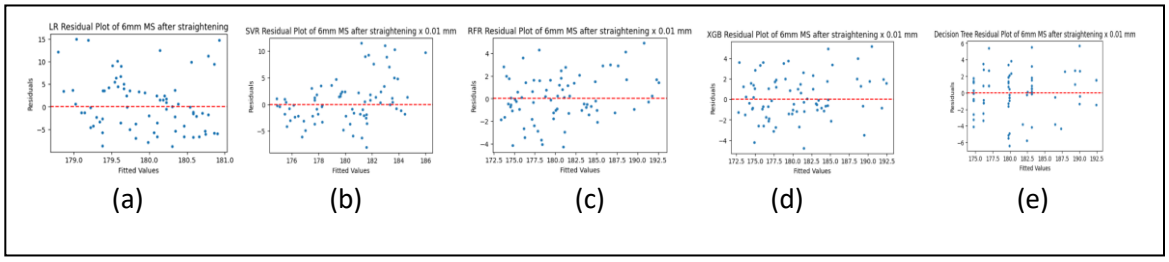

Figure 8.19 Residual Plots for Prediction Results of 6-mm Mild Steel Round Bar after Straightening using (a) LR, (b) SVR, (c) RFR, (d) XGB and (e) DT

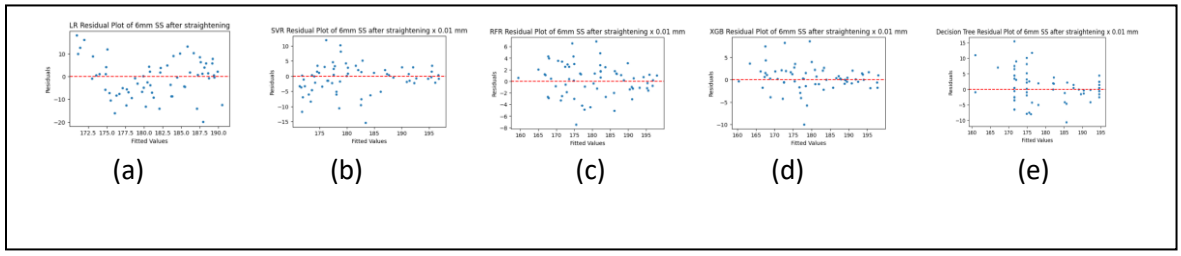

Figure 8.20 Residual Plots for Prediction Results of 6-mm Stainless Steel Round Bar after Straightening using (a) LR, (b) SVR, (c) RFR, (d) XGB and (e) DT

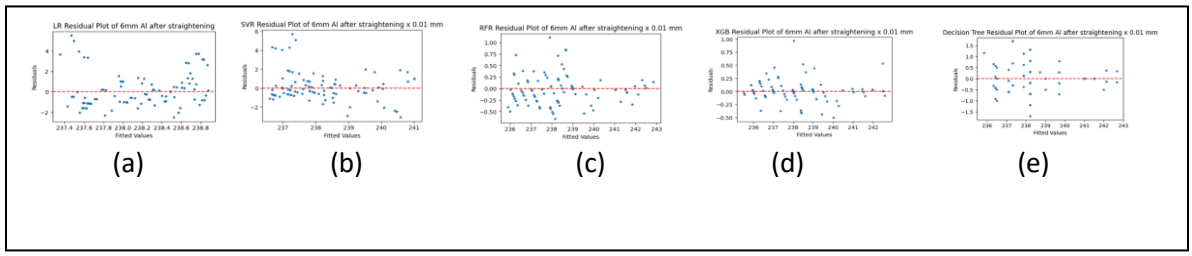

Figure 8.21 Residual Plots for Prediction Results of 6-mm Aluminium Round Bar after Straightening using (a) LR, (b) SVR, (c) RFR, (d) XGB and (e) DT

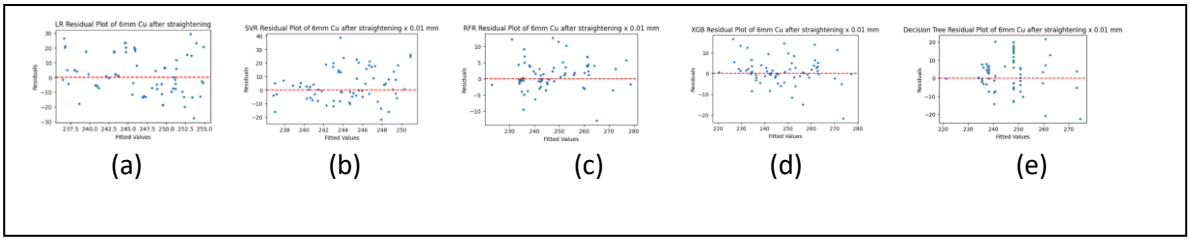

Figure 8.22 Residual Plots for Prediction Results of 6-mm Copper Round Bar after Straightening using (a) LR, (b) SVR, (c) RFR, (d) XGB and (e) DT

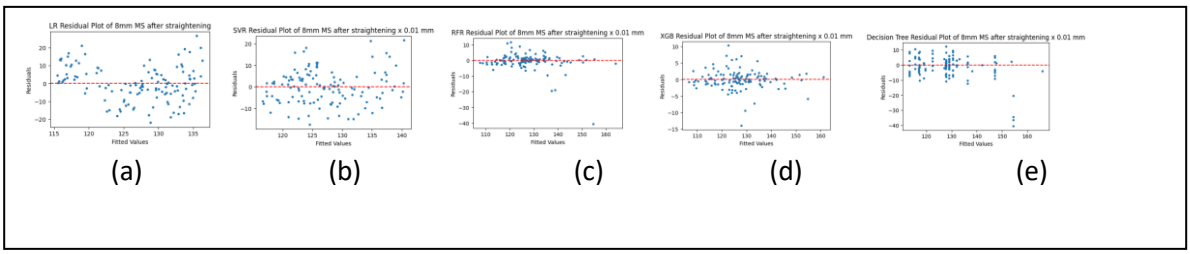

Figure 8.23 Residual Plots for Prediction Results of 8-mm Mild Steel Round Bar after Straightening using (a) LR, (b) SVR, (c) RFR, (d) XGB and (e) DT

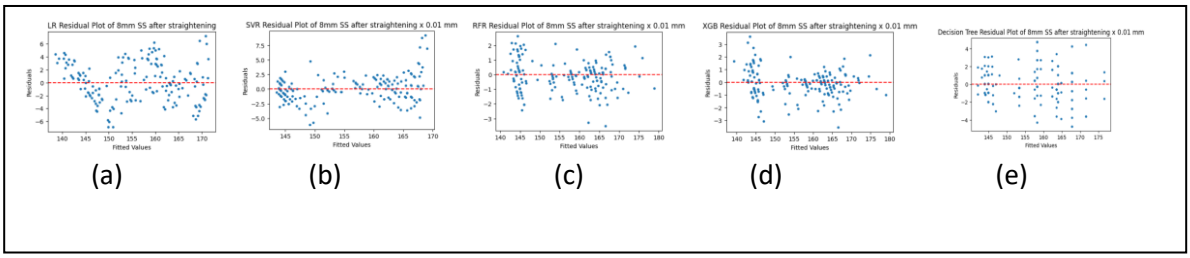

Figure 8.24 Residual Plots for Prediction Results of 8-mm Stainless Steel Round Bar after Straightening using (a) LR, (b) SVR, (c) RFR, (d) XGB and (e) DT

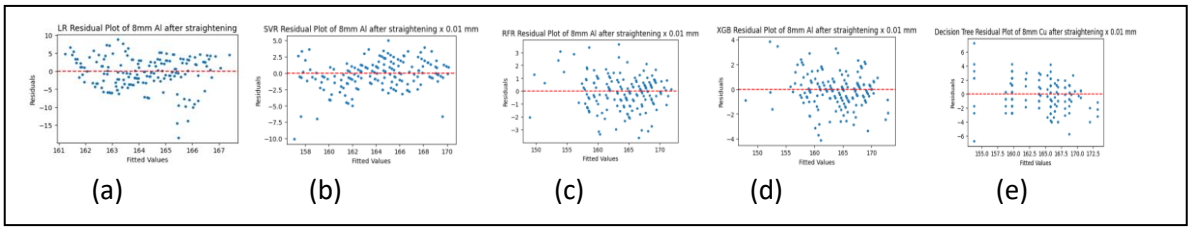

Figure 8.25 Residual Plots for Prediction Results of 8-mm Aluminium Round Bar after Straightening using (a) LR, (b) SVR, (c) RFR, (d) XGB and (e) DT

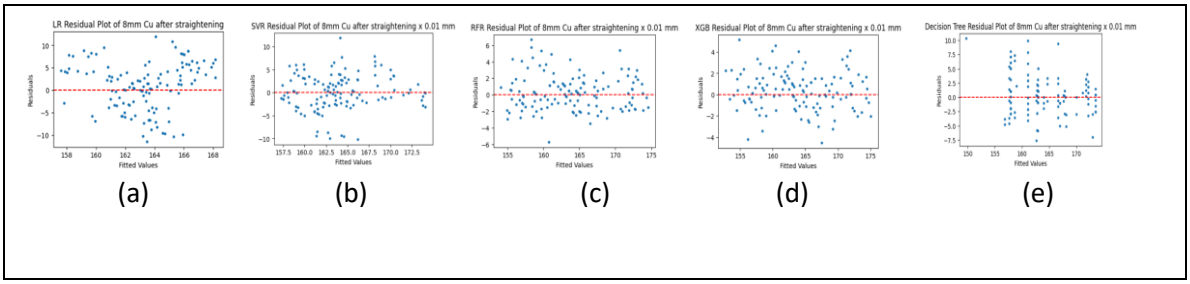

Figure 8.26 Residual Plots for Prediction Results of 8-mm Copper Round Bar after Straightening using (a) LR, (b) SVR, (c) RFR, (d) XGB and (e) DT

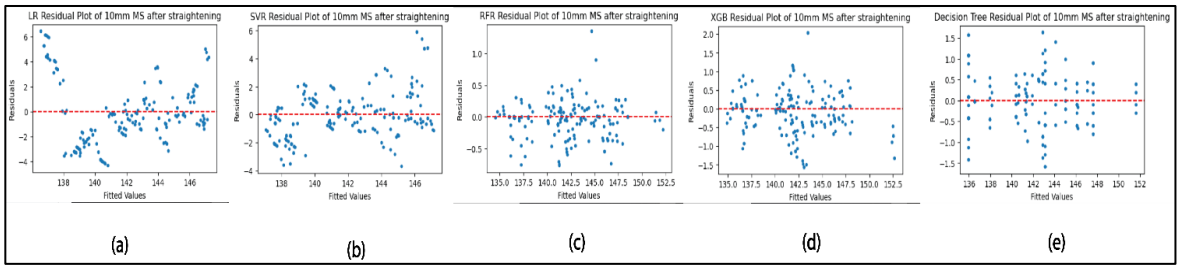

Figure 8.27 Residual Plots for Prediction Results of 10-mm Mild Steel Round Bar after Straightening using (a) LR, (b) SVR, (c) RFR, (d) XGB and (e) DT

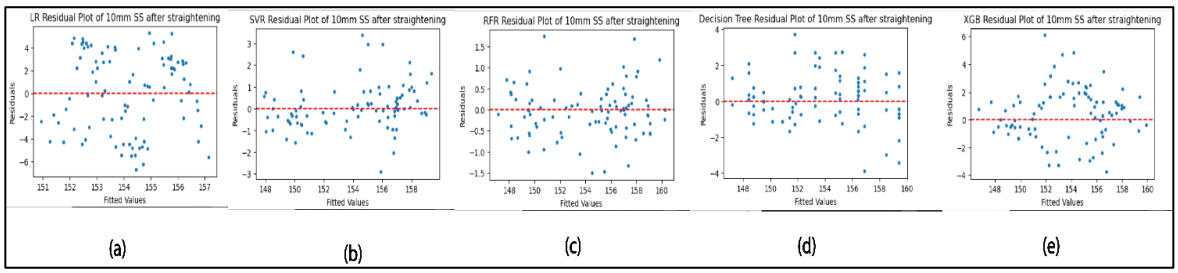

Figure 8.28 Residual Plots for Prediction Results of 10-mm Stainless Steel Round Bar after Straightening using (a) LR, (b) SVR, (c) RFR, (d) XGB and (e) DT

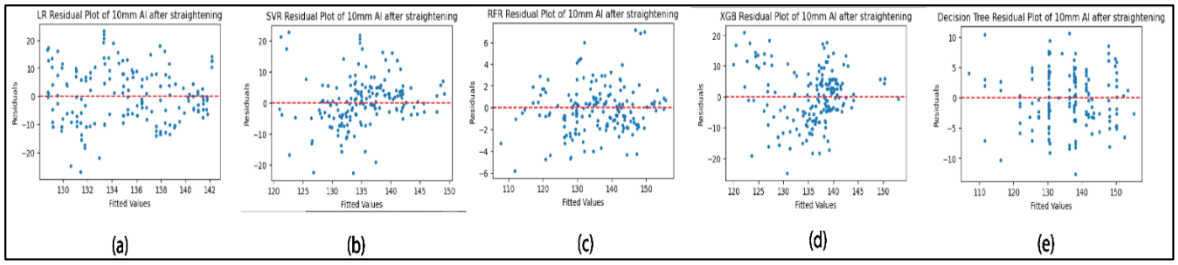

Figure 8.29 Residual Plots for Prediction Results of 10-mm Aluminium Round Bar after Straightening using (a) LR, (b) SVR, (c) RFR, (d) XGB and (e) DT

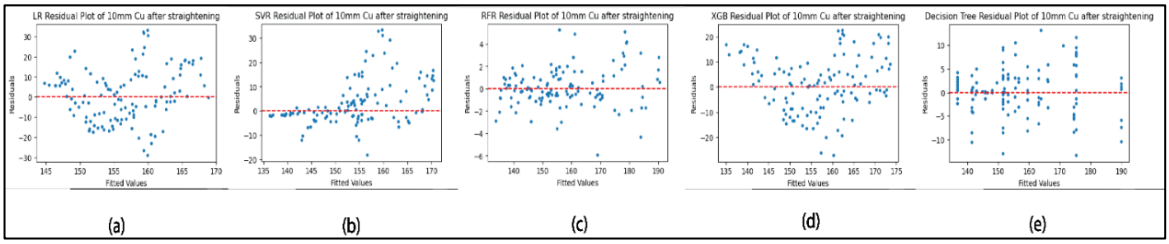

Figure 8.30 Residual Plots for Prediction Results of 10-mm Copper Round Bar after Straightening using (a) LR, (b) SVR, (c) RFR, (d) XGB and (e) DT

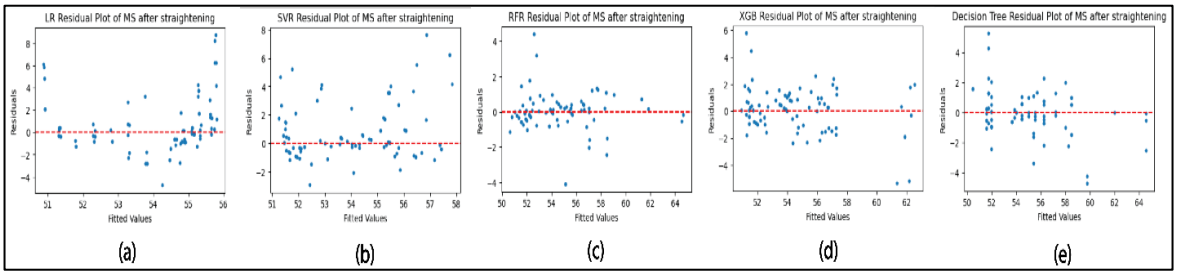

Figure 8.31 Residual Plots for Prediction Results of 12-mm Mild Steel Round Bar after Straightening using (a) LR, (b) SVR, (c) RFR, (d) XGB and (e) DT

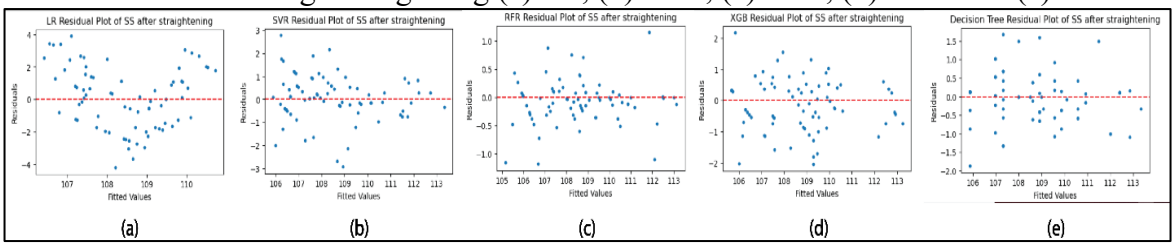

Figure 8.32 Residual Plots of 12-mm Stainless Steel Round Bar after Straightening using (a) LR, (b) SVR, (c) RFR, (d) XGB and (e) DT

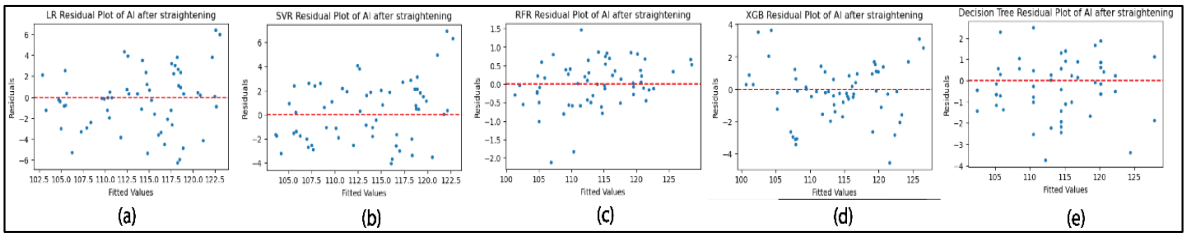

Figure 8.33 Residual Plots of 12-mm Aluminum Round Bar after Straightening using (a) LR, (b) SVR, (c) RFR, (d) XGB and (e) DT

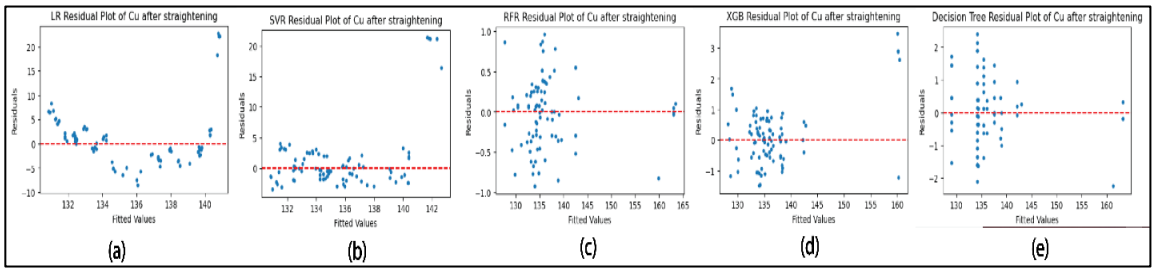

Figure 8.34. Residual Plots of 12-mm Copper Round Bar after Straightening using (a) LR, (b) SVR, (c) RFR, (d) XGB and (e) DT

8.10.3 Evaluation of Computational Metrics

Finally, the results are further assessed using the objective evaluation metrices for regression analysis. Among different such metrices R-squared value (R^2), root mean square error (RMSE), mean absolute error (MAE) and model training time are presented in Table 8.4. As it can be seen that RFR remarkably outperformed other regression models in terms of R^2. In all cases the predictions are in the tune of 0.92 to 0.99 for Aluminium and Copper round bars which convey about 92-99% prediction accuracy for non-ferrous materials using RFR model. The MAE and RMSE of RFR is also visibly less than that of other models under considerations. Another merit of RFR in this study can be listed as the consistency of accurate prediction across all the cases. This vouches the reliability and repeatability potential of RFR based prediction of deformation. It is also seen that apart from RFR, SVR and DT had also resulted considerable amount of accurate prediction with the R^2 values in the range of 0.92 to 0.96 in some cases. Performance of SVR in case of 8-mm and 10-mm SS bars is also satisfactory and performance of DT in case of 8-mm SS bar and 12-mm Copper Bar is also seen quite satisfactory. The performance of XGB is seen satisfactory for 8-mm bars for all materials in the range of 0.92 to 0.98 and for 12-mm Aluminium and Copper bars it exhibits a well performance in the range of value of R^2 from 0.93 to 0.98. The reason for such well performance of all the model can be addressed as lesser non-linearity in the data which is evident from the corresponding box plots where the data points are less scattered. RFR has performed comparatively poor for prediction in case of 6-mm and 8-mm MS and Cu bars. However, a more optimized regression model can

be explored to avoid minor overfitting issue which has caused higher MAE and RMSE in some cases. Nevertheless considering all these results the performance of RFR may be considered as promising and the output of RFR can be integrated to the straightening system as mark up language which can convey the production as well as information of metal round bars between different production processes. It can also interact with management information system (MIS) which can be accessed through internet. Hence management as well as clients can get actual current status of the metal round bars used in machines for production purpose and assigned tasks from any corner of the work using internet. Taking the advantage of platform independent mark up language based development, the presented prediction model can be integrated to the production workflow after getting proper straightness of bars. Moreover, from Table 8.4, it can also be postulated that the slower a model is trained, the higher the accuracy of the prediction.

Table 8.4. Objective Evaluation of Performance by Different Regression Models

		After Straightening																			
		LR			SVR			RFR			XGB			DT							
		6mm	8mm	10 mm	12 mm	6mm	8mm	10 mm	12mm	6mm	8mm	10 mm	12 mm	6mm	8mm	10 mm	12mm	6mm	8mm	10 mm	12mm
Mild Steel	R2	-0.04816	0.15054	0.5753	0.2743	0.48425	0.43271	0.14209	0.50377	0.88356	0.73541	0.99445	0.88188	0.87160	0.92398	0.9775	0.70152	0.80353	0.44098	0.97424	0.76118
	MAE	4.85137	7.59311	2.01635	1.77382	3.13988	6.16830	0.0609	1.43077	1.60610	2.73966	0.20093	0.65905	1.71700	1.87012	0.44945	1.23433	2.02922	4.88020	0.48906	1.02329
	RMSE	6.05342	9.62454	2.55759	2.61532	4.24627	7.86524	0.82078	2.16266	2.01762	5.37145	0.29239	1.05512	2.11873	2.87914	0.58869	1.67728	2.62084	7.80769	0.62984	1.50032
	Model training time (sec)	0.00332	0.00221	0.09984	0.03128	0.01500	0.02555	1.26899	0.0366	0.45258	0.51720	0.97994	0.80834	0.09265	0.09820	0.2247	0.16398	0.00265	0.00361	0.00374	0.003
	Prediction time (sec)	0.00087	0.00048	0.01564	0	0.00486	0.01710	1.66143	0.00863	0.02830	0.02843	0.04688	0.03125	0.00389	0.00280	0	0.00248	0.00089	0.00164	0.01155	0.001
Stainless Steel	R2	0.27369	0.90335	0.16932	0.13053	0.74713	0.94461	0.92111	0.75247	0.91754	0.98793	0.97468	0.96191	0.91049	0.98703	0.73493	0.81953	0.73150	0.96222	0.86549	0.88687
	MAE	6.60720	2.48939	3.00411	1.59811	3.52392	1.66148	0.74509	0.74915	2.19634	0.81575	0.4439	0.27436	1.94506	0.80713	1.53784	0.71227	3.68402	1.43430	1.04768	0.51288
	RMSE	8.20536	3.00560	3.40881	1.90592	4.84153	2.27767	1.05049	1.01692	2.76469	1.06318	0.59517	0.39891	2.88052	1.10209	1.92558	0.86832	4.98896	1.88110	1.37173	0.68749
	Model training time (sec)	0.02458	0.00320	0.10503	0.01561	0.00828	0.04537	0.02479	0.01766	0.40992	0.50433	1.02751	0.88952	0.10725	0.11147	0.15759	0.10686	0.00335	0.00409	0.00801	0.003
	Prediction time (sec)	0.00131	0.00084	0	0	0.00309	0.02309	0.01682	0.00599	0.02914	0.03048	0.04729	0.03124	0.00268	0.00293	0.01562	0.0152	0.00082	0.00091	0	0.00109
Aluminium	R2	0.10755	0.03817	0.14145	0.81398	0.23134	0.75153	0.43399	0.85975	0.96716	0.91834	0.95537	0.99087	0.98560	0.91073	0.28152	0.9355	0.85384	0.78088	0.81962	0.95933
	MAE	1.28590	3.43354	7.83663	2.24946	1.07239	1.67978	5.69465	2.11188	0.24928	0.98873	1.62555	0.48635	0.13669	0.99219	7.12994	1.28971	0.53720	1.67667	3.57689	1.08228
	RMSE	1.70607	4.42881	9.61727	2.89067	1.58334	2.25100	7.80872	2.50995	0.32729	1.29049	2.19268	0.64181	0.21673	1.34922	8.79785	1.70218	0.69044	2.11388	4.40826	1.35167
	Model training time (sec)	0.00174	0.00292	0.004	0.00843	0.01806	0.03630	0.103	0.02458	0.39351	0.46679	1.03301	0.9447	0.12597	0.11392	0.44299	0.16666	0.00250	0.00371	0.00399	0.00852
	Prediction time (sec)	0.00075	0.00054	0.001	0	0.00677	0.01766	0.161	0	0.02794	0.03105	0.045	0.04688	0.00496	0.00302	0.003	0.00878	0.00123	0.00116	0.002	0
Copper	R2	-0.03271	0.29694	0.25959	0.2271	0.10440	0.56959	0.57077	0.44952	0.87808	0.86702	0.98639	0.99647	0.76270	0.90463	0.46473	0.98273	0.44357	0.63284	0.89309	0.97972
	MAE	10.98440	4.27669	10.64231	4.03222	9.57361	2.96553	6.72502	2.75156	3.30167	1.6772	1.30655	0.33472	4.30133	1.41620	9.12212	0.68582	7.75601	2.72821	3.76329	0.79557
	RMSE	13.39550	5.24762	13.13102	6.32536	12.47462	3.86590	9.99788	5.33816	4.60272	2.14880	1.77997	0.42754	6.42122	1.81974	11.16475	0.94546	9.83273	3.57053	4.98964	1.02472
	Model training time (sec)	0.00260	0.00187	0.02	0.01563	0.01023	0.02537	0.03901	0.01963	0.45573	0.48557	1.167	0.81548	0.10870	0.12228	0.17599	0.1836	0.00317	0.00303	0.004	0.00301
	Prediction time (sec)	0.00050	0.00054	0.001	0	0.00312	0.01008	0.02297	0.00944	0.02922	0.02878	0.04201	0.03126	0.00293	0.00283	0.005	0	0.00133	0.00082	0.002	0.002

8.11 Discussion

In this study, experiments have been conducted by developing design of experiments for the measurement of deformations of metal round bars. The experimental results demonstrated that there is a correlation between deformation of the bar along with circumference and length of the bar. The analysis of the regression model shows that straightness has been improved quite significantly after straightening. Reasonable improvement of straightness has been observed in case of non-ferrous materials that is aluminium and copper. The reason could be low modulus of the elasticity of the materials which probably causes less deformation after straightening.

The main contribution of this chapter is to conduct a comparative analysis to explore which machine learning algorithms predicted straightness of round metal bars the best. The experimental results for straightness prediction models have been evaluated through LR, SVR, RFR, XgBoost and DT regression models. By applying ML algorithms on experimental dataset, the results indicate that for all sizes that is of 6-mm, 8-mm, 10-mm and 12-mm round bars, RFR may be considered as overall best regression model in terms of sensitivity and accuracy and this has been achieved by comparing the actual deformation and the predictive deformations. Finally, it can be concluded that the overall performance of RFR for prediction of straightness in terms of circumferential deformations of metal bars may be considered as promising and potential tool.

The present work can be extended towards the hardware implementation of automated sensing and monitoring the deflection readings through data acquisition system. Moreover, this study can as well be extended by selecting the best performed model and optimizing the hyper parameter tuning to achieve 100% accuracy for straightness prediction using large-scale high-performance cloud system. Considering the findings and scope of the future work the proposed machine learning based approach may be considered as an important dimension to the emerging field of effect of straightening process on bars of different materials.

CHAPTER – 9

DISCUSSIONS AND CONCLUDING REMARKS

9.1 Overall Discussions

It is obvious from the above that the determination of quantitative parameters of straightness in metal round bars has been one of the main objectives of the present study. Measurement of deflections associated with the dial gauge experiments as pointed early remains to be one of the outstanding problems for a long time in straightness. It is also known that the deflection, which corresponds to deformation behaviour of metal round bars, changes very rapidly with small spatial extent in the length of the bar such that introduction of any contact type gauge or probe would alter the deformation behaviour drastically. This motivates towards analysis of deformation behaviour by using finite element analysis and machine learning algorithms.

There has been a comprehensive review of previous investigations which has been covered reasonably in detail in Chapter-2 about bar straightening research works done so far and it is evident that there exists enough scope to improve upon the experimental technique using dial gauge as well as to extent the method to analyse both by numerically and predictive modelling using machine learning.

In order to determine the straightness variables quantitatively firstly, we have used the dial gauge method in our laboratory and improved upon the same which is evident from the works presented here. Secondly, different types of analysing technique have been developed to obtain the deformation behaviour of the round bars from the recorded experimental dataset.

The theoretical aspects is dealt in Chapter-3 where important parametric equations found a place that enable to look into the process in a scientific manner. Here in this chapter seven assumptions have been made for deformation analysis of round metal

bars before and after straightening which is necessary for developing theoretical as well as experimental treatments. Some discussions have been given below if any of the assumptions is wrong or not fully satisfying.

If the first assumption is considered wrong or not fully satisfying which means that work hardening is not present in the straightened bar. In that case the deformation results will be affected due to reduced yield strength and increased deformation. The bar will exhibit increased curvature which may lead larger deformations. The material may exhibit the Bauschinger effect showing lower yield strength in reverse direction than in the original direction. The implication could be lower load-carrying capacity and increased failure risk.

If second assumption is wrong or not fully satisfying which means that cross-sectional area of round bar is not circular in pure bending and neutral axis does not pass through the centre then there will be non-uniform distribution of stresses across the sections leading to unexpected deformation patterns. Non-circular cross cross-sections may show distortion under bending load leading to additional stresses and deformations. If the neutral axis does not pass through the centre then there is a possibility of coupling between bending and axial deformation leading to additional stresses and strains which may show complex deformation behaviour thus implying design complexity. The effects of non-circular cross-sections and non-central neutral axis during reverse bending may show significant results. In such cases, careful consideration will be necessary to ensure the structural integrity of the round bars under loading.

If third assumption is wrong or not fully satisfying which means outside shape is not round then deformation results during straightening will vary in several ways. Non-uniform deformations will result into variations in curvature along the bar length leading to difficulty in achieving uniform straightening. Beside this the stress distribution across the cross-section will be non-uniform leading to unexpected deformation pattern. It may also show anisotropic deformation which means there may be direction dependent deformation and different stiffness at different directions.

If fourth assumption is wrong or not fully satisfying which means if cross-section of the bar does not remain on a plane and not at right angles to the axis thus it makes a

case of non-planar cross-section, then during the bar straightening process deformation results will vary on account of warping and distortion. Further, non-planar cross-section can lead to increased residual stresses which can affect behaviour of bar under subsequent loading. Bending loads on non-perpendicular cross-section can cause torsional deformation leading to additional stresses and strains, increased deformation under straightening loads thus potentially may affect bar's straightness and dimensional accuracy.

For fifth assumption, if the strain variation in a bar section at any point is not proportional to the distance from the perpendicular point on the neutral axis, it implies that the beam is not behaving according to the Euler-Bernoulli beam theory. Since it will cause non-proportional strain variation, it will lead to non-linear strain distribution and complex stress distribution.

If sixth assumption is wrong or not fully satisfying which means that the material is not perfectly elastic-plastic then there is a possibility of non-linear stress-strain curve thus material may show non-linear elastic behaviour. Strain curve will not be a straight line. The material may show variable stiffness which will depend on strain level affecting deformation results under bending and reverse bending. The implication is that there will be a possibility of complex deformation behaviour which can lead complex deformation patterns.

If seventh or last assumption is wrong or not fully satisfying which means if stress components are not zero in directions other than longitudinal direction during bar straightening process, the deformation results will vary in several ways leading to multi-axial stress state. This may cause complex stress distribution and interaction between stresses in different directions thus can affect deformation behavior of round bar.

The probabilistic approach in straightening process in Chapter-4 dealt with the probability of final residual curvatures in a domain provided probability density function is available. The mean value and variance thereof for curvature can be evaluated. Statistical aspect of commercially available round bars has been looked into

which have been detailed considering Analysis of Variance (ANOVA) for various helix angles and roller diameters.

As far as practicability in industry is concerned straight round bars are a general requirement in many mechanical industries. When the input raw material is round bar for production of items that needs straight bars, bar straightening plays a significant role. Since round bars are produced in large quantities in rolling industries it is less likely that every round bar will be straight. A large number of round bars require straightening. This is the reason perhaps why several types of straightening machines are available in market. To meet the large demands of straight round bars in major industries, several industries have grown to supply straightened bars using straightening machines.

9.2 Discussion of Experimental Results

The present investigation could be used to determine both qualitative and quantitative information of deformation behaviour of round bars of various sizes and types of materials. The experimental set up has been helpful in getting substantial data before the straightening process which revealed the actual scenario of commercially available bars. Large number of dataset generated out of circumferential measurements of deformation study along the length of the bar for different sizes and types of bars gives an overall scenario of deformation history of round bars. Another outcome of roundness study of bars shows not only dimensional variations but also straightness in length segments along the bar length which is visible from Radar Charts. The results of analysis of data when plotted shows in statistical process control charts shows that diametrical variation of round bars is as such within process control limits hence commercial products are acceptable in industries.

The existing experimental setup used for study of the same round bars after straightening operation. Dataset made out of observation after straightening reveals that straightness actually improves after the process but more significantly in case of non-ferrous materials. This outcome is quite significant in bar straightening study. The possibility of such event could be due to low modulus of elasticity in comparison to

mild steel and stainless steel. From the analysis of scatter plots and box plots, the experimental results show that there is randomness in the deformation data which are non-linear in nature. Surface plots generated out of dataset after straightening which further reveals that straightness improves after round bars pass through cross-roll straightening machines. Straightening of bar being a cold working process has some impact on mechanical properties of the bar materials due to reverse bending which goes beyond yield point where curvatures will undergo change and curvature reduction takes place. The deformation behaviours obtained by using this method (given in chapter-5 & 6) agree quite well with the values obtained numerically (given in chapter- 7 & 8).

9.3 Discussion on Analytical and Numerical Results

From finite element analysis it has been found that commercially available round bars have a considerable amount of deformations at various sections over the length segments. The deformations observed in the diagrams may be a kind of defects in the product which could have possibly occurred during production stage or material handling. Due to deformations, bars are not quite straight at various length segments and curvatures exist. The users will have to take a decision on possible acceptance of these defects i.e. curvatures or take a remedial measure accordingly. It is possible to work on these defects so as to either eliminate or reduce the level of curvatures by taking appropriate remedial measures.

Finite element analysis show that after straightening process through two cross-roll machines, straightness of commercial round bars have fairly improved. The improvement is more significant in case of aluminium and copper round bars thus indicating that straightening is more effective in non-ferrous materials than ferrous materials. Comparison of dataset of deformations for both before and after straightening reveals that with finite element analyses that straightness at various length segments have improved significantly after straightening process. The overall straightness improves in all cases of round bars after two cross-roll straightening process. From quality view point, straightening process would certainly accommodate

a greater number of round bars which would have been otherwise rejected. Bar straightening process is therefore can be considered as economic for the industries.

Observations and measurements through dial gauges generated experimental datasets using experimental set up which have been considered for the purpose of machine learning. These dataset required exploration using box plots and machine learning algorithms for various predictive and residual regression plots. Various algorithms such Linear Regression (LR), Support Vector Regression (SVR), Random Forest Regression (RFR), Extreme Gradient Boosting (XgBoost) and Decision Tree (DT) have been considered for predictive and residual plots of 6-mm, 8-mm, 10-mm and 12-mm diameter round bars. Models executed for prediction and residual plots, and for measuring performance metrics in Python, Jupyter Network and Anaconda prompt environment using Sklearn, Numpy & Pandas libraries resulted with fair accuracy. The results are assessed using objective evaluation metrics for regression analysis. Among different such metrices R-squared value (R^2), root mean square error (RMSE), mean absolute error (MAE) and model training time. It can be seen that RFR remarkably outperformed other regression models in terms of R^2. Predictions are in the tune of 0.92 to 0.99 for Aluminium and Copper round bars in all cases thus conveying about 95-99% accuracy for non-ferrous materials using RFR model whereas for mild steel and stainless steel the accuracy is about 90%. Therefore, the predictive modelling using machine learning models are more effective for non-ferrous materials than ferrous materials.

9.4 Conclusions

A number of conclusions are offered with respect to the present experimental investigation along with the numerical techniques proposed.

(a) The experimental method by using dial gauge is very simple to implement on the metal rods and also to study deformation pattern.

(b) The overall cost of the gadgets, which may be easily constructed with locally available materials, are small in comparison with the conventional optical systems for measuring deflections. Further, the primary cost and overall time

involved to record the deformation pattern are practically insignificant compared to the conventional techniques.

(c) Probabilistic and statistical analysis in the process of bar straightening has been conducted to develop equation for probability of final residual curvatures along the bar length.

(d) Criterion for helix angle of two cross-roll straightening process has been determined as a key parameter.

(e) Deformation analysis of commercial round bars of different materials has been conducted before and after straightening process after measuring the deformations experimentally. Circularity or roundness of straight round bars are studied by using statistical process control analysis before and after straightening based on the experimental observations.

(f) The concept of statistical consideration has been applied to bar straightening process for estimation of final curvature of length segment of a given bar. Application of ANOVA as a part of using statistical process in bar straightening has been implemented based on influencing significant factors of helix angle, roller diameter, bar diameter and modulus of elasticity in a two cross-roll straightening machine.

(g) The statistical approach for checking the quality of bars in terms of straightness and roundness may be useful for manufacturing industries.

(h) FEM can be successfully used for deformation study in round bars to check the validity of statistical results which confirms the utility of commercial bars for further production purposes.

(i) Methodology proposed seems to be a potential tool to study straightness of round bars.

(j) Quantitative analysis of the deformation pattern using both dial gauge method and prediction modelling by machine learning may add significant new capability to the existing straightness measurement techniques and/or to open up entirely new application areas that have not previously been feasible or cost effective.

(k) In spite of limitations of the dial gauge method the proposed technique for

predictive modelling using machine learning algorithm seems to be helpful to estimate quantitative parameters of straightness, at least as a first approximation. The prediction techniques may also be used as a supplementary tool in design in conjunction with the conventional dial gauge experiments and/or with computational method of solution which is gaining more and more acceptance among researchers these days.

(l) By applying machine learning algorithms on experimental dataset, the results indicate Random Forest Regression is the superior regression model in term of sensitivity and accuracy, and this has been achieved by comparing the actual deformation and the predictive deformation. The analysis of the regression model shows that straightness improved quite significantly after straightening.

(m) Reasonable improvement of straightness has been observed in case of non-ferrous materials that is aluminium and copper due to its low modulus of elasticity.

(n) Finally, it can be concluded that the potentiality of the present method to investigate straightness of round metal bars is perhaps beyond question.

Further, in view of simplicity of the proposed methodology as an instructional and research tool potentiality of the method appears to have greatly been enhanced by the development of prediction modelling technique discussed here.

9.5 Novelty and New Contributions

A number of contributions are made by this which may reflect novelty of this research work.

Firstly, the criterion of setting helix angle in two cross-roll straightening machine has been determined and this can now be used scientifically by manufacturing industries.

Secondly, detailing of statistical aspect with ANOVA correlating helix angle, roller diameter, bar diameter and modulus of elasticity is an important outcome of this research work to get improved straightness.

Thirdly, deformation analysis of round metal bars of different materials has been

studied after cross-roll straightening, the results of which show quite improvement as compared to that of results of before straightening.

While using FEM analysis, two key contributions are made which could be considered as novelty of this research work. To begin, deformation analyses of round metal bars of different materials after cross-roll straightening using ANSYS software indicate quite improvement as compared to that of results before straightening. In addition, round metal bars of non-ferrous materials after cross-roll straightening show more significant achievement than that of the ferrous materials.

Moreover, another significant key contribution made which may also be considered as novelty in this research is the use of Machine Learning. The comparative analysis is conducted to explore which machine learning algorithms predicted straightness the best. By applying LR, SVR, RFR, XgBoost and DT algorithms on experimental dataset, the results indicate that for round bars of all sizes, RFR is the best regression model. For aluminium and copper bars the prediction accuracy for RFR model has been found about 90-99%, whereas for mild steel and stainless steel the accuracy is about 90%. Therefore, it can be said that effect of cross-roll straightening process is more significant for non-ferrous materials than ferrous materials. Finally, it can be stated that the overall performance of RFR for prediction of straightness in terms of circumferential deformations of metal bars may be considered as promising and potential tool.

9.6 Limitations

The entire research work was carried out through measurements using dial gauge which is simple in process but quite time consuming for large amount of data. Long bars could not be used due to possible natural sagging that could add to errors in actual measurement of the round bars. Absence of digital electronic measurement system and automation with data acquisition facility limited the research work for very large dataset and fast data acquisition. It is also to be noted here that the present investigation is limited to static condition on metal round bars. However, the periodic measurement

of deformations of actually deployed straight round bars or working shafts as a machine component which is usually dynamic in nature has not been considered.

9.7 Scope of Future Investigations

Experimental validation for criterion of helix angle remains as a future scope along with ANOVA of roller diameter and helix angle. Probability distribution function can be worked out with the help of very large dataset which may help in estimating probability of final curvature in a domain of interest.

The present study can be extended in the emerging field of cross-roll straightening process by analysing the radius of curvatures and corresponding residual stresses of the bars with the help of both experimental and analytical method. Also, the proposed measurement methodology along with the prediction modelling technique can be used for periodic prediction of straightness when round bars or shafts as machine components are dynamic in nature.

Moreover, this study of predictive modelling using machine learning can as well be extended by increasing the numbers of features and optimizing the hyperparameter tuning to achieve 100% accuracy for straightness prediction using large-scale high-performance cloud system. Thus, considering the findings and scope of the future work, the proposed machine learning based approach of deformation analysis may be considered as an important dimension to the emerging field of effect of straightening process on bars of different materials.

REFERENCES

[1] Schleinzer,G., Fischer, F.D., "Residual stresses in new rails", Materials Science and Engineering A288,pp.280–283, 2000. https://doi.org/10.1016/S0921-5093(00)00872-8

[2] Brazier, L. G. "On the flexure of thin cylindrical shells and other 'Thin' sections.", Proc. R. Soc. London A 116:104-114, 1927. https://doi.org/10.1098/rspa.1927.0125

[3] Chakravarty, J., "Theory of Plasticity, Theory of Plasticity", 3/e, ISBN:978-93-80931-71-5, Butterworth-Heinemann, 2008.

[4] Roy, S., Pal, A.K.,"A novel approach for study of straightness in commercially produced round metal bars based on deflection measurements", Applications in Engineering Science, 16 (2023) 100161, https://doi.org/10.1016/j.apples.2023.100161

[5] Kemshall, G.E., Bar Straightening and Bending Equipment, Light Bar and Section Mill Technology, Steel Times, London, vol.202, Iss.3:243-244,246-249,(March 1974). https://www.proquest.com/openview/047cc39b568af3f9ff0866bbed2102f/1.pdf?pq-origsite=gscholar&cbl=1056348

[6] Tokunaga, H. "On the Roller Straightener", Bulletin of the J.S.M.E., Vol.4, No.15, 605, 1961. https://doi.org/10.1299/jsme1958.4.605

[7] Roy, S., Pal, A.K., Rawal, S., "A review on straightening of bars and application of probabilistic approach on Moment-Curvature relationship", IOP Conference Series: Materials Science and Engineering (ICEMEM-2019), 810 (2020), https://doi:10.1088/1757-899X/810/1/012080

[8] Roy, S., Pal, A.K., Das Talukder, N.K., "A Brief Review on Theoretical Aspects of Bar Straightening with Recent Developments in Its Modelling, Simulation, Control System, and Stabilization", Forming the Future, The Minerals, Metals & Materials Series, pp. 2135-2154, (2021), https://doi.org/10.1007/978-3-030-75381-8_180

[9] Roy, S., Pal, A.K., "A Probabilistic Approach on the Estimation of Residual Curvature of Round Bars in Straightening Process with Cross-Roll Arrangements", International Journal of Science and Research (IJSR), ISSN:2319-7064, SJIF (2022): 7.942, Vol.11, Issue 6, June 2022, DOI:10.21275/SR22618185633

[10] Roy, S., Pal, A.K., "Theoretical Approach on Two Factorial Design on Residual Curvature of Bar Straightening in Cross-Roll Arrangements" , Journal of Production Engineering, JPE(2022), Vol.25, No.2, https://doi.org/10.24867/JPE-2022-02-030

[11] Roy, S., Pal, A.K., "Effect of Helix Angle in Cross-Roll arrangements of Bar Straightening Process with Kinematic Reverse Bending", Journal of Production Engineering, JPE(2022), Vol.25, No.2, https://doi.org/10.24867/JPE-2022-02-039

[12] Roy, S., Pal, A.K., "A Statistical Approach for study of Roundness in Commercially Produced Round Metal Bars", European Journal of Theoretical and Applied Science (EJTAS), ISSN 2786-7447, 1(5), 294-306, https://doi.org/10.59324/ejtas.2023.1(5).20

[13] Yu, T.X., Johnson, W., "Estimating the curvature of bars after cross-roll straightening", Proceedings of the 22nd Int. MTDR Conference:517. ISBN: 978-1-349-06283-6, 1982. http://dx.doi.org/10.21275/SR22618185633

[14] Das Talukder, N.K., Johnson, W. "On the arrangements of rolls in cross-roll straighteners", Int. J. Mech. Sci. 23(4): 213-220, 1981. https://www.research-collection.ethz.ch/bitstream/handle/20.500.11850/152929/ETH19928.pdf?sequence=5

[15] Das Talukder, N.K., Singh, A.N. "Mechanics of Bar Straightening, Part-1: General Analysis of Straightening Process", Transaction of the ASME, J. of Manufacturing Science and Engineering, p.p. 224-227, Vol.113, May 1991. https://doi.org/10.1115/1.2899682

[16] Das Talukder, N.K., Singh, A.N. "Mechanics of Bar Straightening, Part-2: Straightening in Cross-Roll Straighteners" Transaction of the ASME, J. of Manufacturing Science and Engineering, p.p. 228-232, Vol.113, May 1991. https://doi.org/10.1115/1.2899683

[17] Whitehouse, D.J. "Surface Metrology",*Measurement Science and Technology, 8*(9), 955-972., 1997. http://doi.org/10.1088/0957-0233/8/9/002

[18] Marcos-B´arcena, M., Sebasti´an-P´erez, M.A., Contreras-Samper, J.P., S´anchez-Carrilero, M., S´anchez-L´opez, M., S´anchez-Sola, J.M., "Study of roundness on cylindrical bars turned of aluminium–copper alloys UNS A92024", Journal of Materials Processing Technology 162–163, pp.644–648, doi:10.1016/j.jmatprotec.2005.02.061

[19] Kalos, P.S., Nandurkar1, K. N., Navale, L.G., "Control of Roundness on Turned Cylindrical Bars Using Artificial Neural Network", Proceedings of the 2007 IEEE IEEM. https://doi.org/10.1109/ieem.2007.4419259

[20] Lu, Hong., Ling He., Leopold Juergen., Zhang, Xiao., Guo, Chang. Qiao., "Improvement on straightness of metal bar based on straightening stroke-deflection model", *Science in China Series E: Technological Sciences,* Feb. 2009, vol. 52, no. 7, 1866-1873. https://doi.org/10.1007/s11431-009-0212-3

[21] Kume, T., Satoh,M., Suwada, T., Furukawa, K., Okuyama,E., "Straightness evaluation using inclinometers with a pair of offset bars", Precision Engineering 39, pp. 173–178, 2015, http://dx.doi.org/10.1016/j.precisioneng.2014.08.006

[22] Tangjitsitcharoen, S., Chanthana, D., "In-process prediction of roundness based on dynamic cutting forces", Int J Adv Manuf. Technol, 94:2229–2238, 2018, https://DOI.org/10.1007/s00170-017-1047-x

[23] Chanthana, D., Tangjitsitcharoen, S., "A study of relation between roundness and cutting force in CNC turning process", Appl Mech Mater 799-800:366–371, 2015. https://doi.org/10.4028/www.scientific.net/amm.799-800.366

[24] Li, Ke-Yang., Chen, Cha'o-Kuang., Yang, Shyue-Cheng., "Profile determination of a tube-straightening roller by envelope theory", Journal of Materials Processing Technology, 94, pp.157-166, 1999. https://doi.org/10.1016/s0924-0136(99)00089-8

[25] Paech, Marcus**.,** **"**Roller straightening process and peripherals", Wire Journal International, 2, pp.76-82, 2001.

[26] Paech, Marcus**.,** **"**Advanced semi-automatic straightening technology", Wire Journal International, pp.74-75, 2008.

[27] Sasaki, Y., Otsu, M., Matsumura, M., Morishita, K., Tanaka, T., Yagi, H., Sekine, Y., Asakawa, M., "Deriving position of bending roll in roll bending of titanium alloy wire for glasses frame", Procedia Engineering 81, 257 – 262, 2014. https://doi.org/10.1016/j.proeng.2014.09.160

[28] Kato, M., Hasegawa, A., Sugyo, S., Nakamura, H., Kobayashi, M., Morimoto, Y., "Straightening technology of round bars using 2-roll rotary Straightener", Procedia Engineering 81,pp. 233 – 238, 11th International Conference on Technology of Plasticity, ICTP 2014, 19-24 October 2014. https://doi.org/10.1016/j.proeng.2014.09.156

[29] Ma, L., Ma, Z., Jia, W., Ly, Y., Jiang, Y., Xu, H., Liu, P., "Research and verification on neutral layer offset of bar in two-roll straightening process", Int J Adv Manuf. Technol, https://DOI.org/10.1007/s00170-015-6899-3 , 2015

[30] Ma. L.,Du, Y., Liu, Z., Ma, Lifeng., "Design of continuous variable curvature roll shape and straightening process research for two-roll straightener of bar", The International Journal of Advanced Manufacturing Technology, 2019, https://doi.org/10.1007/s00170-019-04533-0

[31] Poltarak, Guillermo and Sergio Ferro, S., "A continuous straightening formulation based on minimum curvature variation", Int. J. Materials and Product Technology, Vol. 58, No. 1, 2019. https://doi.org/10.1504/ijmpt.2019.096930

[32] Olson W.A., Bert, *C.* W., "Analysis of Residual Stresses in Bars and Tubes of Cylindrically Orthotropic Materials", Experimental Mechanics, pp. 1966. Pp. 451-457, 1966. https://doi.org/10.1007/bf02326558

[33] Talamani, B., Gordon, J., Perlman, A.B., "Finite element estimation of the residual stresses in roller-straightened rail", Proceedings of IMECE04 2004, ASME International Mechanical Engineering Congress and Exposition, November 13-20, 2004, Anaheim, California USA.

[34] Aris, Rutherford., "Mathematical Modelling Techniques", Dover Publications, 1978. ISBN 0-486-68131-9 (pbk.), Pitman, 1978

[35] Dvorkin, E.N., Medina, F.M., "Finite Element Models for Analyzing the Straightening of Steel Seamless Tubes", Journal of Engineering for Industry, Vol. 111, pp.351-355, 1989. https://doi.org/10.1115/1.3188771

[36] Mischke, J., Jonca, J., "Simulation of the roller straightening process", Journal of Materials Processing Technology, 34,pp. 265-272, 1992. https://doi.org/10.1016/0924-0136(92)90116-A

[37] Macura, P., Petruska, J., "Numerical and experimental simulation of pass rolling", Journal of Materials Processing Technology, 60,pp.55-60, 1996. https://doi.org/10.1016/0924-0136(96)02307-2

[38] Wu, B.J., Chan,L.C., Lee, T.C., Ao, L.W., "A study on the precision modeling of the bars produced in two cross-roll straightening", Journal of Materials Processing Technology, 99,pp.202-206, 2000. https://doi.org/10.1016/s0924-0136(99)00421-5

[39] Widmark, M., Melander,A., Meurling, F., "Low cycle constant amplitude fully reversed strain-controlled testing of low carbon and stainless sheet steels for simulation of straightening operations", International Journal of Fatigue, 22,pp. 307–317, 2000. https://doi.org/10.1016/s0142-1123(99)00127-9

[40] Srimani, S.L., Pankaj, A.C., Basu, J., "Analysis of end straightness of rail during manufacturing", International Journal of Mechanical Sciences, 47,pp. 1874–1884, 2005. https://doi.org/10.1016/j.ijmecsci.2005.07.005

[41] Mutrux, A., Berisha, B., Hochholdinger, B., Hora, P., "Numerical Modelling of Cross Roll Straightening", Metallumformung,7, LS-DYNA Anwenderforum, Bamberg, 2008.

[42] Tian, Y., Huang, Q., Li, J., "Numerical Analysis of Pressure Straightening Process to High Pressure Boiler Tube", Applied Mechanics and Materials, Vols 37-38,pp.723-726, Trans Tech Publications, Switzerland, 2010. https://doi.org/10.4028/www.scientific.net/AMM.37-38.723

[43] Song, H., Wang, P.L., Fu, L.H., Chen, M. and Wang, Z.Q., "Study on the Optimization Straightening Regulation of Heavy Rail Compound Roll Straightening", Advanced Materials Research Vols. 102-104,www.scientific.net, Trans Tech Publications, Switzerland, 2010, https://doi.org/10.4028/www.scientific.net/AMR.102-104.227

[44] Yali,Y., Herong, J., "Three Roller Curvature Scotch Straightening Mechanism Study and System Design", 2012 International Conference on Future Energy, Environment, and Materials, Energy Procedia 16,pp.38 – 44, 2012. https://doi.org/10.1016/j.egypro.2012.01.008

[45] Huang, H., Zheng, H., Du, F. and Wang, W., "Numerical Simulation Analysis on the Ten Cross Rolls Straightening Process of the Heavy Calibre Seamless Steel Tube", Advanced Materials Research Vol. 421, pp 56-59, 2012. https://doi.org/10.4028/www.scientific.net/AMR.421.56

[46] Raab, Z., Hynek,M., "Numerical simulation of cross roll straightening processes", Metal, 23. - 25. 5. 2012, Brno, Czech Republic, EU.

[47] Khromov, I., Kawalla, R., "Simulation of a Steel Wire Straightening Taking into Account Nonlinear Hardening of Material", ETASR - Engineering, Technology & Applied Science Research Vol. 2, No. 6, pp.320-324, 2012. https://doi.org/10.48084/etasr.275

[48] Liu, Z., Wang, Y., Xingchun Yan, X., "A new model for the plate leveling process based on curvature integration method", International Journal of Mechanical Sciences 54, pp.213–224, 2012. https://doi.org/10.1016/j.ijmecsci.2011.10.011

[49] Petruska, J., Navrat, T., "Computational simulation of cross roll straightening", SEECCM III 3rd South-East European Conference on Computational Mechanics, an ECCOMAS and IACM Special Interest Conference, Kos Island, Greece, 12–14 June 2013.

[50] Navrat, T., Petruska, J., "Eulerian Description of Rail Straightening Process", Applied Mechanics and Materials Submitted: 2014-06-30 ISSN: 1662-7482, Vol. 624, pp.213-217, Trans Tech Publications, Switzerland, 2014. https://doi.org/10.4028/www.scientific.net/AMM.624.213

[51] Kaiser, R., Hatzenbichler, T., Buchmayr, B., Antretter, T., "Simulation of the roller straightening process with respect to residual stresses and the curvature trend", Materials Science Forum, Vols 768-769, pp.456-463, Trans Tech Publications, Switzerland, 2014. https://doi.org/10.4028/www.scientific.net/MSF.768-769.456

[52] Petruska, J., Návrat, T., Sebek, F.,"Novel approach to computational simulation of cross roll straightening of bars", Journal of Materials Processing Technology 233, pp. 53–67, 2016. http://dx.doi.org/10.1016/j.jmatprotec.2016.02.004

[53] Zhu, A., Zhu, W., Chen, J., Liu, G., Shen, Y., Wang, X., He, Y., Bai, Y., "Studies on modeling and simulation of straightening machine", WIT Transactions on Engineering Sciences, Vol 113, 2016, doi:10.2495/IWAMA150011

[54] Yu, G., Zhai, R., Zhao, J., Ma, R., "Theoretical analysis and numerical simulation on the process mechanism of two-roller straightening", Int. J. Adv. Manuf.Technol.,2017, https://doi.org/10.1007/s00170-017-1120-5

[55] Hardt,D.E., Hale, M., "Closed Loop Control of a Roll Straightening Process", Annals of the CIRP Vol. 33/1/1984, pp. 137-140, 1984. https://doi.org/10.1016/s0007-8506(07)61396-1

[56] Chandra, A., "Real-Time Identification and Control of Springback in Sheet Metal Forming", Journal of Engineering for Industry, Vol. 109, pp.265-273. August 1987. https://doi.org/10.1115/1.3187128

[57] Kim, S-C, Chung, S-C. "Synthesis of the multi-step straightness control system for shaft straightness process". Mechatronics 12:139-156. 2002. https://doi.org/10.1016/S0957-4158(00)00066-0

[58] Zhao,J., Song, X., "Control strategy of multi-point bending one-off straightening process for LSAW pipes", Int. J. Adv. Manuf. Technol., 72, pp.1615–1624, 2014. https://doi.org/10.1007/s00170-014-5776-9

[59] Nastran, M., Kuzman,K.,"Stabilisation of Mechanical Properties of the wire by roller straightening", Journal of Materials Processing Technology, 125-126, pp.711-719, 2002. https://doi.org/10.1016/s0924-0136(02)00316-3

[60] Aron, M., "Stability conditions for straightened, non-linearly elastic, annular cylindrical sectors", International Journal of Non-Linear Mechanics 41, pp. 672 – 677, 2006. https://doi.org/10.1016/j.ijnonlinmec.2006.04.001

[61] Mishra, A., Gangele, A., Israr, Md., "Application of Taguchi Approach in the Optimization of Roundness of Cylindrical Bars of AISI 1045 Steel", International Journal of Basic and Applied Science, Vol. 02, No. 01, pp.186-194, 2013. Insan Akademika Publications, E-ISSN:2301-4458; P-ISSN:2301-8038

[62] Patel, A.S., Prajapati, J.M., "A review on innovation of wire straightening cutting machine**",** International Journal of Engineering Science and Technology (IJEST), Vol. 3 No. 5, May 2011, pp. 4204-4209, ISSN:0975-5462

[63] Biju, B., Dijin, J.S., Anujith, C., Arun Augustine, Mohammad Anas P., "Design and Analysis of Straightening Mechanism for Commercial Steel Bars". International Research Journal of Engineering and Technology (IRJET) Vol.3 Issue:5, May-2016. p.p.379-383, e-ISSN:2395-0056. p-ISSN:2395-0072 https//www.irjet.net/vol3-issue5

[64] Yu, G., Zhai, R., Zhao, J., Ma, R.,(2018), Theoretical analysis and numerical simulation on the process mechanism of two-roller straightening, International Journal of Advanced Manufacturing Technology. https://doi.org/10.1007/s00170-017-1120-5

[65] Das Talukder, N.K., Singh, A.N., Johnson, W., "Cross-Roll Straighteners and Their Performance", Journal of Materials Processing Technology, 21, pp.101-109, 1990., https://doi.org/10.1016/0924-0136(90)90033-Q

[66] Bewoor A.K., Kulkarni, V.A., "Metrology & Measurement", McGraw Hill Education (India) Private Limited, New Delhi, ISBN: 978-0-07-014000-4.

[67] https://redlux.net/gdandt/straightness

[68] Frederick, C.O., Armstrong, P.J., "A mathematical representation of the multiaxial Bauschinger effect", CEGB Intern Res Rep RD/B/N660 Mater High Temp 24(1):1-26, 1966. ISSN 0960-3409 (Print) https://doi.org/10.3184/096034007x207589

[69] Ludwik, P., "Elemente der technologischen mechanic", Springer Verlag, Berlin., 1909. eBook ISBN978-3-662-40293-1, Softcover ISBN978-3-662-39265-2, https://doi.org/10.1007/978-3-662-40293-1

[70] Drucker, D.C., "A more fundamental approach to plastic stress-strain relations.", In: 1st US National Congress of Applied Mechanics, ASME, New York, 1952.

[71] Davis, E.A., Rose, B.A., Nadai, A., "Theory of Flow and Fracture of Solids", Vol.1, Second Ed. McGraw-Hill, p.20, 1950. http://ci.nii.ac.jp/ncid/BA10558604

[72] Meiwes, K.C., Erdelen-Peppler, M., Brauer, H., "Impact of small-scale reeling simulation on mechanical properties on line pipe steel", Proceedings of the 2014 10th International Pipeline Conference IPC2014, Calgary, Alberta, Canada. 2014. https://doi.org/10.1115/IPC2014-33161

[73] Lascic, B., "Theory and Technology of Quenching", H.M. Tensi, and W. Luty (Eds.), Springer-Verlag, New York, 1992. https://doi.org/10.1007/978-3-662-01596-4

[74] Groover, Mikell. P., "Fundamentals of Modern Manufacturing", John Wiley & Sons, Inc. 2010. http://ci.nii.ac.jp/ncid/BA55024566

[75] Ang, A.H-S., Tang, W.H., "Probability Concepts in Engineering Planning and Design, Basic Principles, Vol.1, John Wiley & Sons Inc., Canada.,1975. https://doi.org/10.2307/2987875

[76] Section Straightening Machine, Make: Kabir Section Straightening Machine, https://www.indiamart.com/proddetail/section-straightening-machine-2808479130.html?pos=1&kwd=section

[77] Section Straightening Machine, Make: Sohal Machine Tools, https://www.indiamart.com/proddetail/section-straightening-machine-280847913.html?pos=1&enqform=1

[78] Stretch Straightening Machine, Make: Cyril Bath Co., North Carolina, USA. https://www.cyrilbath.com/en/products/extrusion-stretch-straightening-and-forming

[79] Schematic diagram of Spinner Straightener, https://www.google.co.in/search?q=spinner+straightener&sca_esv=60fec118eeb925b4&sca_upv=1&sxsrf=ADLYWIL1v6UDRxTwpFAOXvmbL6TITEiDtQ%3A1720177800664&source=hp&ei=iNSHZr7VJJSN2roPt7CRmAU&iflsig=AL9hbdgAAAAAZofimOo0185XnPK-LE18o4ISKSCqjQ2_&oq=spinner+&gs_lp=Egdnd3Mtd2l6IghzcGlubmVyICoCCAAyBBAjGCcyBBAjGCcyBBAjGCcyCBAAGIAEGLEDMggQABiABBixAzIIEAAYgAQYsQMyChAAGIAEGEMYigUyBRAAGIAEMgUQABiABDIIEC4YgAQY1AJIlCZQAFj2EnAAeACQAQCYAfwBoAHCDKoBBTAuNS4zuAEByAEA-AEBmAIIoALNDcICERAuGIAEGJECGNEDGMcBGIoFwgILEAAYgAQYkQIYigXCAhEQLhiABBixAxjRAxiDARjHAcICCxAAGIAEGLEDGIMBwgIQEAAYgAQYsQMYQxiDARiKBcICDhAAGIAEGLEDGIMBGIoFwgIREAAYgAQYkQIYsQMYgwEYigXCAgoQLhiABBhDGIoFwgIQEC4YgAQY0QMYQxjHARiKBcICDRAuGIAEGLEDGEMYigXCAhEQLhiABBixAxiDARjHARivAcICDRAAGIAEGLEDGEMYigXCAhAQLhiABBixAxhDGIMBGIoFwgIKEAAYgAQYFBiHAsICCxAuGIAEGLEDGIMBmAMAkgcFMC4yLjagB6pi&sclient=gws-wiz#vhid=x25XaNuigUrL7M&vssid=

Straightener. Make: Clifford Machines & Technology, South Africa.

[80] https://link.springer.com/chapter/10.1007/978-3-030-75381-8_173

[81] Schematic of experimental setup of Magnetic Pulse Straightening, https://www.researchgate.net/publication/309560512_Hyperplasticity_effect_under_magnetic_pulse_straightening_of_dual_phase_steel/figures

[82] Straightening of Bar in a Two-Roll “Air-Bend”, Straightening Machine, https://www.indiamart.com/atharvamanufacturersconsultant/

[83] Six Roll Straightening Machines. Brand Shivam Engineering. https://www.indiamart.com/proddetail/stainless-steel-tube-straightening-machine-5680873797.html?pos=8&vcdimgform=1

[84] Multi-staggered Roller Straightening Machine. Model:LJ250 10 rolls straightening machine, https://www.chinaironsteel.com/pd.jsp?id=188#_jcp=3_15

[85] Cluster Roll Straightening machine, Vaid Engineering Industries, https://www.indiamart.com/proddetail/multi-roll-straightening-machines-22490494897.html

[86] "Operating Manual" and "Spare Part Catalogue" of Machine No. 453, Super Single Colour Offset Machine (482 mm x 640 mm) 7500 I.P.H. Model No. PO25 Super". Make: Manugraph Industries Ltd., MIDC, Industrial Estate, Shiroli, Kohlapur 416122.

[87] https://www.amazon.in/Upgrade-Engraver-Controller-Extension-180x40mm/dp/B08X67QY74/ref=sr_1_13?crid=2CJ4B8KK8SD1H&dib=eyJ2IjoiMSJ9.n6rd6aL-sLTNRndDuf3n_d2H2NDKcI-vZTrmH5UvMmDPCKzaGjQZwXYnmXCXrsaCcfcw21a_oXRrYxdsiCGeYwlB5I8LANWxIyrK7qIZnv4JdCeLwG_wEGdwccxHzvhUQbfbbIqAxiMipeTicAXnDlM1t0HuvNPl402yKTRfTtY9mrqka8ty1lQrLqhe6STb6-wOqN4Az6EW_L36EkTr6ZjhMD5ZcpcNdE5iGraInJLhebvf0Oq-4pN6SH6R2w5cX5sP6S_8YMJNzTCx2YxPn509EML8ulCe_vjiqDDaumY.9D3Pj84OSAXfvJKXWN8fRJ16u1Sfx2tVyOa5h1t_FN4&dib_tag=se&keywords=cnc+machine&qid=1725439777&sprefix=cnc%2Caps%2C639&sr=8-13

[88] https://www.3idea.in/cnc-router-2457/two-trees-ttc3018s-cnc-router-machine?srsltid=AfmBOoors6rkg_iEjjfh26GWVw-8ixWz0dU1HQvqL3ZwziJ6uz2iXE3o

[89] Montogomery, Douglas C ,"Design and Analysis of Experiments" Eighth Edition, Wiley, 2016. ISBN: 978-81-265-4050-1.

[90] Pai Fan-Yun, Yeh Tsu-Ming & Hung Y.H.(2015). Analysis on Accuracy of Bias, Linearity and Stability of Measurement System in Ball screw Processes by Simulation. Sustainability, 7, 15464-15486. http://doi.org/10.3390/su71115464

[91] Reddy, S. & Rao, C.S. (2016). Optimization of surface roughness, circularity deviation and selection of different Aluminium alloys during drilling for automotive and aerospace industry. Independent Journal of Management & Production [IJM&P), 7(2). http://doi.org/10.14807/ijmp.v7i2.414

[92] Adamctak, S., Zmarzly, P., & Stepien, K. [2016), Identification and analysis of optimal method parameters of the V-block waviness measurements. Bulletin of the Polish Academy of Science, 64[2), 325-332. http://doi.org/10.1515/bpasts-2016-0037

[93] Raghu, S., Mamatha, T.G., Vishnoi, M., Moona, G. & Sharma, R. (2020) Optimization of Turning Parameter for Roundness Investigation using V-block Method. Indian Journal of Advances in Chemical Science, 8(1), 28-31. http://doi.org/10.22607/IJACS.2020.801006

[94] Cuesta E., Gestoa A., Alvareza B.J., Martínez-Pellitero S., Zapico P. & Giganto S. (2019), Dimensional accuracy analysis of Direct Metal Printing machine focusing on roller positioning errors. Procedia Manufacturing, 41, 2-9. https://doi.org/10.1016/j.promfg.2019.07.022

[95] Görög, A. (2022). Influence of the Setting on the Result of Measuring the Roundness of the Cylindrical and Conical Surface. Manufacturing Technology, 22(4). http://doi.org/10.21062/mft.2022.055

[96] https://raw.githubusercontent.com/sroy2605/Bar-Straightening/refs/heads/main/MS-BS.pdf

[97] https://raw.githubusercontent.com/sroy2605/Bar-Straightening/refs/heads/main/SS-BS.pdf

[98] https://raw.githubusercontent.com/sroy2605/Bar-Straightening/refs/heads/main/AL-BS.pdf

[99] https://raw.githubusercontent.com/sroy2605/Bar-Straightening/refs/heads/main/CU-BS.pdf

[100] Mitra, A. "Fundamentals of Quality Control and Improvement". Third Edition, Wiley (2016). ISBN: 978-1-118-70514-8. https://doi.org/10.2307/1268912

[101] Matsuda K., Roy, M., Eiju, T., O'Byrne, J.W., Shepard, C.J.R., "Straightness measurements with a reflection confocal optical system-an experimental study", APPLIED OPTICS, vol.41, No.19, pp.3966-3970, https://doi.org/10.1364/AO.41.003966

[102] Egidi, A., Balsamo, A., Corona, D., Pisani, M., "Investigation on Modulation-Based Straightness Measurement", Sensors, 2023, 2912. https://doi.org/10.3390/s23062912

[103] https://raw.githubusercontent.com/sroy2605/Bar-Straightening/refs/heads/main/MS-AS.pdf

[104] https://raw.githubusercontent.com/sroy2605/Bar-Straightening/refs/heads/main/SS-AS.pdf

[105] https://raw.githubusercontent.com/sroy2605/Bar-Straightening/refs/heads/main/AL-AS.pdf

[106] https://raw.githubusercontent.com/sroy2605/Bar-Straightening/refs/heads/main/CU-AS.pdf

[107] Finite Element Analysis with ANSYS Workbench 2019 R2: A Tutorial Approach, Sham Tickoo, BPB Publications, ISBN: 978-81-944018-1-0, Reprint 2023.

[108] Gribkov, E., Dobronosov, Y., Kukhar, V., Balalayeva, E., Marchenko, I., Hrudkina, N., (2023), "Computer Modelling of Pipe Straightening Process on a Six-Roller Cross-Roll Machine" , IEEE 18th International Conference on Computer Science and Information Technologies (CSIT), https://doi.org/10.1109/CSIT61576.2023.10324256

[109] Xing, S.,(2023), Analytical Modeling for Mechanical Straightening Process of Case-Hardened Circular Shaft, Applied Mechanics,4,715–728, https://doi.org/10.3390/applmech4020036

[110] Awad. M., Khanna, R., "Support vector regression. In: Efficient learning machines", Berkley, CA: Apress. https://link.springer.com/book/10.1007/978-1-4302-5990-9

[111] Wang, J., Chen, Q., Chen, Y. (2004), RBF Kernel Based Support Vector Machine with Universal Approximation and Its Application. In:Yin, FL., Wang,J., Guo, C.(eds.) Advances in Neural Networks – ISNN 2004, Lecture Notes in Computer Science, Vol. 3173, Springer, Berlin, Heidelberg. https://doi.org/10.1007/978-3-540-28647-9_85

[112] Louppe, G. (2014). "Understanding random forests: From theory to practice". arXiv: Machine Learning. https://doi.org/10.48550/arXiv.1407.7502

[113] Sharma G., Khurana, S., Saina, N., Shivansh, Gupta G., (2024), Comparatively analysis of machine learning techniques in air quality index (AQI) prediction in smart cities. International Journal of Systems Assurance Engineering and Management, Vol. 15, No. 7, pp. 3060-3075, https://doi.org/10.1007/s13198-024-02315-w

[114] https://github.com/sroy2605/Code-for-ML/blob/main/Appendix-1%20Code%20for%20Bar%20Straightening%20Machine%20Learning%20Algorithm.txt